DISSERTATION

Titel der Dissertation

Investigating the specificity of human rhinoviruses 2A proteinases

angestrebter akademischer Grad

Doktor/in der Naturwissenschaften (Dr. rer.nat.)

Verfasserin / Verfasser:	Carla Sousa
Matrikel-Nummer:	0548709
Dissertationsgebiet (lt. Studienblatt):	Molekulare Biologie
Betreuerin / Betreuer:	Univ.-Prof. Dr. Tim Skern
Wien, am 19. März 2008	

Acknowledgements

Summary

The picornavirus family is composed of small, non-enveloped viruses which contain a single stranded RNA genome of positive polarity. The genome is translated into one large polyprotein which is then processed into the mature viral proteins by virally encoded proteinases. In human rhinoviruses and enteroviruses, two chymotrypsin-like proteinases, 3C^{pro} and 2A^{pro} carry out these cleavages. 2A^{pro} executes the first cleavage on the polyprotein, cleaving itself from the VP1 capsid protein. 2A^{pro} also cleaves several cellular proteins, amongst which is the eukaryotic initiation factor (eIF) 4G. eIF4G is a scaffolding protein that brings together the cellular capped mRNA and the ribosomes. Thus, the cleavage of this factor leads to the shut off of the cellular translation, as the mRNA is no longer able to reach the ribosome. The viruses can use this reduced translation machinery as they do not need the cap-dependent initiation mechanism to bind the ribosome and synthesize their proteins.

There are more than 100 serotypes of rhinoviruses divided in two genetic groups, A and B. However, the level of sequence identity between the groups A and B is quite variable. For example, there is only 40% amino acid identity between the 2A^{pro} of HRV2 (group A) and HRV14 (group B). Nevertheless, these two proteinases cleave their respective polyproteins at practically the same rate. In contrast, HRV2 2A^{pro} completes the cleavage of eIF4G isoforms I and II at similar times whereas HRV14 2A^{pro} cleaves first eIF4GI and eIF4GII later. In order to understand and identify the residues responsible for the differences in properties of these proteinases, we decided to perform site directed mutagenesis experiments. We found that HRV14 2A^{pro} cannot cleave the eIF4GI cleavage sequence in the polyprotein, due to the presence of the arginine residue at P1. The mutations A104C or A104S in HRV14 2A^{pro} restored cleavage when arginine was present at P1, although not to wild-type levels.

The crystal structure of HRV2 2A^{pro} helped to identify the residues involved in HRV2 2A^{pro} specificity. However, the low level of amino acid identity between HRV2 2A^{pro} and HRV14 2A^{pro} limited the use of this crystal structure for HRV14 2A^{pro}. Therefore, we purified HRV14 2A^{pro} with the objective of solving its crystal structure. We were able to obtain highly purified protein at suitable concentrations for crystallization trials. However, the purified protein appeared to be incorrectly folded. Optimization of the expression and purification methods are needed.

We also wanted to identify new cellular binding partners of 2A^{pro}. To this end, we used a proteomics approach in which cellular proteins complexed with 2A^{pro} were purified and identified by mass spectroscopy. Although we identified some known and some putative binding partners, none of the previously undetected proteins were bound or cleaved by 2A^{pro}.

Optimization is needed in order to lower the amount of false positives and increase the sensitivity for *bona fide* partners.

To know more about the interaction of viral proteinases with eIF4G, we purified a domain of eIF4GII containing the cleavage sites for HRV2 2A^{pro} and the leader proteinase of foot and mouth disease virus and the binding site for eIF4E (cap binding protein). The ultimate aim was to determine the crystal and nuclear magnetic resonance structures of this fragment. The protein was successfully expressed in *E. coli* and labelled with ^{15}N. However, in both cases, the protein was incorrectly folded. Experiments with the eIF4GII complexed with eIF4E need to be done, as there is evidence that eIF4E induces a conformational change in eIF4G which leads to a defined structure.

Zusammenfassung

Die Familie der Picornaviridae besteht aus unbehüllten Viren mit einer einzelsträngigen, linearen RNA mit positiver Polarität als Genom. Dieses wird in ein großes Polyprotein translatiert und von viralen Proteinasen prozessiert. So entstehen die reifen Proteine. In humanen Rhino- und Enteroviren sind zwei Chymotrypsin-ähnliche Proteasen für die Prozessierung verantwortlich: 3C^{pro} and 2A^{pro}. 2A^{pro} führt den ersten Schnitt am Polyprotein aus, indem es sich selbst vom VP1 Kapsidprotein schneidet. Weiters ist sie für die Spaltung diverser zellulärer Proteine verantwortlich, darunter auch der eukaryotische Initiationsfaktor (eIF) 4G. Dieser bringt die zelluläre gecappte mRNA und die Ribosomen zusammen. Eine Spaltung dieses Faktors führt also zu einer Inhibierung der RNA und Proteinsynthese der Wirtszelle. Die virale Translation bleibt davon unbeeinflusst, da sie durch Verwendung einer IRES (internal ribosomal cleavage site) cap-unabhängig ist.

Es gibt mehr als 100 Serotypen von Rhinoviren die in 2 Gruppen eingeteilt werden: A und B. Das Ausmaß der Übereinstimmung dieser beiden Gruppen ist variabel. Zum Beispiel stimmt die Aminosäuresequenz der 2A^{pro} von HRV2 (Gruppe A) und HRV14 (Gruppe B) nur zu 40 % überein. Dennoch schneiden diese beiden Proteinasen ihr jeweiliges Polyprotein im selben Ausmaß. Im Gegensatz dazu, ist die Spaltung des eIF4G unterschiedlich. HRV2 2A^{pro} spaltet die Isoformen eIF4GI and II gleichzeitig, während die HRV14 2A^{pro} zuerst eIF4GI und erst danach eIF4GII schneidet. Um diese unterschiedlichen Eigenschaften zu verstehen und die verantwortlichen Reste zu identifizieren verwendeten wir ortspezifische Mutagenese. HRV14 2A^{pro} kann die eIF4GI Sequenz im Polyprotein nicht schneiden, wegen eines Arginin Restes an der P1 Position. Die Mutationen A104C und A104S in der HRV14 2A^{pro} ermöglichten ein Spaltung von eIF4GI in Anwesenheit eines Arginins in P1 Position, wenngleich nicht auf Wildtyp-Niveau.

Die Kristallstruktur von HRV2 2A^{pro} half jene Reste zu identifizieren, die in die Spezifität der HRV2 2A^{pro} involviert sind. Durch die geringe Sequenzübereinstimmung zwischen den Proteasen der beiden Gruppen kann diese Kristallstruktur aber nur bedingt für die HRV 14 2A^{pro} angewendet werden. Daher purifizierten wir HRV14 2A^{pro} mit dem Ziel, ihre Kristallstruktur zu bestimmen. Wir konnten hoch reines Protein in für die Kristallisation geeigneter Konzentration herstellen. Da das Protein aber falsch gefaltet zu sein scheint, ist eine Optimierung der Expression und Purifikation nötig.

Weiters wollten wir neue zelluläre Bindungspartner der HRV 2A^{pro} identifizieren. Dafür wurde die HRV 2A^{pro} mit zelluläre Proteinen komplexiert, purifiziert und mittel Massenspektroskopie identifiziert. Obwohl wir einige bereits bekannte und einige vermutliche Bindungspartner identifizierten, wurde keines der zuvor undetektierten Proteine von der HRV

2A^{pro} gebunden oder geschnitten. Daher ist eine Optimierung notwendig, um falsch positive Ergebnisse zu minimieren und die Sensitivität für bona fide Partner zu erhöhen.

Um mehr über die Interaktion von viralen Proteasen mit eIF4G zu erfahren, purifizierten wir jene Domaine of eIF4GII die die Spaltungstellen der HRV2 2A^{pro}, der Leaderproteinase des Maul- und Klauensäuchevirus und die Bindungsstelle für eIF4E (cap bindendes Protein) enthält.

Das Ziel war, sowohl die Kristall- also auch die NMR (Nukleare Magnetresonanz) Struktur dieses Fragmentes zu erhalten. Das Protein wurde erfolgreich in E.coli exprimiert und mit ^{15}N markiert. Allerdings war das Protein in beiden Fällen inkorrekt gefaltet. Da es Anzeichen gibt, dass eIF4E eine Konformationsänderung im eIF4E induziert müssen Experimente mit eIF4GII im Komplex mit eIF4E durchgeführt werden.

List of abbreviations

All the abbreviations for amino acids are presented on table 22 in the appendix C.

µCi – microcurie

µl – microlitre

µM - micromolar

4EBP – 4E Binding Protein

aa – amino-acid

AP – Alkaline Phosphatase

APS - Ammonium persulfate

ATCC - American Type Culture Collection

ATP - Adenosine 5'-triphosphate

AUG – starting codon for methionine

BCIP - 5-Bromo-4-chloro-3-indolyl phosphate

°C – degrees centigrade

CaBP – Calmodulin Binding Protein

CAR – Coxsackie and Adenovirus Receptor

CBP – Cap Binding Protein

CD - Cluster of Differentiation

CIP - Calf Intestine Phosphatase

CITE – Cap Independent Translation Enhancer

CREB - cAMP Response Element-Binding

Cryo-EM – cryo Electron Microscopy

CTE – C-Terminal Extension

CV – Coxsackievirus

DAF – Decay Accelerating Factor

DMEM - Dulbecco's Modified Eagle Medium

DMSO - Dimethyl sulfoxide

DNA - Deoxyribonucleic acid

DNase - Deoxyribonuclease

dNTP – deoxynucleotide triphosphate

DTT - Dithiothreitol

ECACC - European Collection of Cell Cultures

ECL - Enhanced chemiluminescence

EDTA - Ethylenediaminetetraacetic

eIF – eukaryotic Initiation Factor

EMCV – Encephalomyocarditis Virus

ER – Endoplasmic Reticulum

Fc - fragment crystallizable

FCS - Foetal Calf Serum

FMDV – Foot and Mouth Disease Virus

FPLC - Fast Protein Liquid Chromatography

g - gram

GST - Glutathione S-transferase

GTP - Guanosine-5'-triphosphate

HAV – Hepatitis A Virus

HEK cells - Human Embryonic Kidney cells

HeLa cells - Henrietta Lacks' cells

HEPES - 4-(2-hydroxyethyl)-1-piperazineethanesulfonic acid

HP – Heparan Sulphate

HRP - Horseradish Peroxidase

HRV – Human Rhinovirus

ICAM – Intercellular Adhesion Molecule

Ig – Immunoglobulin

IPTG - Isopropyl β-D-1-thiogalactopyranoside

IRES – Internal Ribosomal Entry Site

kb – kilobase

kDa - kilodalton

l - litre

L^{pro} – Leader Proteinase

Lab^{pro} – Leader Proteinase ab

Lb^{pro} – Leader Proteinase b

LB – Luria Bertani

LCB - Lysis Cell Buffer

LDL – Low Density Lipoprotein

LGB – Lower Gel Buffer

M - Molar

MAPK - Mitogen-activated protein kinase

MEM - Modified Eagle Medium

MFPL – Max F. Perutz Laboratories

mg – milligram

MHz - Megahertz

ml – millilitre

mm - millimetre

mM – millimolar

mmol - millimol

Mnk1 - (MAPK)-interacting kinase 1

MOI – Multiplicity Of Infection

MOPS - 3-(N-morpholino)propanesulfonic Acid

mRNA – messenger Ribonucleic Acid

MS – Mass Spectroscopy

NBT - Nitro blue tetrazolium

NCBI nr - National Center for Biotechnology Information – non redundant

ng – nanogram

nM – nanomolar

nm – nanometre

NMR - Nuclear Magnetic Resonance

NPC – Nuclear Pore Complex

NTP - Nucleotide triphosphate

*Oct*1 - Octamer Transcription Factor

PABP – PolyA Binding Protein

pBS - PBluescript

PBS - Phosphate Buffered Saline

PBS-T – PBS-Tween

PCR – Polymerase Chain Reaction

Phe – Phenylalanine

pmol - picomol

pol – polymerase

ppm – parts per million

pro - proteinase

PV – Poliovirus

RNA - Ribonucleic Acid

RNase- Ribonuclease

rpm – rotations per minute

RRL - Rabbit Reticulocyte Lysate

SDS - Sodium Dodecyl Sulfate

SDS-PAGE - SDS- Poly-Acrylamide Gel Electrophreis

Sf9 - *Spodoptera frugiperda* cells

SFM – Serum Free Medium

S-MEM - Minimum Essential Medium Eagle Joklik Modification

TAE - Tris-acetate-EDTA

TAP - Tandem Affinity Purification

TB – Terrific Broth

TBP – TATA box Binding Protein

TBq - Tera-becquerels

TCA - Trichloroacetic Acid

TE – Trypsin/EDTA

TEB – Tris/EDTA Buffer

TEMED - Tetramethylethylenediamine

TEV - Tobacco Etch Virus

TF – Transcription Factor

tRNA – transfer Ribonucleic Acid

U - Units

UGB – Upper Gel Buffer

UTR – Untranslated Region

UV – Ultra Violet

V - volts

v - volume

VP – Viral Protein

VPg – Virion Protein genome

w - weight

zVAD.fmk - benzylloxycarbonyl-Val-Ala-Asp(OMe).fluoromethyl ketone

zVAM.fmk - benzylloxycarbonyl-Val-Ala-Met.fluoromethyl ketone

Table of contents

1 Introduction

1.1 Picornaviruses

The family *Picornaviridae* is composed of 9 genera (table 1), all infecting vertebrates. Some are important human and animal pathogens, such as poliovirus (PV) or foot and mouth disease virus (FMDV).

Genus	Members	Serotypes
Enterovirus	Poliovirus, Coxsackievirus, Swine Vesicular Disease Virus	95
Rhinovirus	Common Cold Virus	103
Cardiovirus	Encephalomyocarditis Virus, Theilers Murine Encephalomyelitis Virus, Mengovirus	5
Aphthovirus	Foot-And-Mouth Disease Virus Equine Rhinovirus A	8
Hepatovirus	Including Hepatitis A Virus	3
Parechovirus	Human Parechovirus	4
Erbovirus	Equine Rhinovirus B	2
Kobuvirus	Including Aichi Virus	2
Teschovirus	Including Teschen Disease Virus	11

Table 1: The Genera of the family of Picornaviruses (Fauquet and International Committee on Taxonomy of, 2005).

1.1.1 Human rhinoviruses

Human rhinoviruses (HRV) are the most frequent cause of the common cold, a mild infection of the upper respiratory tract, in humans. The primary sites of infection are the nose and throat (Arruda *et al.*, 1997). However, infection of the lower respiratory tract does occur (Mosser *et al.*, 2005; Papadopoulos *et al.*, 2000). Rhinoviruses are also involved in exacerbation of asthma and pneumonia (Turner, 2007; Xatzipsalti *et al.*, 2005). Furthermore, recent reports show a connection between rhinoviruses and severe respiratory-tract infection in children (Renwick *et al.*, 2007).

There are more than 100 serotypes of HRV which are divided in two genetic groups, A and B, according to sequence data on VP1 and VP4 (Laine *et al.*, 2006; Savolainen *et al.*, 2002). However, recently, a new genotype of HRV, has been identified in patients presenting symptoms of influenza-like disease where no influenza viruses were detected (Lamson *et al.*, 2006). The complete genome of three of these new viruses has been sequenced and

revealed that they belong to a new species, HRV-C (Lau *et al.*, 2007). The genome of HRV-C viruses is relatively small compared with HRV-A and HRV-B. The polyprotein of HRV-C showed 51% amino acid identity with HRV-A and 48% with HRV-B. Phylogenetic analysis of HRV-C strains formed a distinct cluster from HRV-A and HRV-B (figure 1). Out of 26 HRV strains isolated from children with acute respiratory tract infection, 21 were found to belong to the HRV-C group (Lau *et al.*, 2007).
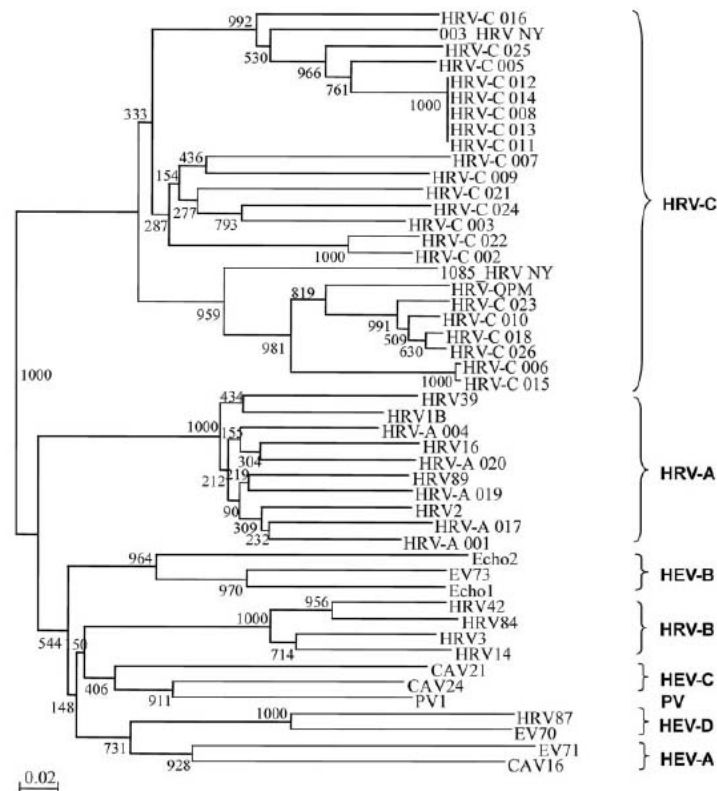
Figure 1: Phylogenetic tree of the VP4 region of 26 HRV strains collected from nasopharyngeal aspirates (Lau *et al.*, 2007).

A second classification system clusters these viruses according to the receptor used to enter the host cell. The major group, which comprises 90% of the serotypes, binds the intercellular adhesion molecule (ICAM) (Greve *et al.*, 1989; Staunton *et al.*, 1989) whereas the minor group utilizes the Low Density Lipoprotein (LDL) receptor (Hofer *et al.*, 1994). Some serotypes can also use the heparan sulphate (HS) receptor as a second receptor (Khan *et al.*, 2007).

1.1.2 Viral particle

Picornaviruses are small, non-enveloped viruses with a single stranded RNA genome of positive polarity. The term picornavirus is derived from the small (pico) size of the viral

particle and their RNA genome. These viruses have a simple structure with a spherical shape of about 30 nm of diameter, arranged in an icosahedral symmetry. The X-ray structures of many picornaviruses are available and were crucial for understanding the viral capsid. Among these structures are PV1 (Hogle *et al.*, 1985), HRV14 (Rossmann *et al.*, 1985), HRV16 (Oliveira *et al.*, 1993), FMDV serotype O (Acharya *et al.*, 1989) and coxsackievirus (CV) B3 (Muckelbauer *et al.*, 1995).

The viral capsid is composed of four structural proteins, VP (Viral Protein) 1, VP2, VP3 and VP4. The precursor of VP2 and VP4 is VP0, which is cleaved during the maturation of the viral particle. VP1, VP2 and VP3 share the same topology despite having different sequences. VP4 is located in the inner surface of the particle. The structure of the capsid proteins is a wedge-shaped, eight stranded, antiparallel β-barrel. One copy of each protein unites to form a protomer, the basic building block of the picornavirus capsid. 60 protomers form the viral capsid (figure 2). The shape similarity shared by the viral proteins facilitates their interaction with one another and their packing in the capsid. The interactions of the β-barrel domains of adjacent proteins form a dense and rigid shell that surrounds the naked RNA genome (Flint, 2004).
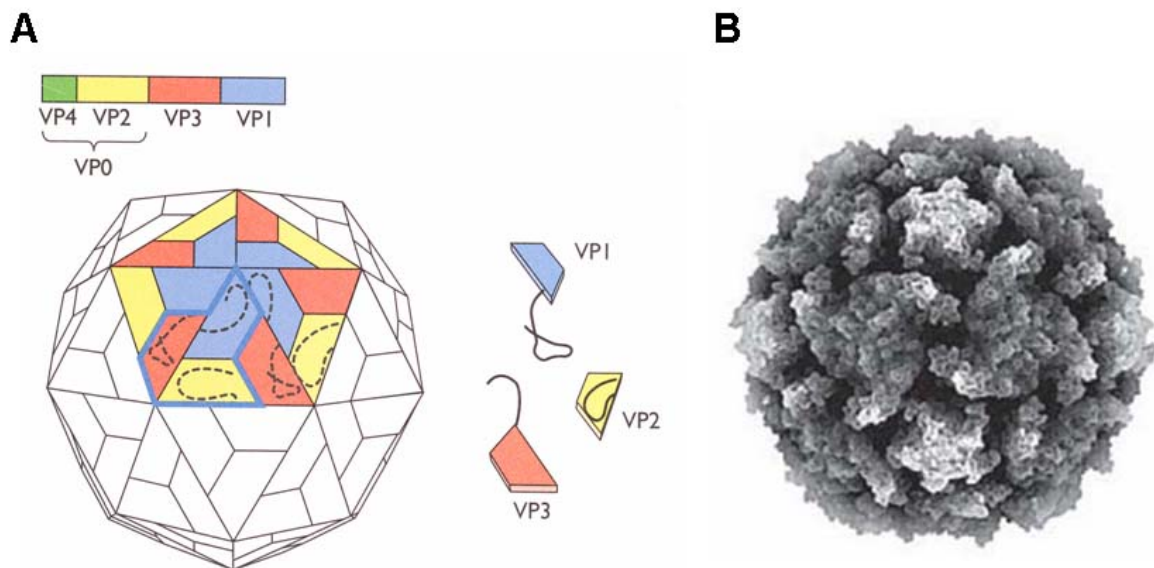
Figure 2: Structure of picornaviruses. A) Representation of the packing of VP1-VP2-VP3 structural units. 60 copies of each viral protein pack tightly forming the viral capsid. The protomer is highlighted in blue and forms two adjacent faces of an icosahedron. VP4 lies on the inner surface of the protein shell. (Flint, 2004) **B)** Poliovirus particle determined from X-ray crystallographic data (Hogle *et al.*, 1985).

The functions of the viral capsid are protection of the genome from the surrounding environment, recognition of cell receptors and thus tissue tropism determination,

3

determination of antigenicity and release of the RNA genome. Despite their similarity, picornaviral capsids vary in some physical properties. For example, cardioviruses, enteroviruses, hepatoviruses and parechoviruses are acid stable and remain infective at pH lower than 3. Other picornaviruses, such as rhinoviruses and aphthoviruses, are labile at pH lower than 6 (Fields *et al.*, 2007). These differences influence the location at which the viruses replicate. For example, rhinoviruses replicate in the respiratory tract whereas enteroviruses are able to replicate in the alimentary tract.

Although many structures of picornaviruses have been solved, there is still no insight into why some genera have a high number of serotypes, such as human rhinoviruses, and others like polioviruses have just few serotypes. The antigenicity of the picornaviruses is determined by the loops that connect the β-strands and the N- and C- terminal sequences that stretch out from the β-barrel domain. These regions contain the main structural differences among VP1, VP2 and VP3 and the major neutralization antigenic sites of the virus.

1.1.3 Picornaviral Genome

Picornaviral genomes are composed of a single stranded RNA molecule of positive polarity, with lengths of 7.1 kb (HRV) to 8.2 kb (FMDV). The viral genome is divided into three regions: the 5' UTR (untranslated region) (0.6 to 1.2 kb), the coding region (6.5 to 7 kb) and the 3' UTR (up to 0.1 kb) that contains a polyA tail of several dozen nucleotides (Agol, 2002). Picornaviral RNA does not possess a 5' cap structure; instead the RNA is covalently linked to the virion protein genome (VPg) (Flanegan *et al.*, 1977; Lee *et al.*, 1977) through a tyrosine residue.

cis-Elements (RNA sequences that regulate the expression of genes located on that same strand) involved in replication and translation of viral RNA are mainly present in the 5' UTR. However, some can be found within the coding region. One *cis*-element present in the 5' UTR is the Internal Ribosome Entry Site (IRES). The IRES is composed of discontinuous RNA segments which associate with each other acquiring a functional conformation (Witherell *et al.*, 1995). This highly structured region of the genome serves as recognition site for the ribosome, ensuring the formation of a pre-initiation template/ribosome complex (Agol, 2002). IRES sequences are formed by approximately 450 nucleotides and contain different sequence and secondary structure among the different picornavirus genera. There are three types of IRES in picornaviruses: type I in entero and rhinoviruses; type II in cardio, aphtho- and parechoviruses and type III in hepatoviruses (figure 3). The classification of IRES was based on sequence comparisons and biochemical or enzymatic probing (Ehrenfeld and Teterina, 2002).
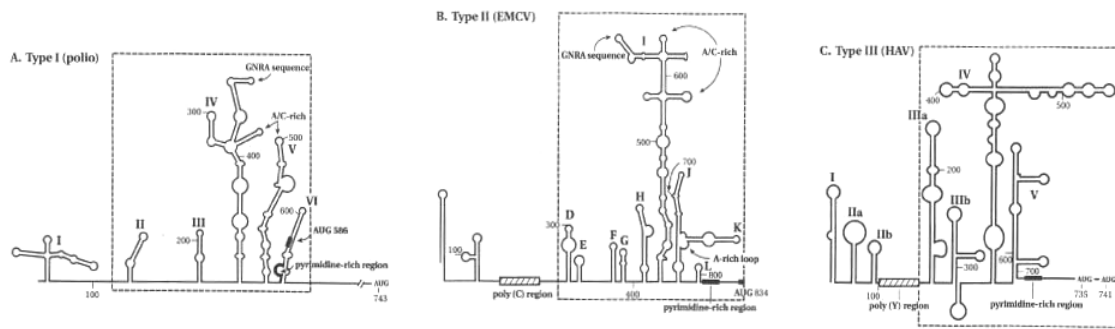
Figure 3: Schematic representation of the predicted stem-loop structures in the (A) poliovirus, (B) encephalomyocarditis virus, and (C) hepatitis A virus 5' UTR of the viral RNAs (Ehrenfeld and Teterina, 2002).

The 5' UTR also contains an oligopyrimidine stretch and an AUG codon separated by about 20 nucleotides which was postulated as being a *cis*-acting element (Beck *et al.*, 1983; Pilipenko *et al.*, 1992). However, it is not clear whether the oligopyrimidine, AUG codon and the spacer function as a single template element or whether they are separated elements in which the spacer determines the position of the AUG codon relative to the IRES (Pilipenko *et al.*, 1995).

Aphthoviruses and cardioviruses contain a polyC tract in their 5' UTR, which varies in length within the several serotypes. In cardioviruses the longer length of the polyC sequence is associated with higher virulence (Fields *et al.*, 2007).

The 3' UTR is shorter than the 5' UTR (47 nucleotides for HRV and up to 125 nucleotides in encephalomyocarditis virus (EMCV)) (Fields *et al.*, 2007). The 3' end contains a pseudoknot which might be involved in the initiation of the synthesis of minus strand RNA (Jacobson *et al.*, 1993). Furthermore, the removal of the polyA tract in PV produces non-infectious RNA (Spector and Baltimore, 1974). However, it was shown recently that the 3' non coding region is not required for HRV and PV infectivity (Brown *et al.*, 2005).

The coding region is composed of a single open-reading frame which is translated as a single polyprotein. Processing of the polyprotein by viral proteinases gives the mature proteins (Fields *et al.*, 2007) (see section 1.1.6) .

1.1.4 Replication cycle

Picornaviruses replicate in the cytoplasm of an infected cell. The replication cycle is divided in three steps: attachment and entry, decoding of genetic information and synthesis of new genomes and finally assembly and release of the particle.

A single replication cycle can take 5 to 10 hours, depending on the virus, temperature, host cell or pH. Figure 4 shows a schematic representation of the picornaviral replication cycle.
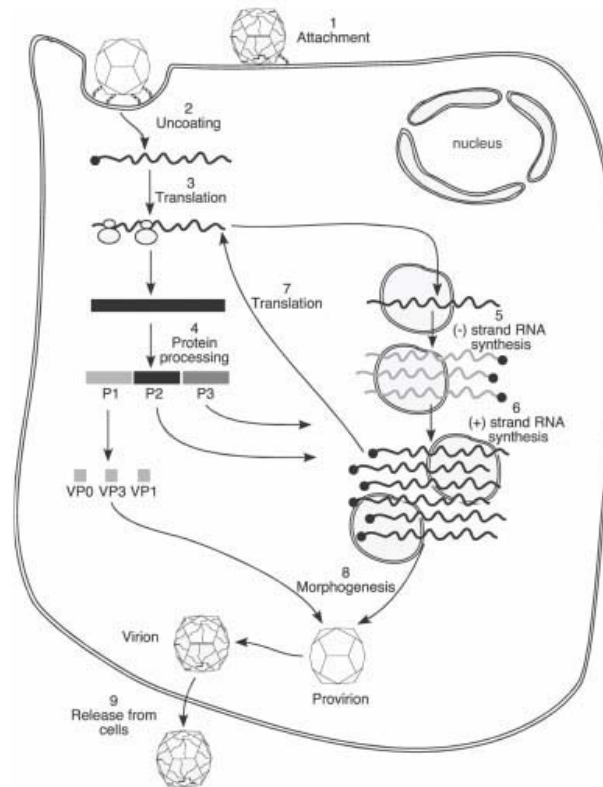
Figure 4: Overview of the picornavirus replication cycle. After binding to the receptor (1) the virus releases its genome and the VPg (virion protein, genome linked) is removed from the viral RNA (2). The RNA is translated (3) into a polyprotein that is co-translationaly cleaved (4) into the the viral proteins. The RNA synthesis is carried out in vesicular membranes where (-) strand RNAs are synthesized by the RNA polymerase (5). The (-) strand RNAs are then used to produce more (+) stand RNAs (6). During early infection the newly synthesized (+) RNA is translated into viral proteins (7) while during late infection it is packed into the viral particles (8), which are finally released upon cell lysis (9) (Fields *et al.*, 2007).

Once the virus enters the cell its RNA needs to be translated as no cellular polymerase can copy it and no viral enzymes are carried within the viral capsid.

Instead of a 5'-terminal cap structure, picornaviruses have an IRES sequence (see section 1.1.3) which allows them to bind to the ribosomes and translate their genome. How the viruses take over the cellular translation machinery will be described in section 1.1.6. In EMCV the central domain of eukaryotic initiation factor (eIF) 4G (see section 1.2.1.1), containing the binding sites for eIF3 (binds directly to the ribosome) and eIF4A (an RNA helicase) remains and stimulates IRES mediated translation (Pestova *et al.*, 2001).

Additionally, FMDV RNA translation is also stimulated by the appearance of proteolytic cleavage products of eIF4G (Ohlmann *et al.*, 1995). An exception is hepatitis A virus (HAV) which requires intact eIF4G (Borman and Kean, 1997).

Upon picornaviral infection, the intracellular membranes of the cell go through rearrangement. The endoplasmatic reticulum (ER) and Golgi apparatus are destroyed and double membrane vesicles fill the cytoplasm (Schlegel *et al.*, 1996). Viral replication occurs on the surface of these membranes. About 50,000 copies of the viral positive-stranded genome are produced in the infected cell, through a negative-stranded intermediate (Fields *et al.*, 2007). The genomic RNA serves as mRNA and as template for synthesis of the negative strand. These processes do not occur simultaneously (Barton *et al.*, 1999).

The synthesis of the negative strand is performed by 3D^{pol}, a RNA dependent RNA polymerase encoded by the virus. Once 3D^{pol} and other essential proteins have been synthesized, the genomic RNA starts to be used as template for the negative-stranded intermediate. The 3D^{pol} together with 3AB, forms two dimensional lattices coating the membranes where the viruses replicate. These structures result in a increase of substrate affinity simply by reducing the collisions between reactants (Lyle *et al.*, 2002).

The shift between translation and replication is controlled by an RNA element at the 5' end of the viral RNA genome, a cloverleaf structure of 64 nucleotides. 3CD (the polymerase precursor) binds to this structure, repressing viral translation and promoting negative stranded RNA synthesis (Gamarnik and Andino, 1998).

After release of the P1 region from the rest of the polyprotein, viral proteinases cleave the VP0-VP3 and VP3-VP1 bonds. Afterwards, one copy of VP0, VP3 and VP1 assemble forming an immature structural unit, the 5S protomer. Five protomers assemble to build a pentamer, which can self-assemble *in vivo* and *in vitro* into empty capsids. There are two models for the insertion of the viral RNA into the capsid. According to the first model, the RNA is inserted into the intact capsid after it is assembled (Jacobson and Baltimore, 1968). The second model states that the pentamers assemble with the RNA to form provirions (Nugent and Kirkegaard, 1995).

The final step of assembly is the cleavage of VP0 into VP2 and VP4 by an unknown proteinase activity. As the scissile bond is not accessible to viral or cellular proteinases, it was suggested that the cleavage can be autocatalytic. The process would involve the Ser10 of VP2 and basic RNA groups that would serve as proton-abstracters as in a serine protease type mechanism (Arnold *et al.*, 1987). However, experiments in which the Ser10 was deleted showed that this residue is not involved in the cleavage mechanism (Harber *et al.*, 1991). Later it was shown that the His195 of VP2 is probably involved in the VP0 cleavage. His195 may activate local bound water molecules that can initiate a nucleophilic attack at VP0

cleavage site (Hindiyeh *et al.*, 1999). This cleavage results in an increase in particle stability and acquisition of infectivity (Lee *et al.*, 1993).

After assembly and maturation, viral particles are released by lysis except for HAV which is released without causing cytopathic effect. The cytopathic effect consists of condensation of chromatin, nuclear blebbing, proliferation of membranous vesicles, changes in membrane permeability, leakage of intracellular components and shrinking of the entire cell (Fields *et al.*, 2007).

1.1.5 Binding to the receptor and cell entry

Picornaviruses use different cell surface molecules as receptors (table 2).

Virus	Receptors
Foot and mouth disesase virus	Heparan sulphate, $\alpha_v\beta_3$, $\alpha_v\beta_8$
Encephalomyocarditis virus	VCAM-1, sialated glycophorin
Polioviruses 1-3	PVR (CD155)
Coxsackieviruses A	ICAM-1, CD55, $\alpha_v\beta_3$, $\alpha_v\beta_6$
Coxsackieviruses B	CAR, CD55 (DAF)
Echoviruses	$A_2\beta_1$-integrin, CD55
Parechovirus 1	$\alpha_v\beta_1$, $\alpha_v\beta_3$
Enteroviruses	CD55, sialic acid
Hepatitis A virus	HAVCR-1
Major group rhinoviruses	ICAM-1, heparan sulphate
Minor group rhinoviruses	LDL receptor family

Table 2: Viruses and their receptors. Adapted from (Fields *et al.*, 2007).

PV, CV and HRV capsids have a five fold axis of symmetry, which is rounded by a deep depression, named the canyon. Many receptors, such as ICAM or CD55, bind to the canyon. Aphthoviruses and cardioviruses do not have these canyons (Fields *et al.*, 2007).

1.1.5.1 Poliovirus

PV uses CD155, an adhesion molecule of the Ig (Immunoglobulin), superfamily. The Ig superfamily receptors have 2 to 5 Ig domains and the viral recognition site lies at the N-terminal domain. This domain penetrates into the picornavirus canyon, causing instability in the capsid, thus facilitating the release of RNA. (Rossmann *et al.*, 2002). Upon receptor binding, conformational changes occur leading to the formation of a pore through which the RNA can enter the cell (Bubeck *et al.*, 2005). Two recent studies suggest that poliovirus enter different cells through different mechanisms (Bergelson, 2008). In the first study, the

results showed that in HeLa and HEK 293 cells, the uncoating occurs within clathrin- and caveolin-independent vesicles in the cell periphery and that it is more than a simple consequence from the interaction with the receptor. It requires energy, an intact cytoskeleton and activity of cellular tyrosine kinases (Brandenburg *et al.*, 2007). The second study showed that in human brain microvascular endothelial cells, viral entry is caveolin and dynamin dependent. The internalization of the caveolar vesicles occurred in response to specific signals from specific ligands. Additionally, the ligation of the virus to the receptor triggered rearrangements of the actin cytoskeleton which were also required for the entry process (Coyne *et al.*, 2007).

1.1.5.2 Coxsackievirus

CVA21 binds DAF (decay accelerating factor) and ICAM-I. CVB bind DAF on the apical surface of the cell, inducing rearrangements that allow the viruses to access to their actual receptor, CAR (coxsackie and adenovirus receptor), that is located in the tight junctions of the cell (Fields *et al.*, 2007).

1.1.5.3 Foot and mouth disease virus

FMDV A12 uses integrin $\alpha_v\beta_3$ for attachment whereas the laboratorial strain FMDV O uses HS (Jackson *et al.*, 1996; Neff *et al.*, 1998). FMDV (and some HRVs) enter the cell by endocytosis and the uncoating process is induced by acidification of the endosome. In these cases, the binding to the receptor does not trigger conformational changes, it just secures the viral particle to the cell so it can enter via endocytic pathway. At pH 6.5, the viral capsid separates itself into pentamers and releases the RNA (van Vlijmen *et al.*, 1998).

1.1.5.4 Human rhinovirus

As mentioned in section 1.1.1, major group human rhinoviruses bind to ICAM-I and minor group human rhinoviruses bind to the LDL receptor family. Although the overall structures of HRV are similar, the binding to their respective receptors is highly specific (Kolatkar *et al.*, 1999). For minor group HRVs, the receptor binding region, situated on the left side of the five fold axis, contains mainly basic residues. Among these residues is a lysine that is conserved in the minor group and seems to play a central role on receptor recognition (Vlasak *et al.*, 2003). The same region of major group HRVs contains mostly uncharged or acidic residues. The nature of the interaction of LDL family receptors was reported to be between acidic residues of the receptor and basic residues of ligands (Yamamoto *et al.*, 1984). Figure 5A shows the surface potential of the HRV2 (minor group) pentamer. The area where the receptor binds was magnified (figure 5B) and compared to

other HRVs of minor and major groups. Blue shows a positive potential and red shows a negative one. A clear difference between groups can be observed (Vlasak *et al.*, 2003).
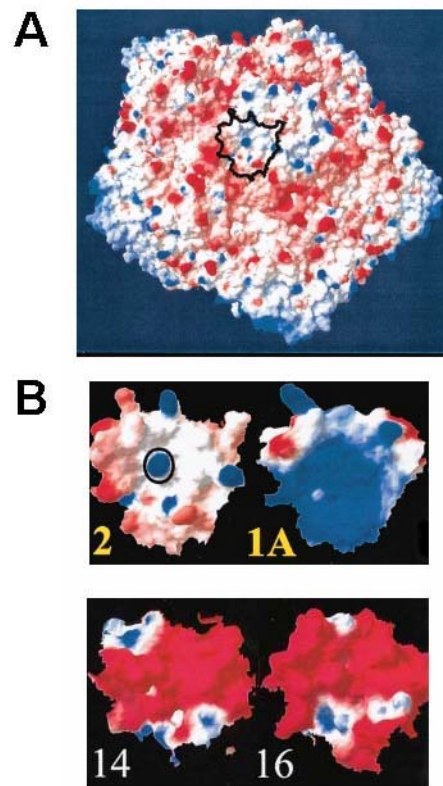
Figure 5: Surface potential of the receptor binding site of several HRVs. A) HRV2 pentamer. **B)** Magnification of the receptor binding sites of HRV2, HRV1A (minor group), HRV14 and HRV16 (major group). Blue areas show positive potential whereas red areas show negative potential. The conserved lysine of minor group viruses is marked by a bold circle in the surface of HRV2. Adapted from Vlasak *et al.*, 2003.

Major group HRVs bind to their receptor ICAM-1 via residues that are located in the canyon (Figure 6) (Kolatkar *et al.,* 1999; Olson *et al.*, 1993). This mode of binding prevents bulky neutralizing antibodies from accessing the receptor binding site (Rossmann *et al.*, 2000). The binding occurs through the distal amino-terminal of ICAM-1. The tip of the most distal domain of ICAM-1 presents a high level of shape and charge complementarity with the wall and floor of the canyon of HRV14 and HRV16 (Kolatkar *et al.,* 1999). This complementarity is not observed in HRV2 (Rossmann *et al.*, 2000).
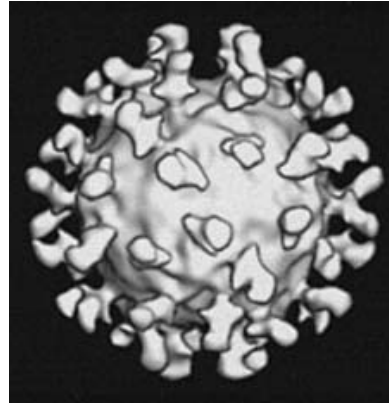
Figure 6: Cryo-EM (cryo electron microscopy) image reconstruction of HRV14 complexed with a soluble fragment of ICAM-1 (Kolatkar *et al.*, 1999).

1.1.6 Polyprotein processing

The polyprotein processing occurs co-translationally via intramolecular cleavages (primary cleavages) and intermolecular cleavages (secondary cleavages). All picornaviruses encode 3C^{pro}, which performs the primary cleavage between 2C and 3A (Fields *et al.*, 2007).

The processing events vary among the different picornaviruses (figure 7). The single picornaviral open reading frame is translated into a long polyprotein which is processed by virally encoded proteinases. The picornaviral polyprotein is divided in three regions: P1, P2 and P3. P1 contains the four capsid proteins VP1 to VP4; P2 and P3 regions contain the non-structural proteins. Cardioviruses and aphthoviruses contain an additional protein, named Leader, preceding the P1 region.

Hepato- and parechoviruses polyprotein processing is the simplest among picornaviruses. These viruses encode only one enzyme with proteolytic activity, 3C^{pro}. 3C^{pro} performs the second primary cleavage between 2A and 2B in the P2 region (Martin *et al.*, 1995) and all the secondary cleavages of the HAV polyprotein, showing an activity profile broader than that of 3C^{pro} of other picornaviruses (Schultheiss *et al.*, 1994). The 2A protein of these viruses has no known function.

In aphthoviruses and cardioviruses, 2A is not active as a proteinase. This protein is released from the polyprotein through a mechanism in which the peptide bond between the last residue of 2A and the first residue of 2B is not formed (Ryan *et al.*, 1999). In this mechanism, the nascent 2A interaction with the exit pore from the ribosome is altered. The orientation of the protein within the peptidyl-transferase center of the ribosome is changed, thus inhibithing the peptide bond formation and releasing the 2A (Ryan *et al.*, 1999). The first encoded protein in aphtho- and cardioviruses is the Leader protein (L). In cardioviruses, the Leader protein has no proteolytic activity and the cleavage at its C-terminus is carried out by 3C^{pro}. However, the leader protein of mengovirus has a role in the antiviral host cell

response, by interfering with the iron homeostasis and inducing NF-κB (Zoll *et al.*, 2002). In contrast to cardioviruses, the aphthoviruses Leader protein is a proteinase (L^{pro}) (Guarne *et al.*, 1998). It cleaves between its own C-terminus and the N-terminus of VP4. The secondary cleavages are performed by 3C^{pro}.

For entero- and rhinoviruses, the primary cleavage that separates the P1 and P2 regions is carried out by 2A^{pro}. The 3C^{pro} performs most of the secondary cleavages. In PV the 3C^{pro} precursor, 3CD^{pro}, cleaves between VP0 and VP3 and between VP3 and VP1 (Jore *et al.*, 1988; Ypma-Wong *et al.*, 1988). Additionally, the 2A^{pro} of PV and some HRV serotypes can cleave the precursor 3CD into the products 3C' and 3D' (Hanecak *et al.*, 1982; McLean *et al.*, 1976). However, the suppression of this cleavage site in PV does not affect viral replication.
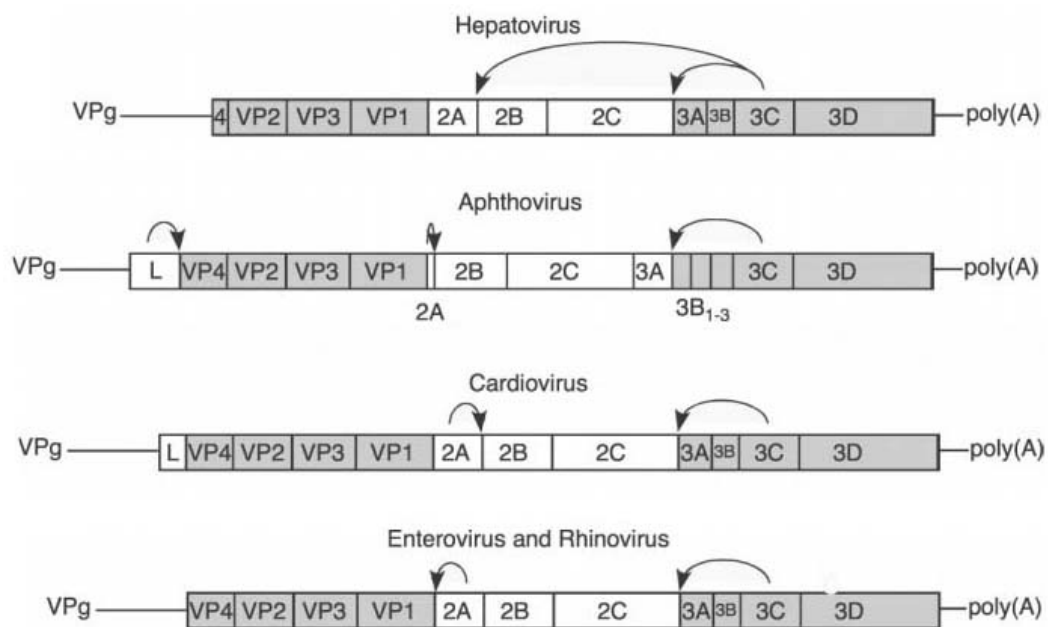
Figure 7: Primary cleavages of picornavirus polyprotein. Hepatoviruses possess the simplest cleavage pattern in wich 3C^{pro} performs all the primary cleavages. In cardioviruses and aphthoviruses 2A releases itself from the 2B protein, although it is not a proteinase. 3C^{pro} separates 2A from the P1 region. FMDV L^{pro} releases itself from the VP4 protein. In enteroviruses and rhinoviruses the 2A^{pro} carries out the cleavage between P1 and P2 regions through autocleavage. Adapted from (Fields *et al.*, 2007).

After a first round of translation, picornaviral proteinases cleave the scaffolding protein eIF4G, whose function is to bring together ribosomes and capped mRNA (figure 8 and section 1.2.1.1). The consequence of eIF4G cleavage is the host cell translation shut-off. The cellular capped mRNA is no longer able to bind to the ribosomes. Therefore the virus

takes over the cell translational machinery, through an IRES sequence present in its genome (section 1.1.3), to synthesize all the proteins necessary for replication and assembly. The cleavage of eIF4G by picornaviral proteinases will be described in detail in sections 1.1.8.1.4 and 1.1.8.3.4.
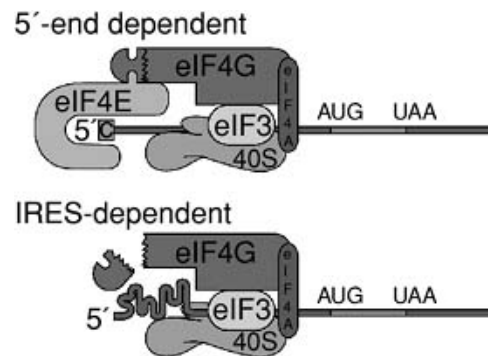
Figure 8: 5' cap-dependent versus IRES-dependent translation initiation. Binding of eIF4E to the 5' cap positions the ribosome on the mRNA. After eIF4G cleavage the 5' capped mRNA can no longer bind the ribosome. However, the IRES can bind the C-terminus of eIF4G which remains from the cleavage and therefore recruit the ribosome.

1.1.7 Picornaviral non-structural proteins

The P1 region contains the structural proteins described in section 1.1.2. P2 and P3 contain the non-structural proteins. This section will not consider those viral proteins with proteinase activity; they will be described in more detail below.

P2 contains the proteins 2A, 2B and 2C. As mentioned above, aphtho- and cardioviruses 2A do not have proteolytic function. However, EMCV 2A seems to be required for efficient translation of EMCV RNA in vivo to neutralize the competition from cellular mRNAs (Svitkin *et al.*, 1998). 2B forms pores on the ER and Golgi membranes. Therefore, it decreases the Ca^{2+} concentration in these organelles and increases the levels of this ion in the cytoplasm. 2B is also involved in the anti-apoptotic response in polioviruses, perhaps due to its ability to disturb the intracellular Ca^{2+} homeostasis (van Kuppeveld *et al.*, 2005). The precursor of 2B, 2BC, is responsible for the accumulation of the Golgi and ER derived vesicles, in the cytosol, where viral replication takes place (Bienz *et al.*, 1994). 2C binds to membranes and RNA. In poliovirus, 2C binds to the 3' end of the negative strand replication intermediate (Goodfellow *et al.*, 2003) and it may have a role in viral encapsidation (Vance *et al.*, 1997).

The P3 region consists of four proteins, 3A to 3D. 3A appears to have a role in altering the ER-Golgi trafficking facilitating the evasion of the host immune system (Choe *et al.*, 2005). 3B is the virion protein genome (VPg) which covalently binds to the 5' end of the

viral RNA (Flanegan *et al.*, 1977). This peptide is cleaved off the RNA upon entry in the cell and is not necessary for translation. However, VPg is found in nascent RNA chains, both positive and negative, (Pettersson *et al.*, 1978) and acts as a primer for RNA synthesis (Paul *et al.*, 1998). Finally, 3D is the RNA dependent RNA polymerase responsible for copying the RNA genome (section 1.1.4) (Crowder and Kirkegaard, 2004; Pata *et al.*, 1995).

1.1.8 Picornaviral Proteinases

1.1.8.1 Leader proteinase (L^{pro})

Two in frame AUG codons that are situated 84 residues apart in the viral polyprotein originate two forms of the Leader proteinase (L^{pro}). When the protein synthesis starts at the first AUG codon Lab^{pro} is produced; when the synthesis starts at the second AUG codon Lb^{pro} is formed (Clarke *et al.*, 1985; Sangar *et al.*, 1987). Both proteins are active and able to perform cleavage from the polyprotein in *cis* and in *trans* (Cao *et al.*, 1995; Medina *et al.*, 1993).

1.1.8.1.1 Properties

L^{pro} is inhibited by general sulphydryl-specific reagents and E-64 (a general inhibitor of cysteine proteinases), implying that this proteinase activity follows a papain like mechanism (Burroughs *et al.*, 1984; Kleina and Grubman, 1992).

1.1.8.1.2 Structure

The structure of Lb^{pro} was solved by X-ray crystallography (Guarne *et al.*, 1998). The proteinase has a papain-like folding with two domains: a α-helical domain (also called left domain) and a β-sheet domain (right domain). In contrast to papain, Lb^{pro} has no prominent surface loops and contains a C-terminal extension (CTE). The CTE structure is very flexible. The active site is formed by the catalytic dyad Cys51 and the His148, at the interface between the two domains (figure 9). Asp163 keeps the active His148 in the correct orientation in respect to the Cys51.
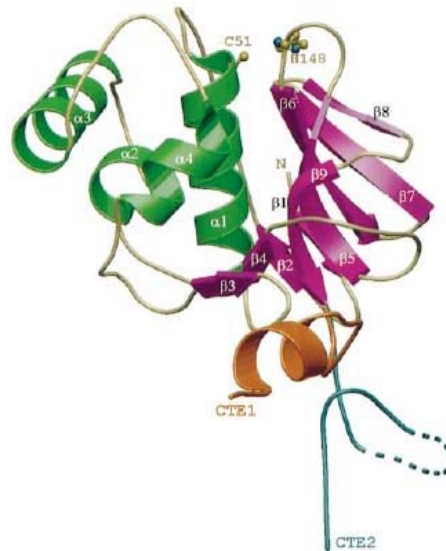
Figure 9: The structure of FMDV Lb^{pro}. α-helices and β-strands are coloured green and magenta, respectively. The CTE is presented in two possible conformations: ordered (orange) and disordered (blue). Two active site residues are shown as ball and stick models (Guarne *et al.*, 1998).

<u>1.1.8.1.3 Specificity</u>

The cleavage sites of L^{pro} are presented in table 3. The structure showed that the most important interactions in the L^{pro} substrate-binding groove are with the residue at the P2 position (Guarne *et al.*, 1998) (the nomenclature P*n*-P1-P1'-P*n*' is that of (Schechter and Berger, 1967)). The protein developed a pocket to anchor a hydrophobic residue at this P2 position. This pocket accepts valine or leucine; however, it does not accept a phenylalanine (table 3).

In contrast, the residues at P3, P1 and P1' are more variable. This might be because P1 and P3 residues point away from the enzyme. At the P1 site, a positively charged residue is well accepted as the Glu96 and Glu147 help to stabilize the positive charge and the side chains provide a hydrophobic environment for the lysine side chain (Guarne *et al.*, 1998). It is not clear why L^{pro} accepts glycine at P1 position in the eIF4G isoforms. Interestingly, the P1' residue is the most variable among the substrates. (Guarne *et al.*, 1998). Although there is no structural information about the interaction of the substrate with the enzyme, comparisons with the papain structure can provide some information on the P1' residue. These analysis show that the Asp164 could accommodate a positively charged residue at the P1' site, as it happens for the cellular substrate, eIF4GI (Skern *et al.*, 2002).

Substrate	Cleavage sites		
	P	*	P'
	54321		1234
Lb^{pro}/VP4	QRKLK	*	GAGQ
eIF4GI	FANLG	*	RTTL
eIF4GII	LLNVG	*	SRRS
eIF4GII not cleaved	FADFG	*	RQTP

Table 3: Lb^{pro} cleavage sites on known substrates. eIF4GII is not cleaved at the analogous sequence to that recognized in eIF4GI (last lane).

1.1.8.1.4 Interaction with cellular proteins

L^{pro} has developed a high level of specificity. Therefore, the only substrates known in the cell are the two isoforms of eIF4G, whose cleavage leads to the host cell translation shut off. As shown in table 3, L^{pro} does not cleave eIF4GII at the analogous site of eIF4GI; instead the cleavage occurs at LNVG*SRRS (Gradi *et al.*, 2004).

1.1.8.2 3C proteinase (3C^{pro})

3C^{pro} was the first viral protein shown to have proteolytic activity through work done in EMCV (Gorbalenya *et al.*, 1979; Palmenberg *et al.*, 1979; Svitkin *et al.*, 1979) and PV (Hanecak *et al.*, 1982; Hanecak *et al.*, 1984).

1.1.8.2.1 Properties

3C^{pro} are inhibited by N-ethylmaleimide, iodocetamide and Hg^{2+} ions (Pelham, 1978), but not by E-64 (Orr *et al.*, 1989). The mechanism of PV 3C^{pro} seems to be similar to the one of serine proteases; however, this mechanism does not involve a thiolate-imidazolium ion pair (Sarkany *et al.*, 2001).

1.1.8.2.2 Structure

3C^{pro} is a single chain protein with homology to chymotrypsin-like serine proteases. The X-ray structure of 3C from HAV (Allaire *et al.*, 1994; Bergmann *et al.*, 1997), HRV14 (Matthews *et al.*, 1994), HRV2 (Matthews *et al.*, 1999) and PV (Mosimann *et al.*, 1997) are available. All these structures contain two topologically equivalent six-stranded β-barrels. A long, shallow groove for substrate binding is situated between the two domains. The catalytic triad is constituted by His40, Cys146 and Glu71 in HRV14, and His44, Cys172 and Asp84 in HAV (Gorbalenya *et al.*, 1989; Kean *et al.*, 1991). Figure 10 shows the structure of PV 3C^{pro}.

A RNA binding site, constituted by basic residues is situated on the opposite side of the active site. Two phenylalanine residues seem to play a role in RNA binding (Matthews *et al.*, 1994). The precursor of 3C^{pro}, 3CD interacts with the viral RNA and plays a role in translational control (Gamarnik and Andino, 1998; Gamarnik and Andino, 2000; Marcotte *et al.*, 2007).
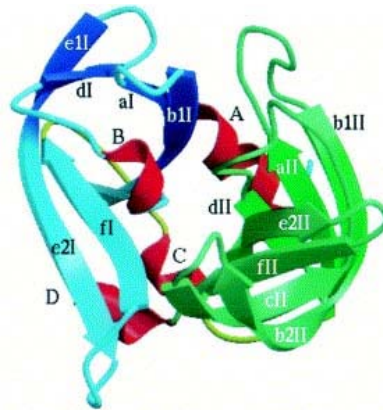
Figure 10: The structure of PV 3C^{pro}. The β-barrels are indicated in blue (domain I) and in green (domain II). The individual four-stranded β-sheets are shown in dark-blue, cyan, and green (Mosimann *et al.*, 1997).

1.1.8.2.3 Specificity

3C^{pro} usually cleaves between Gln*Gly. However, the cleavage sites vary among different genera. PV 3C^{pro} cleaves only between Gln*Gly whereas EMCV 3C^{pro} accepts Glu*Ser or Glu*Ala and FMDV 3C^{pro} recognizes Gln*Leu and Gln*Ile as well. Nevertheless, these sequences are not sufficient for cleavage; the flanking residues are also important for specificity (Ypma-Wong *et al.*, 1988). The residues at P4 and P2 sites are conserved in both HRVs and enteroviruses (an aliphatic residue at P4 and proline at P2). Cardioviruses process substrates that contain proline at P2 and P2' sites. In rhino- and enteroviruses sites P4, P1, P1' and P2' are sensitive to substitutions. HRV14 and PV have a preference for alanine at P4, glutamine at P1, glycine at P1' and proline at P2' (Cordingley *et al.*, 1990; Long *et al.*, 1989). EMCV accepts serine, cysteine, glycine and alanine at P1' but not threonine, isoleucine or tyrosine (Parks *et al.*, 1989).

1.1.8.2.4 Interaction with cellular proteins

PV 3C^{pro} cleaves the transcription factors TFIIIC (Clark *et al.*, 1991), TFIID (Clark *et al.*, 1993) Oct1 and CREB (Yalamanchili *et al.*, 1997b; Yalamanchili *et al.*, 1997c), and the microtubule-associated protein 4 (Joachims *et al.*, 1995). FMDV 3C^{pro} cleaves histone protein

3 (Tesar and Marquardt, 1990) and the initiation factors eIF4A and eIF4GI (Belsham *et al.*, 2000). However eIF4GI cleavage happens later than the cleavage by L^{pro}.

All these cleavages affect host-cell transcription and translation.

1.1.8.3 Entero- and rhinoviruses 2A proteinase (2A^{pro})

In enteroviruses and rhinoviruses, 2A^{pro} is responsible for the initial cleavage of the polyprotein, separating the structural proteins from the non structural ones. It cleaves between its own N-terminus and the C-terminus of VP1. 2A^{pro} also cleave several cellular proteins.

1.1.8.3.1 Properties

2A^{pro} are inhibited by iodocetamide, *N*-ethylmaleinimide and Hg^{2+} ions, but not E-64. Chymostatin and elastatinal (serine proteinases inhibitors) are also efficient against 2A^{pro}. However, leupeptin, another inhibitor of serine and cysteine proteinases, has no effect (Sommergruber *et al.*, 1992). Recently, it was found that a methylated form of the caspase inhibitor benzylloxycarbonyl-Val-Ala-Asp(OMe).fluoromethyl ketone (zVAD.fmk) inhibits 2A^{pro} (Deszcz *et al.*, 2004). Based on structural analysis of zVAD.fmk and HRV2 2A^{pro}, a new inhibitor derived from zVAD.fmk was synthesized. The new compound was named benzylloxycarbonyl-Val-Ala-Met.fluoromethyl ketone (zVAM.fmk). It inhibits specifically 2A^{pro} but not caspases. Therefore, zVAM.fmk is a specific tool to study the roles of 2A^{pro} during viral replication, as the proteinase can be inactivated at specific points of the infectious cycle (Deszcz *et al.*, 2006).

2A^{pro} are also potential drug targets. Crowder and Kirkegaard (2005) showed that PV bearing 2A^{pro} without enzymatic activity can function as dominant negative inhibitors of wild-type growth. In experiments in which cells are co-infected with wild type PV and PV bearing mutations in the 2A^{pro} sequence which make the proteinase inactive, the mutants suppress the growth of the wild type viruses (Crowder and Kirkegaard, 2005). There is evidence that the cleavage between VP1 and 2A^{pro} is exclusively intramolecular (Toyoda *et al.*, 1986). Therefore, the uncleaved VP1-2A can accumulate and co-assemble with wild type VP0 and VP3 forming non-functional capsids, preventing the growth of wild type viruses (Crowder and Kirkegaard, 2005).

1.1.8.3.2 Structure

2A^{pro} are cysteine proteinases with a chymotrypsin-like fold. The X-ray structure of HRV2 2A^{pro} has been solved (Petersen *et al.*, 1999). The NMR structure of CVB4 2A^{pro} is also available (Baxter *et al.*, 2006). 2A^{pro} is composed of an N- and a C-terminal domain, connected by an interdomain loop. This proteinase shows unique characteristics, compared

to other chymotrypsin-like proteinases, the N-terminal domain is not a β-barrel, but a four stranded anti-parallel β-sheet (figure 11). The C-terminal domain is made of a β-barrel and contains a zinc ion that is tightly coordinated by Cys52, Cys54, Cys112 and His114. The zinc ion is essential for the maintenance of the structure and is thought to compensate the reduced size of the N-terminal domain. The zinc ion connects the interbarrel loop with the C-terminal domain, therefore contributing to the stability of the protein (Petersen *et al.*, 1999).

The active site of HRV2 2A^{pro} is composed of a catalytic triad, His18, Asp35 and Cys106 and is topologically similar to the chymotrypsin-like serine proteinases. The histidine shows an unusual flexibility which is stabilized by the aspartate (Petersen *et al.*, 1999). During the interaction with the substrate, chymotrypsin-like proteases develop a negative charge, which is stabilized by a structure named oxyanion hole. The stabilization is achieved by a network of hydrogen bridges, by anchoring the residues 102-108 to a hairpin loop formed by residues 62-65 (Petersen *et al.*, 1999).
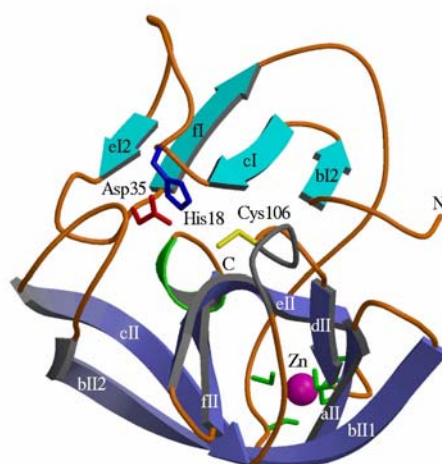
Figure 11: The structure of HRV2 2A^{pro}. Ribbon diagram of the overall structure of HRV2 2A^{pro}.The residues composing the catalytic triad (His18, Asp35 and Cys106), the zinc ion (purple sphere) and the zinc binding site are shown (Petersen *et al.*, 1999).

1.1.8.3.3 Specificity

The minimum length of a substrate for HRV2 2A^{pro} is 9 amino acids, P8 to P1' (Sommergruber *et al.*, 1992). The residues at positions P2 and P1' are of great importance for substrate recognition. P2 residue is able to form hydrogen bonds with Ser83 (in HRV2 2A^{pro} or the equivalent residue in other 2A^{pro}) and seems to provide favourable binding energy. HRV2 2A^{pro} accepts threonine, asparagine and serine at P2. At P1' position, it only processes glycine as Leu19 blocks the access of bulkier residues. The P1 position is more flexible, accepting a variety of amino acids (methionine, leucine, tyrosine, phenylalanine,

threonine and arginine) (Skern *et al.*, 1991; Sommergruber *et al.*, 1992). Moreover, HRV2 2A[pro] processes substrates with tyrosine and methionine at P1 site more efficiently than the wild type alanine (Sommergruber *et al.*, 1992). The structure shows that the substrate binding site, S1, is narrow and deep and is mainly filled with the side chain of Cys101. This characteristics make it possible to accommodate long and flexible side chains, like methionine (Petersen *et al.*, 1999). Additionally, the presence of Glu102 located at the bottom of the pocket provides a negative charge that can support the presence of lysine or arginine at the P1 site.

1.1.8.3.4 Interaction with cellular proteins

The best characterized cleavage of cellular proteins by 2A[pro] is the one of eIF4G, a cellular protein involved in the initiation of protein synthesis. The cleavage of both eIF4GI and II leads to the inhibition of host cell protein synthesis (Gradi *et al.*, 1998b; Svitkin *et al.*, 1999). HRV and CV 2A[pro] were shown to cleave eIF4G directly (Lamphear *et al.*, 1993; Liebig *et al.*, 2002). There is evidence that PV1 2A[pro] also cleaves eIF4G directly (Ventoso *et al.*, 1998). However, there is also evidence that the cleavage of eIF4G by PV1 2A[pro] can occur indirectly, via activation of a not yet identified cellular proteinase. Furthermore, it was shown that PV1 2A[pro] could be modified by caspases (Bovee *et al.*, 1998; Wyckoff *et al.*, 1992; Zamora *et al.*, 2002).

PV and HRV 2A[pro] cleave both isoforms of eIF4GI and II *in vivo* (Gradi *et al.*, 1998a; Gradi *et al.*, 2003). HRV2 2A[pro] recognizes the sequence TLSTR*GPPR on eIF4GI and PLLNV*GSRR in eIF4GII (Gradi *et al.*, 2003). HRV2 2A[pro] binds eIF4GI in a distinct region from the cleavage site (Foeger *et al.*, 2002). Furthermore, the residues 669 to 674 have an important role in the binding process (Foeger *et al.*, 2002). The binding site is probably used to dock the proteinase at some distance from the cleavage site. This shows that the cleavage of eIF4G by 2A[pro] is a multi-step reaction in which the proteinase binds the substrate and afterwards cleaves it (Foeger *et al.*, 2002).

PV and CVB3 2A[pro] cleave the polyA binding protein (PABP) which is involved in several aspects of mRNA metabolism and participates directly in translation initiation (Joachims *et al.*, 1999; Svitkin *et al.*, 2001). The cleavage of PABP seems to correlate better with the host translation shut-off than the cleavage of eIF4G isoforms (Kerekatte *et al.*, 1999).

HRV14 2A[pro] cleaves cytokeratin 8, a member of the intermediate filament family that form the cytoskeleton together with actin filaments (Seipelt *et al.*, 2000). CVB3 2A[pro] cleaves dystrophin in myocytes leading to cardiomyopathy (Badorff *et al.*, 1999). PV 2A[pro] cleaves the TATA-box binding protein (TBP) (Yalamanchili *et al.*, 1997a), reducing transcriptional activity

of the cell. PV 2A^{pro} also cleaves two nuclear pore complex (NPC) proteins, Nup153 and Nup62 (Park *et al.*, 2008).

Picornaviral 2A^{pro} are also involved in apoptosis. CVB3 2A^{pro} is able to induce apoptosis through caspase 8 mediated activation of caspase 3 (Chau *et al.*, 2007). The 2A^{pro} of PV1 and several HRV serotypes induce apoptosis through activation of caspase 3 (Calandria *et al.*, 2004; Deszcz *et al.*, 2005; Deszcz *et al.*, 2004; Goldstaub *et al.*, 2000).

1.2 Translation initiation

1.2.1 Cap-dependent translation

In eukaryotes, more than 10 initiation factors (eIF) are involved in the initiation of protein synthesis. The initiation of translation starts with the formation of the 43S complex by association of the initiator Met-tRNA with the GTPase initiation factor eIF2a (bound to a guanosine triphosphate (GTP)), the 40S ribosomal subunit and several initiation factors (eIF1, eIF3, eIF5 and eIF1A) (Hershey and Merrick, 2000; Lopez-Lastra *et al.*, 2005) (figure 12).
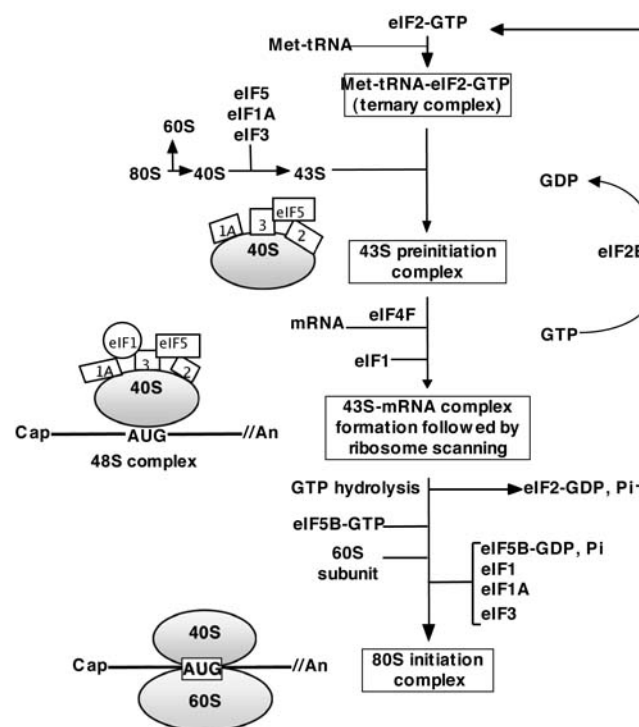
Figure 12: Diagram of translation initiation in eukaryotes (Lopez-Lastra *et al.*, 2005).

The capped mRNA is recognized by the complex eIF4F which consists of the cap binding protein eIF4E, the scaffolding protein eIF4G and the RNA helicase eIF4A (Hershey and Merrick, 2000). This complex binds the 43S pre-initiation complex through interaction of eIF4G with eIF3 (Hentze, 1997; Pain, 1996) and begins to unwind and scan the mRNA for

the correct AUG codon. This activity is dependent on ATP hydrolysis. Once the initiation codon is found, eIF2a hydrolyzes the bound GTP and the pre-initiation factors dissociate from the small subunit (Pollard *et al.*, 2002). Finally, the large ribosomal subunit binds the small subunit and protein synthesis starts.

Of the factors mentioned above, two are relevant for this work, eIF4G and eIF4E.

1.2.1.1 eIF4G

The scaffolding protein eIF4G is a protein of 220 kDa, formerly named p220 and eIF-4γ brings together components of the protein synthesis initiation mechanism (Gradi *et al.*, 1998a; LeFebvre *et al.*, 2006). Two homologues sharing 46% identity have been identified in mammals (Gradi *et al.*, 1998a). Disruption of both isoforms of eIF4G in yeast is lethal (Goyer *et al.*, 1993).

Human eIF4G can be divided in three domains. The N-terminal domain contains the binding sites for PABP and eIF4E (Imataka *et al.*, 1998; Mader *et al.*, 1995). eIF3, eIF4A and RNA bind to the central domain (Imataka and Sonenberg, 1997; Pestova *et al.*, 1996b). The C-terminal domain contains a second binding site for eIF4A (Imataka and Sonenberg, 1997) and a binding site for the protein kinase MnkI (Pyronnet *et al.*, 1999). These sites are shown on figure 13. eIF4G is also specifically cleaved by the picornaviral proteinases Lb[pro] and 2A[pro].
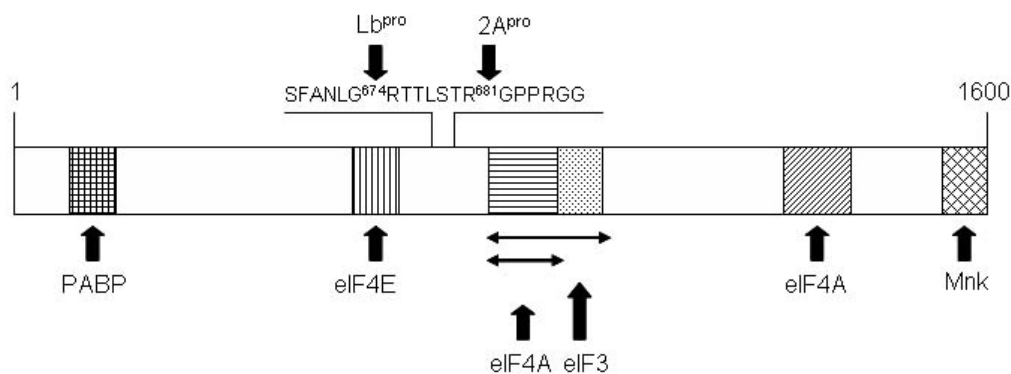
Figure 13: Schematic drawing of eIF4GI. Binding sites for PABP, eIF4E, eIF4A, eIF3 and Mnk as well as cleavage sites of the picornaviral 2A[pro] and Lb[pro] are shown. Adapted from Jackson, 2002 and R. Cencic, PhD thesis 2005.

The N-terminal domain is essential for cap-dependent translation as it contains the eIF4E binding site. The central domain is important for cap-independent translation (Pestova *et al.*, 1996b) and the C-terminal domain has a regulatory function, not being essential for the activity of eIF4G (Morino *et al.*, 2000).

The interaction of eIF4G with PABP and eIF4E simultaneously brings together the 3' and 5' ends of the mRNA forming a pseudo-circular structure which regulates and stimulates translation initiation (Wells *et al.*, 1998) (figure 14).
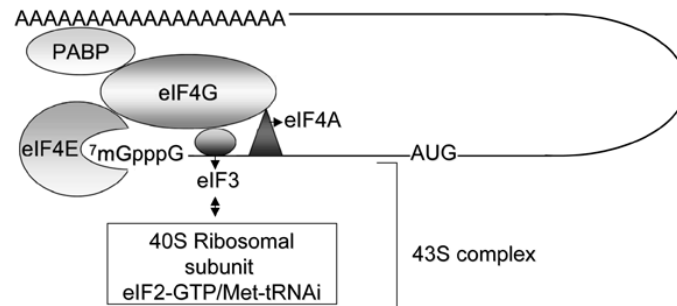
Figure 14: Schematic representation of the initiation translation complex. eIF4G binds PABP and eIF4E bringing together the 3' and 5' ends of the mRNA forming a pseudo-circular structure which regulates and stimulates translation initiation (Lopez-Lastra *et al.*, 2005).

1.2.1.2 eIF4E

eIF4E, also known as the cap binding protein (CBP), recognizes and binds the capped mRNA directly (Haghighat and Sonenberg, 1997). eIF4E is involved in the selection of mRNAs; it therefore plays a role in the regulation of translation (Hershey and Merrick, 2000).

The interaction between eIF4E and the mRNA seems to be regulated by phosphorylation. However, it is not necessary for its function as unphosphrylated eIF4E stimulates translation *in vitro* (Svitkin *et al.*, 1996). In fact, phosphorylation diminishes the ability of eIF4E to bind capped mRNA (Scheper *et al.*, 2002). eIF4E phosphorylation is modulated in response to environmental stress such as heat shock (Duncan *et al.*, 1987) or viral infection (Feigenblum and Schneider, 1993; Kleijn *et al.*, 1996).

Upon eIF4E binding, eIF4G residues 393 to 490 fold into a closed ring-shaped structure of five helical segments (Gross *et al.*, 2003). These interactions are required for optimal growth and maintenance of polysome structure *in vivo*, in yeast (Gross *et al.*, 2003).

1.2.2 Cap-independent translation

Upon picornaviral infection, the cap-dependent translation is inhibited due to the cleavage of eIF4G by picornaviral proteinases. The viral translation is then mediated by the IRES structure present in the viral genome. The IRES structures can recruit the ribosome to an initiator AUG codon (Belsham and Jackson, 2000).

The IRES mediated translation requires almost the complete set of initiation factors except for eIF4E (Pestova *et al.*, 1996a; Pestova *et al.*, 1996b). The complex of eIF4A and

the central domain of eIF4G, missing the eIF4E binding site, can replace the cap-binding protein complex eIF4F during the formation of the 48S pre-initiation complex (Lopez-Lastra *et al.*, 2005) (figure 12). However, the eIFs are not always necessary for cap-independent translation. The hepatitis C virus IRES binds directly the 40S complex without requiring any initiation factor (Ji *et al.*, 2004; Kolupaeva *et al.*, 2000). Thus, the difference of cap-independent from cap-dependent translation relies on how the cleaved eIF4G is anchored to the RNA (Ehrenfeld and Teterina, 2002). The central domain of eIF4G binds directly to the IRES sequence, upstream of the initiation site (Kolupaeva *et al.*, 1998; Pestova *et al.*, 1996b). Additionally, it was shown that the central region of eIF4G is sufficient to deliver a functional ribosomal subunit to mRNA (De Gregorio *et al.*, 1999).

Cap-independent translation seems to occur also on cellular proteins under certain conditions as heat shock or mitosis, in which cellular IRES appear to be involved (Cornelis *et al.*, 2000). However, it is not generally accepted that IRES are involved in cellular translation. Some regions earlier identified as IRES turned out to be cryptic promoters or splicing sites (Kozak, 2005; Kozak, 2007). This subject is still controversial (Kozak, 2001; Schneider *et al.*, 2001)

2 Aim of the work

The aim of the work was to investigate and characterize the 2A^{pro} of HRV2 and HRV14. Although they carry out the same reactions, these two proteins have different properties and characteristics.

HRV2 and HRV14 2A^{pro} cleave their respective polyproteins at similar rates, in contrast, HRV14 2A^{pro} cleaves eIF4GI and II slower than HRV2 2A^{pro}, both *in vitro* and *in vivo* (Gradi *et al.*, 1998b; Svitkin *et al.*, 1999).

What is the structural basis for the observed differences? Based on the structure of HRV2 2A^{pro}, we wanted to perform site directed mutagenesis experiments in order to identify residues that are involved in the difference of specificity presented by these proteinases. However, the low level of identity between HRV2 2A^{pro} and HRV14 2A^{pro} (40%) limits the information which can be sained from the HRV2 2A^{pro}. Therefore, we set out to purify and crystallize HRV14 2A^{pro}. We believe that the determination of this structure would shed light on the specificities and mechanisms of the two 2A^{pro}.

How do the picornaviral proteinases interact with eIF4G? We wanted to obtain information on the nature of the interactions of these proteinases with eIF4G. For that, we planned to purify a fragment of eIF4GII containing the cleavage sites of HRV2 2A^{pro} and the Lb^{pro} of FMDV as well as the binding sites for the Lb^{pro} and eIF4E. We wanted to crystallize and perform NMR experiments with this fragment in order to gain information on its interaction with Lb^{pro} and eIF4E. eIF4E is believed to induce changes in the eIF4G structure which are better recognized by the viral proteinases (Gross *et al.*, 2003; Haghighat *et al.*, 1996; Hershey *et al.*, 1999).

Does 2A^{pro} interact with others cellular proteins? We planned to use the tandem affinity purification (TAP) method developed by Rigaut *et al.*, (1999) to identify new cellular partners for 2A^{pro}

3 Materials and methods

3.1 Tissue culture

3.1.1 Cell lines

Spodoptera frugiperda Sf9 insect cells and HeLa cells Ohio were obtained from European Collection of Cell Cultures (ECACC). HEK 293T cells (CRL-11268) were obtained from the American Type Culture Collection (ATCC).

3.1.2 Media and solutions

Dulbecco's Modified Eagle Medium, Gibco BRL (DMEM) was suplemented with 10% (v/v) Foetal Calf Serum (FCS) (Gibco BRL), 1% (v/v) 100x Penicillin/Streptomycin (Gibco BRL) and 1% (v/v) 200 mM L-Glutamine (Gibco BRL). This medium was used for monolayer culture of HeLa and HEK 293T cells.

Minimum Essential Medium Eagle Joklik Modification (S-MEM) from Sigma was supplemented with 7% Horse serum (Gibco), 1% (v/v) 100x Penicillin/Streptomycin (Gibco BRL), 1% (v/v) 200 mM L-Glutamine (Gibco BRL), 1% (v/v) non essential aminoacids (Bio Whitaker™) and 1% (v/v) Pluronic F-68 (Sigma, 10% w/v). Suspension cultures of HeLa cells were grown in this medium.

SF 900 II SFM (Gibco BRL) medium, used for monolayer and suspension cultures of Sf9 cells, was supplemented with 2% FCS (Gibco), 1% (v/v) 100x Penicillin/Streptomycin (Gibco BRL) and 1% (v/v) 200 mM L-Glutamine (Gibco BRL).

Reduced Serum Medium modified of MEM (Eagle's) (OPTI-MEM Gibco BRL) was used for transfection of HEK 293T cells.

For transfection of Sf9 cells we used Grace's Insect Cell Culture Medium Modified (Gibco BRL).

The buffer used to wash the cells was Phosphate Buffered Saline (PBS). The 10 x stock contains 14 mM KH_2PO_4, 27 mM KCl, 43 mM Na_2HPO_4 and 1370 mM NaCl dissolved in H_2O.

The antibiotic solutions were prepared in 1x PBS and contained 60 mg/L Penicillin G potassium salt, 100 mg/L of Streptomycine sulphate and 58 mg/L of glutamine.

The cells were detached from the culture flasks using a solution od 0.5% trypsin and 0.53 mM EDTA (TE) (Gibco BRL).

3.1.3 Cell culture

3.1.3.1 HeLa and HEK 293T cells

Cells were cultured either in Petri-dishes or flasks (Nunc, Corning) with DMEM medium supplemented with FCS, antibiotics and glutamine (see 3.1.2) at 37°C in presence of 5% CO_2. Before reaching complete confluence, the cells were washed with 1x PBS and incubated with just enough TE (see 3.1.2) to cover the cells at 37°C for no more than 5 minutes. Once detached from the surface, the cells were taken up in fresh medium and transferred to a new flask at a suitable dilution.

For preparation of HeLa S10 extracts (see 3.5.2.2) HeLa cells were also grown in suspension. A suspension culture was set up from 5 confluent 175 cm^2 flasks that were split and transferred into a glass spinner flask containing one litre of S-MEM medium (see 3.1.2). The cultures were kept at 37°C with 5% CO_2 and the cell density was mantained between $2x10^5$ and $8x10^5$ cells/ml.

3.1.3.2 Sf9 insect cells

Cells were cultured in flasks (Nunc, Corning) or in glass conical flasks for the liquid cultures with SF 900 II SFM medium supplemented with FCS, antibiotics and glutamine (see 3.1.2) at 27°C in a humidified chamber. Before reaching complete confluence or a density superior to $2x10^6$ cells/ml, the cells were split. For the monolayer culture, the cells were washed with 1x PBS and fresh medium was added. The cells were detached from the flask by scraping with a glass Pasteur pipette and transferred to a new flask at a suitable dilution. The liquid cultures were simply diluted in fresh medium at a suitable dilution and kept with rotation at 120 rpm.

3.1.4 Cell counting

After the cells were trypsinised and detached from the flask surface, they were taken up in a known volume of fresh medium. 10 µl of the cell suspension were loaded onto a haemocytometer (Neubauer improved counting chamber) and cells were counted under a light microscope.

3.1.5 Freezing and thawing of cells

HEK 293T cells growing logarithmically were washed twice with 1x PBS, trypsinized, taken up in fresh medium and centrifuged at 1000 rpm for 5 minutes at 4°C. The supernatant was disposed off and the cells were washed with 1x PBS and spun down at 1000 rpm for 5 minutes at 4°C. The cells were finally resuspended in 90% FCS and 10% DMSO, transferred into cryo tubes (Nunc) and stored at -80°C in a freezing container (Nalgene) for two days

before transfer to liquid nitrogen for long term storage. The same procedure was used for Sf9 cells except that they were grown in suspension and were stored in Sf-900 II SFM medium containing 7.5% DMSO. The cell density of the stocks was 2×10^6 cells/ml.

The recovery from the liquid nitrogen was done by quickly warming the cells to 37°C in a water bath for 2 to 3 minutes and transferring them to 10 ml of fresh medium. A centrifugation at 1200 rpm for 4 minutes at room temperature followed and the pellet was resuspended in fresh medium and added to a new flask. Sf9 cells were kept in monolayer culture during the adaptation from 20% FCS to 2% FCS supplemented medium and then were transferred to suspension cultures.

3.2 Bacterial culture

3.2.1 Bacterial strains

The bacterial strain used for modification and amplification of plasmids was *E. coli* Top10F´ (F-mcrAΔ(mrr-hsdRMS-mrcBC) Φ80*lac*ZΔm15Δ*lac*X74*rec*A1deoR*ara*D139(*ara-leu*)7697 *gal*U *gal*K rpsL (Str^R) endA1 nupG) (Invitrogen). For expression of recombinant proteins we used the strains *E. coli* BL21 (DE3) LysS (*hsd*D *gal* (λc*I*ts857 *ind*1 Sam7 *nin*5 *lac*UV5-T7*gene*1) (Novagen) and *E.coli* JM101 (*Sup*E *thi* Δ(*lac*-proAB) F' [*tra*D36 *pro*AB$^+$ *lac*I^q *lac*ZΔM15) (Pharmacia). The strain *E. coli* DH10Bac™ (F$^-$ *mcr*A Δ(*mrr-hsd*RMS-*mcr*BC) Φ80*lac*ZΔM15 Δ*lac*X74 *rec*A1 *end*A1 *ara*D139 Δ(*ara, leu*)7697 *gal*U *gal*K λ-*rps*L *nup*G / bMON14272 / pMON7124) (Invitrogen) was used to introduce genes into a baculovirus shuttle vector (bacmid).

3.2.2 Media and antibiotics

Luria-Bertani (LB) medium (Roth) contains 10 g/l of tryptone, 5 g/l of yeast extract and 10 g/l of NaCl. The pH is adjusted 7.0 and the medium is autoclaved before use.

Another medium used for bacterial growth was the Terrific Broth (TB) medium which is prepared with 12 g/l bacto-tryptone, 24 g/l yeast extract and 4 ml/l glycerol. After autocleavage a solution of 100 ml/l of 0.17 M KH_2PO_4/ 0.72 M K_2HPO_4 is added.

To express recombinant proteins labelled with ^{15}N, the bacteria are grown in minimal medium. To obtain this medium we prepare a solution of 33.7 mM $Na_2HPO_4.2H_2O$, 22 mM KH_2PO_4, 8.5 mM NaCl and 18.7 mM $^{15}NH_4Cl$. This solution is autoclaved and added to a filtered sterilized solution of 2 mM $MgSO_4$, 1% trace elements, 0.4% glucose, 0.3 mM $CaCl_2$, 1 µg/ml biotine, 1 µg/ml thiamine and suitable antibiotics.

The solid bacteria medium is obtained by addition of 1.5% Bacto-agar (Roth) to liquid media before autoclaving. When the medium temperature reaches 50°C, antibiotics are added to the final concentrations and poured into Petri dishes.

The antibiotics used in this work were Ampicillin sodium salt (Sigma) dissolved in H_2O (100mg/ml) and Chloramphenicol (Calbiochem) dissolved in absolute ethanol (34 mg/ml). The working dilutions of these antibiotics were 100 µg/ml.

3.2.3 Plasmids

Table 4 shows the plasmids used throughout this work.

Plasmid	Function
pCITE-1 (Novagen)	*In vitro* transcription
pCITE-A1 (pCITE-1 modified by Andreas Roetzer (Roetzer, 2004))	*In vitro* transcription
pET3b (Novagen)	Protein expression in bacteria
pET 11d (Novagen)	Protein expression in bacteria
pGEX-6P-1 (Amersham Pharmacia Biosciences)	Protein expression in bacteria
pBluescript I KS (Stratagene)	Blunt end cloning
pMZI (J. K. Greenblatt)	Protein expression in mammalian cells
pVgRXR (Invitrogen)	Transfection of mammalian cells
pFastBac (Invitrogen)	Transformation of the bacterial strain *E. coli* DH10Bac™
pproExHTA (Invitrogen)	Protein expression in bacteria

Table 4: List of the plasmids used in this work. The origin of each plasmid is shown in brackets.

3.2.4 Preparation of competent cells

A 3 ml overnight culture was diluted into 200 ml LB medium and incubated at 37°C with rotation at 180 rpm. When the cell density reached an OD_{600} of 0.6, the bacteria were collected into 50 ml sterile falcon tubes and centrifuged for 10 minutes at 4300 rpm at 4°C (*Heraeus* Megafuge 1.0R). The pellet was resuspended in 25 ml of ice cold 0.1 M $CaCl_2$, incubated for 25 minutes on ice and centrifuged as described above. The pellet was taken in 10 ml of ice cold 0.1 M $CaCl_2$ and kept at 4°C overnight without rotation. 2 ml of 80% glycerol were added and mixed gently with the bacterial solution, which was then divided in 200 µl aliquots, snap frozen in liquid nitrogen and stored at -80°C.

3.2.5 Transformation

An aliquot of competent cells was thawed on ice for 10 minutes and incubated with DNA (10 µl of a ligation or 1 µl of a plasmid) for 15 minutes on ice. A heat shock was then

applied to the cells for 45 seconds at 42°C. The cells were chilled on ice for 2 to 3 minutes, upon which 400 µl of LB medium was added. The cells were incubated at 37°C for 30 minutes and plated in Petri-dishes containing the appropriate medium and antibiotics. Incubation at 37°C overnight followed.

3.3 DNA methods

3.3.1 Preparation of plasmid DNA from bacteria

3.3.1.1 DNA miniprep

A 3 ml culture of bacteria grown overnight was harvested by centrifugation at 14,000 rpm for 30 seconds at room temperature (eppendorf centrifuge 5415 C) and the cell pellet resuspended in 100 µl of Solution I (50 mM glucose, 25 mM Tris-HCl pH 8.0 and 10 mM EDTA). To lyse the cells, 200 µl of Solution II (0.2 N NaOH,1 % (w/v) SDS) were added, the suspension was mixed gently and incubated for not more than 5 minutes at room temperature. Precipitation of proteins and chromosomal DNA was done by addition of 150 µl Solution III (3 M potassium acetate, 11.5 % (v/v) acetic acid) and again gentle mixing. Alternatively, the solutions S1, S2 and S3 from the Nucleobond AX plasmid Midi Kit (Macherey-Nagel) were used. The precipitate was separated by centrifugation for 5 min at 14,000 rpm at 4°C (eppendorf centrifuge 5417 R). The supernatant containing the plasmid DNA was transferred to a new tube and the DNA was precipitated by addition of 1 ml of absolute ethanol. The DNA pellet was dissolved in 200 µl of TEB buffer (10 mM Tris-HCl pH 8.0, 1 mM EDTA) and mixed with 200 µl of 5 M LiCl. After centrifugation 5 minutes at 14,000 rpm at 4°C (eppendorf centrifuge 5417 R), the supernatant was transferred to a new tube and the DNA again precipitated with 1 ml of absolute ethanol. Finally the DNA pellet was resuspended in an appropriate volume of H_2O. This plasmid quality is suitable for digestions (include 10 % (v/v) RNAse A (Sigma) at a concentration of 0.1 mg/ml) and sequencing reactions.

3.3.1.2 DNA midiprep

Higher amounts of pure plasmid DNA (up to 500 µg) were obtained with the Nucleobond AX plasmid Midi Kit (Macherey-Nagel) used according to the instructions of the manufacturer.

3.3.2 DNA separation on agarose gels

DNA was mixed with 1/10 of the total volume of 10x loading buffer (1 mM EDTA pH 8.0, 0.1 % (w/v) Orange G, 10 % (w/v) Ficoll in 0.5x TAE (20 mM Tris base, 5 mM sodium acetate, 1 mM EDTA, adjust to pH 8.2 with HCl)) and separated according to size on

agarose (GenXpress) gels. Depending on the size of DNA to be separated, the percentage of agarose dissolved in 0.5x TAE was between 0.7 and 1.5 % (w/v). Gels were run with 2 to 8 V/cm (power pac 300, Biorad) in 0.5x TAE in wide mini-sub® or mini-sub® cell GT tanks (Biorad) and DNA was visualized after ethidium bromide staining (dilute 10 mg/ml stock solution 1:10,000 in 0.5x TAE) under UV (ultraviolet) light. The intensity of the DNA was compared to a λDNA (promega) *Hind*III digested marker (see Appendix B).

3.3.3 Enzymatic reactions

3.3.3.1 Restriction digestions of DNA

Restriction endonucleases and 10x reaction buffers (New England Biolabs) were used following the instructions of the manufacturer. Analytical digestions were performed in a total volume of 20 μl with 0.5 to 1 μg DNA and preparative digestions in a total volume of 100 μl with 2 to 5 μg DNA.

3.3.3.2 Ligation of DNA Fragments with T4 DNA Ligase

A typical 20 μl reaction contained 50 ng of restricted vector DNA and 20 ng of insert DNA in 1 mM ATP, 1x T4- DNA ligase buffer (30 mM Tris-HCl pH 7.8, 10 mM $MgCl_2$, 10 mM DTT, 1 mM ATP) and 0.5 μl T4-DNA ligase (New England Biolabs, 400 U/μl). The reactions were incubated from 4 hours to overnight at room temperature.

3.3.3.3 Phosphorylation of DNA 5´ ends

Phosphorylation of 5´ ends was performed using T4 Polynucleotide Kinase (New England Biolabs, 5 U/μg DNA) in the buffer supplied with the enzyme (70 mM Tris-HCl pH 7.6, 10 mM $MgCl_2$, 5 mM DTT) and 1 mM ATP. The reaction was incubated for 30 min at 37°C prior to phenol/$CHCl_3$ extraction and ethanol precipitation (see 3.3.4.1 and 3.3.4.2).

3.3.3.4 Filling-in of DNA 5´ recessed ends

0.5 μl of T4 DNA polymerase (New England Biolabs, 3 U/μl) were added to a fresh PCR product (see 3.3.6) prior to its purification and incubated 10 minutes at 37°C. The reaction was then stopped with 0.5 μl of a 0.5 M EDTA solution pH 8.0. The DNA was extracted with phenol/$CHCl_3$ and precipitated with ethanol (see 3.3.4.1 and 3.3.4.2).

3.3.3.5 Dephosphorylation of DNA 5´ ends

In order to avoid self-ligation, cleaved vectors were incubated with 1 U/pmol DNA ends of calf intestine phosphatase (CIP) (New England Biolabs) in 20 mM Tris-HCl pH 8.0 for 45 minutes at 37°C. The enzyme was inactivated by incubation at 65°C for 45 minutes. Afterwards, the reaction mixture was purified by elution from an agarose gel (see 3.3.4.3).

3.3.4 Purification of DNA Solutions

3.3.4.1 Phenol/Chloroform extractions

To purify DNA from enzymes or other proteins and to remove other contaminants, 1% (v/v) 0.5 M EDTA pH 8.0 and 1 volume of Tris-HCl pH 7.5 saturated phenol (Sambrok *et al.*, 1989) were added to the DNA solution and vortexed for 5 to 10 seconds. Phases were separated by centrifugation for 2 min at 14,000 rpm at room temperature (eppendorf centrifuge 5415 D) and the upper aqueous phase transferred into a new tube. After re-extraction with 1 volume of $CHCl_3$, the upper aqueous phase was ethanol precipitated (see below).

3.3.4.2 Ethanol Precipitation

To purify or concentrate DNA, 10 % (v/v) 3 M sodium acetate pH 5.6 and 2 volumes of absolute ethanol were added to the DNA solution. The mixture was incubated at -20°C for at least 20 minutes and centrifuged for 15 min at 14,000 rpm at room temperature (eppendorf centrifuge 5415 D). After discarding the supernatant, the pellet was air dried and taken up in an appropriate volume of H_2O.

3.3.4.3 Elution of DNA Fragments from the Gel

Elution of DNA from agarose gels was performed with the Wizard® SV Gel and PCR Clean-Up System kit from Promega. The instructions of manufacturer were followed.

3.3.5 DNA quantification

The concentration of DNA solutions was determined by UV spectroscopy at 260 nm in a photometer (BioPhotometer, eppendorf). OD_{260} of 1 corresponds to 50 µg/ml of DNA. Dilutions of 1/100 of the DNA solutions were prepared in H_2O and measured against a blank containing only H_2O.

3.3.6 Amplification of DNA fragments by PCR (polymerase chain reaction)

A standard PCR reaction of 50 µl contained 10 ng of template DNA, 0.2 µg of each primer, 1x Taq-polymerase buffer (supplemented with the enzyme), 0.2 mM dNTPs (Invitrogen) and 0.6 U DyNAzyme II (Finnzyme) or 3 U of *Pfu* DNA polymerase I (Promega) (for PCR products larger than 800 base pairs or to be cloned in expression vectors). The aqueous solution was overlaid with one drop of mineral oil and the PCR reaction was done in a Perkin Elmer DNA Thermal Cycler (Perkin) machine. DNA was denaturated at 94°C and amplified in 20 to 35 cycles of denaturating at 94°C for 30 seconds, 30 to 90 seconds of

annealing temperature (based on the melting temperature of the primers) and 30 to 90 seconds of extension temperature at 72°C (68°C for *Pfu*I (Promega)). A final step of extension temperature was done for 10 minutes at 72°C (68°C for *Pfu*I (Promega)).

3.3.7 Site directed mutagenesis

3.3.7.1 Cassette Cloning

Cassette cloning consists in substituting, through digestion and ligation, a small DNA fragment (up to 40 to 50 nucleotides) with a new fragment bearing the desired mutations. Two primers complementary to each other, containing the desired mutations and the same restriction sites used to digest the vector, were phosphorylated and ligated into a digested and dephosphorylated vector (see 3.3.3.3 and 3.3.3.5).

Before the ligation reaction, the primers had been phosphorylated. 1 µg of each primer was added to 1 mM ATP, 1x PNK (polynucleotide kinase) reaction buffer (70 mM Tris-HCl, 10 mM $MgCl_2$, 5 mM dithiothreitol (DTT), pH 7.6), 5 U of PNK (New England Biolabs) and H_2O in a total volume of 20 µl. The solution was overlaid with one drop of mineral oil and a single cycle of incubation at 37°C for 30 minutes, 90°C for 30 seconds and 37°C for 5 minutes was done using a Perkin Elmer DNA Thermal Cycler (Perkin) machine.

The ligations were transformed into *E. coli* Top 10 F´ (Invitrogen) and the new plasmid bearing the desired mutations was extracted and purified (see 3.2.5 and 3.3.3.2).

3.3.7.2 Cycle PCR

This method allows the introduction of a mutation by amplifying the complete plasmid. The proof reading *Pfu* DNA Polymerase I (Promega) and a PCR machine with a heated lid (T3 Thermocycler Biometra) were used. The mutagenesis was performed using two primers complementary to each other bearing the mutation. Base pair exchange of up to 6 nucleotides is possible with this method. The mutated nucleotides lay in the middle of the primer, flanked by 12 wild type nucleotides. To introduce the mutations, 20 cycles of denaturing at 95°C for 2 minutes, 1 minute at usually 40°C (depending on the number of nucleotides to be exchanged) and elongation for 2 minutes per kb of the template at 68°C, were performed. The PCR reaction was set up with different dilutions of DNA (1 µg, 1 µg 1:10, 1 µg 1:100) (see 3.3.6). As a negative control a PCR was performed without the primers. 10 µl of the PCR reaction were tested on an agarose gel (see 3.3.2). The remaining 40 µl were digested with 1 µl *Dpn*I (20 U/µl, New England Biolabs) for at least 5 hours to remove the methylated template DNA. 10 µl of the undigested DNA were used for transformation in E.Coli Top 10 F´ (see 3.2.5).

3.3.8 Sequencing reactions

DNA sequencing was performed using the ABI PRISM 310 Genetic Analyzer and the BigDye Terminator v3.1 Cycle Sequencing Kit (Applied Biosystems) according to the instructions of the manufacturer. Dilution of the BigDye Terminator mix with 5x sequencing buffer (100 mM Tris-HCl pH 9.0, 10 mM $MgCl_2$) was optional. The sequencing reaction was composed as follows: 0.2 µg plasmid DNA, 1 µl primer (4 to10 pmol/µl), 2 µl BigDye Terminator mix, 3 µl 5x sequencing buffer added to water in a total volume of 20 µl.

The reaction was performed in a heated lid thermocycler (T3 Thermocycler Biometra). 30 cycles were performed with 30 sec at 96°C, 10 sec at 50°C and 4 min at 60°C. The reaction was cleaned by spinning through Millipore UltrafreeMC columns packed with Sephadex G-50 (DNA-grade, Pharmacia) for 3 minutes at 2500 rpm.

Alternatively the DNA samples and primers were sent to be sequenced in the Service Department of IMP (Institute of Molecular Pathology) Vienna, headed by Gotthold Schaffner.

3.3.9 List of primers

3.3.9.1 Primers for cloning

Label	Sequence and description (orientation 5' to 3')
TIM979	ACTGGAATTCGGTTTAGGACCGCGG Sense primer to introduce HRV14 2A^{pro} in the vector pGEX-6P1; *Eco*RI site
TIM1302	CCGGTAATTAAGAAGAGGAAAGGTGACATTAAATCCCGTGGTTTAGGACCGC Sense oligo to introduce Arg in P1 position of HRV14 VP1 2A^{pro}; *Age*I, *Sac*II sites
TIM1303	GGTCCTAAACCACGGGATTTAATGTCACCTTTCCTCTTCTTAATTA Antisense oligo to introduce Arg in P1 position of HRV14 VP1 2A^{pro}; *Age*I, *Sac*II sites
TIM1304	CCGGTAATTAAGAAGAGGAAAGGTGACATTAAATCCTATGGTCCAGGACCGC Sense oligo to introduce Leu in P2' position of HRV14 VP1 2A^{pro}; *Age*I, *Sac*II sites
TIM1305	GGTCCTGGACCATAGGATTTAATGTCACCTTTCCTCTTCTTAATTA Antisense oligo to introduce Leu in P2' position of HRV14 VP1 2A^{pro}; *Age*I, *Sac*II sites
TIM1315	CCGGTAATTAAGAAGAGGCGGACAACCCTTAGCACCTATGGGCCCCCACGGC Sense oligo to introduce Tyr in P1 position of HRV14 VP1-(eIF4GI)- 2A^{pro}; *Age*I, *Sac*II sites
TIM1316	CGTGGGGGCCCATAGGTGCTAAGGGTTGTCCGCCTCTTCTTAATTA Antisense oligo to introduce Tyr in P1 position of HRV14 VP1-(eIF4GI)- 2A^{pro}; *Age*I, *Sac*II sites
TIM1322	ATACAGGAAAGTCCGTACTATCCCAAA Sense primer to introduce the mutation E84P in HRV2 2A^{pro}

Label	Sequence and description (orientation 5' to 3')
TIM1323	TTTGGGATAGTACGGACTTTCCTGTAT
	Antisense primer to introduce the mutation E84P in HRV2 2A^{pro}
TIM1324	ATTGAAGGAAGCGAGTATTACCCAAGT
	Sense primer to introduce the mutations N86S P87E in HRV14 2A^{pro}
TIM1325	ACTTGGGTAATACTCGCTTCCTTCAAT
	Antisense primer to introduce the mutations N86S P87E in HRV14 2A^{pro}
TIM1327	CCGGTAATTAAGAAGAGGAAAGGTGACATTTCATCCTATGGTTTAGGACCGC
	Sense oligo to introduce Ser in P3 position of HRV14 VP1 2A^{pro}; *Age*I, *Sac*II sites
TIM1328	GGTCCTAAACCATAGGATGAAATGTCACCTTTCCTCTTCTTAATTA
	Antisense oligo to introduce Ser in P3 position of HRV14 VP1 2A^{pro}; *Age*I, *Sac*II sites
TIM1329	ATTGAAGGAAACGAGTATTACCCAAGT
	Sense primer to introduce the mutation P87E in HRV14 2A^{pro}
TIM1330	ACTTGGGTAATACTCGTTTCCTTCAAT
	Antisense primer to introduce the mutation P87E in HRV14 2A^{pro}
TIM1331	CATGCCATGGGTTTAGGACCTAGGTACGG
	Sense primer to introduce HRV14 2A^{pro} in pET11d-TAPtag; *Nco*I site
TIM1332	CATGCCATGGCCTGTTCCTCTGCGATACA
	Antisense primer to introduce HRV14 2A^{pro} in pET11d-TAPtag; *Nco*I site
TIM1333	CATGCCATGGGCCCCAGTGACATGTATGT
	Sense primer to introduce HRV2 2A^{pro} in pET11d-TAPtag; *Nco*I site
TIM1334	CCATGCCATGGCTTGTTCTTCAGCACAATG
	Antisense primer to introduce HRV2 2A^{pro} in pET11d-TAPtag; *Nco*I site
TIM1336	CATGGGATCCATGTCCCCTATACTAGGT
	Sense primer to introduce the GST tag plus PreScission cleavage site in the vector pFastBac; *Bam*HI site
TIM1337	CATGGAATTCGGGCCCCTGGAACAGAAC
	Antisense primer to introduce the GST tag plus PreScission cleavage site in the vector pFastBac; *Bam*HI site
TIM1338	ATCTGGATTGAAGAAAACCCTTATTAC
	Sense primer to introduce the mutation G85E in HRV14 2A^{pro}
TIM1339	GTAATAAGGGTTTTCTTCAATCCAGAT
	Antisense primer to introduce the mutation G85E in HRV14 2A^{pro}
TIM1340	ATCTGGATTGAAGAAAGCGAGTATTAC
	Sense primer to introduce the mutations G85E N86S P87E in HRV14 2A^{pro}
TIM1341	GTAATACTCGCTTTCTTCAATCCAGAT
	Antisense primer to introduce the mutations G85E N86S P87E in HRV14 2A^{pro}

Label	Sequence and description (orientation 5' to 3')
TIM1342	TATGAAATACAGGGAAGTGAGTACTAT
	Sense primer to introduce the mutation E82G in HRV2 2A^{pro}
TIM1343	ATAGTACTCACTTCCCTGTATTTCATA
	Antisense primer to introduce the mutation E82G in HRV2 2A^{pro}
TIM1344	CCCCTCTCCACCAAAGATCTGACCACA
	Sense primer to introduce the *Bgl*II restriction site upstream the PV1-VP1 2A^{pro} cleavage site; *Bgl*II site
TIM1345	TGTGGTCAGATCTTTGGTGGAGAGGGG
	Antisense primer to introduce the *Bgl*II restriction site upstream the PV1-VP1 2A^{pro} cleavage site; *Bgl*II site
TIM1346	AACAAAGCGGTGTATACTGCAGGTTAC
	Sense primer to introduce the *Bst*Z17 I restriction site downstream the PV1-VP1 2A^{pro} cleavage site; *Bst*Z17 I site
TIM1347	GTAACCTGCAGTATACACCGCTTTGTT
	Antisense primer to introduce the *Bst*Z17 I restriction site downstream the PV1-VP1 2A^{pro} cleavage site; *Bst*Z17 I site
TIM1348	GATCTGACCACACGTGGATTCGGACACCAAAACAAAGCGGTGTA
	Sense oligo to introduce Arg in P1 position of PV1-VP1 2A^{pro}; *Bgl*II, *Bst*Z17 I sites
TIM1349	TACACCGCTTTGTTTTGGTGTCCGAATCCACGTGTGGTCA
	Antisense oligo to introduce Arg in P1 position of PV1-VP1 2A^{pro}; *Bgl*II, *Bst*Z17 I sites
TIM1353	GAATTCGCCATCACAGTCCAGAGA
	Sense primer to introduce eIF4GII residues 445 to 744 in the vector pFastBac; *Eco*RI site
TIM1354	GAATTCCTATTAATCGGCTTGGCTGTCTCG
	Antisense primer to introduce eIF4GII residues 445 to 744 in the vector pFastBac; *Eco*RI site
TIM1392	GGGGTTGGGCCGTGCGAGCCAGGAGAC
	Sense primer to introduce the mutation A104C in HRV14 2A^{pro}
TIM1393	GTCTCCTGGCTCGCACGGCCCAACCCC
	Antisense primer to introduce the mutation A104C in HRV14 2A^{pro}
TIM1394	GGGGTTGGGCCGTCAGAGCCAGGAGAC
	Sense primer to introduce the mutation A104S in HRV14 2A^{pro}
TIM1395	GTCTCCTGGCTCTGACGGCCCAACCCC
	Antisense primer to introduce the mutation A104S in HRV14 2A^{pro}
TIM1396	GGTGAGGGCCCTGCTGAACCAGGTGAC
	Sense primer to introduce the mutation C101A in HRV2 2A^{pro}

Label	Sequence and description (orientation 5' to 3')
TIM1397	GTCACCTGGTTCAGCAGGGCCCTCACC
	Antisense primer to introduce the mutation C101A in HRV2 2A^{pro}
TIM1398	GGTGAGGGCCCTAGTGAACCAGGTGAC
	Sense primer to introduce the mutation C101S in HRV2 2A^{pro}
TIM1399	GTCACCTGGTTCACTAGGGCCCTCACC
	Antisense primer to introduce the mutation C101S in HRV2 2A^{pro}
TIM1411	CTCGAGTCATTAGTGGTGGTGGTGGTGGTGCTGTTCCTCTGCGATACA
	Antisense primer to introduce HRV14 2A^{pro} plus a His tag in the vector pGEX-6P1; *Xho*I site
TIM1472	GCGGAATTCTTTCATCCTGAAAGAGACC
	Sense primer to introduce eIF4GII residues 552 to 744 in the vector pGEX-6P1; *Eco*RI site
TIM1473	GCGGAATTCTCACTAATCATCGGCTTGGCTGTC
	Antisense primer to introduce eIF4GII residues 552 to 744 in the vector pGEX-6P1; *Eco*RI site
TIM1474	CACCGCTCGAGATGGGCCCCAGTGACATGTATG
	Sense primer to introduce HRV2 2A^{pro} in the vector pMZI; *Xho*I site
TIM1475	CGCGCACATATGTTGTTCTTCAGCACAATGG
	Antisense primer to introduce HRV2 2A^{pro} in the vector pMZI; *Nde*I site
TIM1476	CACCGCTCGAGATGGGTTTAGGACCTAGGTACG
	Sense primer to introduce HRV14 2A^{pro} in the vector pMZI; *Xho*I site
TIM1477	CGCGCACATATGCTGTTCCTCTGCGATACAC
	Antisense primer to introduce HRV14 2A^{pro} in the vector pMZI; *Nde*I site
TIM1492	GCGGAATTCTCACTAGTGGTGGTGGTGGTGGTGATCATCGGCTTGGCTGTC
	Antisense primer to introduce eIF4GII residues 552 to 744 plus a His tag in the vector pGEX-6P1; *Eco*RI site
TIM1518	GACCGCTCGAGATGGAATTCCACATGCCTCAGATCACT
	Sense primer to introduce HIV 1 protease in the vector pMZI; *Xho*I*, Eco*RI sites
TIM1519	GCACATATGTCGAAGGATCCCAATTCCCAAGAAATT
	Antisense primer to introduce HIV 1 protease in the vector pMZI; *Nde*I*, Bam*HI sites
TIM1520	GACCGCTCGAGATGGGCCCCTATGGACATCAATC
	Sense primer to introduce CBV4 2A^{pro} in the vector pMZI; *Xho*I site
TIM1521	CGCGCACATATGCTGTTCCATTGCATCATC
	Antisense primer to introduce CBV4 2A^{pro} in the vector pMZI; *Nde*I site
TIM1522	GACCGCTCGAGATGGAACTGACACTGTAC
	Sense primer to introduce FMDV Lb^{pro} in the vector pMZI; *Xho*I site

Label	Sequence and description (orientation 5' to 3')
TIM1523	CGCGCACATATGTTTGAGCTTGCGTTGAACC
	Antisense primer to introduce FMDV Lb^{pro} in the vector pMZI; *Nde*I site
TIM1532	CTTTAAATTTTTCGTCAATTGGGATCC
	Sense primer to delete two stop codons in HIV 1 protease cloned in the vector pMZI; *Mfe*I, *Bam*HI sites
TIM1533	GGATCCCAATTGACGAAAAATTTAAAG
	Antisense primer to delete two stop codons in HIV 1 protease cloned in the vector pMZI; *Mfe*I, *Bam*HI sites
TIM1544	CGCGCCATGGGATTTCATCCTGAAAGAGACC
	Sense primer to introduce eIF4GII residues 552 to 744 in the vector pET11d; *Nco*I site
TIM1545	GCGCCCATGGTCACTAGTGGTGGTGGTGGTGGTGATCATCGGCTTGGCTGTC
	Antisense primer to introduce eIF4GII residues 552 to 744 plus a His tag in the vector pET11d; *Nco*I site
TIM1546	CGCGCCATGGGTTTAGGACCTAGGTAC
	Sense primer to introduce HRV14 2A^{pro} in the vector pET11d; *Nco*I site
TIM1547	GCGGATCCTCACTAGTGGTGGTGGTGGTGGTGCTGTTCCTCTGCGATAC
	Antisense primer to introduce HRV14 2A^{pro} plus a His tag in the vector pET11d; *Bam*HI site

Table 5: List of primers used for cloning experiments.

3.3.9.2 Primers for sequencing

Label	Sequence (orientation 5' to 3')	Target
TIM31	GTTTGCTGAATCAGG	HRV14 VP1; antisense
TIM69	CACATCAATAGGGCGCA	HRV14 2A^{pro}; sense
TIM197	TCAATGCTTGAAGGAGC	pGEX-6P1 and pFastBac-GST inserts; sense
TIM258	GAATTCGATCCCTTGTTCTTCAGCACA	HRV2 2A^{pro}; antisense
TIM315	CCCACAAATTGATAAG	pGEX-6P1 and pFastBac-GST inserts; sense

Label	Sequence (orientation 5' to 3')	Target
TIM326	GGAATTCTGGCCCCAGTGACATGTA	HRV2 2A^{pro}; sense
TIM768	GAATCGGGATCCCTATCACTGTTCCTCTGCGATACACTC	HRV14 2A^{pro}; antisense
TIM847	CCAGGAGACGCCGGTGGGATT	HRV14 2A^{pro}; sense
TIM848	AATCCCACCGGCGTCTCCTGG	HRV14 2A^{pro}; antisense
TIM967	ACCAGGTGACGCAGGTGGAAAGT	HRV2 2A^{pro}; sense
TIM1109	TCTGAGATGCATGAATCTATTTTGGTATCTTATTCATCA	HRV2 2A^{pro}; sense
TIM1312	ATACATCAAGGTTTAGTG	HRV14 2A^{pro}; sense
TIM1331	CATGCCATGGGTTTAGGACCTAGGTACGG	HRV14 2A^{pro}; sense
TIM1332	CATGCCATGGCCTGTTCCTCTGCGATACA	HRV14 2A^{pro}; antisense
TIM1333	CATGCCATGGGCCCCAGTGACATGTATGT	HRV2 2A^{pro}; sense
TIM1334	CATGCCATGGCTTGTTCTTCAGCACAATG	HRV2 2A^{pro}; antisense
TIM1336	CATGGGATCCATGTCCCCTATACTAGGT	GST; sense
TIM1337	CATGGAATTCGGGCCCCTGGAACAGAAC	GST; antisense
TIM1346	AACAAAGCGGTGTATACTGCAGGTTAC	PV1 2A^{pro}; sense
TIM1350	GACCAAGGTCACCTCCAA	PV1 2A^{pro}; sense
TIM1351	TCCATGGCTTCTTCTTCG	PV1 2A^{pro}; antisense
TIM1391	CTACAAATGTGGTATGGC	pFastBac inserts; antisense
TIM1518	GACCGCTCGAGATGGAATTCCACATGCCTCAGATCAC	HIV 1 protease; sense
TIM1519	GCACATATGTCGAAGGATCCCAATTCCCAAGAAATT	HIV 1 protease; antisense

Label	Sequence (orientation 5' to 3')	Target
TIM1520	GACCGCTCGAGATGGGCCCCTATGGACATCAATC	CBV4 2A^{pro}; sense
TIM1521	CGCGCACATATGCTGTTCCATTGCATCATC	CBV4 2A^{pro}; antisense
TIM1522	GACCGCTCGAGATGGAACTGACACTGTAC	FMDV Lb^{pro}; sense
TIM1523	CGCGCACATATGTTTGAGCTTGCGTTGAACC	FMDV Lb^{pro}; antisense
M13(-40)	GTTTTCCCAGTCACGAC	Bacmid (Invitrogen) inserts; sense
M13 rev	CAGGAAACAGCTATGAC	Bacmid (Invitrogen) inserts; antisense
T7promoter	TAATACGACTCACTATAGGG	pET11d inserts; sense
T7terminator	GCTAGTTATTGCTCAGCGG	pET11d inserts; antisense

Table 6: List of primers used for sequencing.

3.4 RNA methods

3.4.1 *In vitro* transcription

2 to 5 µg of plasmid DNA were used to perform *in vitro* transcription experiments. First, the plasmid DNA was cleaved with a restriction enzyme cleaving just downstream of the protein coding sequence. Then, the linearized DNA was purified performing a phenol/CHCl$_3$ extraction followed by ethanol precipitation (see 3.3.4.1 and 3.3.4.2) and resuspension in H$_2$O. Finally, a typical transcription reaction composed of the cleaved plasmid DNA, 5 mM DTT, 1x transcription buffer (40 mM Tris-HCl, pH 7.9, 10 mM NaCl, 6 mM MgCl$_2$, 2mM spermidine) (Promega), 0.25 mM of all four NTPs (Amersham), 120 U RNasin (Promega) and 18 U of T7 RNA Polymerase (Promega) was performed in a total volume of 100 µl for 90 minutes at 37°C.

The template DNA was removed after the reaction by addition of 30 U DNase I (Invitrogen) and 40 U RNasin (Promega) followed by an incubation of 20 min at 37°C. The RNA was extracted with phenol/CHCl$_3$ (see 3.3.4.1) and precipitated with 1/5 volumes of 8 M NH$_4$OAc and 2.5 volumes of absolute ethanol for a maximum of 15 minutes at -80°C. After

centrifugation for 15 minutes at 14,000 rpm at 4°C (eppendorf centrifuge 5417 R), the RNA pellet was washed with 500 µl 70 % ethanol and resuspended in 25 µl of H_2O. The quality of the RNA was checked on an agarose gel containing 0.1 % (w/v) SDS. Before staining the gel with ethidium bromide (10 mg/ml stock solution 1:10,000 in 0.5x TAE), the SDS was removed by shaking the gel in H_2O for 30 to 60 minutes.

3.4.2 *In vitro* translation

Translation reactions were performed at 30°C in a volume of 10 µl (or multiples of 10 µl, depending on how many aliquots needed to be taken at different time points) and composed of 70% of Rabbit Reticulocyte Lysate (RRL) (Promega), 8 U of RNasin (40 U/µl, Promega), 20 µM of amino acids mix without methionine (Promega), 4 µCi of [^{35}S]-Methionine (37 TBq/mmol, Hartmann Analytics) and 10 to 50 ng of RNA.

After pre-incubation for 2 minutes at 30°C, translation was started by addition of the RNA. At different time points, aliquots were taken and the reaction was stopped by adding 1/10 volumes of 20 mM unlabelled cysteine/methionine in Laemmli sample buffer and moving the samples to ice. In the experiments using the inhibitor zVAM.fmk, the inhibitor was added 10 minutes after translation initiation. Negative controls were done with DMSO (the solvent of zVAM.fmk) and without RNA.

Translation products were analysed by the polyacrylamide gel electrophoresis system described by Dasso & Jackson (1989) and fluography (see 3.5.6.3 and 3.5.6.4) or by Western Blot Analysis (see 3.5.7). The volumes loaded on the polyacrylamide gels were 2 µl of a 10 µl reaction for the fluography and 3 µl of a 10 µl reaction for the Western Blot Analysis.

3.5 Protein methods

3.5.1 Protein expression

3.5.1.1 Protein expression in LB and TB media

Expression of recombinant proteins was performed in *E. coli* BL21(DE3)LysS for pET vectors or in *E. coli* JM101 for pGEX vectors. A single colony was grown in LB or TB media containing the suitable antibiotics. The LB or TB media were inoculated 1:10 with the overnight culture. The culture was incubated at 37°C on a shaker at 160 to 180 rpm. Once the cell density reached an OD_{600} between 0.5 and 0.6, induction with the appropriate concentration of IPTG (Isopropyl β-D-1-thiogalactopyranoside) was started depending on the protein being expressed. The temperature was shifted to 20°C, 30°C or maintained at 37°C (this was also protein specific) and the cells were incubated for several hours or overnight.

Cells were harvested by centrifugation at 5000 rpm, 10 min, 4°C on Sorvall RC5C or RC5C *plus* centrifuges. The cell pellets were snap-frozen in liquid nitrogen and stored at -80°C.

3.5.1.2 Protein expression in M9 minimal medium

Protein expression in M9 Minimal medium was performed in *E. coli* BL21(DE3)LysS. A single colony was inoculated in M9 minimal medium containing the appropriate antibiotics. The M9 minimal medium was inoculated with 1% of the pre-culture and incubated at 37°C on a shaker at 160 rpm. Once the cell density reached an OD_{600} above 0.5, induction with 0.1 mM IPTG was started and the cells incubated for 5 hours shaking at 37°C. Cells were harvested by centrifugation at 5000 rpm, 10 min, 4°C on Sorvall RC5C or RC5C *plus* centrifuges. The cell pellets were snap-frozen in liquid nitrogen and stored at -80°C.

3.5.1.3 Protein expression in Sf9 cells

The protein expression in insect Sf9 cells was performed using the Bac-to-Bac® Baculovirus Expression System from Invitrogen. The instructions of the manufacturer were followed.

3.5.1.3.1 Transfection of Sf9 cells to generate a recombinant baculovirus

$9x10^5$ Sf9 cells/well were seeded in a 6 well plate in 2ml of Sf-900 II SFM complete media (containing 50 units/ml penicillin and 50 µg/ml streptomycin). The plate was incubated at 27°C for 1 hour to allow the cells to attach. The transfection samples were prepared in 12 x 75 mm sterile tubes. 2 µg of purified bacmid were diluted in 100 µl of unsupplemented Grace's media and in other tube 6 µl of Cellfectin® Reagent (Invitrogen) were also diluted in 100 µl of unsupplemented Grace's media. The diluted bacmid and Cellfectin® Reagent were then combined, mixed gently and incubated for 45 minutes at room temperature. Meanwhile the cells were washed two times with 2 ml of unsupplemented Grace's media. After the incubation, 0.8 ml of unsupplemented Grace's media were added to the transfection mix and this was added to the cells. An incubation period of 5 hours at 27°C followed, after which the transfection mix was removed and 2 ml of complete growth media (Sf-900 II SFM media containing 50 units/ml penicillin and 50 µg/ml streptomycin) were added to the cells. The plate was incubated in a humidified incubator at 27°C for 72 hours (time at which the viral infection was visible).

3.5.1.3.2 Preparation of the P1 viral stock and amplification

The media of the transfection was collected and transferred to a 15 ml falcon. After a centrifugation at 800 rpm for 5 minutes at room temperature, the supernatant was transferred

to a new falcon tube. This corresponds to the P1 viral stock. Short term storage was at 4°C protected from light; long term storage was at -80°C, also protected from light.

The amplification of the viral stock was done as recommended by the manual Bac-to-Bac® Baculovirus Expression System from Invitrogen. 2×10^6 cells/ well were seeded in a 6 well plate in 2ml of Sf-900 II SFM complete media. The plate was incubated at 27°C for 1 hour to allow the cells to attach. 400 µl of the P1 viral stock were added to each well and the plate was incubated at 27°C in a humidified chamber for 48 hours. The isolation of the viral stock P2 was as for viral stock P1.

3.5.1.3.3 Virus titer determination using end-point dilution

5×10^3 cells/well in Sf-900 II SFM complete media (100µl) were seeded in a 96 well plate and incubated 1 hour at room temperature to allow the cells to attach. Dilutions of the viral stock from 10^{-2} to 10^{-12} in Sf-900 II SFM complete media were prepared. 100 µl of each dilution were added to the cells (12 wells per dilution). One row of 12 wells was not infected and left for control. An incubation at 27°C in a humidified chamber followed for 6 to 10 days. After that, the number of infected wells was counted. The wells considered infected contained lysed cells and the wells non-infected contained a confluent layer of cells. The method used to determine the virus titer was the one described by Reed and Muench (Reed and Muench., 1938).

3.5.1.3.4 Expression of the recombinant protein

A time course experiment was done to determine the optimal level of expression. 6×10^5 cells/well were seeded on a 24 well plate in Sf-900 II SFM complete media and incubated 1 hour at room temperature to allow the cells to attach. The media was removed and replaced with 300 ml of fresh one. The viral stock was added at a MOI (multiplicity of infection) of 5 and the plate was incubated at 27°C in a humidified chamber. The supernatants were harvested at the time points 24, 48, 72 and 96 hours. The samples were boiled with ½ volumes of 2x Laemli sample buffer for 5 minutes and analyzed on SDS-PAGE gels (see 3.5.6.1).

Once the conditions for expression were optimized the method was scaled up to liquid cultures of 200 ml. The cells were transferred to 1 litre conical flasks at a concentration of 2×10^6 cell/ml in Sf-900 II SFM complete media and directly infected with the appropriate amount of viral stock. The incubation was at 27°C in a humid chamber with constant rotation at 120 rpm. After expression, the cells were harvested by centrifugation at 1200 rpm, 5 minutes at 4°C. The supernatant was then treated with glutathione sepharose beads in order to purify the recombinant protein.

3.5.2 Preparation of cell extracts

<u>3.5.2.1 Bacterial crude cell extracts</u>

The bacterial pellets stored at -80°C after expression were thawed on ice and resuspended in 30 ml/litre of expression of the appropriate buffer. Cell disruption was achieved by sonication using the device Homogenizer Sonopuls HD 200 from Bandelin. The probe tip used was the MS 73D at a 40% cycle 4 times 30 seconds and one continuous cycle for 30 seconds, on ice. The samples were centrifuged at 18,000 rpm in Sorvall RC5C or RC5C *plus* centrifuges, for 30 minutes at 4°C. For small scale experiments the pellets were resuspended in 1 to 1.5 ml of buffer and sonicated at a 20% cycle twice for 30 seconds and one continuous cycle for 30 seconds, on ice. The centrifugation to separate the soluble fraction (supernatant) from the unsoluble one (pellet), was done in an eppendorf centrifuge 5417R at 14,000 rpm for 30 minutes at 4°C.

The buffers used to ressuspend the bacterial pellets varied with the proteins being purified. HRV2 2A^{pro}, eIF4GII and eIF4E were resuspended in buffer A (50 mM Tris-HCl pH 8.0, 1 mM EDTA, 5 mM DTT, 5% glycerol, 50 mM NaCl). HRV14 2A^{pro} was also resuspended in buffer A, however at pH 9.0. In some experiments eIF4E was resuspended in LCB buffer (20 mM Hepes pH 7.5, 0.2 mM EDTA, 100 mM KCl). All the proteins used in GST pull down assays were taken up in ΔX buffer (150 mM NaCl, 10 mM EDTA, 50 mM Tris-HCl pH 7.4).

<u>3.5.2.2 HeLa S10 extracts</u>

A 1 litre suspension culture (see 3.1.3.1) of HeLa Ohio Flow cells in logarithmic phase (4 to 5x10^5 cells/ml) was harvested at 1200 rpm, 10 min, 4°C (Beckmann J6-HC centrifuge). Cells were then washed one time with 50 ml of ice cold 1x PBS and twice with 25 ml of ice cold 1x PBS. After each wash, the cells were spun down at 1000 rpm for 8 minutes at 4°C on a Heraeaus Megafuge 1.0R centrifuge. The pellet was taken in 1.5 volumes of hypotonic lysis buffer (2 to 3 ml) (10 mM HEPES-KOH pH 7.2, 10 mM KOAc, 1.5 mM Mg(OAc)$_2$, 2 mM DTT) and left on ice for 10 minutes to allow the cells to swell. The lysis and homogenization occurred by application of 250 to 300 strokes of a suitable Wheaton Dounce homogenizer. The lysis was controlled by staining the cells with trypan blue and observing them at a light microscope (more than 95% of the cells should be lysed). The cells were transferred to a 30 ml glass tube (Correx) and centrifuged at 4°C for 5 minutes at 3000 rpm to remove the cell debris and nuclei. The speed was increased to 13,000 rpm for another 20 minutes in order to separate the mitochondria. The centrifugation was done in a Sorvall RC5C *plus* centrifuge with a Sorvall HB-4 rotor. The white lipid layers visible on the supernatant were removed. The extract was dialysed for 3 hours (see 3.5.4.1) against 1 litre of dialysis buffer (10 mM

HEPES-KOH pH 7.2, 90 mM KOAc, 1.5 mM Mg(OAc)$_2$, 1 mM DTT), transferred to a clean 30 ml glass tube (Correx) and centrifuged at 13,000 rpm for 10 minutes at 4°C (Sorvall HB-4 rotor). After removing the lipid layer, aliquots of 380 µl were prepared, snap-frozen in liquid nitrogen and stored at -80°C. The extract concentration was between 15 and 20 mg/ml.

3.5.3 Protein purification

3.5.3.1 Batch purification

3.5.3.1.1 binding to glutathione sepharose beads

An aliquot of 1 ml glutathione sepharose beads (Amersham Biosciences) per litre of expression was washed three times with the appropriate buffer, mixed with bacterial extract containing the GST fusion protein (see 3.5.2.1) and incubated for 4 hours to overnight at 4 °C with rotation for binding. Unbound proteins to the beads were removed by washing the beads 3 times with the appropriate buffer.   Beads with bound GST fusion proteins were stored as 50 % slurry in buffer at -80 °C. Aliquots were checked on an SDS- PAGE.

3.5.3.1.2 Cleavage with preScission^{TM} Protease

The cleavage of the fusion protein from the GST tag was done by incubation for 24 hours rotation at 4 °C with preScission^{TM} Protease (Amersham Biosciences, 1 U/100 µg protein). Supernatants were separated by centrifugation at 1500 rpm for 1 minute at 4°C (eppendorf centrifuge 5417R) and beads washed 3 times with buffer, keeping the supernatants. The protein could then be purified by Size Exclusion Chromatography (see 3.5.3.2.3).

3.5.3.1.3 GST pull down

Glutathione sepharose beads coated with GST fusion proteins were incubated in ΔX buffer (see 3.5.2.1) with 8 µl of RRL (Promega) for 2 hours at 4°C. After washing 3 times with ΔX buffer the proteins were eluted by boiling in Laemmli sample buffer for 5 minutes. The samples were resolved by electrophoresis and visualized by ECL detection of Western blot membranes (see 3.5.7)

3.5.3.1.4 binding to m^{7}GTP beads

eIF4E samples eluted from a Mono 10/10 column (see 3.5.3.2.2) were dialysed against binding buffer (20 mM MOPS pH 7.6, 0.25 mM DTT, 0.1 mM EDTA, 50 mM NaF, 100 mM KCl) for 3 times for 1 hour at 4°C (see 3.5.4.1). After dialysis, the protein samples were incubated with 100 µl of m^{7}GTP beads (Amersham Biosciences) per 500 µl of sample, overnight at 4°C with rotation. After washing the unbound proteins 3 times with binding

buffer, the eIF4E was eluted by addition of 500 μl of elution buffer (20 mM MOPS pH 7.6, 0.25 mM DTT, 0.1 mM EDTA, 50 mM NaF, 550 mM KCl) and incubation for 3 hours at 4°C with rotation. The centrifugations were done at 1500 rpm for 1 minute at 4°C on an eppendorf centrifuge 5417R.

3.5.3.2 FPLC purification methods

Protein purification was performed based on size exclusion, affinity and anion exchange, using the ÄKTA FPLC (Fast Protein Liquid Chromatography) system from Amersham Biosciences. All the columns were purchased from Amersham Biosciences. 2 ml fractions were collected using an automatic fraction collector connected to the ÄKTA FPLC system. Purification experiments and cleaning of the columns were performed according to the instructions of the manufacturer. Fractions were analysed by SDS-PAGE (see 3.5.6.1).

3.5.3.2.1 Affinity purification

Proteins bearing a His tag were purified using the HisTrap FF 1 ml affinity column. Protein samples of 30 to 60 ml were loaded on the column and eluted with a gradient of imidazole. The gradient program was as follows: 5 column volumes of 100% binding buffer (50 mM Tris- HCl pH 8.0 or 9.0 (depending on the protein being purified), 50 mM NaCl), 20 column volumes of 0% to 100% of elution buffer (50 mM Tris- HCl pH 8.0 or 9.0 (depending on the protein being purified), 50 mM NaCl, 500 mM imidazole) and 5 column volumes of 100% elution buffer.

3.5.3.2.2 Anion Exchange Chromatography

Proteins differing in electrostatic charge were separated via anion exchange chromatography. Protein samples containing 5 to10 mg protein were loaded on a MonoQ 10/10 with a column volume of 8 ml. The proteins were eluted by using a gradient of NaCl. The gradient program was as follows: 2.5 column volumes of 100% binding buffer (50 mM Tris-HCl pH 8.0, 1 mM EDTA, 5 mM DTT, 5% glycerol, 50 mM NaCl), 2.5 column volumes of 0% to 20% of elution buffer (50 mM Tris-HCl pH 8.0, 1 mM EDTA, 5 mM DTT, 5% glycerol, 1 M NaCl), 15 column volumes of 20% to 60% of elution buffer, 2.5 column volumes of 60% to 100% of elution buffer and 2.5 column volumes of 100% elution buffer.

3.5.3.2.3 Size Exclusion Chromatography

Purification of proteins based on molecular weight differences was performed via size exclusion chromatography. Sample volumes of 0.5 to 2 ml were loaded in a HiLoad 26/60 Superdex 75 prep grade column. The samples were separated by passing 1.2 column

volumes of buffer A (50 mM Tris-HCl pH 8.0 or 9.0 (depending on the protein being purified), 1 mM EDTA, 5 mM DTT, 5% glycerol, 50 mM NaCl).

.

3.5.3.5 TAP purification

3.5.3.5.1 Strategy 1 (adapted from Rigaut G. *et al.* 1999)

The TAP (tandem affinity purification) method allows the purification of protein complexes under native conditions, without prior knowledge of their composition, which are then identified by mass spectroscopy (MS). This method is fast and can be used with a relatively small number of cells. The TAP tag consists of two proteins, protein A of *Staphylococcus aureus* (15.3 kDa) and a calmodulin binding peptide (CaBP, 3.0 kDa), which are separated by the cleavage sequence recognized by the Tobacco Etch Virus (TEV) protease (Rigaut *et al.*, 1999).

The expression of the proteins of interest was done in BL21(DES3)LysS cells (see 3.5.1.1). The pellet of 1 litre expression was resuspended in 12 ml of buffer A (50 mM Tris-HCl pH 8.0, 1 mM EDTA, 5 mM DTT, 5% glycerol, 50 mM NaCl) and sonicated (see 3.5.2.1). The centrifugations to separate soluble from insoluble fractions were performed at 16,000 rpm for 35 minutes at 4°C. The supernatant (soluble fration), supplemented with 10 mM of Tris-HCl pH 8.0, 150 mM of NaCl and 0.1% Igepal CA-630 (Sigma) (final concentrations), was added to 600 µl of IgG sepharose beads (Amersham), previously washed 3 times with 2 ml of IPP150 buffer (10 mM Tris-HCl pH 8.0, 150 mM NaCl, 0.1% Igepal CA-630 (Sigma)). The incubation was done at 4°C for 2 hours with rotation. After incubation the IgG sepharose beads were spun down, the supernatant was removed and the beads were washed 3 times with 2 ml of TEV cleavage buffer (10 mM Tris-HCl pH 8.0, 150 mM NaCl, 0.1% Igepal CA-630 (Sigma), 0.5 mM EDTA, 1 mM DTT (added just before use)). The IgG sepharose beads were then divided in two fresh tubes (approximately 300 µl of beads per tube), one for the negative control (no incubation with HeLa S10 extracts) and one for incubation with the HeLa S10 extracts. The positive controls were incubated with 50 mg of Hela S10 extracts for 2 hours at 4°C with rotation. After spinning down, the supernatant was removed and the beads were washed 3 times with 2 ml of IPP150 buffer and 3 times with TEV cleavage buffer. 300 µl of TEV cleavage buffer plus 100 units of TEV protease (Invitrogen) were added to the IgG sepharose beads and incubated overnight at 4°C with rotation. The IgG sepharose beads were spun down and the supernatant was collected to a fresh tube, to which 1 volume of IPP150 calmodulin binding buffer (10 mM β-mercaptoethanol, 10 mM Tris-HCl pH 8.0, 150 mM NaCl, 1 mM Mg-acetate, 1 mM imidazole, 2 mM $CaCl_2$, 0.1% Igepal CA-630 (Sigma)) was added. The IgG sepharose beads were washed 3 times with 300 µl of IPP150 calmodulin binding buffer. The supernatants from the washing steps were added to the same tube containing the first eluate. The final 1200 µl were added to 200 µl of calmodulin beads

(Stratagen), previously washed with 3 times with 2 ml of IPP150 calmodulin binding buffer. The mix was incubated at 4°C for 90 minutes with rotation. The beads were spun down, the supernatant was removed and the beads were washed 3 times with 2 ml of calmodulin binding buffer. The elution was performed with IPP150 calmodulin elution buffer (10 mM β-mercaptoethanol, 10 mM Tris-HCl pH 8.0, 150 mM NaCl, 1 mM Mg-acetate, 1 mM imidazole, 2 mM EGTA, 0.1% Igepal CA-630 (Sigma)). 200 µl of elution buffer were added to the beads and incubated 5 minutes at room temperature with agitation. The supernatant was collected after the beads were spinned down. 5 different 200 µl fractions were eluted. All the centrifugations to spin down beads were done at 1500 rpm for 1 minute at 4°C.

Protein precipitation

The precipitation procedure was as described by Ozols (1990). A solution of sodium deoxicholate (20 mg/ml) was added to the samples to a final concentration of 150 µg/ml followed by incubation at 4°C for 30 minutes with rotation. A 20% solution of trichloroacetic acid (TCA) was added to a final concentration of 6% and the mix was incubated on ice for 1 hour. The sample was centrifuged at 2500 rpm at 4°C for 45 minutes. The supernatant was removed and the pellet was ressuspended in 50 µl of 150 mM NaHCO$_3$ pH 8.8; 43.8 mM Tris-HCl pH 6.8 and 3% SDS. After protein quantification (see section 3.5.5) the samples were sent for analysis by mass spectroscopy.

3.5.3.5.2 Strategy 2 (adapted from Anne–Claude Gingras 2003)

The genes of interest were cloned in the vector pMZI, which contains a TAP tag and was constructed to transiently transfect human cells (Zeghouf *et al.*, 2004). The expression of the proteins was carried out using the Ecdysone-Inducible Mammalian Expression System from Invitrogen. The cell line used for the experiments was the HEK 293T.

Transfection and protein expression

2×10^6 cells/well were seeded in a 6 well plate in antibiotic-free media one day prior to transfection. Cells were 80 to 90% confluent on the day of the transfection. 2 µg of the pMZI vector carrying the gene of interest plus 2 µg of the vector pVgRXR from the expression system (Invitrogen) were diluted in 250 µl of OptiMEM media (Gibco) at room temperature and divided in 5 aliquots of 50 µl. 10 µl of lipofectamin 2000 (Invitrogen) were also diluted and throughly mixed in 250 µl of OptiMEM medium and incubated at room temperature for 5 minutes. 50 µl of the lipofectamin 2000 solution were added to each aliquot of the tubes containing the plasmid DNA. The final mix was incubated at room temperature for 20 minutes. Meanwhile, the cells were washed with 1 ml of 1x PBS and 1.5 ml of DMEM (Gibco) supplemented with 2% FCS, antibiotic-free was added. The 5 aliquots of 100 µl containing

lipofectamine and DNA were distributed equally over the well. The transfected cells were incubated at 37°C in a humidified chamber for 4 hours. Then, the cells were trypsinized with 200 µl of trypsin/EDTA solution (Gibco) (see 3.1.3.1), neutralized by addition of 800 µl of DMEM (Gibco) supplemented with 10% FCS, antibiotic-free and seeded in a 150 mm cell culture dish. The cells were incubated overnight at 37°C in a humidified chamber in 30 ml of DMEM (Gibco) supplemented with 10% FCS, antibiotic-free. On the next day, the media was changed to DMEM (Gibco) supplemented with 10% FCS and 50 units/ml penicillin and 50 µg/ml streptomycin plus the desired concentration of ponasterone A (Invitrogen) to start the induction of protein expression. Large scale experiments were induced for 48 hours.

Small scale experiments were performed in 6 well plates in which 200 µl of the trypsinized transfected cells were used.

Protein purification

The cells were washed 3 times with 10 ml of 1x PBS and then were lysed in 1 ml of lysis buffer (10% glycerol, 50 mM HEPES-KOH pH 8.0, 100 mM KCl, 2 mM EDTA, 0.1% Igepal CA-630 (Sigma), 2 mM DTT, 1x sigma protease inhibitor, 10 mM NaF, 0.25 mM NaOVO$_3$, 5 nM calyculin A, 50 mM β-glycerolphosphate) for 30 minutes at 37°C and harvested by scraping. To improve the protein recovery, two cycles of freeze and thaw in liquid nitrogen intercalated with 37°C incubation were done. The cell debris was spun down for 10 minutes at 14,000 rpm at 4°C. The supernatant was recovered and incubated, in batch, with 100 µl of IgG sepharose beads (Amersham) (previously washed 3 times with 1 ml of lysis buffer), at 4°C for 2 hours with rotation. The beads were spun down and the supernatant removed. The beads were then washed 3 times with 1 ml of lysis buffer and 3 times with 1 ml of TEV buffer (10 mM Hepes-KOH pH 8.0, 150 mM NaCl, 0.1% Igepal CA-630 (Sigma), 0.5 mM EDTA, 1 mM DTT). 300 µl of TEV buffer plus 100 units of TEV protease (Invitrogen) were added to the IgG sepharose beads and incubated overnight at 4°C with rotation. Afterwards, the IgG sepharose beads were spun down and the supernatant was transferred into a fresh tube to which 1 volume of calmodulin binding buffer (10 mM β-mercaptoethanol, 10 mM Hepes-KOH pH 8.0, 150 mM NaCl, 1 mM MgOAd, 1 mM imidazole, 0.1% Igepal CA-630 (Sigma), 2 mM CaCl$_2$) was added. The IgG sepharose beads were washed 3 times with 300 µl of calmodulin binding buffer; the supernatants from the washing steps were then added to the first supernatant. The final 1200 µl were added to 100 µl of calmodulin beads (Stratagen) (previously washed 3 times with 1 ml of calmodulin binding buffer). 1/250 volumes of 1M CaCl$_2$ were added to the mix and incubated at 4°C for 90 minutes with rotation. The mix was spun down, the supernatant was removed and the calmodulin beads were washed 2 times with calmodulin binding buffer and 3 times with calmodulin rinsing buffer (50 mM NH$_4$HCO$_3$, 75 mM NaCl, 1 mM MgOAc, 1 mM imidazole, 2

mM $CaCl_2$). The protein elution was done by addition of 200 µl of calmodulin elution buffer (50 mM NH_4HCO_3, 25 mM EGTA), followed by incubation at room temperature for 5 minutes with agitation. The calmodulin beads were spun down and the supernatant recovered to a fresh tube. The elution was repeated 4 times. The final eluates were frozen at -80°C until protein quantification and mass spectroscopy analysis.

All the spin-down centrifugations were done at 4°C, 1500 rpm for 1 minute.

3.5.4 Buffer exchange and protein concentration

3.5.4.1 Dialysis

Dialysis was used for buffer changing. The protein solution was introduced into a bag of a semi-permeable membrane made of cellulose acetate with a cut-off of 10 kDa prepared as recommended by the manufacturer (Sigma). The sample was dialysed against the desired buffer. A ratio of 100 times the volume of buffer compared to sample volume was used. Dialysis was performed at 4°C in a beaker under slow stirring of the bag from 3 hours to overnight. During the dialysis process the buffer was changed from 2 to 3 times.

3.5.4.2 Protein concentration

Amicon Ultra Centrifugal Filter Devices (Millipore) were used to concentrate protein samples. The instructions of the manufacturers were followed. The centrifugations were carried out at 4°C at maximum speed on a Megafuge 1.0R Hearaeus centrifuge for volumes inferior to 4 ml and on an eppendorf centrifuge 5810R for volumes from 4 to 15 ml.

3.5.5 Protein quantification

Quantification of proteins was performed with the kit BCA - Protein Assay Reagent A from Pierce. The quantification was done following the microplate procedure provided with the kit.

The Nanodrop spectrophotometer ND-1000 from Peqlab was also used to quantify protein samples. The instructions of the manufacturer were followed.

3.5.6 SDS- Poly-Acrylamide Gel Electrophreis (SDS-PAGE)

3.5.6.1 SDS-PAGE (Laemmli, 1970)

SDS-Poly-Acrylamide Gel Electrophoresis (PAGE) was performed in Hoefer slab gel units or in the mini-PROTEAN® 3 system from Biorad, assembled according to the instructions of the manufacturers. The separating gel was poured, overlaid with 70% ethanol and rinsed with H_2O after polymerization. Afterwards, the stacking gel was prepared, the gel unit assembled and the gel overlaid with 1 x running buffer (25 mM Tris base, 0.2 M Glycine,

0.1 % (w/v) SDS). Protein samples mixed with Laemmli sample buffer (10 % (v/v) Glycerol, 5 % (v/v) β-Mercaptoethanol, 3 % (w/v) SDS, 62 mM Tris, 5 % (w/v) Bromophenol Blue, pH adjusted to 6.8 with HCl) were denatured for 5 min (20 minutes in case of bacterial cultures taken in 1x Laemmli sample buffer) at 95 °C and loaded onto the gel. Separation of protein samples including a protein marker (Biorad prestained protein marker, 161-0373 (see appendix B)) was performed at up to 20 mA in a power pac 300 from Biorad.

Acrylamide content	6 %	10 %	12.5 %	15 %
4x Lower Gel Buffer (ml)	1.5	1.5	1.5	1.5
30 % Acryl-/Bisacrylamide (ml)	1.2	2	2.5	3
H_2O (ml)	3.3	2.5	2	1.5
10 % APS (μl)	36	36	36	36
TEMED (μl)	3.6	3.6	3.6	3.6

Table 7: Composition of Separating Gels (Laemmli, 1970). APS: Ammonium peroxidisulafte; TEMED: N,N,N´,N´-Tetramethyl-ethylene diamine.

The lower gel buffer (LGB) is kept in stock 4x concentrated and contains 1.5 M Tris base pH 8.8 and 0.4 % SDS. The upper gel buffer (UGB) is also kept in 4x concentarted stocks and is composed of 0.5 M Tris base pH 6.8 and 0.4 % SDS.

The stoks of acrylamide/bisacrylamide are prepared by dissolving 29% acrylamide (w/v) and 1% N,N´Methylene Bisacrylamide (w/v) in H_2O, followed by filtration.

The stacking gel solution is prepared by adding 12.5 ml of UGB and 6.5 ml of 30% acrylamide to 31 ml of H_2O. For each gel, 2 ml of this solution are mixed with 12 µl 10 % (w/v) APS and 4 µl TEMED before pouring.

3.5.6.2 SDS-PAGE Gradient gels

Gradient gels were prepared from two starting mixes containing 7% and 20% bis/acrylamide. The solutions were combined gradually with the help of a mixer and pumped into the gel units with Minipuls 2 pump from Gilson.

3.5.6.3 SDS-PAGE (Dasso and Jackson, 1989)

In order to better separate *in vitro* translation products, a protocol resulting in higher resolution of proteins was used (Dasso and Jackson, 1989). Acrylamide and bisacrylamide were prepared as separate solutions and only mixed directly before preparing the SDS-PAGE. The composition of the separating gel was as listed in table 8.

Acrylamide content	6 %	12.5 %	15 %	17.5 %	20 %
4x Lower Gel Buffer (ml)	1.5	1.5	1.5	1.5	1.5
30 % (w/v) Acrylamide (ml)	1.2	2.5	3	3.5	4
2.5 % (w/v) Bisacrylamide (ml)	0.209	0.209	0.209	0.209	0.209
H_2O (ml)	3.06	1.8	1.26	0.758	0.261
10 % (w/v) APS (µl)	30	30	30	30	30
TEMED (µl)	3	3	3	3	3

Table 8: Composition of separating gels (Dasso & Jackson, 1989).

The stacking gel was composed of 333 µl 30 % (w/v) acrylamide, 104 µl 2.5 % (w/v) bisacrylamide, 500 µl 4x UGB, 1.06 ml H_2O, 20 µl 10 % (w/v) APS and 2 µl TEMED. When the translation products were detected by radiolabelling and fluography (3.5.6.4); the [^{14}C]-labelled protein marker CFA626 from Amersham Biosciences was used (see appendix B).

3.5.6.4 Fluorography

[^{35}S]-methionine labelled proteins were separated on SDS-PAGE. The gel was washed twice for 15 minutes at room temperature with rotation in Enhancer solution (1M sodium salicylate, 45% methanol) to increase the signal and lower the background. After drying with vaccum on Whatman^{TM} 3MM paper, the gel was exposed to a KODAK BioMax MR film overnight at -80°C.

3.5.6.5 Coomassie Staining of Polyacrylamide Gels

The gels were stained by incubation for 1 hour in commassie staining buffer (0.4 % (w/v) Biorad Commassie Brilliant Blue R250, 45 % (v/v) methanol, 10 % (v/v) acetic acid, filter before use) and destained by exchanging the staining buffer by water and boiling the gel for several times in the microwave. Gels were vacuum-dried (Slab Gel Dryer SGD 4050, Savant) on Whatman^{TM} 3MM paper for 1 hour at 80°C.

3.5.6.6 Silver Staining of Polyacrylamide Gels

In order to obtain higher detection sensitivity, proteins were visualized by silver staining. Proteins were fixed by incubating the gels for 1 hr in fixing solution (50 % methanol, 12 % acetic acid, 0.05 % formaldehyde). Subsequently, the gels were washed three times for 20 minutes with 50 % ethanol. For sensitization, gels were placed in 0.02 % $Na_2S_2O_3$ for 1 minute and washed three times 20 seconds with H_2O. The gels were then incubated with staining solution (0.2 % AgNO3, 0.075 % formaldehyde) for 20 minutes and washed twice for

20 seconds with H_2O. Proteins were developed with developing solution (6% Na_2CO_3, 0.0004% $Na_2S_2O_3.5H_2O$, 0.05% formaldehyde) for 10 minutes or until the protein bands became visible. Washing was done twice for 2 minutes with H_2O. The development was stopped by incubation with stopping solution (50 % methanol, 12 % acetic acid) for 10 min and the final washing was performed in 50% methanol for 20 minutes.

3.5.7 Western blot analysis

For western blot analysis, protein samples and prestained protein marker (Biorad prestained protein marker, 161-0373 (see appendix B)) were separated on SDS-PAGE. The proteins were then transferred onto a membrane. For that, Immobilon™-P Transfer Membrane (Millipore) was pre-soaked in methanol and placed together with 4 pieces of Whatman™ 3MM paper and 2 pads in the plastic support (Biocom). The transfer was performed in the omniPAGE Blot mini (Biocom) filled with transfer buffer (1 % (w/v) glycine, 20 % (v/v) methanol, 25 mM Tris base pH 8.8) for 2 hrs at 400 mA. The transfer efficiency was verified by staining the membrane with Ponceau S solution (Sigma) and washing with H_2O.

The immunoblot analysis was started by saturating the non-specific binding sites via incubation with blocking buffer (0.2 % Tween 20, 0.2 % I-Block (Tropix) in 1x PBS) for 30 minutes shaking. Subsequently, the membrane was incubated with the primary antibody for 1 hour or overnight (in presence of 0.002% NaN_3) at 4°C with rotation, followed by three times washing for 10 minutes in 1x PBS/T (1.4 mM KH_2PO_4, 2.7 mM KC, 4.3 mM Na_2HPO_4, 137 mM NaCl, 0.1% Tween 20). Incubation with the secondary antibody followed for 1 hour at 4°C with rotation.

For detection of alkaline phosphatase (AP) conjugated secondary antibodies, the membrane was washed with tap water and incubated with 5 ml alkaline phosphatase buffer (5 mM MgCl2, 100 mM NaCl, 100 mM Tris-HCl pH 9.6) supplemented with 25 µl NBT (Nitro blue tetrazolium) (5 % (w/v) in 90 % dimethylformamide) and 25 µl BCIP (2.5 % (w/v) 5-bromo-4-chloro-3-indolyl phosphate disodium salt, Sigma) until the proteins were visible (1 to 2 minutes). The colour reaction was stopped with H_2O.

For horseradish peroxidase conjugated (HRP) antibodies, the detection was performed with the Super Signal® West Pico chemiluminescent substrate kit from Pierce. After incubation with the secondary antibody the membrane was washed three times 10 minutes with 1x PBS/T and 2 times 10 minutes with 1x PBS and covered with a 1:1 mix of solutions of the detection kit for 5 minutes. The solution was removed and the membrane was wrapped in SaranWrap and exposed to an autoradiography film (CL-X Posuse™ Film, Pierce).

Primary antibodies	Dilution
rabbit anti eIF4GI (N-terminal, antiserum, gift from R. Rhoads, Shreveport, LA)	1:8000
rabbit anti β-actin (polyclonal, Sigma)	1:200
rabbit anti PABP (polyclonal, gift from Luiza Deszcz, MFPL)	1:1000
mouse anti eIF1α (polyclonal, gift from J. Pelletier, McGill Uni., Montreal)	1:2000
rabbit anti HRV2 2A^{pro} (antiserum, gift from Andrea Reischl, MedUni Vienna)	1:1000
goat anti GST (polyclonal, GE Healthcare)	1:10,000

Table 9: List of primary antibodies used in this work.

Secondary antibodies	dilution
His Probe™ HRP conjugated (Pierce)	1:10,000
anti rabbit HRP conjugated (Jackson)	1:20,000
anti goat HRP conjugated (Jackson)	1:20,000
anti rabbit AP conjugated (Sigma)	1:5000
anti mouse AP conjugated (Biorad)	1:10,000

Table 10: List of secondary antibodies used in this work.

3.5.8 Maldi-Tof Mass Spectroscopy analysis

Maldi-TOF MS (Matrix assisted laser desorption ionization time of flight mass spectrometry) allows the identification of proteins that are separated by SDS-PAGE (see 3.5.6.1) and e.g. silverstained (see 3.5.6.6) and digested enzymatically, preferentially with trypsin. The peptide masses from the enzymatic digest are then compared to theoretical mass values in the databases by using the Mascot and Peptide Search softwares. The measurements were done at the Mass Spectrometry Facility of Max F. Perutz Laboratories headed by Professor Gustav Ammerer.

3.5.9 NMR (Nuclear Magnetic Resonance)

NMR is a method used to determine the structure of a protein in solution and investigate protein dynamics. The influence of a ligand on protein structure and/or dynamics can be measured in the absence or presence of for example a substrate. The measurements were done by Dr. Georg Kontaxis at the Computational and Structural Biology department of Max F. Perutz Laboratories.

3.5.10 Determination of protein melting point

Protein stability can be measured by determination of its melting temperature, which is defined as the temperature at which the protein denatures. When a protein is heated above its characteristic thermal stability point (protein melting point) significant unfolding leads to exposed hydrophobic chains. This phenomenon can be measured by addition of a specific dye which is non-fluorescent in a hydrophilic environment and fluorescent in a hydrophobic environment (Yeh *et al.*, 2006). The protein is mixed with the dye and the temperature of the mix is increased constantly. When the protein reaches the melting point, it starts to unfold and consequently exposes the hydrophobic residues, which trigger the dye to emit fluorescence allowing the determination of the melting temperature easily.

The purified proteins were mixed with the SYPRO Orange dye (Invitrogen) in several dilutions, from 0.1 to 1 mg of protein mixed with 1x to 150x concentrated dye (see table 11). The dilutions were made to find the optimal ratio Protein/dye. The melting temperature was measured in a real-time PCR machine (Biorad) using a single cycle from 20°C to 95°C, in which the temperature was increased 1°C each 30 seconds.

Protein (mg)	SYPRO Orange dye (x times concentrated)		
0,1	10x	5x	1x
0,2	30x	15x	5x
0,3	50x	30x	10x
0,5	150x	100x	50x
1	150x	100x	50x

Table 11: Dilutions of protein/SYPRO Orange dye for protein melting point detection.

3.5.11 Enzymatic reactions of proteins

To measure the cleavage of β-actin and eIF1α by HRV2 and HRV14 $2A^{pro}$, 8µl of RRL (promega) or 50 mg of HeLa cell extracts (see 3.5.2.2) were incubated with 100 ng of HRV2 and HRV14 $2A^{pro}$ at 30°C (overnight with the HeLa extracts and 2 hours with the RRLs) in buffer A (50 mM Tris-HCl pH 8.0 , 50 mM NaCl, 1 mM EDTA, 5 mM DTT, 5% glycerol). the total volume was 10 µl. The reaction was stopped by placing the sample on ice and adding 10 µl of 2x Laemmli sample buffer. Controls were made with non-incubated samples and incubation with buffer only. The samples were then analyzed by SDS-PAGE (3.5.6.1), followed by immunoblotting using the appropriate antibody (3.5.7).

4 Results

4.1 Specificity of HRV 2A proteinases

The 2A[pro] used in this work are from HRV2, which belongs to the genetic group A and enters the cell via LDL receptor; and HRV14, a member of the genetic group B which binds to ICAM-I. Our work was focused on investigating the substrate specificity of the 2A[pro] of these two viruses.

4.1.1 Polyprotein and eIF4GI processing

HRV2 and HRV14 2A[pro] share only 40% identity at the amino acid level. The kinetics of both proteins for self cleavage is very similar. For HRV2 2A[pro] in the rabbit reticulocyte lysate (RRL), 50% of the self-cleavage of VP1-2A[pro] is complete at 20 minutes and the complete cleavage is achieved between 60 and 120 minutes (figure 15A). HRV14 2A[pro] reaches 50% cleavage at 30 minutes and finishes self-processing between the first and second hours as HRV2 2A[pro] (figure 15B).
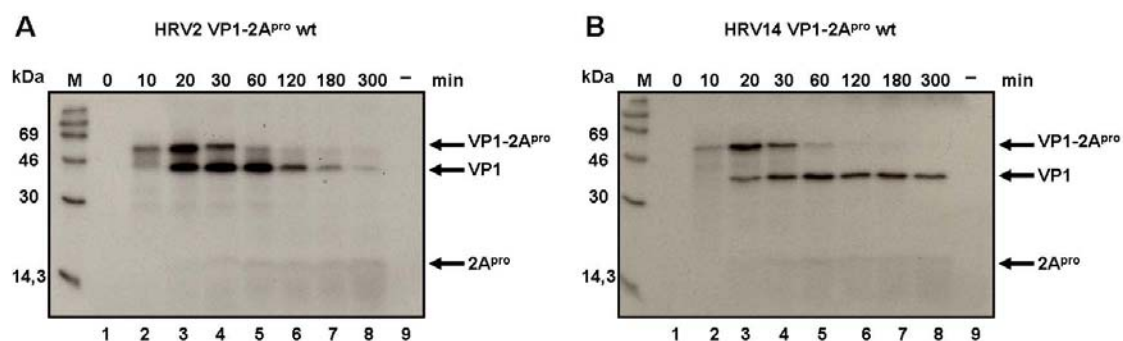
Figure 15: Fluorography of a 17.5% SDS-PAGE showing an in vitro translation experiment. A) HRV2 VP1-2A[pro] wild-type; **B)** HRV14 VP1-2A[pro] wild-type. RRLs were incubated with or without 10 ng/µl of the indicated mRNAs as described in section 3.4.2. 10 µl samples were taken at the indicated time points after mRNA addition and protein synthesis was terminated by addition of unlabeled methionine and cysteine and Laemmli Sample Buffer. Aliquots were analyzed on SDS-PAGE for protein synthesis and thus self-processing of 2A[pro]. Lane 9 corresponds to the negative control (without RNA) taken at the latest time point.

RRLs contain the eIF4GI and II, which are cleaved by 2A[pro]. Therefore, we can observe eIF4GI cleavage by 2A[pro] by simply analysing the extracts where the proteinases were translated via western blot against eIF4GI. In contrast with self cleavage, we observed

that the cleavage of eIF4GI does not occur at similar rates for HRV2 and HRV14 2A^{pro}. HRV2 2A^{pro} cleaves the translation factor during the first hour whilst HRV14 2A^{pro} cleavage is only observed after two hours and is not complete after five hours. Figure 16 shows an immunoblot against eIF4GI of the same samples of figure 15.
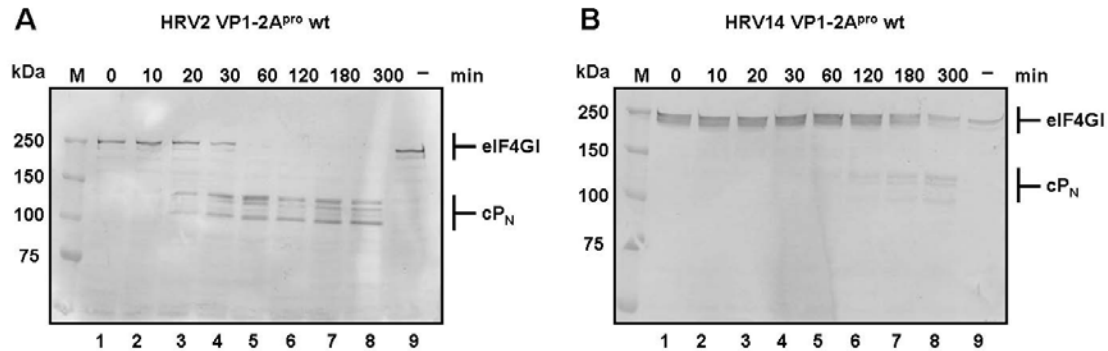

Figure 16: Immunoblot of 6% SDS-PAGE of the samples from figure 15 showing cleavage of eIF4GI by A) HRV2 VP1-2A^{pro} and B) HRV14 VP1-2A^{pro}. The proteins were detected by immunoblotting using the eIF4GI N-terminal antiserum (1:8000).

We compared the HRV2 and HRV14 2A^{pro} cleavage sites with the eIF4GI cleavage site recognized by HRV2 2A^{pro}. The cleavage sites of HRV2 and HRV14 are shown in table 12. The HRV14 2A^{pro} cleavage sites of eIF4GI and II have not been determined yet. However, CV and PV cleave eIF4GI at the same sequence as HRV2 2A^{pro} (Lamphear *et al.*, 1993; Zamora *et al.*, 2002). This supports the possibility that HRV14 2A^{pro} recognizes the same sequence on eIF4GI. In order to determine whether the eIF4GI cleavage site can be recognized in the context of the polyprotein, we substituted the cleavage sequence on the polyprotein by the sequence recognized by HRV2 2A^{pro} in eIF4GI. The result is presented in figure 17. HRV2 2A^{pro} self-processing of the new cleavage site is slower than that of the wild type, but the eIF4GI cleavage sequence is well tolerated in the polyprotein context (figure 17A). However, HRV14 2A^{pro} is not able to recognize this sequence in the same context. The first indications of cleavage could only be observed 180 minutes after translation initiation (figure 17B).

Substrate	Cleavage sites		
	P	*****	**P'**
	54321		**1234**
HRV 2 polyprotein	IITTA (850)	*	GPSD
HRV14 polyprotein	DIKSY (856)	*	GLGP
PV1 polyprotein	DLTTY (881)	*	GFGH
eIF4GI	TLSTR (681)	*	GPPR
eIF4GII	PLLNV (699)	*	GSRR

Table 12: 2A^{pro} cleavage sites on the respective polyproteins and eIF4G homologues. The viral polyprotein sequences represent the C terminus of VP1 and the N terminus of 2A^{pro}, respectively. Numbers in bold indicate the positions of amino acid residues relative to the cleavage site. The numbers in brackets refer to the P1 residue in the polyproteins and eIF4G isoforms. The cleavage sites on eIF4G isoforms are the ones recognized by HRV2 2A^{pro} (Gradi *et al.*, 2003).
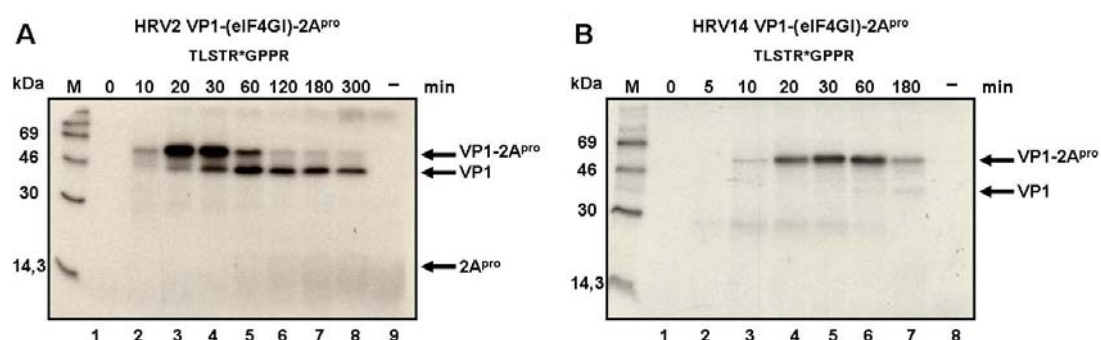
Figure 17: Fluorography of a 17.5% SDS-PAGE showing the processing of HRV2 and HRV14 VP1-2A^{pro} bearing the eIF4GI cleavage site. A) HRV2 VP1-(eIF4GI)-2A^{pro}; **B)** HRV14 VP1-(eIF4GI)-2Apro. RRLs were incubated with or without 10 ng/µl of the indicated mRNAs as described in section 3.4.2. Samples were taken at the indicated time points after mRNA addition and protein synthesis was terminated by addition of unlabeled methionine and cysteine and Laemmli Sample Buffer. Aliquots were analyzed on SDS-PAGE for protein synthesis and thus self-processing of 2A^{pro}. Lane 9 correspond to the negative control (without RNA) taken at the latest time point.

After observing such a different result for the two proteinases, we wanted to know in more detail which residues are responsible for such a difference. The cleavage sequences of HRV14 2A^{pro} and eIF4GI differ significantly at the positions P3 (serine instead of lysine), P1 (arginine instead of tyrosine) and P2' to P4' (ProProArg instead of LeuGlyPro) (the nomenclature Pn-P1-P1'-Pn' is that of Schechter and Berger 1967). To find out which of these substitutions were responsible for the absence of cleavage, we decided to change the

eIF4GI cleavage sequence back to the HRV14 wild type by introducing one residue at the time. As the P1 position is known to be important in defining specificity in chymotrypsin-like enzymes (Brändén and Tooze, 1999), we chose to start by replacing the P1 arginine with tyrosine (figure 18). Indeed this substitution was sufficient to restore HRV14 2A^{pro} self-cleavage to almost wild type levels.
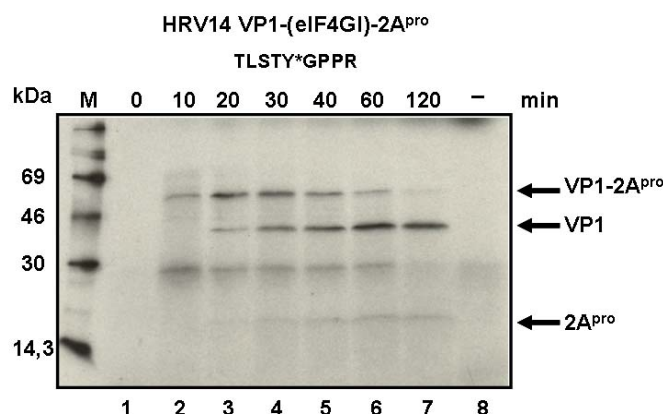

Figure 18: Fluorography of a 17.5% SDS-PAGE showing the processing of HRV14 VP1-2A^{pro} bearing the eIF4GI cleavage site in which the P1 residue arginine was substituted by tyrosine. RRLs were incubated with or without 10 ng/µl of the indicated mRNAs as described in section 3.4.2. Samples were taken at the indicated time points after mRNA addition and protein synthesis was terminated by addition of unlabeled methionine and cysteine and Laemmli Sample Buffer. Aliquots were analyzed for protein synthesis by SDS-PAGE and thus self-processing of 2A^{pro}. Lane 8 correspond to the negative control (without RNA) taken at the latest time point.

To see whether the tyrosine at P1 position is also crucial for recognition of the cleavage site in the wild type sequence, we performed the reverse experiment. Replacing the wild type tyrosine by an arginine gave us the construct HRV14 VP1 (Y289R) 2A^{pro}. Figure 19A shows that the HRV14 2A^{pro} can no longer perform self-cleavage, even after 7 hours of translation. However, some non-specific protein degradation is observed after 2 hours. As controls, we used the constructs HRV14 VP1 (K287S) 2A^{pro} and HRV14 VP1 2A^{pro} L2P which contain a serine at P3 position and a proline at P2' position respectively (as in the eIF4GI cleavage sequence). These mutations do not affect HRV14 2A^{pro} performance whatsoever (figure 19B and 19C). The band seen at 30 kDa visible in figures 19B and 19C is an unspecific product formed by the RRL itself as it is present also in the negative control. In conclusion, these results show that HRV2 and HRV14 2A^{pro} differ markedly in their specificity at P1. HRV2 2A^{pro} can accept arginine at P1 whereas HRV14 2A^{pro} cannot.
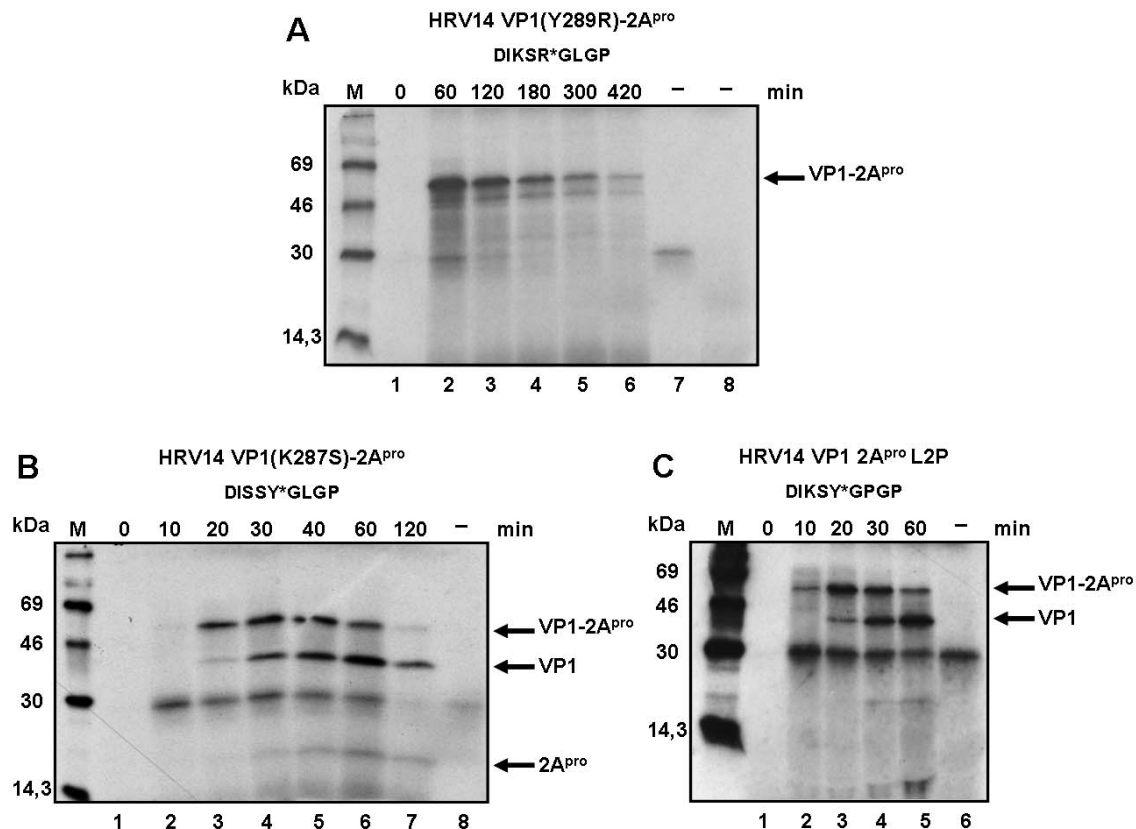
60

Figure 19: Fluorography of a 17.5% SDS-PAGE showing processing of HRV14 VP1-2A^{pro} containing several substitutions at the cleavage site. A) HRV14 VP1 (Y289R) 2A^{pro}; **B)** HRV14 VP1 (K287S) 2A^{pro} **C)** HRV14 VP1 2A^{pro} L2P. RRLs were incubated with or without 10 ng/µl of the indicated mRNAs as described in section 3.4.2. 10 µl samples were taken at the indicated time points after mRNA addition and protein synthesis terminated by addition of unlabeled methionine and cysteine and Laemmli Sample Buffer. Aliquots were analyzed for protein synthesis by SDS-PAGE and thus self-processing of 2A^{pro}. Lanes 7 and 8 in panel A are the negative control at 60 and 420 minutes respectively. Lanes 8 and 6 in panel B and C respectively correspond to the negative control (without RNA) taken at the latest time points.

The HRV14 genome is more similar to enteroviruses than to other rhinoviruses (Wang *et al.*, 1998) and the cleavage site of HRV14 2A^{pro} on the polyprotein is more related to PV than to other rhinoviruses (table 12). The amino acid identity between the HRV14 2A^{pro} and PV1 is 47% (figure 20); the residue at position P1 is tyrosine for both proteinases (table 12). For these reasons, we decided to replace the P1 tyrosine on PV1 cleavage site by an arginine and see whether the PV1 2A^{pro} is affected as HRV14 2A^{pro}. The pCITE PV1 VP1 2A^{pro} (constructed by Andreas Roetzer (Roetzer, 2004)) was modified into pCITE PV1 VP1 (Y302R) 2A^{pro}. Figure 21 shows that the presence of an arginine at P1 site slightly delays PV1 2A^{pro} self-processing. 50% cleavage of the wild type substrate is reached between 30

and 60 minutes, whilst for the mutant it happens between 60 and 120 minutes. In conclusion, PV1 2A^{pro} self-processing differs from that of HRV14 2A^{pro}.


```
HRV14_2A    1 GLGPRYGGIYTSNVKIMNYHLMTPEDHHNLIAPYPNRDLA 40
PV1_2A      1 GFGHQNKAVYTAGYKICNYHLATQDDLQNAVNVMWSRDLL 40

HRV14_2A   41 IVSTGGHGAETIPHCNCTSGVYYSTYYRKYYPIICEKPTN 80
PV1_2A     41 VTESRAQGTDSIARCNCNAGVYYCESRRKYYPVSFVGPTF 80

HRV14_2A   81 IWIEGNPYYPSRFQAGVMKGVGPAEPGDCGGILRCIHGPI 120
PV1_2A     81 QYMEANNYYPARYQSHMLIGHGFASPGDCGGILRCHHGVI 120

HRV14_2A  121 GLLTAGGSGYVCFADIRQLECIAEEQ---            146
PV1_2A    121 GIITAGGEGLVAFSDIRDLYAYEEEAMEQ            149
```

Figure 20: Sequence alignment between HRV14 2A^{pro} and PV1 2A^{pro}. HRV 14 2A^{pro} shares 47% with PV1 2A^{pro}. Conserved residues are represented in blue.
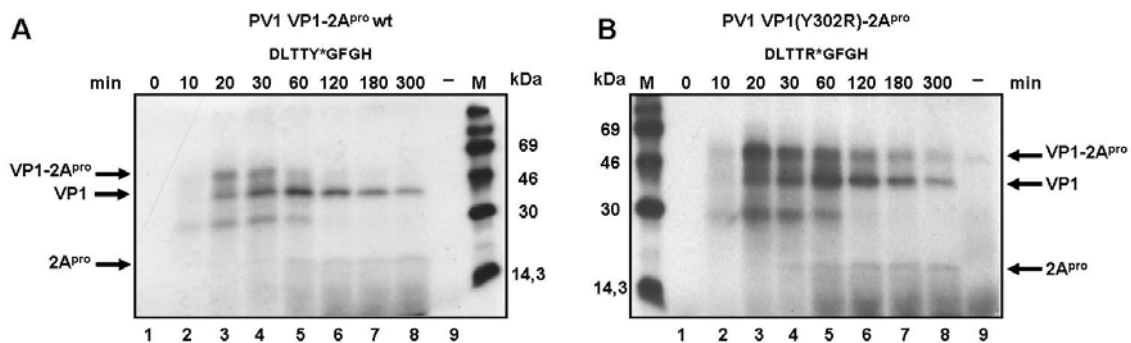
Figure 21: Fluorography of a 17.5% SDS-PAGE showing the processing of PV1 VP1-2A^{pro} wild type (A) and a mutant containing an arginine at P1 site (B). A) PV1 VP1 2A^{pro} wild type; **B)** PV1 VP1 (Y302R) 2A^{pro}. RRLs were incubated with or without 10 ng/µl of the indicated mRNAs as described in section 3.4.2. Samples were taken at the indicated time points after mRNA addition and protein synthesis terminated by addition of unlabeled methionine and cysteine and Laemmli Sample Buffer. Aliquots were analyzed for protein synthesis by SDS-PAGE and thus self-processing of 2A^{pro}. Lanes 9 correspond to the negative control (without RNA) taken at the latest time point.

After these observations, we used the structure of HRV2 2A^{pro} solved by Petersen *et al.* (1999) to look for non-conserved regions that might be important for the interaction between the active site of the proteinase and the substrate. One of these regions is formed by the residues 82 to 85 (85 to 88 in HRV14 2A^{pro}) which form one side of the substrate-binding cleft (Petersen *et al.*, 1999). These residues are part of a β-hairpin loop named the dityrosine flap that rotates and allows the proteinase to accommodate the P2 threonine in HRV2 2A^{pro} (Petersen *et al.*, 1999). We thought that this might be an important region as it is

in close contact with the substrate and is not conserved between HRV2 and HRV14. The replacement of these residues on the HRV14 2A^{pro} that contains an arginine at P1 by the equivalent residues of HRV2 2A^{pro} did not have any effect on the recognition of the substrate (figure 22, A to D). HRV14 2A^{pro} is still unable to recognize the cleavage sequence and all the material remains unprocessed. The opposite experiment replacing the residues 82 to 85 on HRV2 2A^{pro}, bearing the eIF4GI cleavage sequence, by the corresponding residues of HRV14 2A^{pro} also did not have any effect on the performance of the HRV2 2A^{pro} (figure 22, E and F).
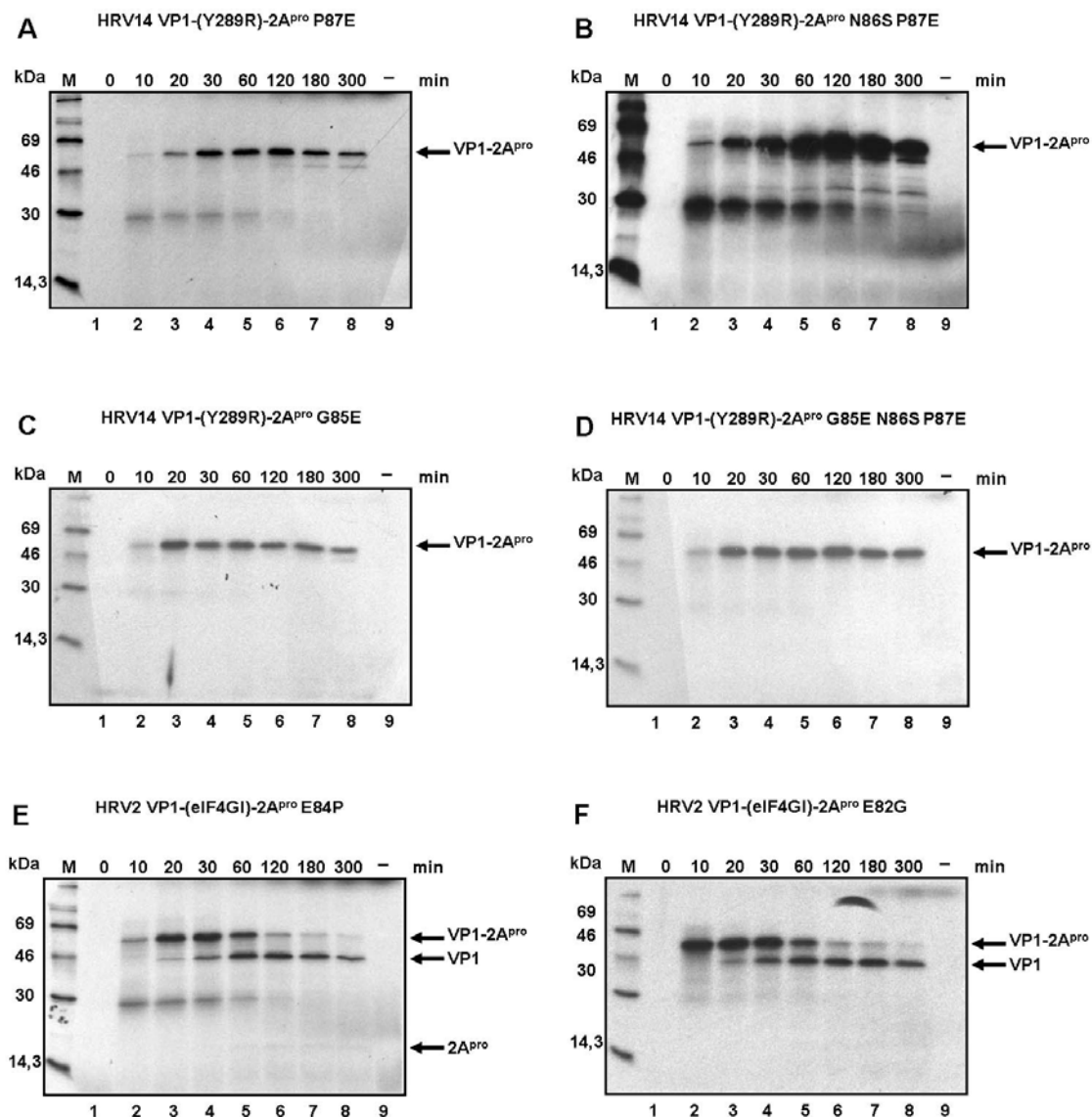
Figure 22: Fluorography of a 17.5% SDS-PAGE showing the processing of HRV14 and HRV2 VP1-2A^{pro} bearing several mutations on the 2A^{pro} sequence. A) HRV14 VP1 (Y289R) 2A^{pro} P87E; **B)** HRV14 VP1 (Y289R) 2A^{pro} N86S P87E; **C)** HRV14 VP1 (Y289R) 2A^{pro} G85E; **D)** HRV14 VP1 (Y289R) 2A^{pro} G85E N86S P87E; **E)** HRV2 VP1-(eIF4GI)-2A^{pro} E84P; **F)** HRV2 VP1-(eIF4GI)-2A^{pro} E82G. RRLs were incubated with or without 10 ng/µl of the indicated mRNAs as described in section

63

3.4.2. Samples were taken at the indicated time points after mRNA addition and protein synthesis terminated by addition of unlabeled methionine and cysteine and Laemmli Sample Buffer. Aliquots were analyzed for protein synthesis by SDS-PAGE and thus self-processing of 2A[pro]. Lanes 9 correspond to the negative control (without RNA) taken at the latest time point.

Further analysis of HRV2 2A[pro] structure showed that the side chain of Cys101 protrudes into the S1 pocket (figure 23). This is the site on the enzyme that recognizes the P1 substrate residue. At the bottom of the pocket, the presence of Glu102 provides a negative charge which presumably assists in accepting the positive charge of the arginine at position P1 (Petersen *et al.*, 1999) (figure 23). The equivalent residues to Cys101 and Glu102 in HRV14 2A[pro] are Ala104 and Glu105, respectively. Therefore, we wanted to know whether the replacement of the Ala104 for a cysteine would influence the performance of HRV14 VP1 (Y289R) 2A[pro].
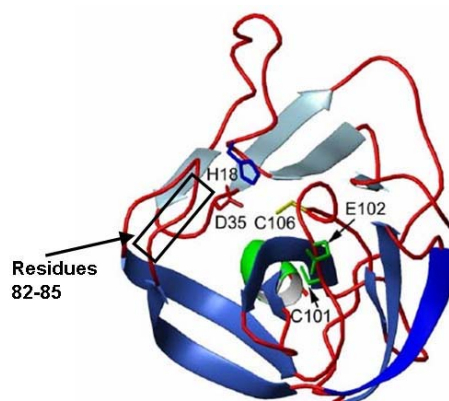
Figure 23: The structure of HRV2 2A[pro]. Ribbon diagrams of the overall structure of HRV2 2A[pro]. The single α-helix is shown in green, the β-strands of the N-terminal and C-terminal domains are shown in silver and deep blue, respectively. The three residues of the catalytic triad (His18, Asp35 and Cys106) are shown as well as the residues Cys101 and Glu102. Residues 82 to 85 are marked with a black rectangle.The figure was generated using the program Molscript (Kraulis, 1991) and was a kindly prepared by Christina Mayer.

We obtained further support for investigating this residue by analysing 2A[pro] sequences of other picornaviruses. This revealed that the residue at position 101 (for HRV2 2A[pro]) is related to the residue at the P1 site (table 13). Group A rhinoviruses contain an alanine, phenylalanine or valine at the P1 site and always a cysteine at position 101. Group B rhinoviruses and all three serotypes of polioviruses have a tyrosine at the P1 site and an alanine at position 104 (correspondent to 101 in HRV2 2A[pro]). Finally coxsackie B1, B3, B4,

B5 and B6 viruses contain a threonine at the P1 site and a serine at position correspondent to 101 in HRV2 2A^{pro} (table 13).

Virus	Cleavage site	Active site
	----------VP1--------->< --------------------------2A^{pro}-->	
	P1	**101** <u>106</u>
HRV2	.....TRPIITT**A** * GPSDMYV^7..............	^{97}GEGPCEPGD<u>C</u>GGKL^{110}....^{142}
HRV89 (genetic group A)	.....DVFTVTN**V** * GPSSMFV^7..............	^{97}GEGPCEPGD<u>C</u>GGKL^{110}....^{142}
HRV14 (genetic group B)	.....RKGDIKS**Y** * GLGPRYG^7..............	^{100}GVGPA**E**PGD<u>C</u>GGIL^{113}....^{146}
Poliovirus type 1	.....STKDLTT**Y** * GFGHQNK^7..............	^{100}GHGFA**S**PGD<u>C</u>GGIL^{113}....^{149}
Coxsackievirus B4	.....ERASLIT**T** * GPYGHQS^7..............	^{101}ATGF**S**EPGD<u>C</u>GGIL^{114}....^{150}

Table 13: Occupancy of the P1 residue of the 2A^{pro} cleavage site and residue 101 or its equivalent of 2A^{pro}. The numbers refer to the residue position on the 2A^{pro}. The P1 or equivalent residues are shown in bold face. The active site residue cysteine (residue 106 in HRV2 2A^{pro}) is underlined. The sequence identifiers are: POLG_HRV2; POLG_HRV89; POLG_HRV14; POLG_POL1M AND POLG_CXB4J (Sousa *et al.*, 2006).

In the light of these relationships, we also decided to replace the Ala104 in HRV14 2A^{pro} by serine. Indeed the activity of HRV14 2A^{pro} is partially recovered in both mutants (figure 24). The cleavage product is observed after 1 hour of translation, in contrast with the wild type alanine at position 104, in which no cleavage product is observed even after 7 hours of translation (figure 19A). The mutant with a serine at residue 104 is more efficient than the mutant bearing a cysteine at the same position (compare figure 24A with figure 24B).
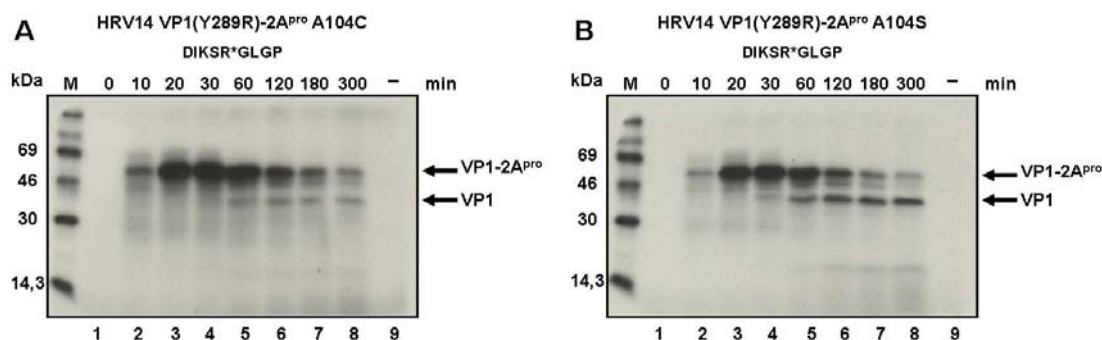
Figure 24: Fluorography of a 17.5% SDS-PAGE showing the processing of HRV14 VP1-2A^{pro} **containing an arginine at the P1 site and a mutation in position 104. A)** HRV14 VP1 (Y289R) 2A^{pro} A104C; **B)** HRV14 VP1 (Y289R) 2A^{pro} A104S. RRLs were incubated with or without 10 ng/µl of the indicated mRNAs as described in section 3.4.2. 10 µl samples were taken at the indicated time points after mRNA addition and protein synthesis terminated by addition of unlabeled methionine and cysteine and Laemmli Sample Buffer. Aliquots were analyzed for protein synthesis by SDS-PAGE and thus self-processing of 2A^{pro}. Lanes 9 correspond to the negative control (without RNA) taken at the latest time point.

In an additional experiment we wanted to investigate whether the change from a cysteine to an alanine (and serine, like in CBV4) in position 101 (equivalent residue to 104 in HRV14 2A^{pro}) in HRV2 2A^{pro} would also affect self-processing. Figure 25 shows that the processing of HRV2 VP1 2A^{pro} C101A and HRV2 VP1 2A^{pro} C101S are not affected by these mutations. The activity of HRV2 2A^{pro} remains at wild type levels. It seems that the residue at this position is important for the acceptance of bulky residues at the P1 site but not when the P1 residue has a small side chain such as alanine.
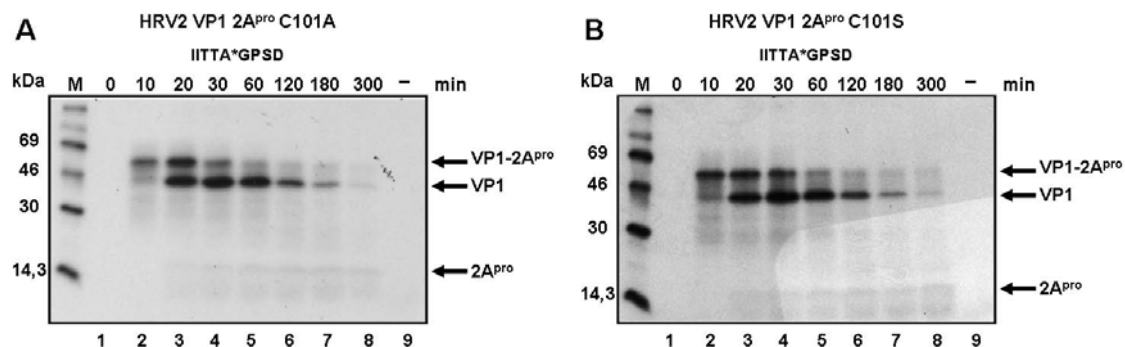
Figure 25: Fluorography of a 17.5% SDS-PAGE showing the processing of HRV2 VP1-2A^{pro} **containing a mutation in position 101. A)** HRV2 VP1 2A^{pro} C101A; **B)** HRV2 VP1 2A^{pro} C101S. RRLs were incubated with or without 10 ng/µl of the indicated mRNAs as described in section 3.4.2. Samples were taken at the indicated time points after mRNA addition and protein synthesis terminated by addition of unlabeled methionine and cysteine and Laemmli Sample Buffer. Aliquots were analyzed for protein synthesis by SDS-PAGE and thus self-processing of 2A^{pro}. Lanes 9 correspond to the negative control (without RNA) taken at the latest time point.

4.1.2 Specific inhibition of 2A^{pro} by zVAD.fmk and zVAM.fmk

Recently, Deszcz *et al.* (2004) showed that human rhinoviruses are inhibited by the caspase inhibitor zVAD.fmk, which was developed to inhibit caspases (fmk binds to SH groups of an adjacent cysteine residue causing irreversible inhibition) (Deszcz *et al.*, 2004).

The inhibitor is methylated on the aspartic acid residue so that it can cross the cell membrane. Once inside the cell, endogenous esterases remove the methyl group, allowing the compound to inhibit caspases. Rhinoviral replication is blocked due to specific inhibition of the 2A^{pro} by the methylated form of zVAD.fmk. The methyl group satisfies the preference of HRV2 2A^{pro} for hydrophobic residues at P1. As the aspartic acid is not accepted at this position by HRV 2A^{pro}, the unmethylated form of zVAD.fmk has no inhibitory effect.

Based on these observations, Deszcz *et al.* (2006) designed a new inhibitor derived from zVAD.fmk. The aspartate was replaced by a methionine, which had been shown to be a better substrate than alanine for HRV2 2A^{pro} (Skern *et al.*, 1991). The new compound was named zVAM.fmk and has no influence on caspase inhibition. Therefore, zVAM.fmk is a specific inhibitor of HRV 2A proteinases (Deszcz *et al.*, 2006). It inhibits 2A^{pro} from several rhinoviruses (HRV2, HRV14 and HRV16) both *in vivo* and *in vitro* as well as CVB4 *in vitro*.

We wanted to know whether this inhibitor is also effective against PV *in vitro*. Therefore, we used the pCITE vector containing the sequence of VP1 and 2A^{pro} of PV1 (construct from Andreas Roetzer (Roetzer, 2004)) to obtain the RNA. This RNA was *in vitro* translated in presence and absence of zVAM.fmk. In a initial time course experiment of 1 hour, we tried to inhibit PV1 2A^{pro} by adding 50 µM of zVAM.fmk. The inhibitor was added 10 minutes after translation initiation; control reaction mixtures contained DMSO only, as zVAM.fmk is dissolved in DMSO. This concentration was shown to inhibit HRV14 2A^{pro} (Deszcz *et al.*, 2006); however, it has no effect on PV1 2A^{pro} (figure 26A). Therefore, we raised the concentration of zVAM.fmk to 100 µM and 200 µM. Once again zVAM.fmk was added 10 minutes after initiation of protein synthesis. Figure 26B shows that zVAM.fmk has no effect in the self-processing of PV1 2A^{pro} *in vitro*, even at concentrations as high as 200 µM.
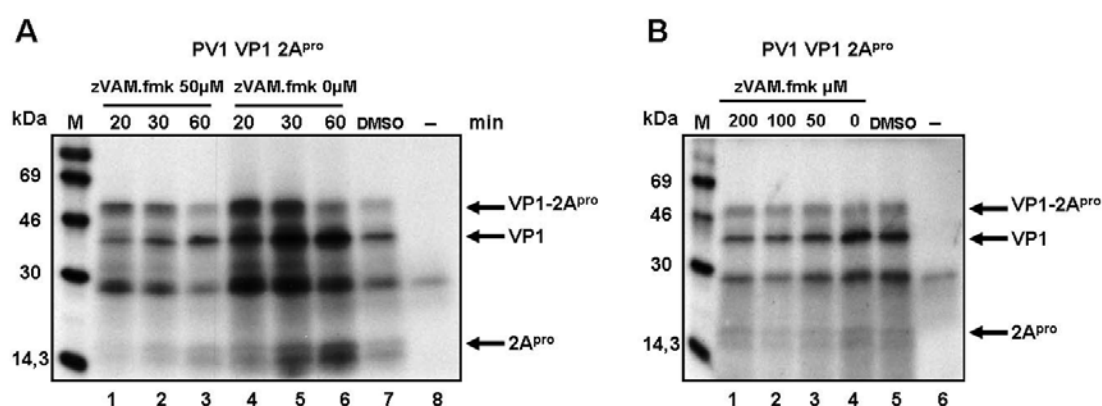

Figure 26: 17.5% SDS-PAGE showing the inhibition of self-processing of HRV2 and HRV14 2A^{pro} by zVAM.fmk. A) Autoradiogram of a time course of in vitro translation of PV1 VP1 2A^{pro}. Ten minutes after the start of protein synthesis, zVAM.fmk was added to a final concentration of 50 µM.

Samples were taken at the times indicated, and 2A^{pro} self-cleavage from VP1 was examined. In lane 7, translation was performed using 0.05% DMSO only, and lane 8 shows the negative control without RNA taken at the latest time point. **B)** Autoradiogram of the in vitro translation products of RNAs from PV1 VP1 2A^{pro}. Ten minutes after the start of protein synthesis, zVAM.fmk was added to a final concentration of 200 µM, 100 µM, or 50 µM (lanes 1 to 3). After 60 min of translation, samples were taken and analyzed. Lane 4 shows 60 minutes translation of the RNAs without any inhibitor; translation was also performed in the presence of 0.2% DMSO only (lane 5) and without RNA (lane 6).

4.2 Analysis of HRV14 2A^{pro}

4.2.1 Expression and purification

It was shown in section 4.1.1 that HRV14 2A^{pro} has a different substrate specificity compared to HRV2 2A^{pro}. HRV2 2A^{pro} cleaves a substrate bearing an arginine at P1 position; HRV14 2A^{pro} is unable to do so unless the residue in position 104 is a cysteine or a serine. Even then, the cleavage is delayed and incomplete compared to wild type levels. Another important difference observed was the cleavage of eIF4GI and II. eIF4GI cleavage by HRV14 2A^{pro} is significantly delayed compared to HRV2 2A^{pro} (figure 16) and the same is true for eIF4GII (Schmid, 2002). Moreover, the susceptibility of HRV14 2A^{pro} to the inhibitor zVAM.fmk seems to be different from that of HRV2 2A^{pro}. HRV14 2A^{pro} is more sensitive to zVAM.fmk in self-processing and more resistant to the inhibitor during the intermolecular cleavage; this is opposite to the results with HRV2 2A^{pro} (Deszcz *et al.*, 2006).

To find explanations for these differences, we wished to obtain the three-dimensional structure of HRV14 2A^{pro}. Therefore, we set out to clone the HRV14 2A^{pro} C109A (the inactive form of the proteinase) carrying a C-terminal His tag into the plasmid pGEX-6P1, which contains an N-terminal GST tag (figure 27).
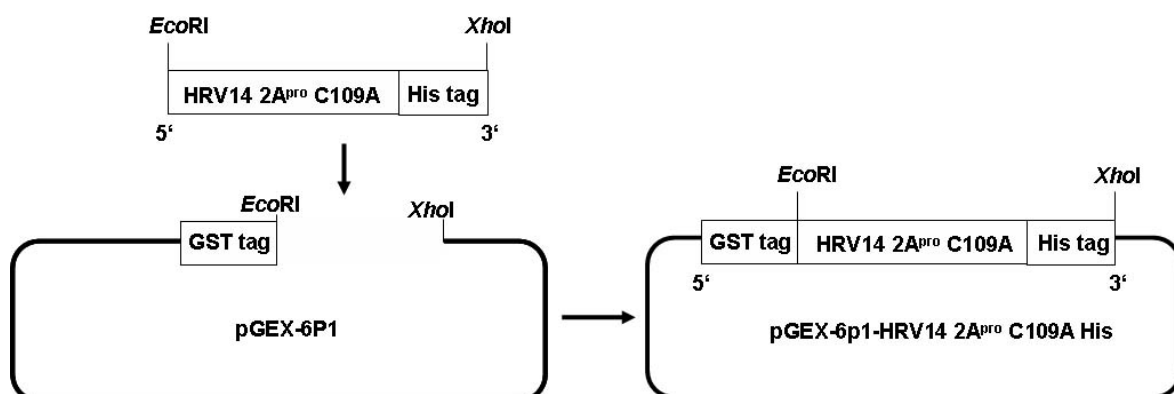

Figure 27: Cloning strategy to introduce the inactive form of HRV14 2A^{pro} carrying a His tag into pGEX-6P-1. pGEX-6P-1-HRV14 2A^{pro} C109A. The ORFs were amplified with primers containing *Eco*RI (primer named TIM979) and *Xho*I (primer named TIM1411) restriction sites. The reverse primer contained also 6 histidines before two stop codons.

The inclusion of the His tag was based on previous results. The expression of HRV14 2A^{pro} with a GST tag alone gave two products: the complete 2A^{pro} and a truncated form which was lacking the C-terminus (Cencic, 2005). We thought that by introducing an additional C-terminal tag, we would be able to purify the intact 2A^{pro}. The introduction of the His tag indeed prevented the formation of the truncated form as can be observed in figure 28B. After cleavage from the GST tag, there was only one band visible corresponding to the intact protein with the His tag. The binding of the protein to Ni^{2+} column showed that the His tag was present, and therefore that the protein was not truncated (figure 29B).

As the pGEX-6P1 vector is under control of the *tac* promoter, we used the bacterial strain JM101 for the expression. These cells contain the *lacI*^{q} gene that encodes a repressor protein which binds to *lac* operator sequences and blocks transcription of down-stream sequences. However, the *lacI*^{q} gene product dissociates from the lac operator in the presence of IPTG (Amann *et al.*, 1988). The optimal conditions to express this protein were 0.1 mM of IPTG and incubation at 16°C for 5 hours (figure 28A). The volume of bacterial culture was 2 litres.
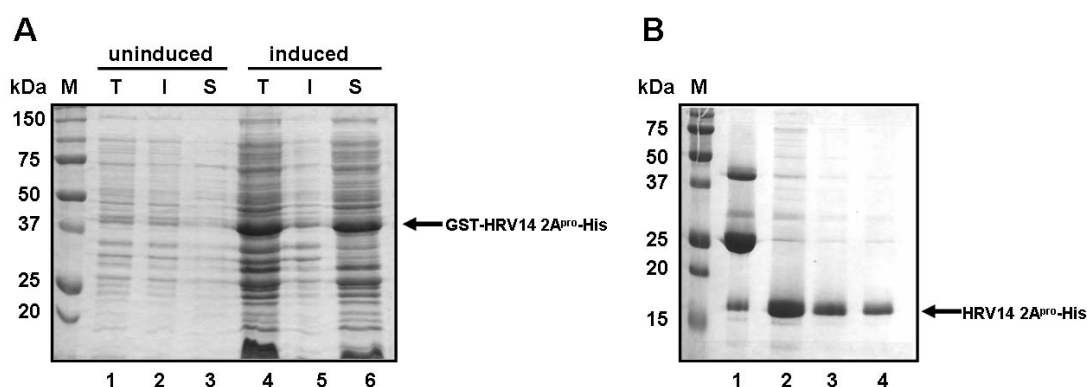
Figure 28: Coomassie stained SDS-PAGE (10% (A) and 15% (B) polyacrylamide) of the expression of HRV14 2A^{pro}-GST-His (A) and the protein after incubation with PreScission proteinase (Amersham) (B). Protein standards in kDa are shown in line M. A) T: total fraction; I: insoluble fraction; S: soluble fraction. The expression was carried out at 16°C with 0.1 mM IPTG for 5 hours. Lanes 1 to 3 show the uninduced samples, lanes 4 to 6 the induced samples. 2μl of each sample were loaded on the gel (0.02% of the sample total volume). B) 40 units of PreScission proteinase (Amersham) were added to the soluble fraction and incubated with glutathione-sepharose beads. Lane 1 shows the beads after washing; lanes 2 to 4 show the collected supernatants with the HRV14 2A^{pro}-His. 10μl of each sample were loaded (1% of the sample total volume).

After binding and cleavage from the glutathione beads (figure 28B) in buffer A, the fractions were pooled and dialysed against phosphate buffer (500 mM NaCl, 20 mM Na-phosphate pH

7.4) according to the manufacturer of the His Trap FF 1ml column (Amersham Biosciences) instructions. Unfortunately, the protein precipitated in the new buffer.

We repeated the expression using the same conditions described above and obtained similar results. However, this time we loaded the sample on the His Trap FF 1ml column (Amersham Biosciences) without changing the buffer. The column was equilibrated with Binding Buffer (50 mM NaCl and 50 mM Tris-HCl pH 8.0) and the sample was eluted with Elution Buffer (50 mM NaCl, 50 mM Tris-HCl pH 8.0, 500 mM imidazole) (figure 29A). However, the DTT present in the sample (which was diluted in 50mM Tris-HCl pH 8.0, 50 mM NaCl, 1mM EDTA 5 mM DTT and 5% glycerol) was enough to alter the column properties (its colour changed from light green to dark brown) and most of the protein did not bind to the column. Nevertheless, we examined the fractions and pooled those from lanes 3 to 7 (figure 29B) and stored them at 4°C.
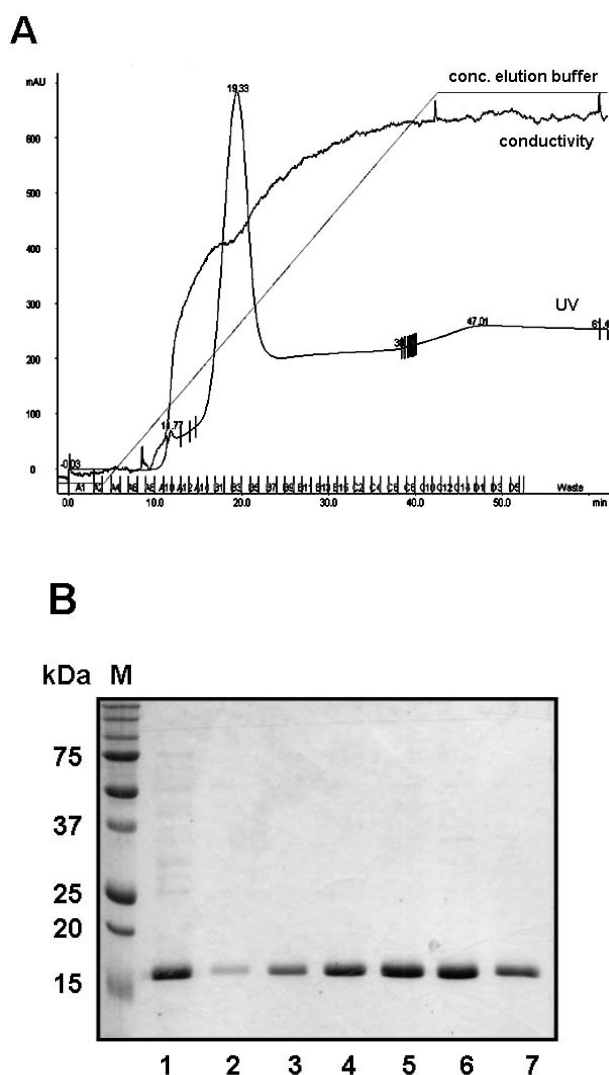
Figure 29: A) Chromatogram of HRV14 2A^{pro}-His purification performed on a HisTrap column 1 ml (Amersham). The UV units are presented in micro-arbitrary units and each fraction corresponds to 2 ml. **B) Coomassie stained 15% SDS-PAGE of the fractions collected.** Lane 1 shows the soluble fraction before loading the column (3µl of 12 ml) and lanes 2 to 7 show the fractions collected (10µl of 2ml). Protein standards in kDa are shown in line M.

After two days at 4°C, the protein had however once again precipitated. To verify the reasons for the precipitation, we dialysed the sample overnight against buffer A at pH 9.0, at 4°C. This was sufficient to re-dissolve the protein. Therefore, we decided to use buffers at pH 9.0 for future purifications.

For the next purification, we expressed 8 litres of bacterial culture under the same conditions described above, except that the buffer used to dissolve the pellet was 50 mM NaCl and 50 mM Tris-HCl pH 9.0. The major part of the expressed HRV14 2A^{pro} was insoluble (figure 30A). However, we incubated the soluble fraction with glutathione-sepharose beads (1 mL of beads per litre of culture) and found a high amount of fusion protein. Figure 30B shows the amount of HRV14 2A^{pro} cleaved from 1 mL of beads.
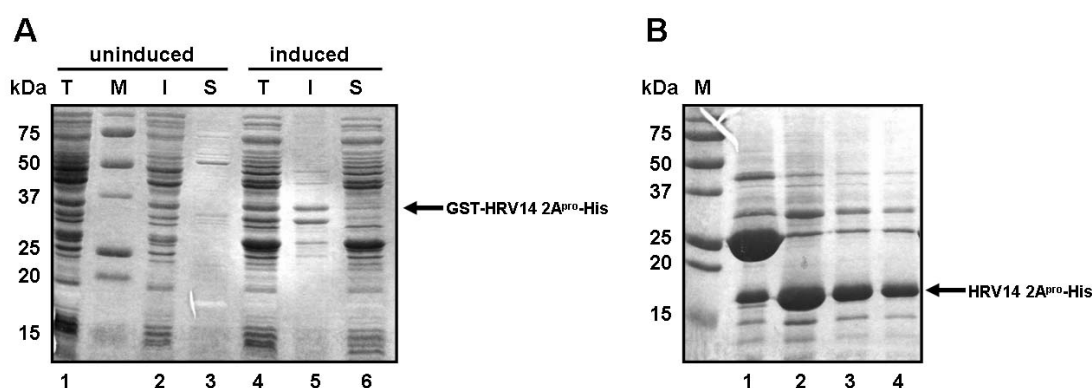

Figure 30: Coomassie stained 12.5% SDS-PAGE of the expression of HRV14 2A^{pro}-GST-His (A) and the protein after incubation with PreScission protease (Amersham) (B). A) T: total fraction; I: insoluble fraction; S: soluble fraction. The expression was carried out at 16°C with 0.1 mM IPTG overnight. Lanes 1 to 3 show the uninduced samples; lanes 4 to 6 the induced samples; 1.5µl of the samples was loaded (0.01% of the sample total volume). **B)** 40 units of PreScission protease (Amersham) were added to the soluble fraction and incubated with glutathione-sepharose beads. Lane 1 shows the beads after washing; lanes 2 to 4 show the collected supernatants with the HRV14 2A^{pro}-His. 10µl of the samples were loaded (1% of the sample total volume). Protein standards in kDa are shown in line M.

After pooling all the fractions, we had a final volume of 24 mL of protein solution which were loaded on a His Trap FF 1ml column (Amersham Biosciences), previously equilibrated with

the same buffer in which the protein was ressuspended. The elution buffer contained 50 mM NaCl, 50 mM Tris-HCl pH 9.0 and 500 mM imidazole. Figure 31A shows the chromatogram of the purification and the protein eluted from the column.
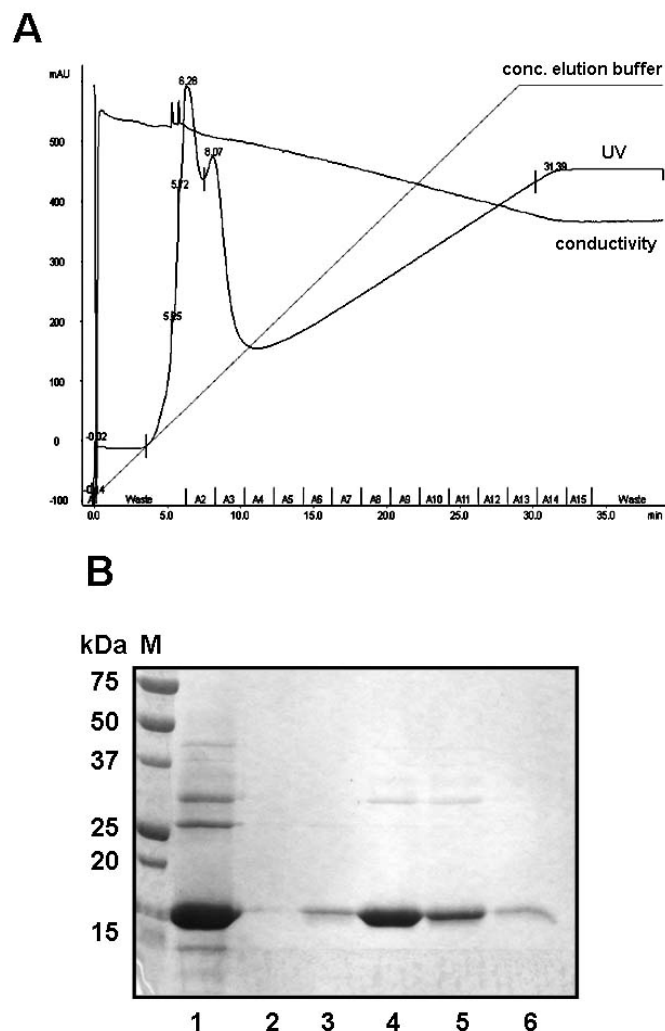

Figure 31: A) Chromatogram of HRV14 2A^{pro}-His purification performed on a HisTrap column 1 ml (Amersham). The UV units are presented in micro-arbitrary units and each fraction corresponds to 2 ml. **B) Coomassie stained 12.5% SDS-PAGE of the fractions collected.** Lane 1 shows the soluble fraction before loading the column (3µl of 24 ml); lane 2 the flow-through; lane 3 the collected waste fraction and lanes 4 to 6 show the fractions collected (10µl of 2ml), which correspond to the fractions A2 to A4 from the peak observed on the chromatogram. Protein standards in kDa are shown in line M.

The fractions from lane 4 to 6 were pooled, concentrated to 2 mL and injected on a HiLoad 26/60 Superdex prep grade column (Amersham Biosciences) for separation by gel filtration. As figure 32B shows, most of the protein is eluted with the flow through, which corresponds to peak 1 of figure 32A.
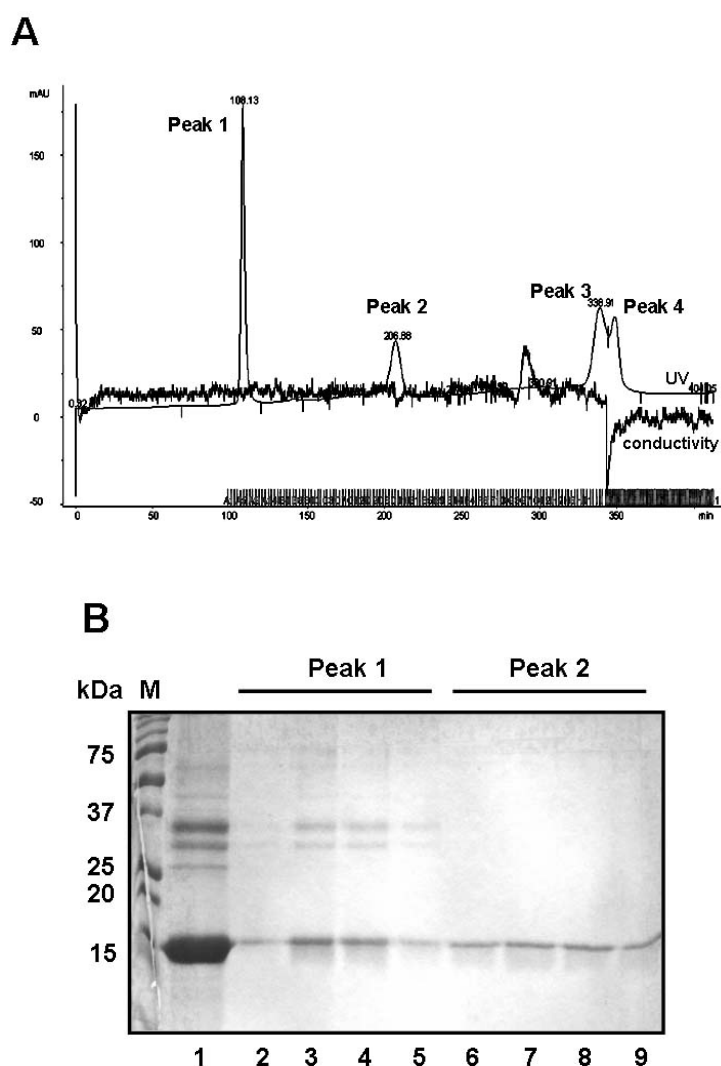
A

B

Figure 32: A) Chromatogram of gel filtration performed on a superdex 26/60 column. The UV units are presented in micro-arbitrary units and each fraction corresponds to 2 ml. **B) Coomassie stained 12.5% SDS-PAGE of the fractions collected.** Lane 1 shows the sample before loading the column (10µl of 2ml); lanes 2 to 5 show the fractions of peak 1 of the chromatogram; lanes 6 to 9 show the fractions peak 2 (10µl of 2 ml). Peaks 3 and 4 had no protein (data not shown). Protein standards in kDa are shown in line M.

However, peak 2 (figure 32A) contained some highly purified protein. After pooling the samples from lanes 6 to 9 (figure 32B), they were concentrated from 10 ml to 400 µl. The final concentration was 2,83 mg/ml (figure 33).
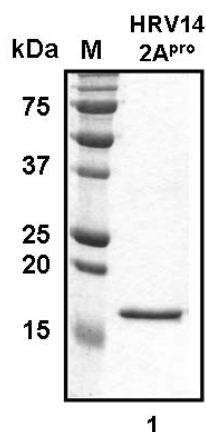
Figure 33: Coomassie stained 12.5% SDS-PAGE of the concentrated HRV14 2A^{pro}-His. Protein standards in kDa are shown in line M. The amount of loaded protein was 2 µg.

As the protein was very pure, we decided to proceed with the preliminary experiments for crystallization. The first step consists in the determination of the melting temperature of the protein, which gives information on the folding state of a protein (Yeh *et al.*, 2006). For that, a fluorescent dye, which is sensitive to the nature of the solvent in which it is diluted, is mixed with the protein. The dye is non-fluorescent in a hydrophilic environment and fluorescent in a hydrophobic environment (Yeh *et al.*, 2006). The protein is mixed with the dye and the temperature of the mix is constantly increased. When the protein reaches its melting point, it starts to unfold and consequently exposes the hydrophobic residues, which trigger the dye to emit fluorescence allowing a simple determination of the melting temperature. A typical melting temperature curve presents a sigmoid shape, from which is possible to determine the melting temperature of the tested sample (figure 34).
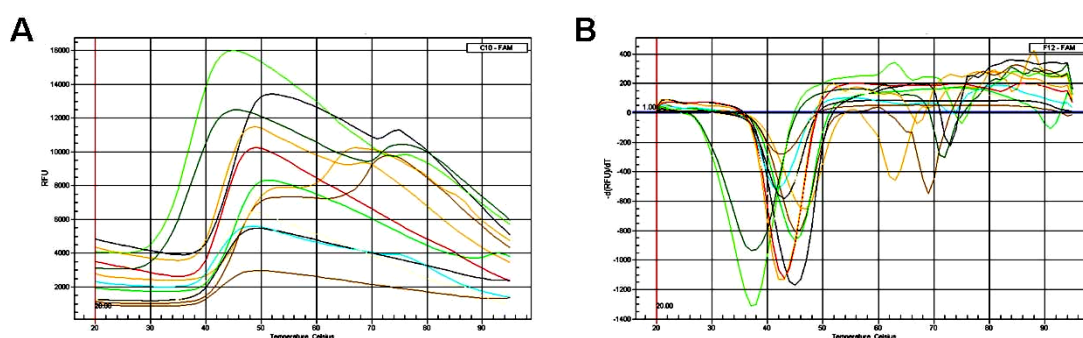

Figure 34: Determination of the melting temperature of a protein. A) Graphic showing a typical melting temperature curves of a purified protein. **B)** Graphic showing the derivative of (A) indicating that the melting temperature is about 40°C. Each line represents a different dilution of protein and dye. Data obtained from the N2B/3 proteinase from tick-born encephalitis virus, provided by Martina Kurz and Zhu Junping.

74

The purified HRV14 2A^{pro} was mixed with the SYPRO Orange dye (Invitrogen) in several dilutions. The melting temperature was measured in a real-time PCR machine (Biorad) using a single cycle from 20°C to 95°C in which the temperature was increased 1°C every 30 seconds. However, the final graphic shows a decrease in fluorescence. This indicates that the HRV14 2A^{pro} is unstructured at room temperature, most likely aggregated (figure 35).
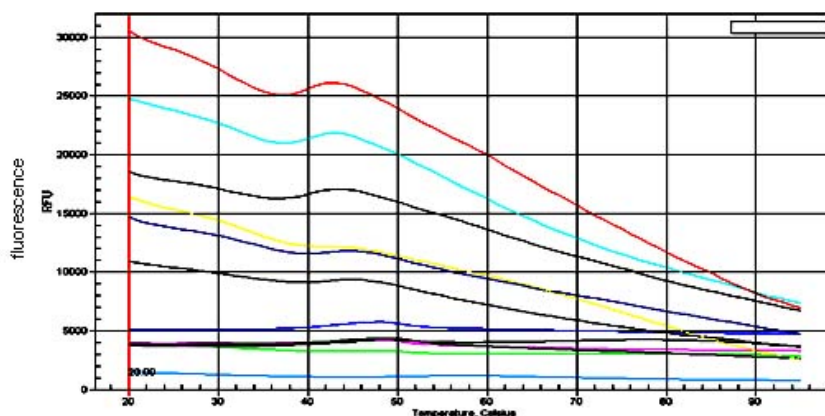

Figure 35: Graphic showing the melting temperature curve of HRV14 2A^{pro}-His. Each line represents a different dilution of protein and dye (see section 3.5.10, table 11 for the setup of the mix of protein with SYPRO).

The next step was to change the strategy to increase further the expression whilst reducing the purification steps by removing the GST tag. HRV14 2A^{pro} C109A was amplified and introduced together with a His tag in the pET11d vector using the restriction sites *Nco*I and *Bam*HI (figure 36). This plasmid was then transferred to the bacteria strain BL21(DE3)LysS. These cells carry a chromosomal copy of the T7 RNA polymerase gene under control of the *lacUV5* promoter, which make them suitable to express genes cloned in appropriate T7 expression vectors such as pET11d. Additionally, this strain of BL21 cells encodes the T7 lysozyme, an inhibitor of T7 RNA polymerase. The expression of this inhibitor suppresses basal expression of T7 RNA polymerase prior to induction (Studier, 1991).
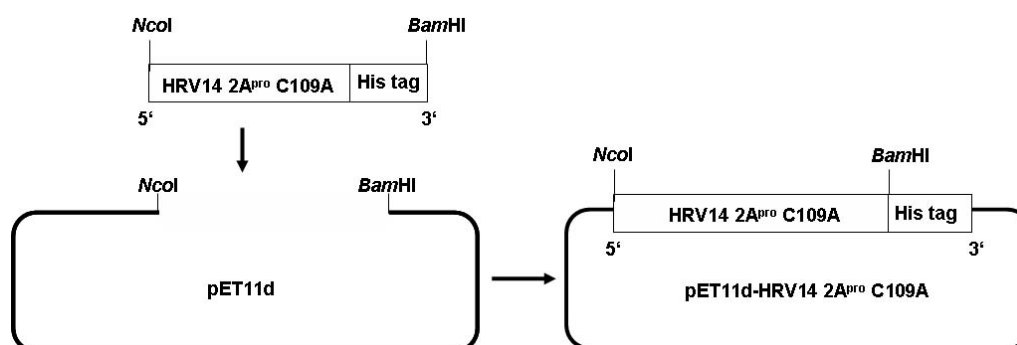
Figure 36: Cloning strategy to introduce the inactive form of HRV14 2A^{pro} carrying a His tag into pET11d. pET11d-HRV14 2A^{pro} C109A His. The ORFs were amplified with primers containing *Nco*I (primer named TIM1546) and *Bam*HI (primer named TIM1547) restriction sites. TIM1547 contains also 6 histidines before two stop codons.

We tested several temperatures, concentrations of IPTG and times of incubation. The conditions which gave the highest amount of soluble protein turned out to be an overnight incubation 1 of litre of bacterial culture at 16°C with 0.03 mM IPTG (figure 37, compare lanes 3, 6 and 9).
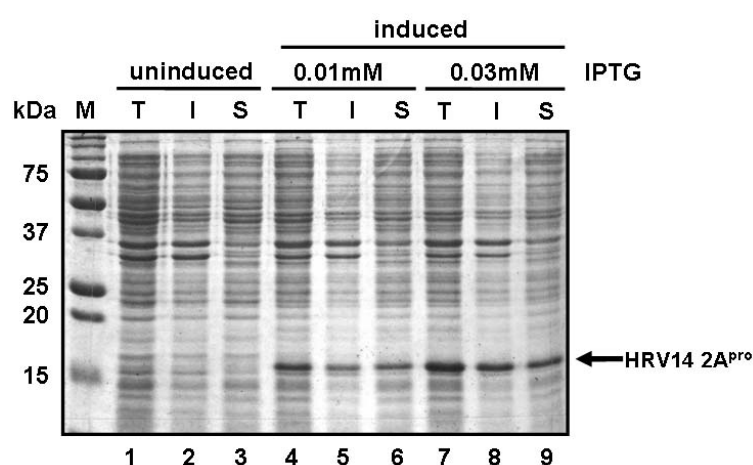

Figure 37: Coomassie stained 12.5% SDS-PAGE of the expression HRV14 2A^{pro}-His. T: total fraction; I: insoluble fraction; S: soluble fraction. The expression was carried out at 16°C with 0.01 and 0.03mM IPTG overnight. Lanes 1 to 3 show the uninduced samples; lanes 4 to 6 the induced samples with 0.01mM IPTG; lanes 7 to 9 show the induced samples with 0.03mM IPTG. 3µl of the samples was loaded (0.005% of the sample total volume). Protein standards in kDa are shown in line M.

The bacterial pellet was dissolved in 30 mL of 50 mM NaCl and 50 mM Tris-HCl pH 9.0 and loaded on a His Trap FF 1ml column (Amersham Biosciences) pre-equilibrated with the

same buffer. The protein was eluted with 50 mM NaCl, 50 mM Tris-HCl pH 9.0 and 500 mM IPTG. Figure 38 shows the results.
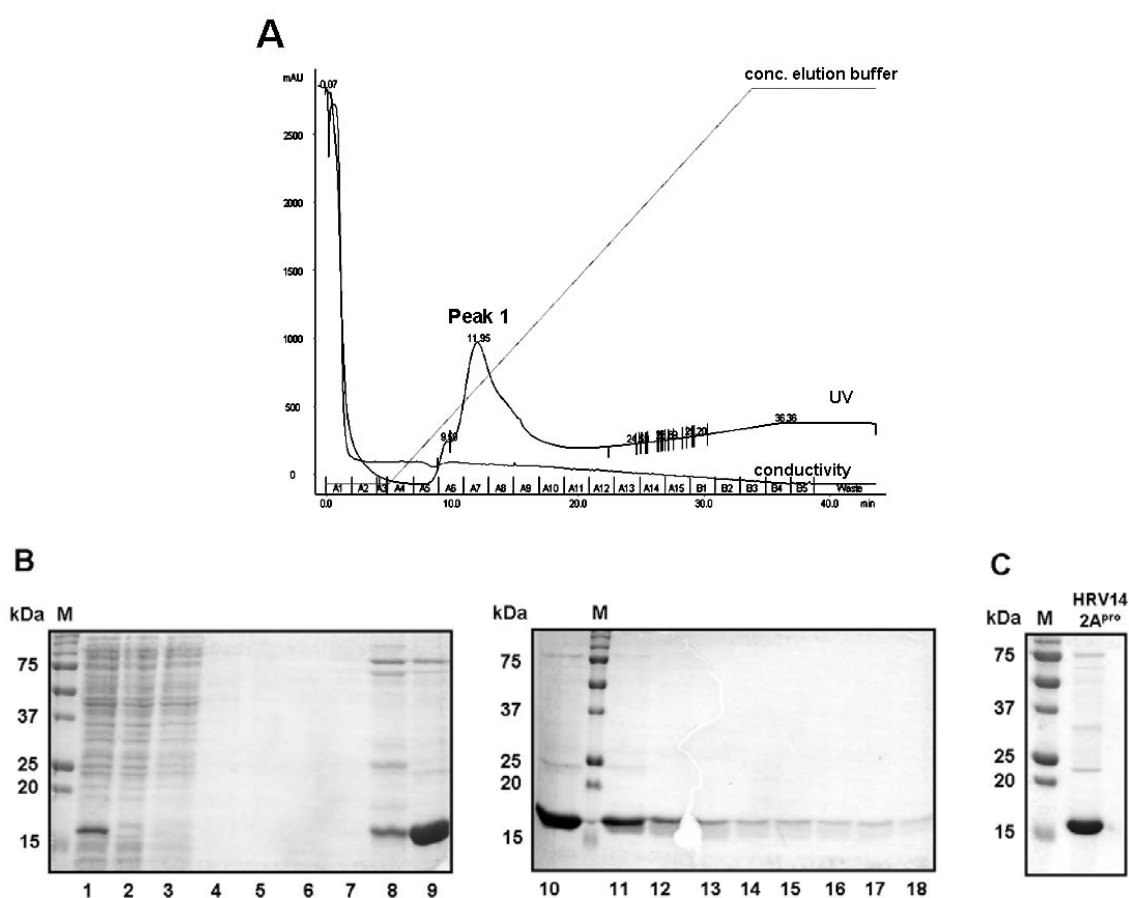

Figure 38: A) Chromatogram of HRV14 2A^{pro}-His purification performed on a HisTrap column 1 ml (Amersham). The UV units are presented in micro-arbitrary units and each fraction corresponds to 2 ml. **B) Coomassie stained 12.5% SDS-PAGE of the fractions collected.** Lane 1 shows the soluble fraction before loading the column (3µl of 60 ml); lane 2 the soluble fraction after loading the column (flow through) (3µl of 60 ml) and lanes 3 to 18 show the fractions collected (10µl of 2ml) of peak 1 (see (A)). Protein standards in kDa are shown in line M. **C) Coomassie stained 12.5% SDS-PAGE of the concentrated (pool of lanes 9 to 13 of panel B) HRV14 2A^{pro}-His.**

The fractions from lanes 9 to 13 of figure 38B were pooled and concentrated to 900 µl (figure 38C) and loaded on a HiLoad 26/60 Superdex prep grade column (Amersham Biosciences) for separation by gel filtration (figure 39). Once again, most of the protein is eluted with the flow through (peak 1, figure 39A); this probably indicates aggregation. For this reason, we did not proceed to the melting temperature determination. Optimization of the purification method is thus necessary. One possibility is to increase the concentration of NaCl in future purifications. Unfotunately, these experiments fall out of the time frame of this project.
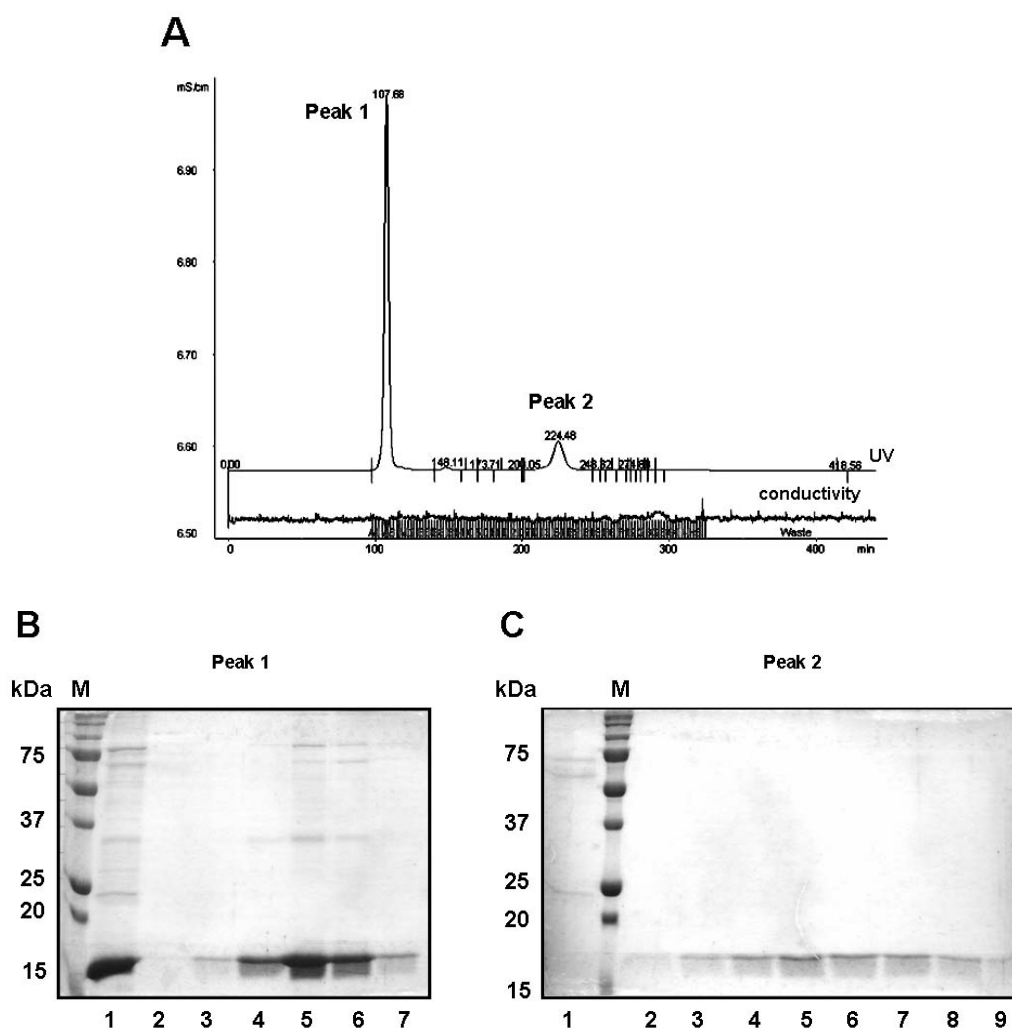
Figure 39: A) Cromatogram of gel filtration performed on a superdex 26/60 column. The UV units are presented in micro-arbitrary units and each fraction corresponds to 2 ml. **B) and C) Coomassie stained 12.5% SDS-PAGE of the fractions collected.** Lane 1 on panel B shows the sample before loading the column (10µl of 900 µl); lanes 2 to 7 show the fractions of peak 1 of the chromatogram; lanes 1 to 9 of panel C show the fractions corresponding to peak 2 of the chromatogram (10µl of 2 ml). Protein standards in kDa are shown in lines M.

4.3 Analysis of eIF4GII

4.3.1 Expression and purification

eIF4G is a scaffolding protein which brings the capped mRNA and the ribosome together. This protein is cleaved during picornaviral replication (Etchison *et al.,* 1982) leading to the so called cellular translation shut-off, allowing the viruses to take over the ribosome and express their own proteins as the viral translation is cap independent. eIF4G has two isoforms, eIF4GI and eIF4GII, which have the same function in the cell (Gradi *et al.,* 1998a). The translation shut-off, induced by the viral infection is only achieved when both isoforms

are cleaved (Svitkin *et al.*, 1999). There is evidence that the cleavage of eIF4G by picornaviral proteinases is more efficient in the presence of the initiation factor eIF4E. It is believed that eIF4E may induce a change in the eIF4G structure that is better recognized by the viral proteinases (Gross *et al.*, 2003; Haghighat *et al.*, 1996; Hershey *et al.*, 1999). To investigate this idea, we set out to obtain structural data on the interaction of eIF4G with eIF4E and picornaviral proteinases. We began with eIF4G, selecting a fragment of eIF4GII comprising the residues 445 to 744 that contain the cleavage sites recognized by HRV2 2A^{pro} and FMDV Lb^{pro}, the binding site for eIF4E and the binding sites for FMDV Lb^{pro} and HRV2 2A^{pro}.

We started by using the plasmid pGEX-6P1- eIF4GII (aa 445 to 744) with the flag tag (a gift from A. Gradi, figure 40).
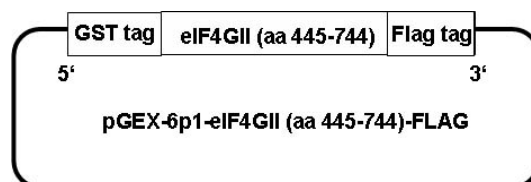

Figure 40: Scheme for the pGEX-6P1-eIF4GII-(aa 445-744)-FLAG vector provided by A. Gradi.

JM101 cells were transformed with the plasmid and the expression of eIF4GII was induced with IPTG. We tested several expression conditions, using different temperatures, different concentrations of IPTG and different times of incubation. Figure 41 shows a typical expression at 37°C with 0.1 mM IPTG for 5.5 hours. We never saw a clear over-expression of the protein. Nevertheless, we incubated the soluble fraction with glutathione-sepharose beads and we could observe that the protein which has a molecular weight of 64 kDa, was present (figure 41, lane 7).
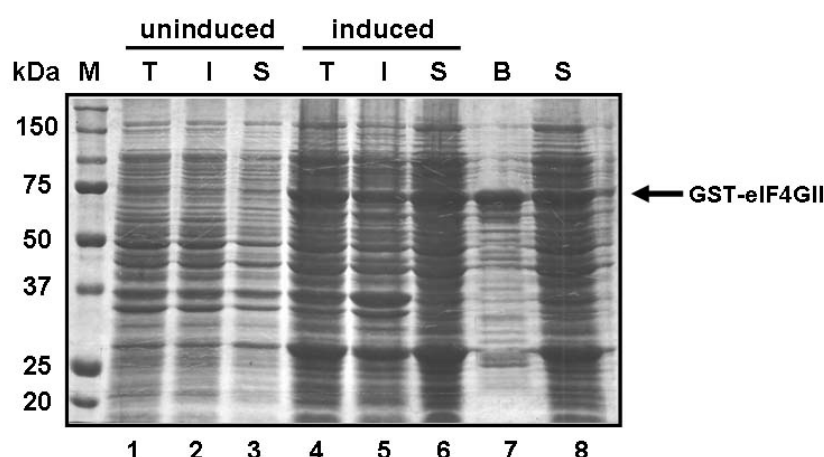
Figure 41: Coomassie stained 10% SDS-PAGE of the expression eIF4GII-GST aminoacids 445 to 744. Lane M shows the protein standards in kDa. T: total fraction; I: insoluble fraction; S: soluble fraction. The expression was carried out at 37°C with 0.1 mM IPTG for 5.5 hours. Lanes 1 to 3 show the uninduced samples; lanes 4 to 6 the induced samples; lane 7 the soluble fraction after incubation with glutathione-sepharose beads (B) and line 8 shows the supernatant after incubation with the beads (S); the volume loaded was 5µl (0.02% of the sample total volume).

After expressing 4 litres of bacterial culture using the same conditions used for the experiment illustrated in figure 41, we incubated the soluble fraction with 1 ml of glutathione beads per litre of expression and subsequently incubated the same beads (after washing) with preScission proteinase. Figure 42 shows a coomassie stained gel with 0.3% of the total amount of eIF4GII (3 ml) after cleavage from the glutathione beads. The eIF4GII fragment has a molecular weight of 37 kDa after cleavage. GST tag remained in the beads (lane 1). The higher molecular weight bands show uncleaved material and the bacterial chaperonin GroEL which was identified by mass spectroscopy and will be mentioned later (lanes 2 to 4).
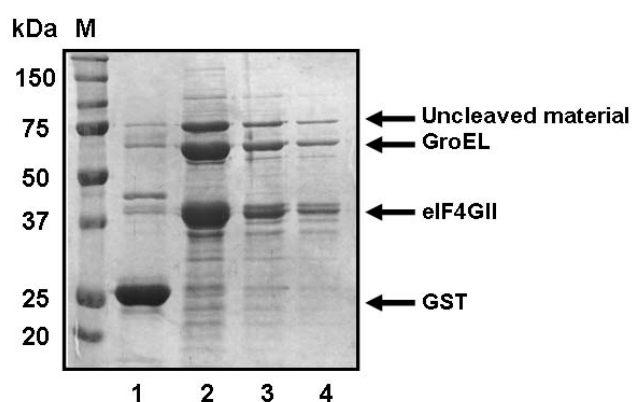

Figure 42: Coomassie stained 10% SDS-PAGE of eIF4GII aminoacids 445 to 744 after cleavage from the GST-tag. 40 units of PreScission protease (Amersham) were added to the soluble fraction

incubated with glutathione-sepharose beads. Lane 1 shows the beads after washing with the GST tag; lanes 2 to 4 show the collected supernatants with the 37 kDa fragment corresponding to eIF4GII, uncleaved material and the bacterial chaperonin GroEL which was identified by mass spectroscopy. Protein standards in kDa are shown in line M. 10μl of the samples were loaded (1% of the sample total volume).

The samples from lanes 2 to 4 were pooled and concentrated to 2 ml and loaded on a HiLoad 26/60 Superdex prep grade column (Amersham Biosciences) for gel filtration (figure 43A)
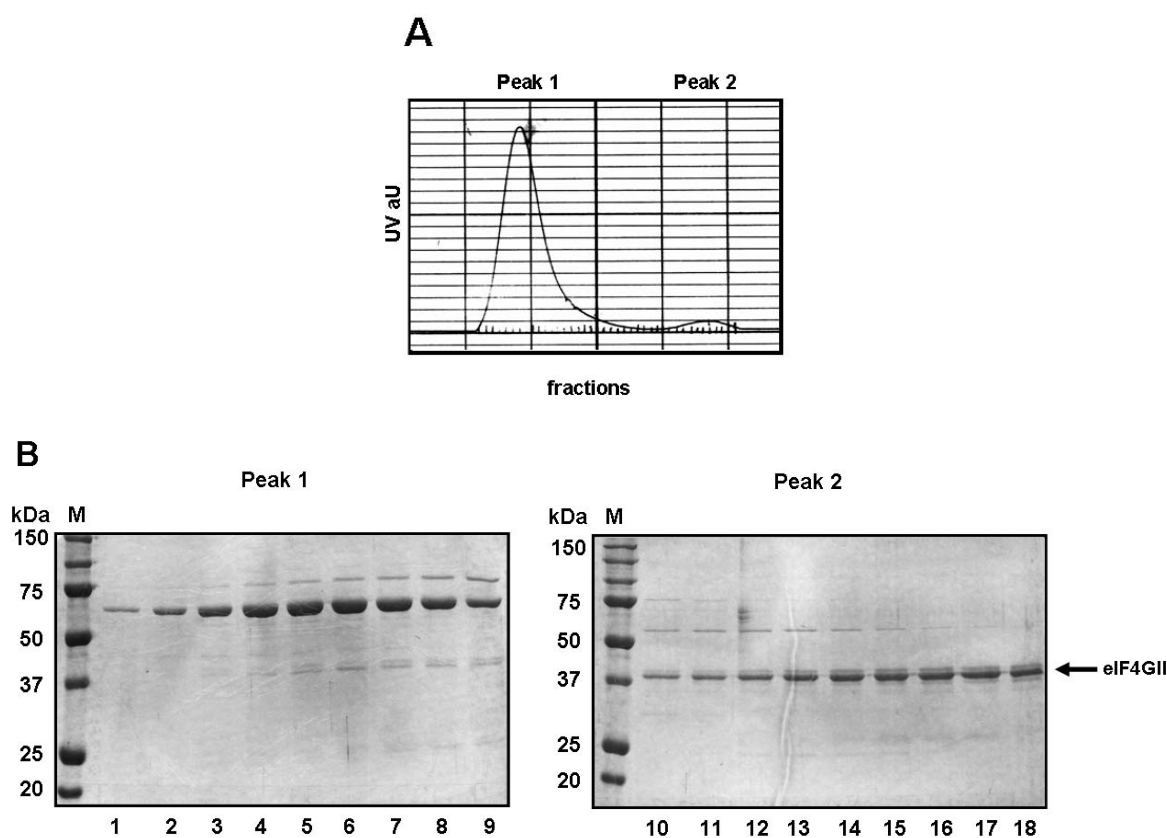

Figure 43: A) Chromatogram of gel filtration of the sample from figure 42, after being concentrated to 2 ml, performed on a superdex 26/60 column. The UV units are presented in micro-arbitrary units and each fraction corresponds to 2 ml. **B) Coomassie stained 10% SDS-PAGE of the fractions corresponding to peak 1 and 2 respectively.** Protein standards in kDa are shown in line M. 10μl of the samples were loaded (0.5% of the sample total volume).

The fractions of lanes 12 to 15 and lanes 16 to 18 of figure 43B were pooled and concentrated to 700 μl and 1.5 ml, respectively. Figure 44 shows a coomassie stained gel with 5μl of each sample after concentration.
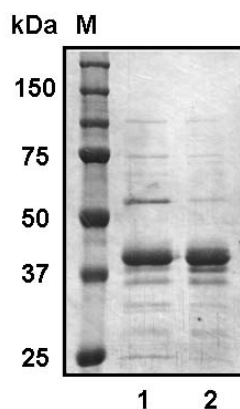
Figure 44: Coomassie stained 10% SDS-PAGE of the pooled and concentrated fractions of eIF4GII. Lane 1 corresponds to lanes 12 to 15 of figure 43B and lane 2 to lanes 16 to 18 lanes of figure 43B. Protein standards in kDa are shown in line M. 5µl of the samples were loaded (0.7% (line 1) and 0.3% (line 2) of the sample total volume).

As the amount of protein obtained (0.8 mg) and the purity were not sufficient, we decided to change the strategy of purification and use an insect cell purification system. We used the Sf9 cells and the Bac-to-Bac Baculovirus Expression System from Invitrogen.

First, we started by introducing the GST tag (amplified from the vector pGEX-6P1) into the pFastBac vector using the restriction sites *Bam*HI and *Eco*RI (figure 45A). Secondly we introduced the eIF4GII, amplified from the pGEX-6P1- eIF4GII (aa 445 to 744) flag tag, using the restriction site for *Eco*RI, on both 5' and 3' ends. The vector was digested with *Eco*RI and the eIF4GII DNA was introduced at the C-terminus of the GST tag (figure 45B).
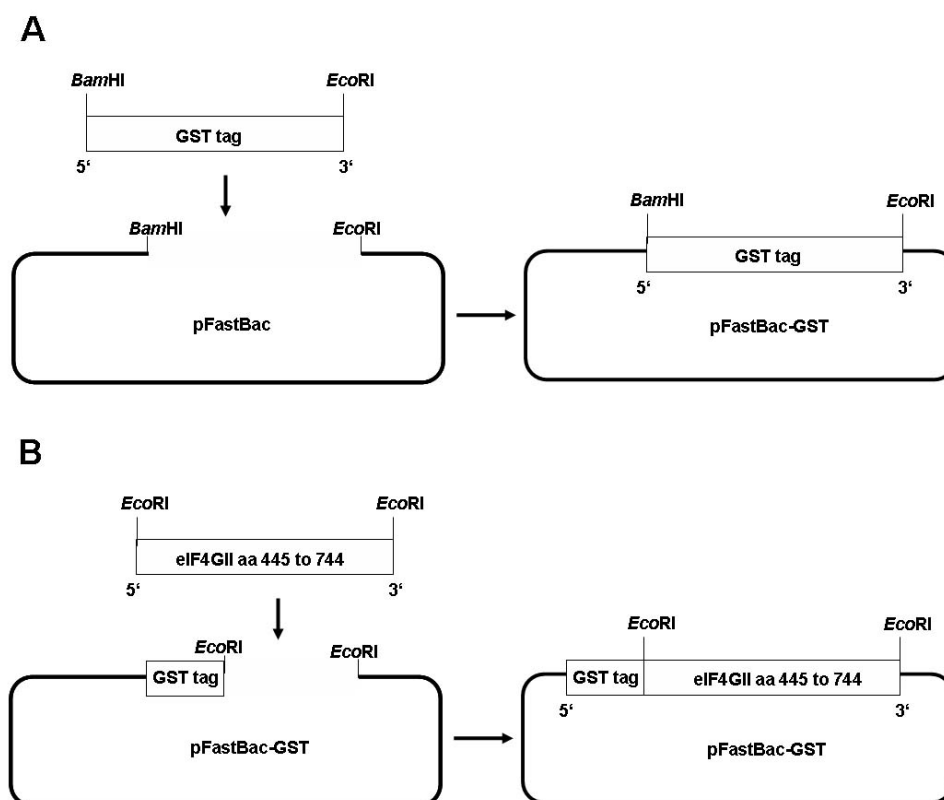
Figure 45: Cloning strategy to introduce the GST tag and eIF4GII residues 445 to 744 into the pFastBac vector (Invitrogen). A) The tag was amplified from the pGEX-6P-1(Amersham Pharmacia Biosciences) vector with the primers TIM1336 and TIM1337 and introduced into pFastBac. **B)** The eIF4GII, amplified with the primers TIM1353 and TIM1354, was then introduced in the *Eco*RI restriction site.

The new vector pFastBac-GST-eIF4GII aa 445 to 744 was used to transform DH10Bac™ cells from Bac-to-Bac Baculovirus Expression System. These cells contain enzymes that help to integrate the construct into the baculovirus genome. After confirming that the integration of the eIF4GII with the GST tag was correct, the DNA was used to infect Sf9 cell which are susceptible to the infection by the baculovirus of the system used. As the baculovirus replicates, it also expresses the protein added to its genome. After the virus has induced cell lysis, the expressed protein can be collected from the supernatant.

Figure 46 shows a western blot performed after the infection of 6×10^5 Sf9 cells in 24 well plates. After 48 hours of infection with an MOI of 5, the expression of eIF4GII-GSTtag is evident (figure 46B).
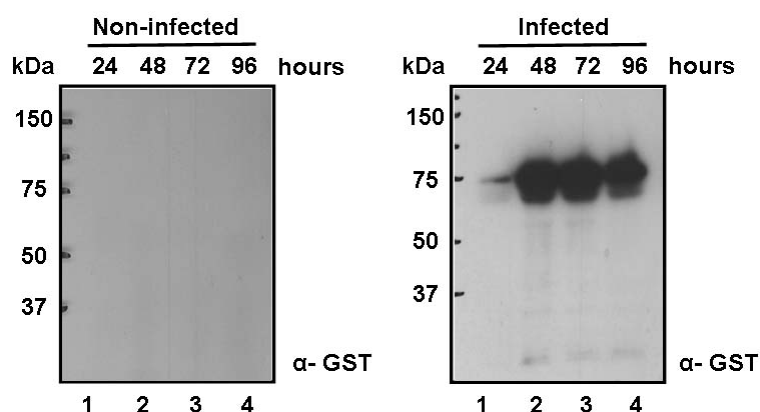
Figure 46: immunoblot of 12.5% SDS-PAGE showing the expression of eIF4GII-GST. The proteins were detected by immunoblotting using the GST antiserum (1:1000). The left panel shows the non infected samples and the right panel the infected ones. Samples were collected at 24, 48, 72 and 96 hours post infection (lanes 1, 2, 3, 4, respectively). 10µl of the samples plus 10 µl of Laemli sample buffer were loaded (3.3% of the sample total volume). Protein standards in kDa are shown on the left side of the panels.

The experiment was scaled up to 200 ml suspension culture with a cell density of $2x10^6$ Sf9 cells/ml (see section 3.5.1.3.4). The supernatant was collected after 48 hours and incubated with glutathione-sepharose beads, after which the eIF4GII was cleaved from the GST tag with PreScission proteinase (Amersham) and eluted from the beads (figure 47). Surprisingly, the gel did not show a band with the predicted size of the eIF4GII fragment (37 kDa). The slowest migrating band (above 37 kDa) appearing in lane 3 of figure 47 was too large to be eIF4GII after cleavage. As the size of this band is similar to that of PreScission proteinase (data not shown) we assumed that it is the PreScission proteinase itself.
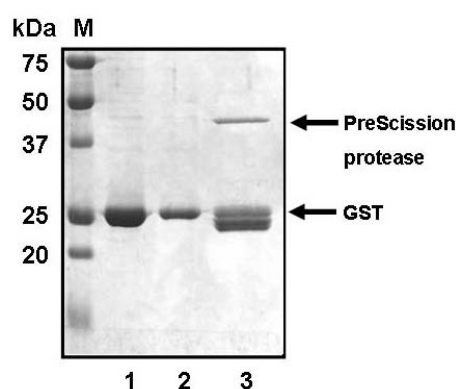

Figure 47: Coomassie stained 10% SDS-PAGE of eIF4GII after incubation with PreScission protease (Amersham). Lanes 1 and 2 show purified GST (5 and 3 µl respectively); lane 3 shows the supernatant collected from the glutathione-sepharose beads (5µl of 1 ml). Protein standards in kDa are shown in line M.

Figure 47 (lane 3), also shows three bands at the length of the GST tag. The upper band running at about 25 kDa in lane 3 is the GST tag (compare size with purified GST in lanes 1 and 2). We think that the remaining two bands can be eIF4GII after PreScission cleavage. We considered this hypothesis because PreScission proteinase is itself HRV14 3C^{pro} which is known to recognize Gln*Gly sequences for cleavage. The eIF4GII fragment that we expressed also contains the Gln*Gly sequence (red in figure 48). Although the adjacent residues to the Gln*Gly site are not those favoured by HRV14 3C^{pro} (Cordingley *et al.*, 1990; Long *et al.*, 1989), we believe that the HRV14 3C^{pro} which cleaved the protein from the GST tag could also have cleaved the expressesd eIF4GII fragment. An argument that support our hypothesis is that FMDV 3C^{pro} was shown to cleave eIF4GI in a different site from that expected for 3C^{pro}, at the sequence Glu711*Pro712 (figure 48) (Strong and Belsham, 2004).

The reason why this fragment purified from Sf9 cells was cleaved whereas the same fragment purified from bacteria was not may indicate that the expression in eukaryotic cells could have introduced some post-translational modifications that affected the folding of the protein, making it recognizable by the HRV14 3C^{pro}.
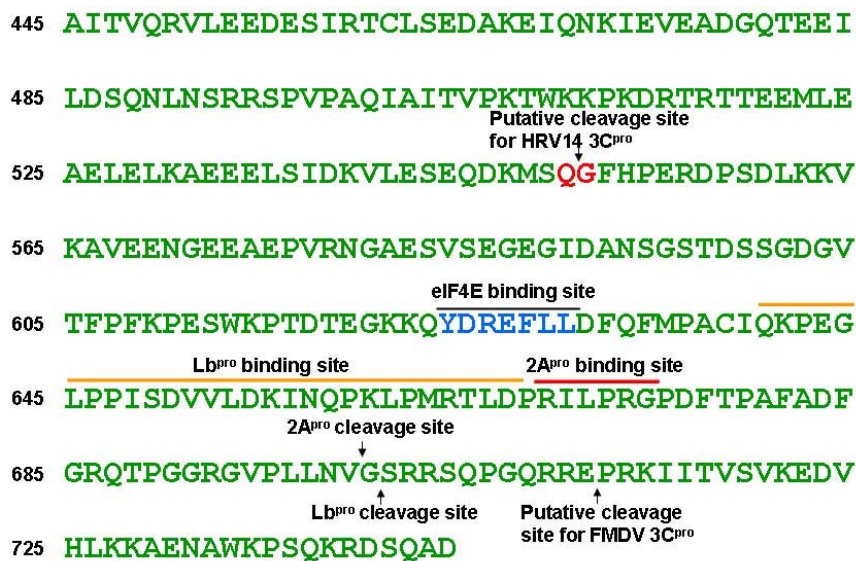
Figure 48: fragment of eIF4GII (residues 445 to 744) cloned in pGEX-6P1 (Amersham). Red marks the putative cleavage site for PreScission protease (HRV14 3C^{pro}) (Amersham); blue shows the eIF4E binding site; the orange line shows the residues important for Lb^{pro} binding in eIF4GI and the red line shows the residues important for 2A^{pro} binding in eIF4GI (Foeger *et al.*, 2002). The cleavage sites for 2A^{pro} and Lb^{pro} are marked (Gradi *et al.*, 2004). Finally the cleavage site of FMDV 3C^{pro} correspondent to eIF4GI is also marked (Strong and Belsham, 2004). The numbers on the left refer to the first residue of eIF4GII on each line.

Since the fragment C-terminal to the Gln*Gly sequence contains all the regions we are interested in, we decided to clone it in the pGEX-6P1 vector and try to express it again in bacteria, as this is a simpler system. The new eIF4GII fragment starts with the aminoacid Phe552 and ends with a His tag after the Glu744. The insert was amplified from the vector pGEX-6P1- eIF4GII (aa 552 to 744) flag tag introducing the restriction sites for *Eco*RI. Once again the plasmid pGEX-6P1 was digested with *Eco*RI and the insert was introduced after the 3' end of the GST tag (Figure 49).
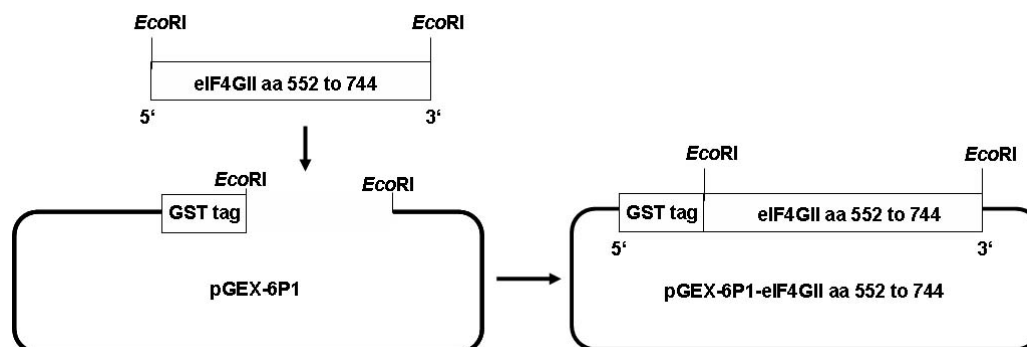
Figure 49: Cloning strategy to introduce the fragment corresponding to the residues 552 to 744 of eIF4GII into pGEX-6P-1. pGEX-6P-1-eIF4GII 552-744. The ORFs were amplified with the primers TIM1472 and TIM1354.

The amount of expressed protein from pGEX-6P-1-eIF4GII 552-744 was higher than with the larger fragment; however the recovery after incubation with glutathione beads was still not high enough for structural studies (figure 50).
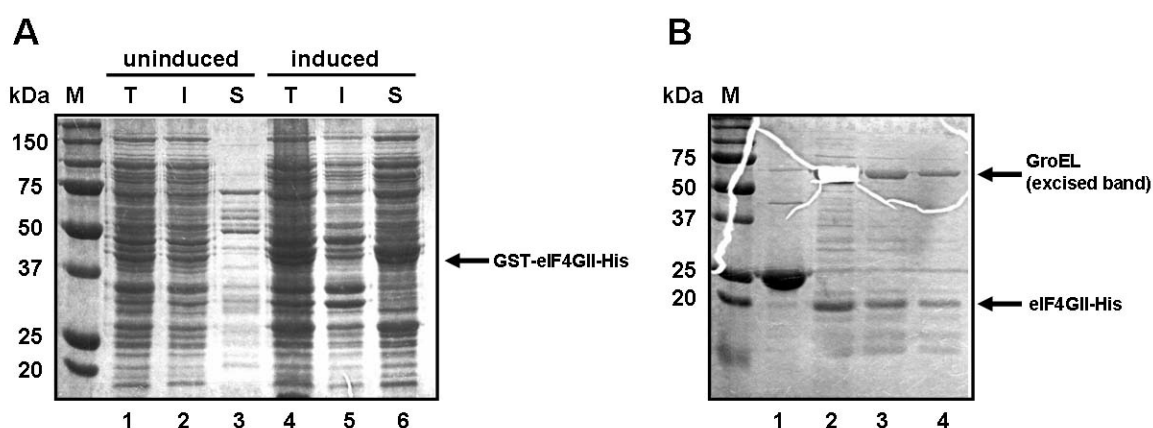
Figure 50: Coomassie stained 10% SDS-PAGE of the expression eIF4GII-GST-His aminoacids 552 to 744 (A) and the protein after incubation with PreScission protease (Amersham) (B). A) T: total fraction; I: insoluble fraction; S: soluble fraction. The expression was carried out at 20°C with 0.5

mM IPTG overnight. Lanes 1 to 3 show the uninduced samples; lanes 4 to 6 the induced samples; 3µl of the samples were loaded (0.015% of the sample total volume). **B)** 40 units of PreScission protease (Amersham) were added to the soluble fraction and incubated with glutathione-sepharose beads. Lane 1 shows the beads after washing; lanes 2 to 4 show the collected supernatants with the eIF4GII. 10µl of the samples were loaded (1% of the sample total volume). The upper arrow indicates a protein which is systematically co-purified with eIF4GII and was identified as GroEL chaperone from *E. coli* by mass spectroscopy (excised band of lane 2). Protein standards in kDa are shown in line M.

The excised band on lane 3 (figure 50B) corresponds to a protein which was systematically co-purified with the eIF4GII fragment. We thought that it could be a binding partner. Consequently, we sent it for mass spectroscopy identification. The results showed that this protein is the *E. coli* chaperone GroEL (data not shown).

As the yield and purity of the new eIF4GII fragment were not satisfactory, we decided to try the expression using a different plasmid and a different bacteria strain. The chosen plasmid was the pET11d (Novagen) which can be expressed with the cells BL21(DE3)LysS. The smaller fragment of eIF4GII (aminoacids 552 to 744) with the C-terminal His tag was introduced into the pET11d plasmid using the restriction enzyme *Nco*I. The new plasmid was named pET11d-eIF4GII aa 552 to 744 His tag (figure 51).
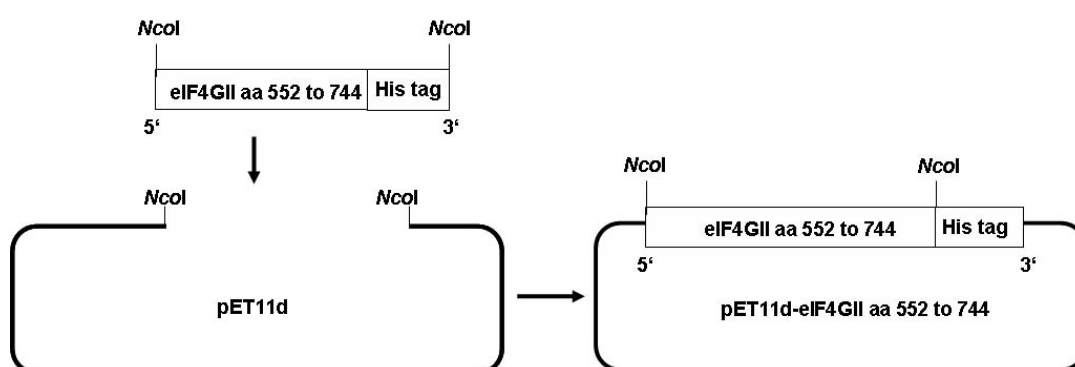

Figure 51: Cloning strategy to introduce the fragment corresponding to the residues 552 to 744 of eIF4GII carrying a His tag into pET11d. pET11d-eIF4GII 552-744 His. The ORFs were amplified with the primers TIM1544 and TIM1545. TIM 1545 contains also 6 histidines before two stop codons.

We started by optimizing the expression at small scale (25 ml of bacterial culture), trying several temperatures, concentrations of IPTG and times of incubation. Figure 52A shows that the protein is well expressed and soluble at 37°C with 0.1mM IPTG for 5 hours. As the band that we thought to correspond to eIF4GII runs at a higher molecular weight than the predicted (22.2 kDa, compare with figure 50B), we performed some experiments to confirm the content of this band. Figure 52B presents a western blot against the His tag

showing that the band above 25 kDa corresponds to the eIF4GII fragment. The reason why eIF4GII is only visible in the total and soluble fractions might be due to the low efficiency of the sonication, as the amount of protein is rather low in the insoluble fraction (figure 52A, lane 5). The probe used for detection was a nickel (Ni^{2+}) activated derivative of horseradish peroxidase (HRP) (HisProbe™-HRP, Pierce) prepared to detect poly-histidine-tagged proteins. Additionally, a sample of this band was sent for mass spectroscopy analysis, which confirmed that this protein is indeed the eIF4GII fragment (data not shown).
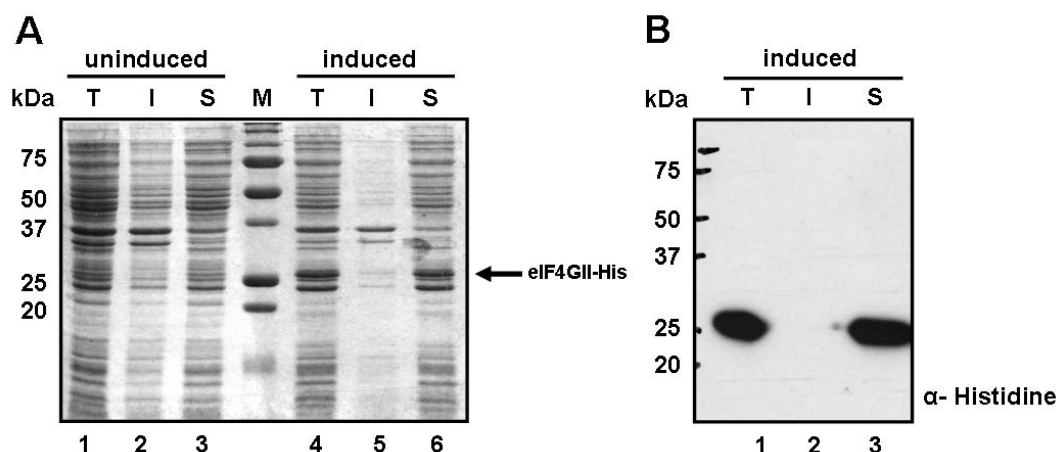

Figure 52: Coomassie stained 12.5% SDS-PAGE of the expression eIF4GII-GST aminoacids 552 to 744. A) Lane M shows the protein standards in kDa. T: total fraction; I: insoluble fraction; S: soluble fraction. The expression was carried out at 37°C with 0.1 mM IPTG for 5 hours. Lanes 1 to 3 show the uninduced samples; lanes 4 to 6 the induced samples. 3µl of the samples were loaded (0.005% of the sample total volume). **B)** Immunoblot of 12.5% SDS-PAGE showing the expression of eIF4GII (induced fractions corresponding to lane 4 to 6 of figure 52A). The proteins were detected by immunoblotting using an anti-histidine probe: nickel (Ni^{2+}) activated derivative of horseradish peroxidase (1:10,000) (HisProbe™-HRP, Pierce).

The conditions chosen for expression at large scale were the same shown in figure 52A for the small scale. We incubated 1 litre of bacterial culture at 37°C for 5 hours with 0.1 mM of IPTG. The soluble fraction was loaded on a His Trap FF 1ml column (Amersham Biosciences) equilibrated with 50 mM NaCl, 50 mM Tris-HCl pH 8.0. The proteins were eluted by a gradient of imidazole (elution buffer: 50 mM NaCl, 50 mM Tris-HCl pH 8.0, 500 mM imidazole). Figure 53A shows the result of the FPLC purification, in which one single peak can be observed. 10 µl of each fraction from the FPLC purification were loaded on a 12.5% SDS-PAGE. The fractions 9 to 15, corresponding to the peak seen in figure 53A contain a band with the expected molecular weight for the eIF4GII fragment expressed (figure 53B).
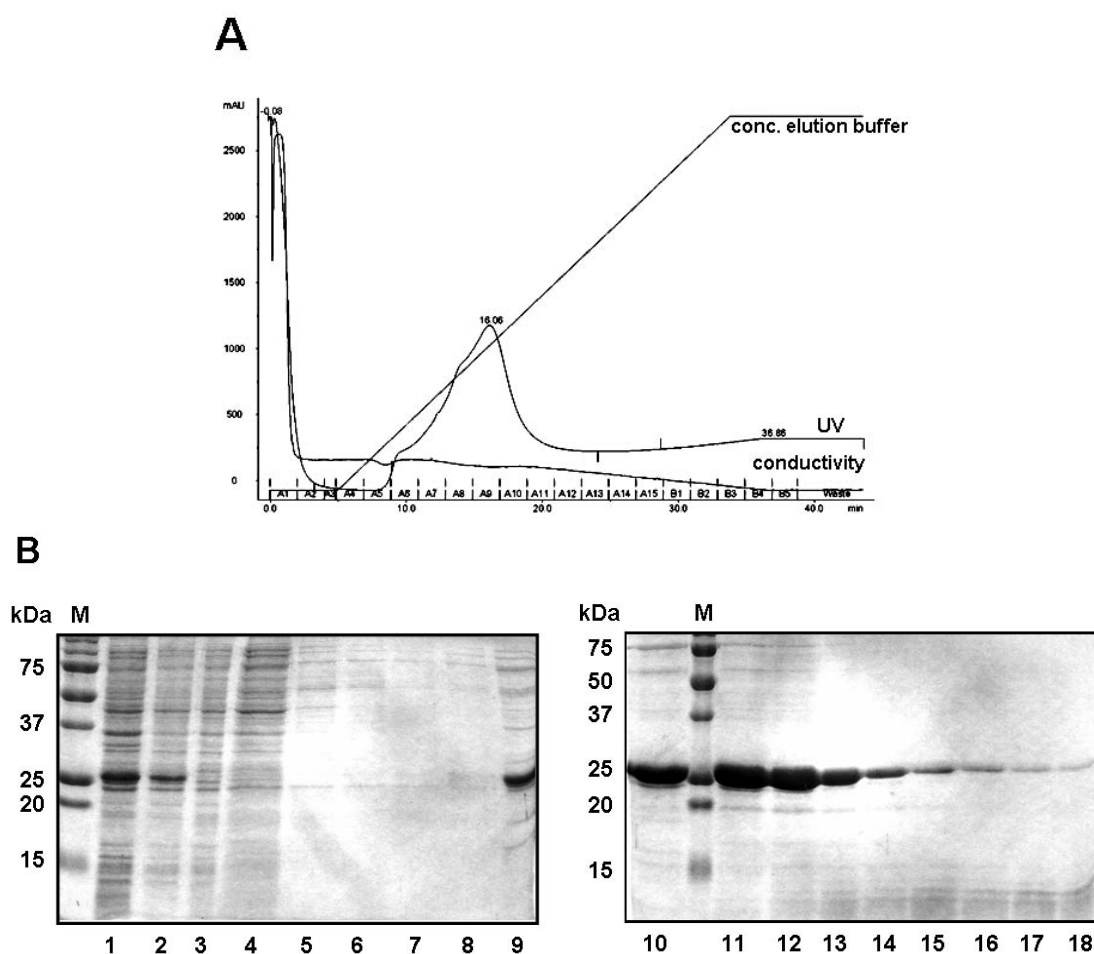
Figure 53: A) Chromatogram of eIF4GII-His aminoacid 552 to 744 performed on a HisTrap column 1 ml (Amersham). The UV units are presented in micro-arbitrary units and each fraction corresponds to 2 ml. **B) Commassie stained 10% SDS-PAGE of the fractions collected.** Lane 1 shows the total fraction before loading the column (3µl of 60 ml); lane 2 the soluble fraction before loading the column (3µl of 60 ml); lane 3 the flow-through and lanes 4 to 18 show the fractions collected (10µl of 2ml). Protein standards in kDa are shown in line M.

The fractions of lanes 9 to 10 and 11 to 15, containing the eIF4GII fragment (figure 53, panel B) were pooled separately and dialysed against buffer A overnight (in order to remove the imidazole). Afterwards the two samples were concentred to 600 µl each (figure 54).
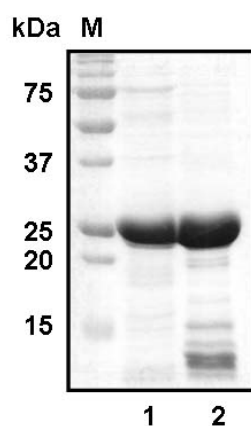
89

Figure 54: Commassie stained 12.5% SDS-PAGE of the pooled and concentrated fractions of eIF4GII. Lane 1 corresponds to the pool of lanes 9 and 10 of figure 53B and lane 2 corresponds to the pool of lanes 11 to 15 of figure 53B. Protein standards in kDa are shown in line M. 2µl of 600 µl of the samples were loaded).

These two samples were pooled together to a total volume of 1.2 ml and loaded on a HiLoad 26/60 Superdex prep grade column (Amersham Biosciences) for separation by gel filtration (figure 55A). The fractions corresponding to the peaks 1 and 2 are shown in figure 55B.
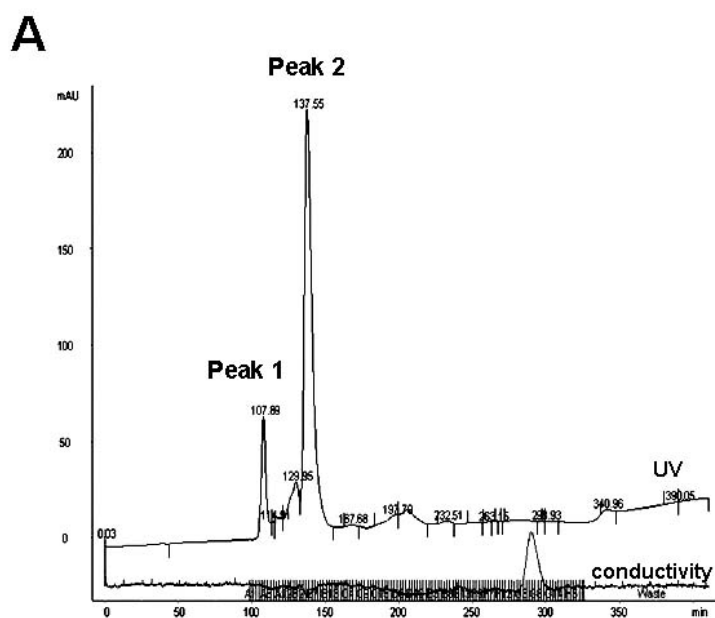
B
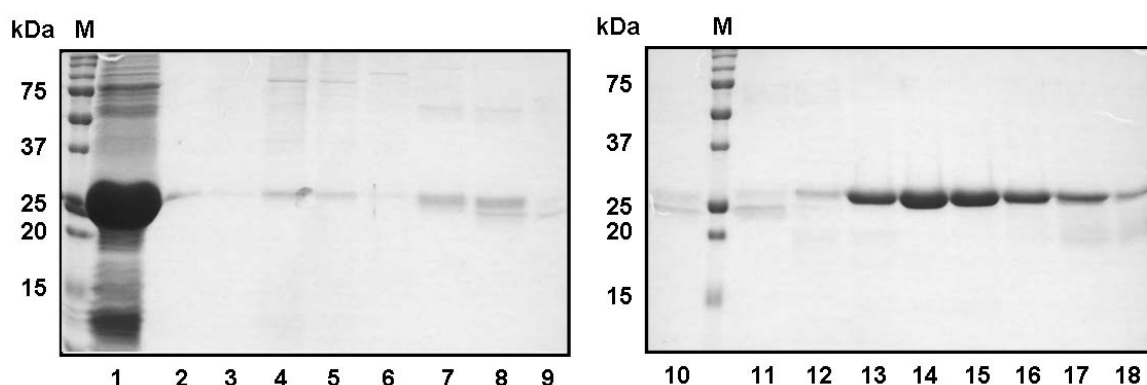
Figure 55: A) Chromatogram of gel filtration performed on a superdex 26/60 column. The UV units are presented in micro-arbitrary units and each fraction corresponds to 2 ml. **B) Commassie stained 10% SDS-PAGE of the fractions collected.** Lane 1 shows the sample before loading the column (10μl of 1.2 ml); lanes 2 to 9 show the fractions of peak 1 of the chromatogram; lanes 10 to 18 show the fractions correspondent peak 2 of the chromatogram (10μl of 2 ml). Protein standards in kDa are shown in line M.

Fractions of lane 13 to lane 16 of figure 55B (a total amount of 8 ml) were pooled and concentrated to 600 μl. The concentration of the purified protein was 2.4 mg/ml; a sample of 5 μg was examined for purity on a polyacrilamide gel (figure 56).
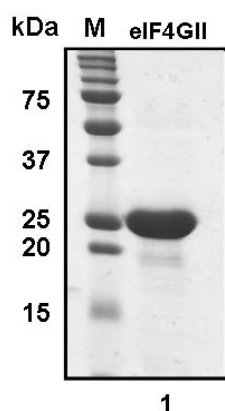
Figure 56: Commassie stained 12.5% SDS-PAGE of the pooled and concentrated fractions 13 to 16 of eIF4GII of figure 55B. Protein standards in kDa are shown in line M. The amount of sample loaded was 5 μg.

The next step was to determine the melting temperature of the purified eIF4GII, in order to find the best conditions to set up the crystals. For that SYPRO Orange dye (Invitrogen) was used. As explained in section 4.2.1, this dye is sensitive to the nature of the solvent in which it is diluted when it is mixed with the protein. The determination of the

91

melting temperature of a protein can give information about its folding status. Unfortunately, the eIF4GII fragment tested seems to be unstructured in solution, as the results show no melting temperature curve (figure 57). For comparison with a typical melting curve of a correctly folded protein see figure 34.
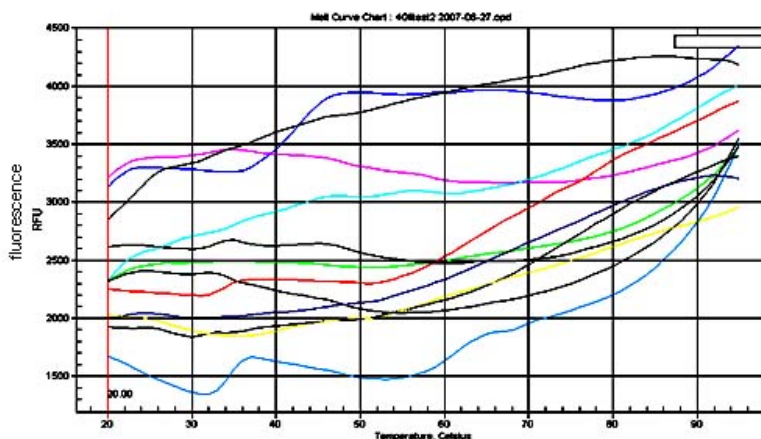
Figure 57: Melting temperature curve of eIF4GII-His amino acids 552 to 744. Each line represents a different dilution of protein (see section 3.5.10, table 11 for the setup of the mix of protein with SYPRO).

4.3.2 NMR analysis

An alternative way to determine protein structures by crystallography is nuclear magnetic resonance (NMR). NMR is based on a quantum mechanical magnetic phenomenon of the nucleus named spin (I). The hydrogen nucleus (^{1}H) has a half integer spin and is the most important nucleus to study proteins. Other relevant nuclei for biological studies are ^{15}N, ^{13}C and ^{31}P. The "spinning" nucleus can be pictured as a rotative positive charge which generates a magnetic field. Without an external magnetic field, the direction of the axis of spin is random; however, when such a field is present each "nuclear magnet" adopts a specific orientation. For nuclei with spin -1/2, two orientations are possible, a low energy state (α) and a high energy state (β). α aligns in the same direction as the applied field and β aligns at the opposite direction. The spins in the α state are slightly more abundant than the spins in the β state, which makes NMR an intrinsically insensitive technique.

The NMR phenomenon corresponds to transition between α and β energy levels and it occurs when an appropriate amount of energy (resonance) is supplied to the system by a pulse of electromagnetic radiation at a frequency of v_L. The higher the external magnetic field, the greater is the difference in energy between the α and β states and the more sensitive is the NMR experiment. Despite the intrinsic insensitivity of the technique, NMR is

very useful when applied to small molecules. It gives information on molecular dynamics, protein folding and intra and intermolecular interactions. Additionally, the method is carried out in solution, resembling the native physiological conditions.

Chemical shift

The electrons that surround the nucleus "shield" it from the static field, B_0 as they also interact with the magnetic field. The electron density is directly proportional to the shielding, so the higher the electron density the lower is the resonance frequency. Thus, nuclei that are bonded to electronegative atoms experience NMR transitions of higher energy. The resonance frequencies, in NMR are expressed in independent manner of B_0: the chemical shift scale (δ).

$$\delta_{ppm} = (\nu_{obs} - \nu_{ref}) / \nu_0 * 10^6$$

in which ν_{obs} is the frequency of a resonance of interest, ν_0 is the spectrometer frequency and ν_{ref} is the frequency of a signal from a chosen reference compound. The units of chemical shift are dimensionless and expressed in parts per million (ppm). This allows NMR spectra from spectrometers with different operating frequencies to be compared directly. The reference substance is dependent on the nucleus under analysis. It was conventioned that the ppm scale should show the zero at the right side. An "upfield" shift corresponds to an increase in nuclear shielding and a lower resonance frequency. Chemical shifts in proteins are influenced by noncovalent interactions, namely hydrogen bonding and proximity and relative orientation of carbonyl groups and aromatic rings. These interactions can give information of the local environment of a nucleus in a protein and are a function of the secondary and tertiary structures. For example, upfield shifts are observed in α-helices whereas β-sheets are shifted to lower fields.

Chemical shifts are very sensitive to a large number of variables such as structural, electronic, magnetic and dynamic. Chemical shifts give a tremendous amount of information on the system under investigation. For instance, large shift dispersion indicates that a protein is well structured and suitable for further measurements and calculations. Figure 58 shows a typical spectrum of a well structured protein. In this case, the shift dispersion is between 1 and 7 ppm.
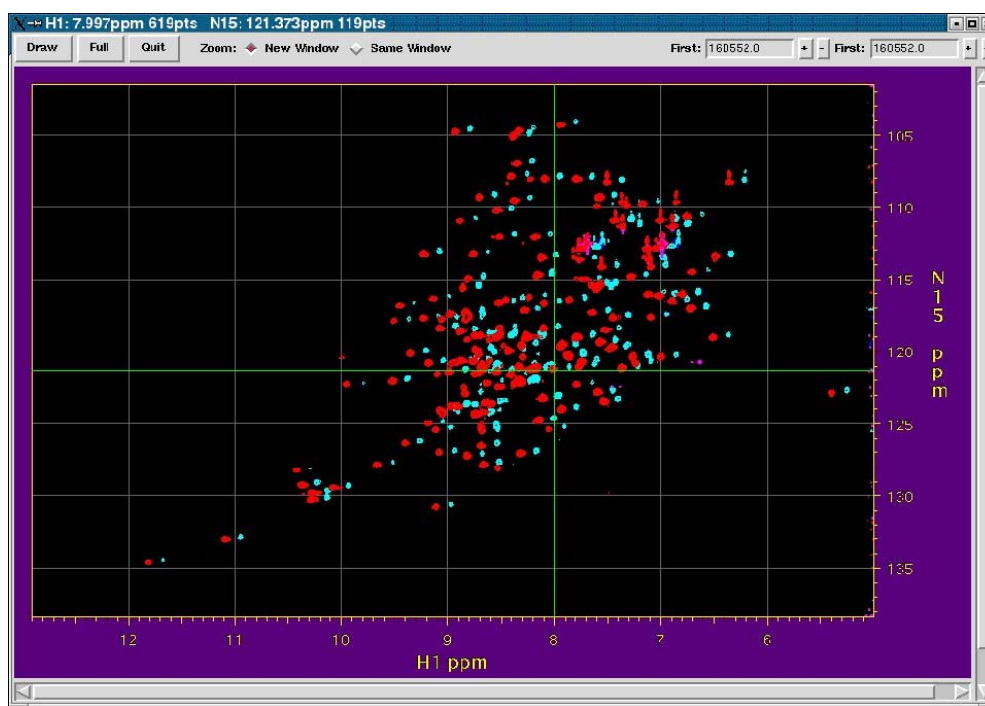
Figure 58: Superimposition of ^{1}H-^{15}N-HSQC of ^{15}NLb^{pro}C51A and ^{1}H-^{15}N-HSQC of ^{15}N/^{13}C Lb^{pro}C51A. The ^{15}N labelled sample is drawn in blue and the double labelled one in red. The two spectra are shifted somewhat to make the corresponding peaks better visible. Thus, they lie next to and not on top of each other. Figure taken from R. Cencic PhD thesis, 2005.

Relaxation time

Another important concept is the relaxation time. Relaxation corresponds to a process by which the excited spin state, responsible for the NMR signal, returns to equilibrium. Two relaxation mechanisms can be observed: longitudinal relaxation (T1) which measures the exchange of a spin excess of energy with the surroundings and how difficult the process is; and transversal relaxation (T2) which measures how efficient is the exchange of energy between spins. An isolated nuclear spin would present rather long relaxation times; however, within molecules, relaxation can be induced by exchange of energy with the surrounding or other spins in the same molecule. The relaxation rates are specifically related to molecule motion and are very important to study molecular dynamics.

In order to begin the determination of the NMR structure of eIF4GII, we expressed the protein in minimal medium containing ^{15}N labelled ammonium chloride as the sole source of nitrogen. The conditions of the expression were the same used to express pET11d-eIF4GII aa 552 to 744 His tag, and the plasmid was the also the same. Figure 59 shows the FPLC chromatogram after purification on the His Trap FF 1ml column (Amersham Biosciences) and the fractions correspondent to the peaks observed.
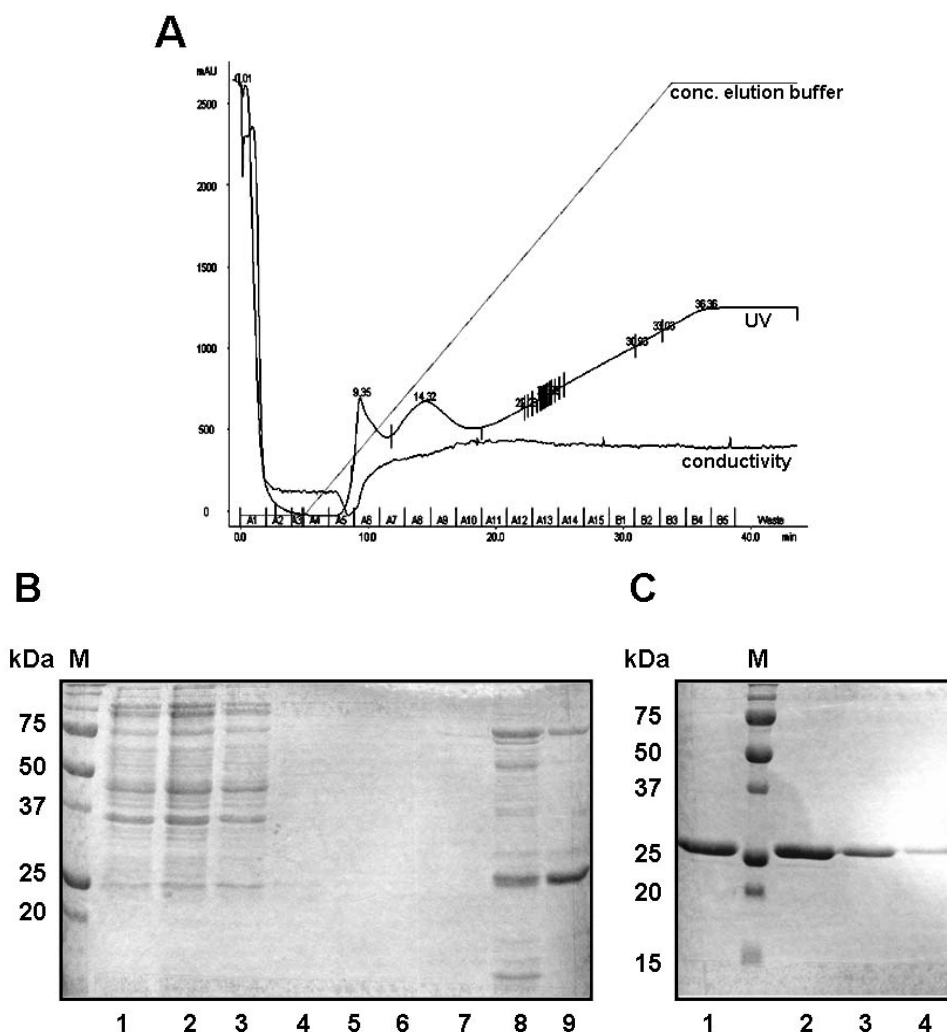
Figure 59: A) Chromatogram of eIF4GII-His aminoacid 552 to 744 performed on a HisTrap column 1 ml (Amersham). The UV units are presented in micro-arbitrary units and each fraction corresponds to 2 ml. **B) and C) Commassie stained 10% SDS-PAGE of the fractions collected.** Lane 1 on panel B shows the soluble fraction before loading the column (3μl of 60 ml); lane 2 the flow-through and lanes 3 to 9 and 1 to 4 of panel C show the fractions collected (10μl of 2ml). Protein standards in kDa are shown in line M.

Fractions of lines 1 to 4 of figure 59C (8 ml) were pooled and concentrated to 250 μl (figure 60). The concentration of the protein is 150 μM. This concentration is far form optimal as the measurements are normally done at concentrations higher than 1 mM. Nevertheless, we decided to perform a preliminary measurement. As for NMR experiments the proteins do not need to be highly pure, we did not perform a gel filtration. Instead the sample was directly measured.
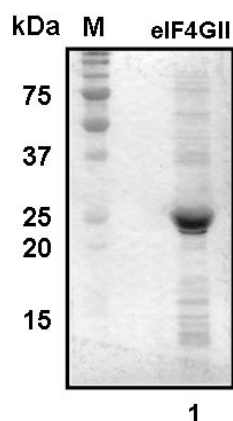
Figure 60: Commassie stained 12.5% SDS-PAGE of the pooled and concentrated fractions of eIF4GII. Protein standards in kDa are shown in line M. 2 µg of protein were loaded.

The measurements were done by Georg Kontaxis (MFPL). The measurements were done at 25°C with 5% D_2O in buffer A (50 mM Tris-HCl pH 8.0, 50 mM NaCl, 1 mM EDTA, 5 mM DTT, 5% glycerol) in a 800 MHz Varian Inova device. Figure 61 shows the spectrum of ^{15}N-eIF4GII alone in red. There is only a small ^1H shift dispersion which is between 7.5 and 9 ppm. This, as explained above, indicates that the protein is not well structured. One possible reason for these results is that eIF4GII might need another factor, such as eIF4E (Gross *et al.,* 2003; Haghighat *et al.,* 1996; Hershey *et al.*, 1999) or Lb[pro], to acquire a defined structure. We added Lb[pro] at a four fold excess; however, no differences were observed (blue spectrum, figure 61). The remaining factor to check was eIF4E and we decided to purify this protein to see whether this idea is correct.
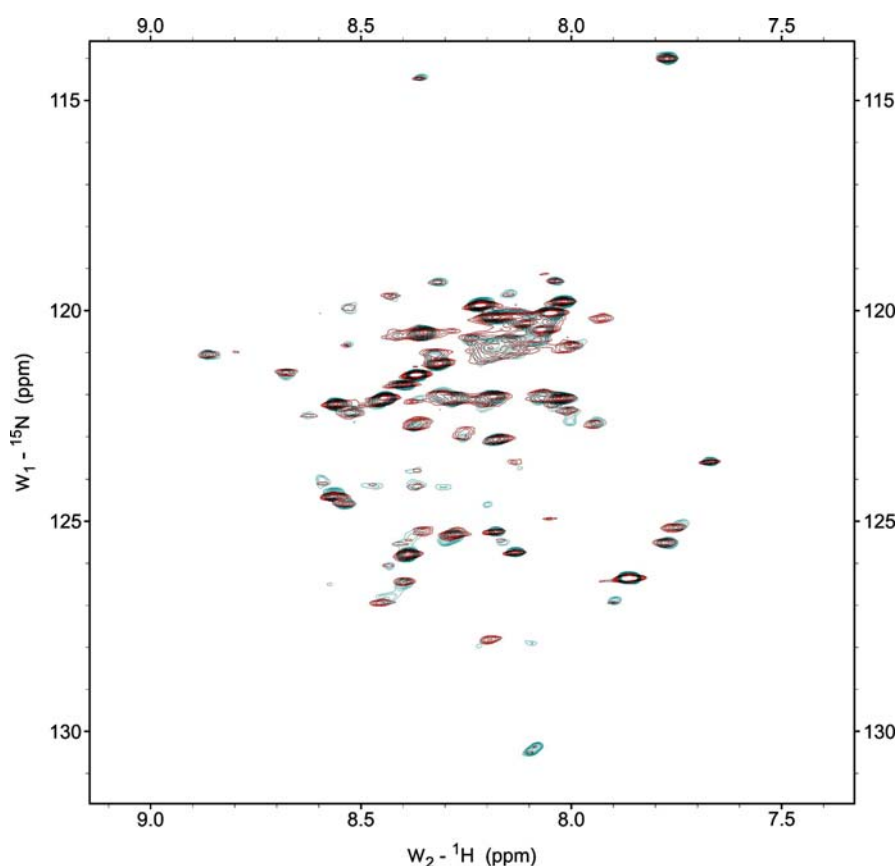
Figure 61: Superimposition of ^{15}N-eIF4GII (red) and ^{15}N-eIF4GII plus FMDV Lb (blue). The ^{1}H shift dispersion between 7.5 and 9 ppm indicates that the protein is not folded.

4.3.3 eIF4E expression and purification

As the attempts to crystallize and obtain the NMR structure of a fragment of eIF4GII (which contains the binding site for eIF4E, see section 4.3.2) were not successful, we decided to express and purify the mouse eIF4E. We chose the mouse isoform because it shares 98% identity with the human eIF4E and it was already cloned in an expression vector. It was shown previously that Lb^{pro} can cleave eIF4GI more efficiently in the presence of eIF4E (Gradi *et al.*, 2004). eIF4E induces a change on eIF4GI conformation that makes it accessible to the proteinase. For this reason, we wanted to add eIF4E to the labelled eIF4GII, in order to perform new NMR measurements and see whether eIF4GII acquires a folded structure.

We started the expression using the vector pET3b-meIF4EΔ27 which lacks the first 27 amino acids at the N-terminus, making the protein more stable (a kind gift from Jerry Pelletier, McGill University, Montreal). It also lacks a tag. The binding sites for the cap structure, 4EBP and eIF4G remain in the truncated protein. The protein was well expressed with the conditions used (30°C with 0.1 mM IPTG for 5 hours); however, it was completely insoluble, under these conditions (figure 62).

97

Figure 62: Commassie stained 12.5% SDS-PAGE of the expression eIF4EΔ27. T: total fraction; I: insoluble fraction; S: soluble fraction. The expression was carried out at 30°C with 0.1 mM IPTG for 5 hours. Lanes 1 to 3 show the uninduced samples; lanes 4 to 6 the induced samples; 3.5µl of the samples were loaded (0.012% of the sample total volume). Protein standards in kDa are shown in line M.

As there was a second plasmid available (gift from Regina Cencic, McGill University, Montreal), we decided to try to express it instead of trying other conditions with the first plasmid. The new plasmid is named ₚproExHTA-meIF4E wt which contains the complete sequence of the mouse eIF4E and an N-terminal His tag (figure 63).
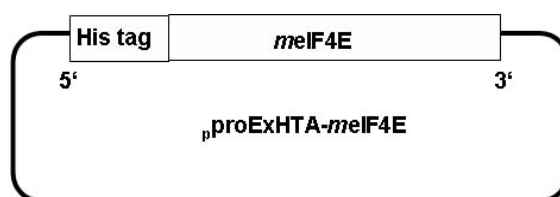
Figure 63: Scheme for the ₚpro ExHTA-meIF4E vector provided by Regina Cencic.

Once again, we tested several expression conditions, using different media for expression and different buffers for the cell extracts. Figure 64 shows four different conditions used to express eIF4E. The expression was carried out at 16°C with 0.1 mM IPTG for 5 hours in all cases. The growth media and the buffers used to resuspend the pellets were different (see section 3.2.2 and for buffers composition section 3.5.2.1). In panel A, the expression was done in Terrific Broth (TB) medium and the pellet was resuspended in buffer A. Panel B shows the expression in TB medium and ressuspension of the pellet in Lysis Cell

Buffer (LCB) buffer. In panel C the expression was carried out in Luria Bertoni (LB) medium and the pellet was taken in buffer A. Finally, in panel D the expression was done in LB medium and the pellet was resuspended in LCB buffer. The optimal procedure was expression in TB medium. The buffer used to resuspend the soluble fraction was buffer A.
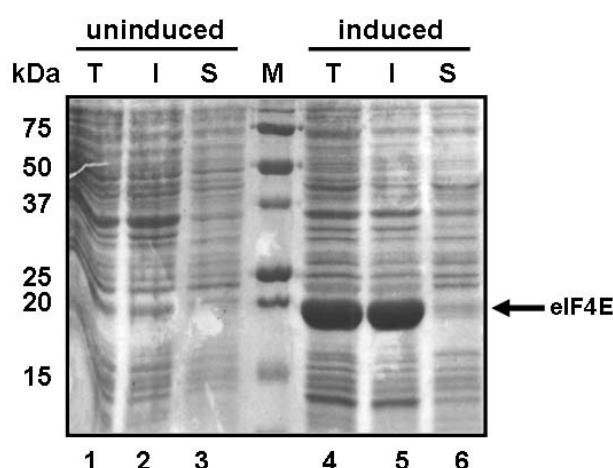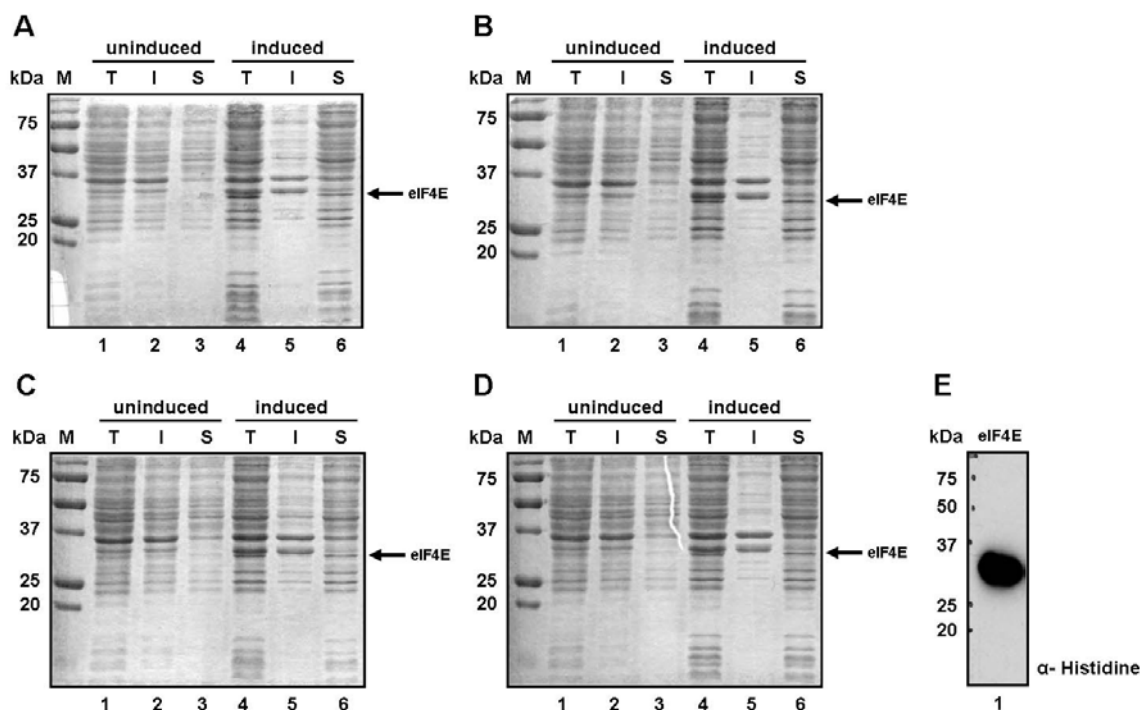

Figure 64: Commassie stained 12.5% SDS-PAGE of the expression eIF4E. T: total fraction; I: insoluble fraction; S: soluble fraction. The expression was carried out at 16°C with 0.1 mM IPTG for 5 hours. Lanes 1 to 3 show the uninduced samples; lanes 4 to 6 the induced samples; 3.5µl of the samples were loaded (0.35% of the sample total volume). Protein standards in kDa are shown in line M. **A)** Expression in TB medium and pellet ressuspended in buffer A; **B)** Expression in TB medium and pellet ressuspended in LCB buffer; **C)** Expression in LB medium and pellet ressuspended in buffer A; **D)** Expression in LB medium and pellet ressuspended in LCB buffer; **E)** Immunoblot of 12.5% SDS-PAGE showing the fraction of lane 6 of panel A blotted against an anti histidine serum (HisProbe™-HRP, Pierce) (1:10,000).

As a first attempt at purification, we loaded the soluble fraction on a His Trap FF 1ml column (Amersham Biosciences) equilibrated with 50 mM NaCl, 50 mM Tris-HCl pH 8.0. The proteins were eluted by a gradient of imidazole (elution buffer: 50 mM NaCl, 50 mM Tris-HCl pH 8.0, 500 mM imidazole). However, eIF4E failed to bind the column (data not shown). After repeating the expression, we decided to use a mono Q 10/10 column (figure 65) for purification.
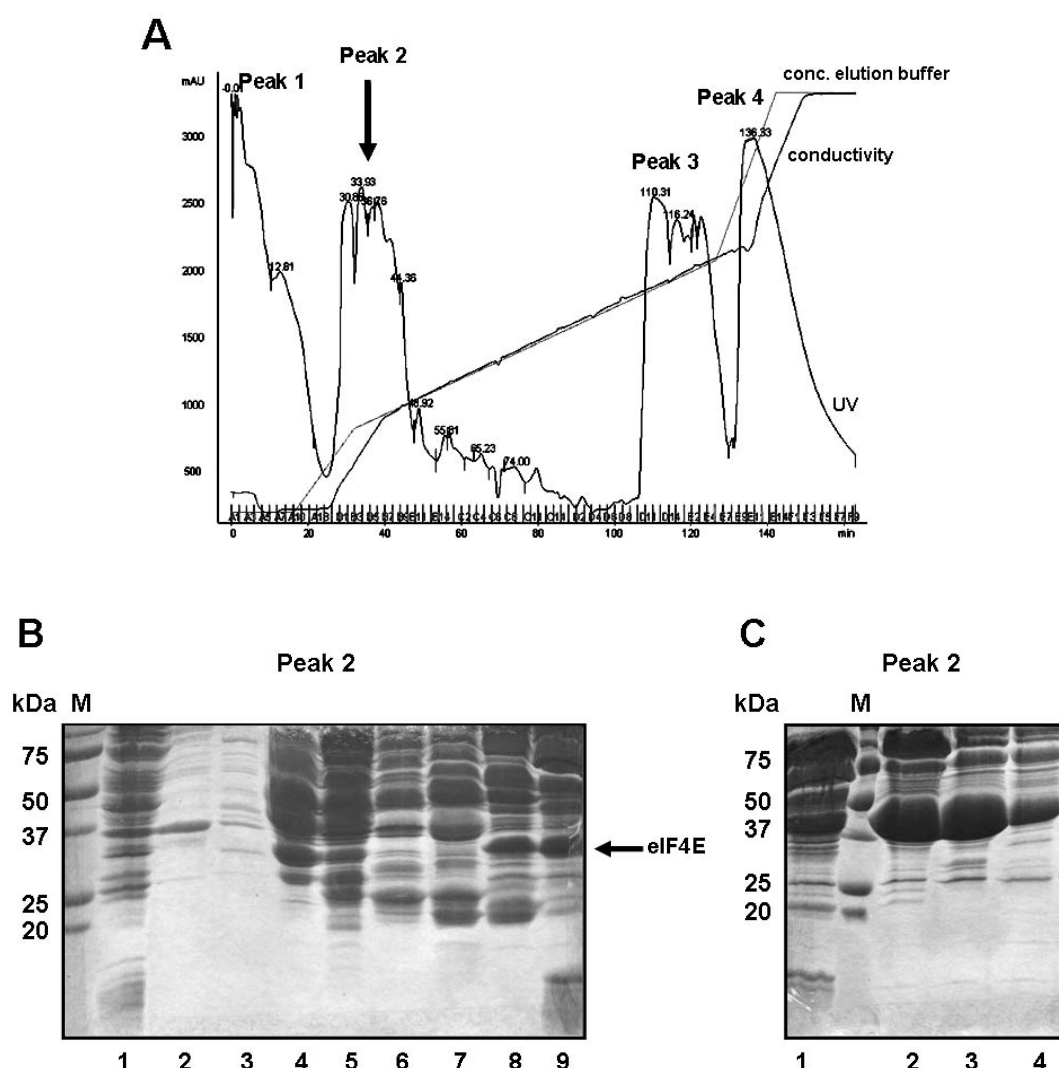
Figure 65: A) Chromatogram of eIF4E performed on a MonoQ 10/10 column (Amersham). The UV units are presented in micro-arbitrary units and each fraction corresponds to 2 ml. **B) and C) Commassie stained 10% SDS-PAGE of the fractions collected.** Lane 1 on panel B shows the soluble fraction before loading the column (3µl of 60 ml); lane 2 the flow-through and lanes 3 to 9 and 1 to 4 of panel C show the fractions collected (10µl of 2ml) of peak 2. peaks 1, 3 and 4 had no protein with the relevant weight (data not shown). Protein standards in kDa are shown in line M.

The fractions of lanes 8 and 9 of figure 65B, which had a band running at the weight predicted for eIF4E were dialysed against a buffer containing 20 mM MOPS, 0.25 mM DTT, 0.1 mM EDTA, 50 mM NaF and 100 mM KCl, 3 times one hour at 4°C. Afterwards they were incubated with 100µl of m^{7}GTP beads for 3 hours at 4°C. After incubation the beads were washed 2 times with the same buffer and the eIF4E was eluted with a new buffer (20 mM MOPS, 0.25 mM DTT, 0.1 mM EDTA, 50 mM NaF and 500 mM KCl). After washing and elution the protein was highly pure (figure 66, lane 4).
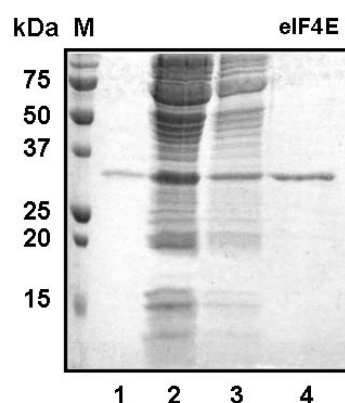
Figure 66: Commassie stained 12.5% SDS-PAGE of eIF4E eluted from m^{7}GTP beads. Lane 1 shows 2µl (of 60 µl) of m^{7}GTP beads after elution; lane 2 the eIF4E fraction after incubation; lane 3 the washing buffer and line 4 the eluate containing the purified eIF4E. 10µl of 1 ml were loaded in lanes 2 to 4. Protein standards in kDa are shown in line M.

The protein was then concentrated from 8 ml to 250 µl and quantified (100µM). Figure 67 shows the concentrated protein (A) and an immunoblot of the same sample performed with an anti-histidine probe (B). This concentration is rather low for NMR experiments. Additionally, as it needs to be complexed with eIF4GII ^{15}N labelled at least at a ratio of 1:1, the protein will be too diluted to obtain reasonable measurements. For these reasons we need to purify higher and more concentrated amounts of eIF4E. Then this protein will be used with eIF4GII ^{15}N labelled in NMR experiments. These experiments are not presented as they fall out of the time frame of this project.
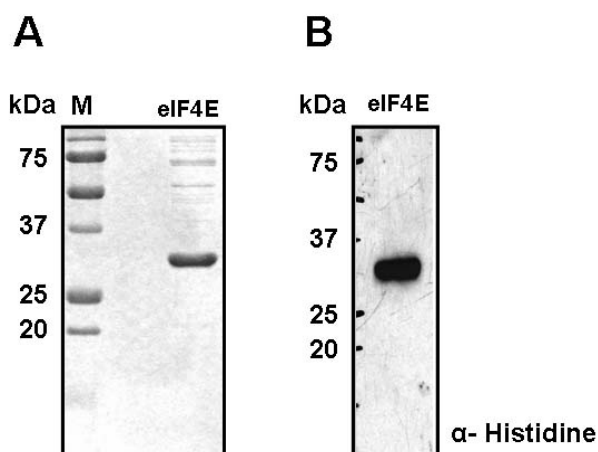
Figure 67: eIF4E after purification and concentration. A) Commassie stained 12.5% SDS-PAGE of the concentrated eIF4E. Protein standards in kDa are shown in line M. 3µg of the sample was loaded. **B**) Immunoblot of 12.5% SDS-PAGE showing the sample of panel A blotted against an anti histidine probe (HisProbe™-HRP, Pierce) (1:10,000).

4.4 Screening for HRV2 and HRV14 2A^pro binding partners

4.4.1 Expression and purification of the protein complexes

HRV 2A^{pro} bind and cleave several cellular proteins such as eIF4G and cytokeratin 8 (Foeger *et al.*, 2002). We wanted to identify further binding partners of HRV2 2A^{pro} and HRV14 2A^{pro} in the host cell by using a modified version of the method developed by Rigaut *et al.* (1999). The tandem affinity purification (TAP) method allows the purification of protein complexes under native conditions, without prior knowledge of their composition. The proteins isolated are then identified by mass spectroscopy (MS). This method is fast and can be used with a relatively small number of cells. The TAP tag consists of two proteins, protein A of *Staphylococcus aureus* (15.3 kDa) and a calmodulin binding peptide (CaBP, 3.0 kDa) which are separated by the cleavage sequence recognized by the Tobacco Etch Virus (TEV) protease. Figure 68 shows a schematic representation of the method.
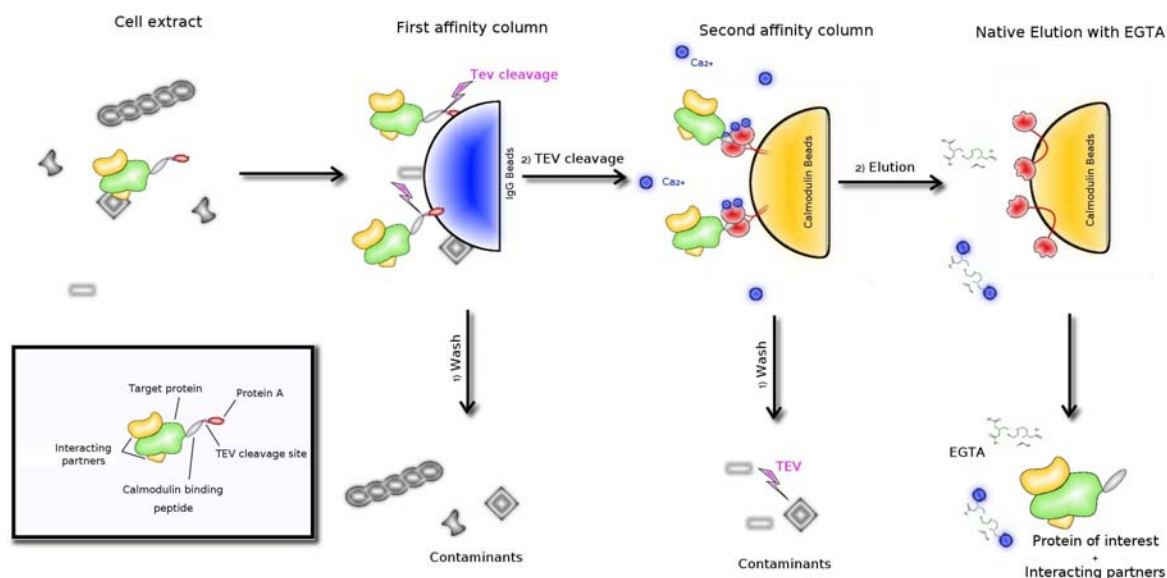
Figure 68: Overview of TAP procedure (adapted from Rigaut *et al.*, 1999).

We started by introducing the TAP tag (20.5 kDa) into the expression vector pET11d (Novagen) using the restriction sites *Sma*I and *Nco*I. The vector was digested with *Nco*I; the TAP tag was extracted from the pBluescript vector with the restriction enzymes *Sma*I and *Nco*I. The introduction of the TAP tag into the vector eliminated the *Nco*I site on the 3' end of the insert; therefore the *Nco*I site on the 5' end of the tag could be used for further cloning (figure 69).
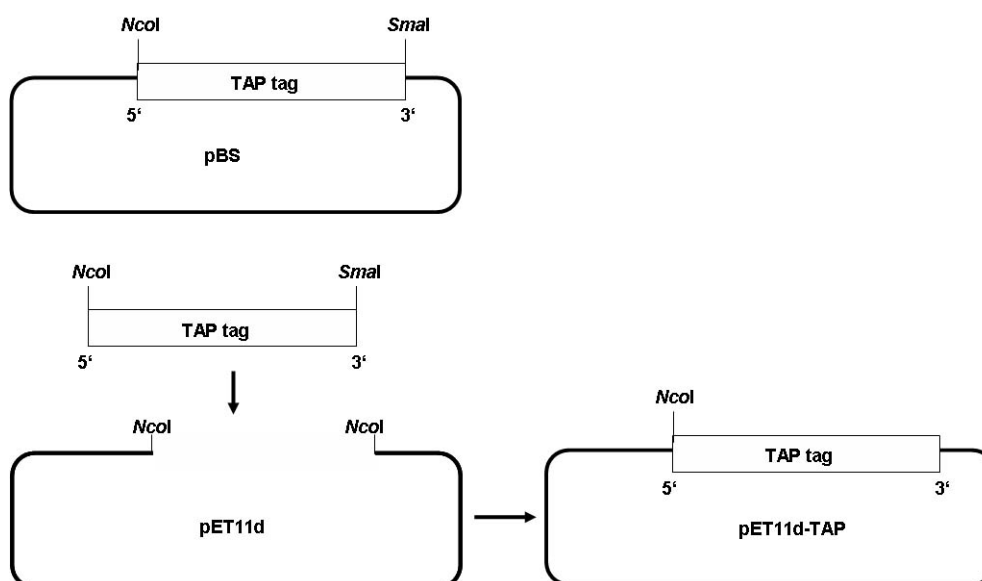
Figure 69: Cloning strategy to introduce the TAP tag into pET11d. The tag was cut from the pBS (PBluescript) vector with *Nco*I and *Sma*I and introduced into pET11d digested with *Nco*I only. Consequently, the *Sma*I and the 3' end *Nco*I restriction sites were eliminated.

Once the vector pET11d-TAP was ready, the inactive forms of HRV2 2A^{pro} (16.2 kDa) and HRV14 2A^{pro} (16.0 kDa), in which the active cysteine had been substituted by an alanine, were introduced in frame with the TAP tag. The new vectors were named pET11d-TAP-HRV2 2A^{pro} C106A and pET11d-TAP-HRV14 2A^{pro} C109A (figure 70). The expressed proteins with the TAP tag have a size of 36.7 kDa and 36.5 kDa respectively.
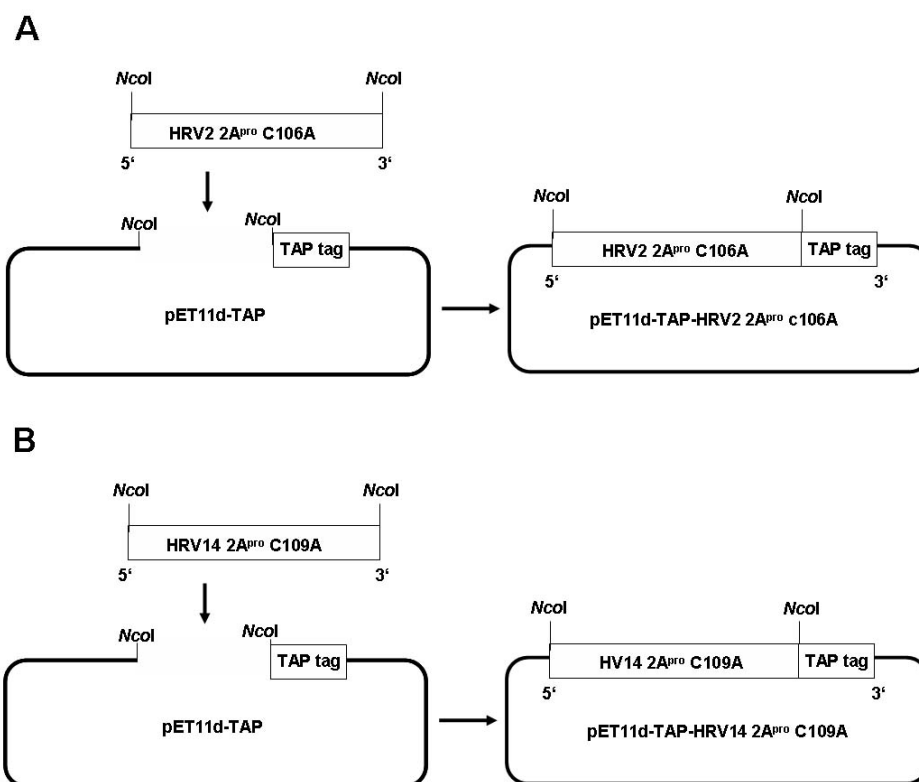
A

B

Figure 70: Cloning strategy to introduce the inactive forms of HRV2 and HRV14 2A^{pro} into pET11d-TAP. A) pET11d-TAP-HRV2 2A^{pro} C106A. **B)** pET11d-TAP-HRV14 2A^{pro} C109A. The ORFs were amplified with the primers TIM1333 and TIM1332 (A) and TIM1331 and TIM1332 (B) and introduced into pET11d digested with *Nco*I. The TAP tag is C-terminal.

The bacteria strain BL21(DES3)LysS was used to express the plasmids described above. We tested several expression conditions, such as temperature, IPTG concentration and time of incubation. Figure 71 shows a typical coomassie stained gel of samples collected after expression. The conditions of expression were 1 litre of bacterial culture incubated at 30°C with 0.5 mM IPTG for 5 hours. The expression of the TAP tag only is evident (figure 71A), whilst the expression of the inactive HRV2 and HRV14 2A^{pro} is not visible (figure 71B and 71C).
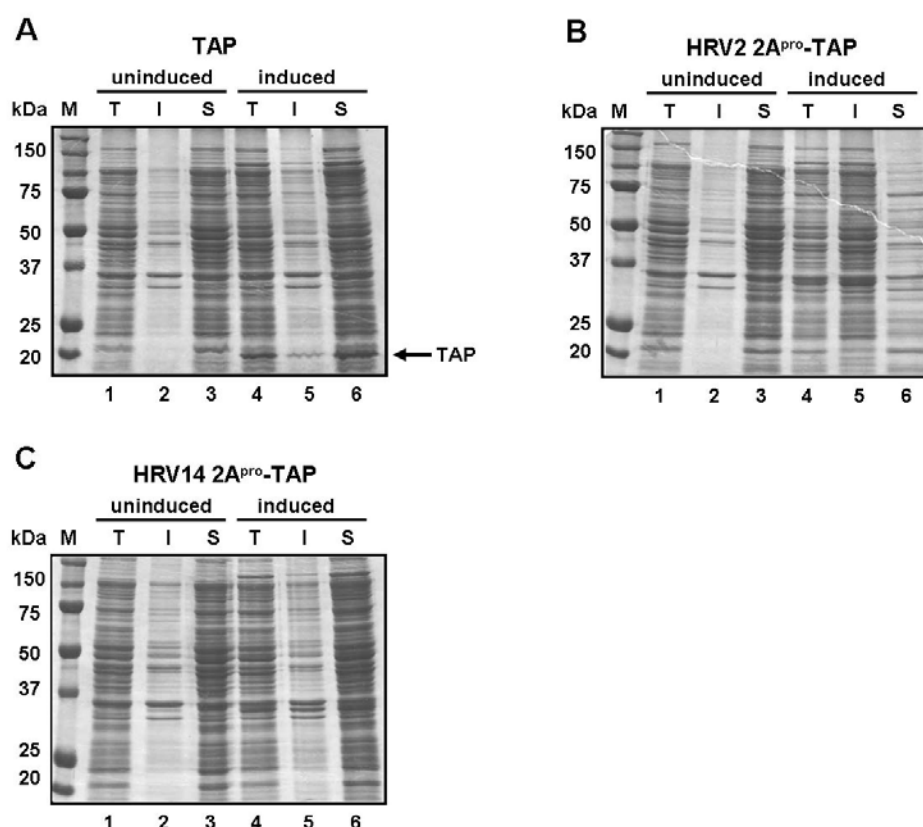
Figure 71: Commassie stained 10% SDS-PAGE of the expression of: A) Tap tag, B) HRV2 2A^{pro}-TAP and C) HRV14 2A^{pro}-TAP. Lane M shows the protein standards in kDa. T: total fraction; I: insoluble fraction; S: soluble fraction. The expression was carried out at 30°C with 0.5 mM IPTG for 5 hours. The samples were mixed with 2x Laemmli sample buffer; the volume loaded was 4µl (0.4% of the sample total volume).

We thought that the amount of expressed proteins was not high and probably they were not visible in the crude extract. Therefore, we decided to incubate the soluble fractions with IgG beads (Amersham Biosciences) for 1 hour at 4°C, in order to remove non-specific proteins and concentrate the tagged proteins. As can be observed in figure 72, the expressed 2A^{pro} and TAP tag were easily identified on a coomassie stained gel. The bands observed at above 50 kDa and 25 kDa correspond to the heavy and light chains of IgG, respectively.
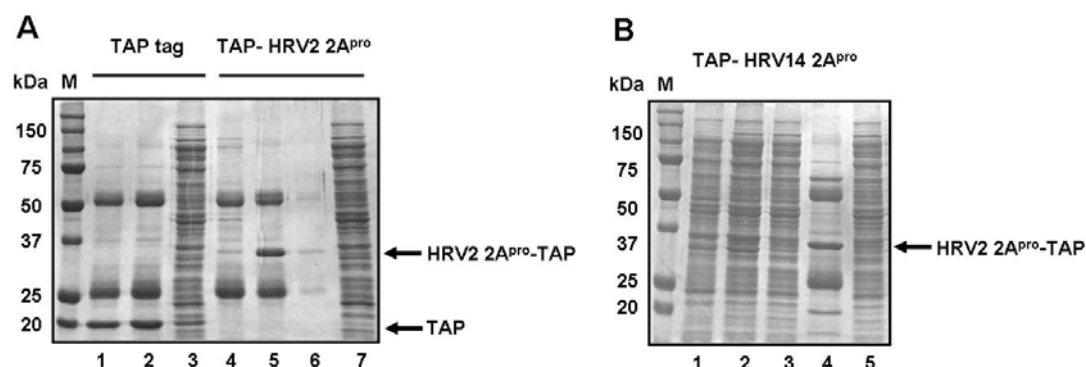
Figure 72: Commassie stained 10% SDS-PAGE of the soluble fractions from the expressions of TAP, HRV2 2A^{pro}-TAP and HRV14 2A^{pro}-TAP. A) TAP and HRV2 2A^{pro}-TAP: lanes 1, 2, 4, 5 and 6 show the soluble fractions after incubation with IgG beads; lanes 1 and 5 were expressed at 30°C with 0.5 mM IPTG; lanes 2 and 6 were expressed at 30°C with 1mM IPTG; lane 4 was expressed at 37°C with 1mM IPTG; lanes 3 and 7 are the supernatants after incubation. **B)** HRV14 2A^{pro}-TAP: lane 1 shows the total fraction of the uninduced expression (30°C, 0.5 mM IPTG); lane 2 the total fraction of the expressed protein; lane 3 the soluble fraction of the expressed protein; lane 4 the soluble fraction after incubation with IgG beads and lane 5 shows the supernatant after incubation. The samples were mixed with 2x Laemmli sample buffer; the volume loaded was 4µl (0.16% of the sample total volume). The bands observed at above 50 kDa and 25 kDa correspond to the heavy and light chains of IgG, respectively. Lane M shows the protein standards in kDa.

The samples bound to the IgG beads were further incubated with 50 mg of HeLa cells S10 extracts (see section 3.5.2.2) so that any putative binding partners of HRV2 and HRV14 2A proteinases could bind them. Subsequently, the method described by Rigaut *et al.* (1999) was used to purify any complexes. Figure 73 shows the result after purification and protein precipitation. The precipitation step was necessary to remove the detergent present in the buffer used to elute the complexes from the calmodulin beads (Ozols, 1990). The final pellet was ressuspend in 50 mM of ammonium hydrogencarbonate (NH$_4$HCO$_3$).
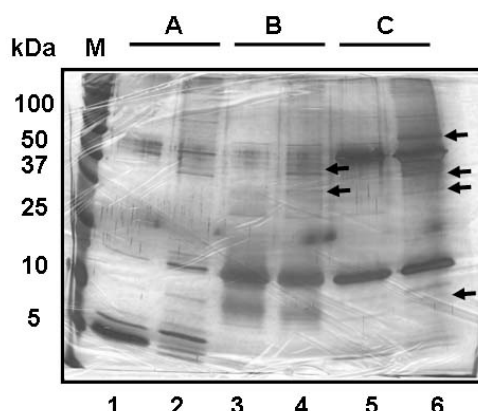
Figure 73: Silver stained 7 to 20% SDS-PAGE of TAP (A), HRV2 2A^{pro}-TAP (B) and HRV14 2A^{pro}-TAP (C). Lane M shows the protein standards in kDa. Lanes 2, 4 and 6 were incubated with 50 mg of HeLa cells extracts; lanes 1, 3 and 5 were not incubated (negative controls). The arrows indicate proteins that are not present on the negative controls. The samples were mixed with 2x Laemmli sample buffer; the volume loaded was 5µl (2.5% of the sample total volume).

Several proteins were present only in the samples incubated with HeLa extracts (indicated by the arrows in figure 73) and not in the negative controls. We decided therefore to send those samples to be analysed by mass spectroscopy. The results are shown in appendix A.

4.4.2 Analysis of the putative binding partners

Table 14 shows some of the proteins that were co-purified with HRV2 2A^{pro}-TAP and HRV14 2A^{pro}-TAP. We selected these proteins due to their function in the cell and due to the fact that other proteins with similar functions are cleaved by picornaviral 2A^{pro} (see 1.1.8.3.4). We focused on ribosomal proteins, translation and transcription factors, RNA binding proteins and proteins involved in cell structure.

Identified proteins	function
eIF4GI	translation
PABP	translation
eEF1α	translation
ß-actin	cell structure and integrity
hnRNP U	RNA binding protein
S17	Ribosomal protein
RAP74	Transcription factor
RBAF600	Interaction with retinoblastoma protein

Table 14: Proteins purified with the TAP method and identified by mass spectroscopy. These proteins were selected for further investigation due to their function in the cell.

One candidate, the retinoblastoma-associated factor 600 (RBAF600), was excluded after literature research revealed that this factor binds calmodulin (Nakatani *et al.*, 2005). As we could not obtain antibodies against ribosomal protein S17, hnRNPU protein and eukaryotic translation elongation factor 1 alpha (eIF1 α), they were also excluded from future research. Finally, we considered the protein eIF4GI, binding to HRV2 2A^{pro}, as a positive control for this method (Foeger *et al.*, 2002) as well as the PABP, which is cleaved by CVB3 2A^{pro} (Kerekatte *et al.*, 1999) and PV 3C^{pro} (Kuyumcu-Martinez *et al.*, 2002). β-actin was chosen as putative HRV 2A^{pro} binding partner.

We started the analysis of the putative interaction of β-actin with HRV2 and HRV14 2A^{pro} by performing GST pull downs to confirm its binding to 2A^{pro}. Figure 74 shows ~1 µg of the expressed GST tag, HRV2 2A^{pro} C106A - GST and HRV14 2A^{pro} C109A - GST expressed in JM101 cells and bound to glutathione-sepharose beads.
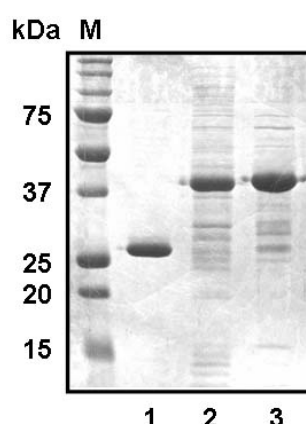
Figure 74: Commassie stained 12.5% SDS-PAGE of GST tag (lane 1), HRV2 2A^{pro} C106A – GST (lane2) and HRV14 2A^{pro} C109A – GST (lane 3).

These samples were incubated with 8 µl RRL overnight at 4°C, and after elution of the proteins from the beads with Laemmli sample buffer, we performed western blots against eIF4GI, PABP and β-actin. We chose RRL to perform the incubations because these extracts come from mammalian cells and contain all the proteins that we decided to test (Pelham and Jackson, 1976). The results of the experiment are shown in figure 75. eIF4GI and PABP bind to HRV2 2A^{pro} but not to HRV14 2A^{pro} (figure 75A and B). However, as HRV14 2A^{pro} is known to cleave eIF4GI and PABP (personal communication of Luiza Deszcz), the fact that the pull-down experiments do not show an interaction between the HRV14 2A^{pro} and these two proteins could indicate that the affinity of HRV14 2A^{pro} for PABP and eIF4GI is low or that the binding is reversible, as it was observed for the interaction between Lb^{pro} and eIF4GI (Foeger *et al.*, 2002). β-actin does not bind neither HRV2 2A^{pro} nor HRV14 2A^{pro} (figure 75C).
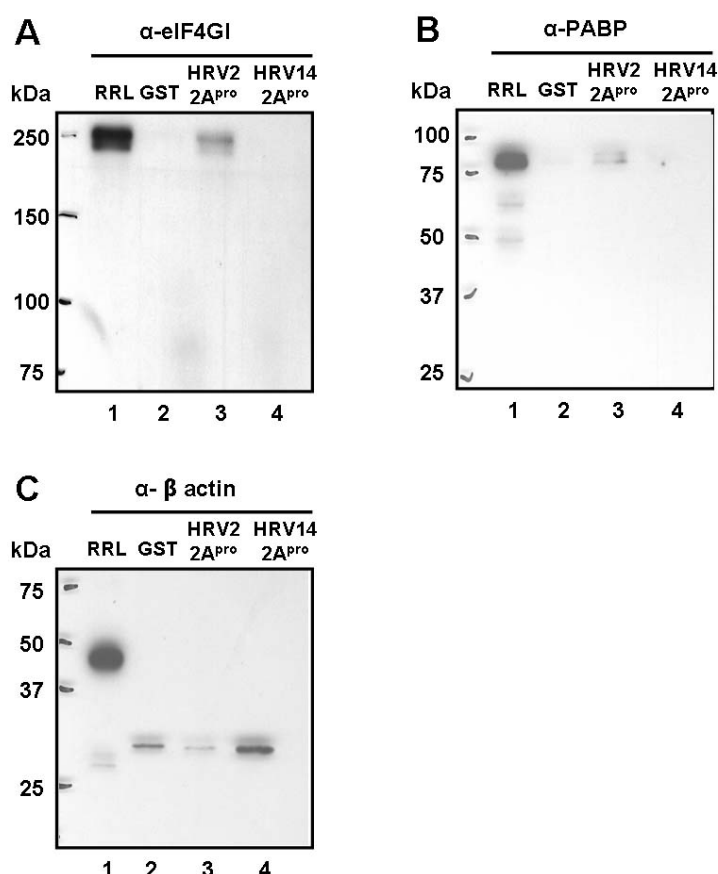
Figure 75: GST pulldown of eIF4GI (6% SDS-PAGE) (A), PABP (12.5% SDS-PAGE) (B) and β-actin (12.5% SDS-PAGE) (C). Glutathione-Sepharose beads coated with purified GST (lane 2) and with GST- HRV2 2A^{pro} and GST- HRV14 2A^{pro} (lanes 3 and 4, respectively). Lane 1 shows the input loading, corresponding to 2μl of RRL. The bound proteins were detected by immunoblotting using the antisera of eIF4GI (1:8000), PABP (1:1000) and β actin (1:1000). Protein standards in kDa are shown on the left side of the panel.

Although β-actin does not bind HRV2 or HRV14 2A^{pro}, we still wanted to see whether this protein is cleaved by the viral proteinases, as the interaction could be too weak to be observed with GST-pulldown experiments. Additionally, we also tested the eIF1α for cleavage as we were able to obtain an antibody against it (gift from Regina Cencic). To this end, we incubated 8μl of RRL (promega) and 50 mg of HeLa cell extracts with 100 ng of HRV2 and HRV14 2A^{pro} at 30°C (overnight with the HeLa extracts and 2 hours with the RRLs) and performed a western blot against β-actin and the eIF1α. PAPB was used as control for the cleavage by HRV 2A^{pro} (Luiza Deszcz, personal communication). Figure 76 shows that HRV2 2A^{pro} is not able to cleave either β-actin or eIF1α. HRV14 2A^{pro} is also not able to cleave eIF1α under the conditions used.
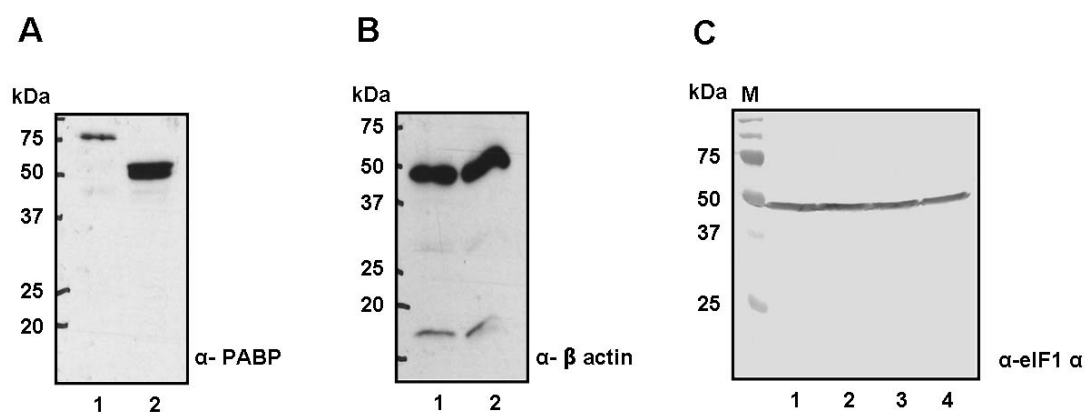
Figure 76: Immunoblot of 12.5% SDS-PAGE of β actin, PABP and eIF1 α. 50 mg of HeLa cell extracts or 8 μl of RRL (Promega) were incubated with 100 ng of recombinant HRV2 and HRV14 2A^{pro} at 30°C during 2 hours (RRL) or overnight (HeLa extracts). **A)** α-PABP (1:1000); lane 1 shows RRLs without HRV2 2A^{pro}; lane 2 RRLs incubated with HRV2 2A^{pro}. **B)** anti β-actin (1:1000); lane 1 shows RRLs without HRV2 2A^{pro}; lane 2 RRLs incubated with HRV2 2A^{pro}. **C)** α-eIF1α (1:2000); lane 1 shows Hela cell extracts not incubated; lane 2 HeLa cell extracts incubated without proteinases; lane 3 Hela cell extracts incubated with HRV2 2A^{pro} and lane 4 RRLs incubated with HRV14 2A^{pro}.

4.4.3 Alternative approach for expression and purification of the protein complexes

The results shown above were not satisfactory. Therefore, we decided to modify the method. Instead of over-expressing the HRV2 and HRV14 2A^{pro} in bacteria, we decided to transiently transfect human cells with the same proteinases. We used the pMZI vector, developed by Zeghouf *et al.* (2003) which was given to us by J. K. Greenblatt. This vector contains an ecdysone promoter and the TAP tag. The ecdysone promoter allows the use of the Ecdysone-Inducible Mammalian Expression System (Invitrogen). In this system we use ponasterone A, an analogue of ecdysone, to induce the expression of the gene cloned downstream of the promoter. As mammalian cells are not responsive to ecdysone or analogs, the basal levels of transcription are very low (Ecdysone-Inducible Mammalian Expression System, version E, Invitrogen).

The inactive forms of HRV2 2A^{pro} and HRV14 2A^{pro} were cloned into pMZI vector using the restriction enzymes NdeI and *Xho*I, in frame with the TAP tag which is located in the 3' end of the construct (figure 77). The new vectors were named pMZI-HRV2 2A^{pro} C106A and pMZI-HRV14 2A^{pro} C109A.
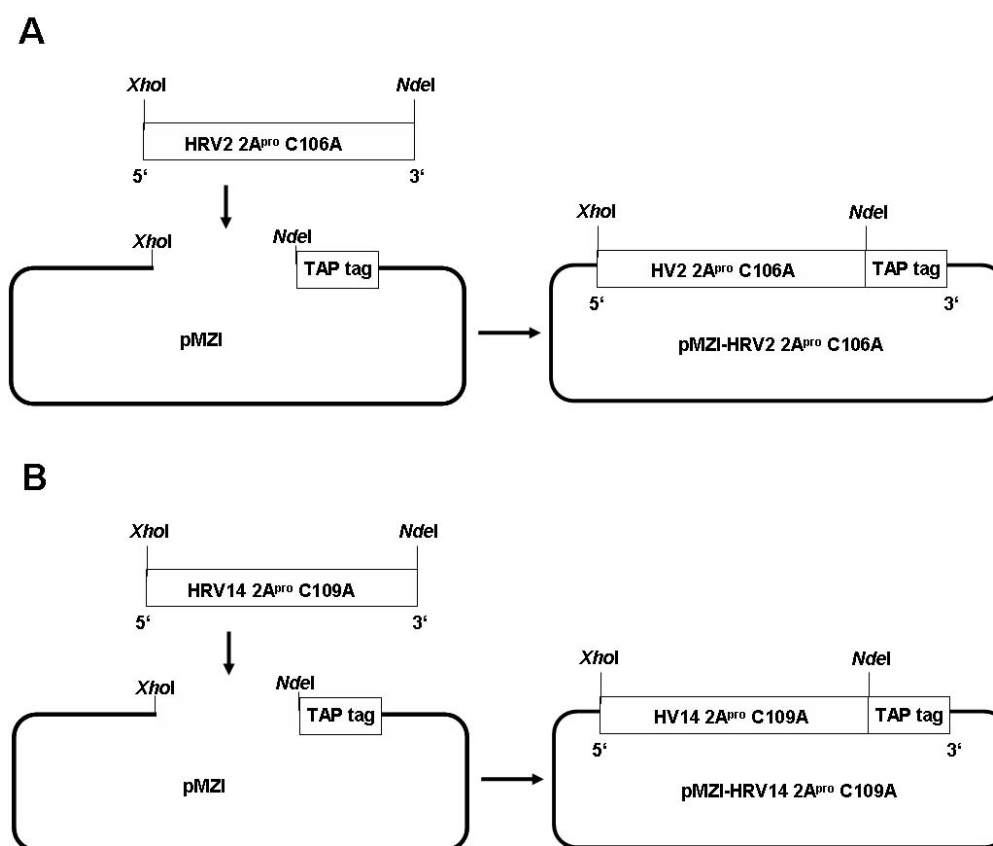
Figure 77: Cloning strategy to introduce the inactive forms of HRV2 and HRV14 2A^{pro} into pMZI.
A) pMZI-HRV2 2A^{pro} C106A. **B)** pMZI-HRV14 2A^{pro} C109A. The ORFs were amplified with the primers TIM1474 and TIM1475 (A) and TIM1476 and TIM1477 (B) and introduced into pMZI digested with *Nde*I and *Xho*I. The TAP tag is C-terminal.

HEK 293T cells are highly transfectable (ATCC). Therefore we chose these cells for this set of experiments, in which the pMZI vectors were co-transfected with the vector pVgRXR from the Ecdysone-Inducible Mammalian Expression System (Invitrogen). The transfection was done using lipofectamin 2000 from Invitrogen, following the manufacturer instructions. The expression was induced using ponasterone A (Invitrogen) and cell extracts were prepared from several time points to observe the progress of the protein expression. Figure 78 shows the result of the first small scale transfection (6 well plate), in which the expressed HRV2 2A^{pro}-TAP and HRV14 2A^{pro}-TAP can be observed. For the protein detection, we used a polyclonal antibody against HRV2 2A^{pro} which also detects the protein A domain of the TAP tag. Protein A binds to the Fc region of the antibody.
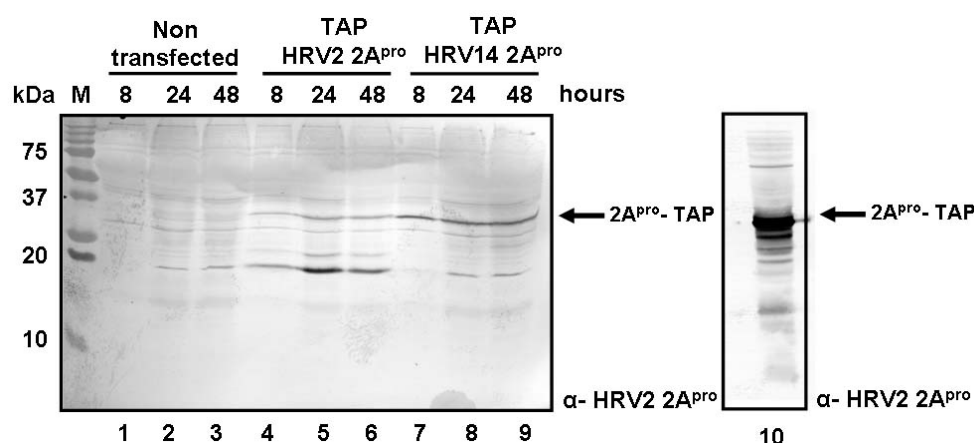
Figure 78: immunoblot of 12.5% SDS-PAGE showing the expression of HRV2 2A^{pro}-TAP and HRV14 2A^{pro}-TAP after a small scale transfection of HEK-293T cells. The proteins were detected by immunoblotting using the HRV2 2A^{pro} antiserum (1:1000). Protein standards in kDa are shown in line M. Lane 10 shows a positive control for the immunoblot (HRV2 2A^{pro}-TAP). The antiserum used is targeting the protein A, which is part of the TAP tag.

After confirming that the transfection was successful, we performed large scale experiments using the protocol described by Anne-Claude Gingras (see section 3.5.3.5.2). However, the large scale experiments did not show any expression of 2A^{pro}; only the TAP tag alone is expressed (figure 79).
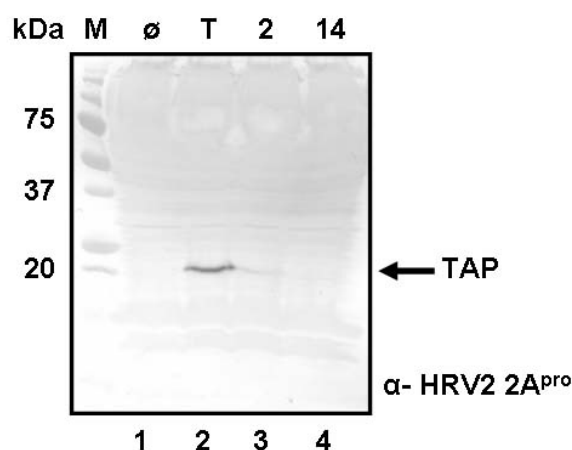
Figure 79: Immunoblot of 12.5% SDS-PAGE showing the expression of HRV2 2A^{pro}-TAP and HRV14 2A^{pro}-TAP after transfection of 2x10^6 HEK-293T cells and 48 hours expression. The proteins were detected by immunoblotting using the HRV2 2A^{pro} antiserum (1:1000). Lane 1 shows the non transfected sample; lane 2 the TAP tag; lanes 3 and 4 show HRV2 2A^{pro}-TAP and HRV14 2A^{pro}-TAP respectively. Protein standards in kDa are shown in line M. The antiserum used is targeting the protein A, which is part of the TAP tag.

113

As the TAP tag is visible on the western blots, a possible technical error could be excluded. Instead, we thought of the possibility of the HRV2 and HRV14 2A^{pro} being toxic for the cells. For this reason we wanted to know how cells react to other viral proteins. Can HEK 293T cells overexpress other 2A^{pro} or proteinases of other viruses? To this end, we cloned the inactive forms of HIV 1 proteinase (provided by Petra Schlick (Schlick, 2004)), CVB4 2A^{pro} (constructed by Andreas Roetzer (Roetzer, 2004)) and FMDV Lb^{pro} (constructed by Regina Cencic (Cencic, 2005)) into the pMZI vector using the restriction enzymes *Nde*I and *Xho*I (figure 80). The new vectors are pMZI-HIV1^{pro} D25A D125A (encodes a protein product of 42.5 kDa), pMZI-CBV4 2A^{pro} C110A (encodes a protein product of 37.0 kDa) and pMZI-FMDV Lb^{pro} C51A (encodes a protein product of 40.3 kDa).
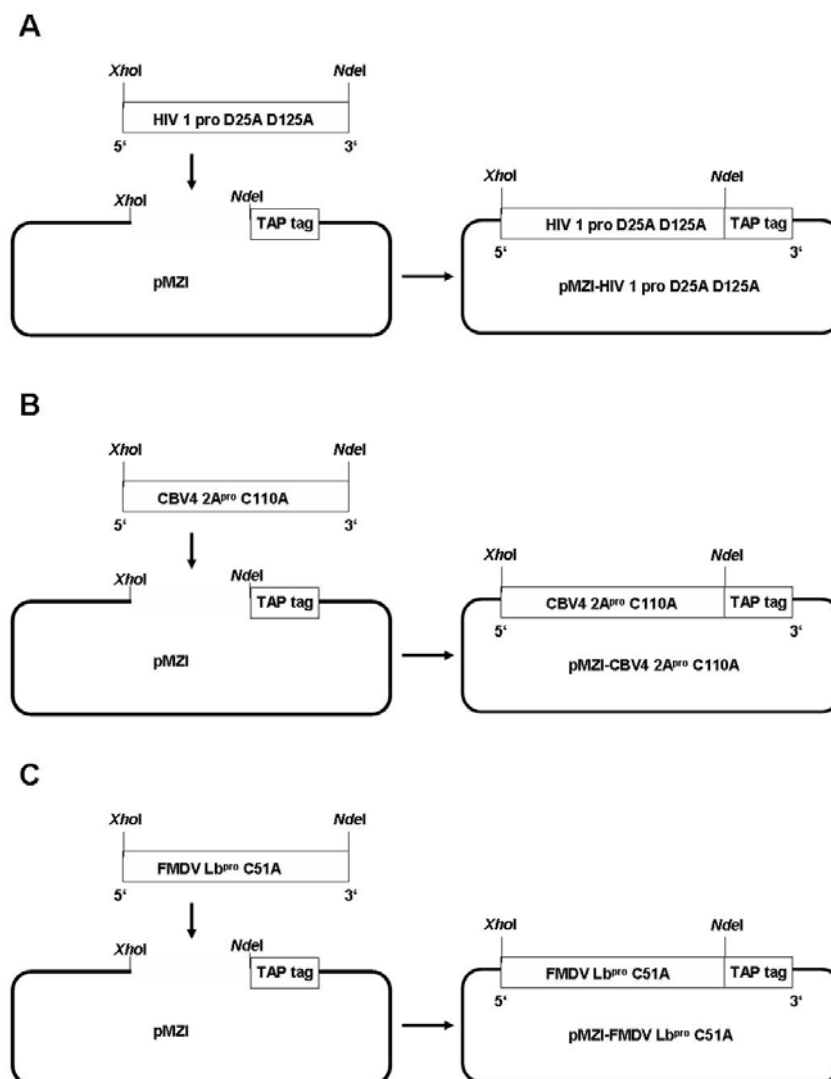
Figure 80: Cloning strategy to introduce the inactive forms of HIV1 protease, CBV4 2A^{pro} and FMDV Lb^{pro} into pMZI. A) pMZI-HIV1^{pro} D25A D125A (primers TIM1518 and TIM1519). **B)** pMZI-

CBV4 2A^pro C110A (primers TIM1520 and TIM1521). **C)** pMZI-FMDV Lb^pro C51A (primers TIM1522 and TIM1523). The ORFs were introduced into pMZI digested with *Nde*I and *Xho*I. The TAP tag is C-terminal.

These plasmids were transfected into HEK 293T cells. The protein complexes were purified via the same methods used for pMZI-HRV2 2A^pro C106A and pMZI-HRV14 2A^pro C109A. The expression was induced for 48 hours with different concentrations of ponasterone A. Only pMZI-FMDV Lb^pro was successfully expressed (figure 81).
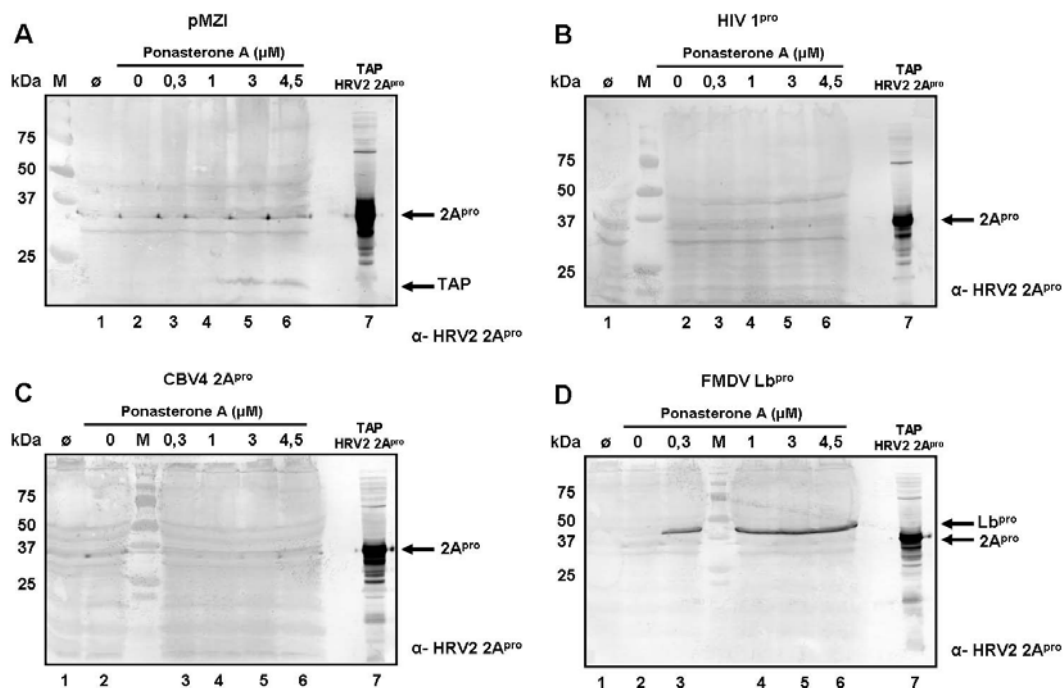
Figure 81: immunoblot of 12.5% SDS-PAGE showing the expression pMZI-TAP (A), HIV 1^pro-TAP (B), CBV4 2A^pro-TAP (C) and FMDV Lb^pro-TAP after a large scale transfection of HEK-293T cells and 48 hours expression (D). The proteins were detected by immunoblotting using the HRV2 2A^pro antiserum (1:1000). Lane 1 shows the non transfected sample; lanes 2 to 6 show the induction with different concentrations of ponasterone A. Lane 7 shows a positive control for the immunoblot (HRV2 2A^pro-TAP). Protein standards in kDa are shown in line M. The antiserum used is targeting the protein A, which is part of the TAP tag.

The eluted fractions of pMZI-FMDV Lb^pro and pMZI from the calmodulin beads were quantified and loaded on a 7 to 20% SDS-PAGE for silver staining (figure 82) and sent for mass spectroscopy analysis. Lb^pro cleaved of the protein A (first part of the TAP tag) has a molecular weight of 22.8 kDa and it was not observed on the gel. The band running at 37 kDa (figure 82, lane 2) might be glyceraldehyde-3-phosphate dehydrogenase or annexin A2,

according wtih the results presented in tables 20 and 21 (appendix A). Unfortunately none of the 28 proteins identified appeard to be a promising candidate for a binding partner. Also, the one the protein that is known to bind Lb^{pro}, the eIF4GI is missing. Possibly the amount of purified protein complexes was not sufficient for mass spectroscopy detection.
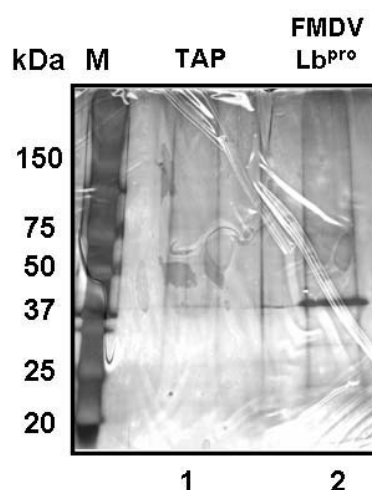
Figure 82: Silver stained 7 to 20% SDS-PAGE of TAP FMDV Lb^{pro}-TAP. After transfection and expression for 48 hours in HEK-293T cells, the cells were lysed and the supernatants were purified using the TAP tag protocol (see section 3.5.3.5.2). The volume loaded was 15µl (3.7% of the sample total volume). Protein standards in kDa are shown in line M.

The new strategy for the TAP tag protocol is closer to physiological conditions. Although the viral proteins are still over-expressed, the interaction with the cellular components occurs in biological conditions where the proteins are in native conditions and functional. This difference from first method is an improvement as it can help to minimize the number of false positives. However, it is necessary to determine whether over-expression of picornaviral proteinases in human cells, even in their inactive forms, is harmful for the cells. Of all the proteinases tested, only the FMDV Lb^{pro} was successfully expressed, though the results from the TAP purification failed to show any promising binding partners. Therefore, further experiments must be done to optimise and scale-up the method.

5 Discussion

HRV are responsible for about 50% of the common cold. Although common cold is not a severe infection it has a major economic impact. It is estimated that $40 billion are spent every year in the United States to treat common cold (Fendrick *et al.*, 2003). Therefore, it is very important to study and understand these viruses.

There has been constant research to find a vaccine against HRV. However the large number of HRV serotypes makes this task very difficult as one serotype is not neutralized by antibodies produced against other serotype. An alternative approach is to develop antiviral drugs against the non-structural proteins.

Until recently, picornaviral 3C^{pro} and its precursor 3CD have been seen as the main potential drug targets. 3C^{pro} is the most well studied picornaviral proteinase as it performs the majority of the maturation cleavages on the polyprotein. Among the inhibitors developed against these proteins is the rupintrivir (formerly known as AG-7088), an irreversible inhibitor of rhino- and enteroviruses 3C^{pro} (Binford *et al.*, 2005). Rupintrivir has been tested in clinical trials and the results showed that this inhibitor is able to moderate the severity of the symptoms and reduce the viral load during infection (Binford *et al.*, 2007). Another inhibitor similar to rupintrivir is "compound 1" ((E)-(S)-4-((S)-2-(3-[(5-methyl-isoxazole-3-carbonyl)-amino]-2-oxo-2H-pyridin-1-yl)-pent-4-ynoylamino)-5-((S)-2-oxo-pyrrolidin-3-yl) pent-2-enoic acid ethyl ester), which also demonstrated broad-spectrum activities against several HRV serotypes tested *in vitro* (Patick *et al.*, 2005). These inhibitors interact with conserved residues of 3C^{pro} suggesting efficacy against a broad number of serotypes (Matthews *et al.*, 1999).

However, as mentioned in sections 1.1.8.3.1 and 4.1.2 HRV 2A^{pro} of picornaviruses are potential targets for antiviral drugs. Yet, these proteins vary greatly among the different serotypes. In order to develop effective inhibitors, it is of great importance to understand the substrate specificity of the different rhinoviral 2A^{pro}.

The work in this thesis covered three aspects in order to characterize two rhinoviral 2A^{pro}, namely the investigation of the specificity of HRV2 and HRV14 2A^{pro} during substrate recognition, the expression and purification of HRV14 2A^{pro} and the cellular initiation factor eIF4GII for structural studies as well a the search for new cellular binding partners of picornaviral proteinases.

5.1 Specificity of HRV 2A proteinases

The first part of this work was centred on determining the substrate specificity of the 2A^{pro} of HRV2 and HRV14. These two proteins share only 40% amino acid residues. We showed that HRV2 and HRV14 2A^{pro} have different kinetics when processing eIF4GI *in vitro*

(figure 16) and we wanted to know which residues are responsible for the differences observed.

We found that HRV14 2A^{pro} is not able to process the polyprotein when the cleavage sequence is that of eIF4GI. In contrast, HRV2 2A^{pro} processes a polyprotein bearing the eIF4GI cleavage sequence at practically wild type levels. One caveat could be that it is necessary to determine the sequence cleavage in eIF4GI for HRV14 and other group B rhinoviruses to see whether the same site is used for cleavage. However, as eIF4GI is cleaved by CV and PV 2A^{pro} at the same sequence as HRV2 2A^{pro} (Lamphear *et al.*, 1993; Zamora *et al.*, 2002), the hypothesis that HRV14 2A^{pro} can cleave eIF4GI at the same sequence seems plausible. Actually, our results showed that a single modification on the cleavage sequence of eIF4GI was sufficient to HRV14 2A^{pro} recognize the cleavage site. This modification was made at P1 position in which we replaced the arginine by a tyrosine (the residue recognized by HRV14 2A^{pro} in the polyprotein). We then introduced new mutations at P3 and P2' sites which also show differences among the two proteinases. The results showed that these mutations did not produce any effect on the performance of the protease, enhancing the significance of the P1 site for substrate recognition by HRV14 2A^{pro}.

Considering that HRV B group rhinoviruses, amongst them HRV14 2A^{pro}, are closer related to enteroviruses than to group A rhinoviruses (Laine *et al.*, 2005), we wanted to see whether PV1 2A^{pro} was also unable to recognize an arginine at P1 position. We would have expected a result similar to HRV14 2A^{pro} as the wild type residue at P1 position in the polyprotein is a tyrosine for both HRV14 and PV (table 13). Additionally, the sequence identity is higher between HRV14 2A^{pro} and PV1 2A^{pro} than between HRV14 2A^{pro} and HRV2 2A^{pro} (figure 83). Surprisingly, the outcome of this experiment was only a slight delay on the activity of the 2A^{pro}. This indicates that the 2A^{pro} specificity lies mainly in the non-conserved regions of the protein.

A


```
HRV2_2A     1 - - GPSDMYVHVGNLIYRNLHLFNSEMHESILVSYSS-DLI 37
HRV14_2A    1 GLGPRYGGIYTSNVKIMNYHLMTPEDHHNLIAPYPNRDLA 40

HRV2_2A    38 IYRTNTVGDDYIPSCDCTQATYYCKHKNRYFPITVTSHDW 77
HRV14_2A   41 IVSTGGHGAETIPHCNCTSGVYYSTYYRKYYPIICEKPTN 80

HRV2_2A    78 YEIQESEYYPKHIQYNLLIGEGPCEPGDCGGKLLCKHGVI 117
HRV14_2A   81 IWIEGNPYYPSRFQAGVMKGVGPAEPGDCGGILRCIHGPI 120

HRV2_2A   118 GIVTAGGDNHVAFIDLRHFHC-AEEQ 142
HRV14_2A  121 GLLTAGGSGYVCFADIRQLECIAEEQ 146
```

B

```
HRV14_2A    1 GLGPRYGGIYTSNVKIMNYHLMTPEDHHNLIAPYPNRDLA  40
PV1_2A      1 GFGHQNKAVYTAGYKICNYHLATQDDLQNAVNVMWSRDLL  40

HRV14_2A   41 IVSTGGHGAETIPHCNCTSGVYYSTYYRKYYPIICEKPTN  80
PV1_2A     41 VTESRAQGTDSIARCNCNAGVYYCESRRKYYPVSFVGPTF  80

HRV14_2A   81 IWIEGNPYYPSRFQAGVMKGVGPAEPGDCGGILRCIHGPI 120
PV1_2A     81 QYMEANNYYPARYQSHMLIGHGFASPGDCGGILRCHHGVI 120

HRV14_2A  121 GLLTAGGSGYVCFADIRQLECIAEEQ---            146
PV1_2A    121 GIITAGGEGLVAFSDIRDLYAYEEEAMEQ            149
```

C

Figure 83: Analysis of HRV2, HRV14 and PV1 2A^pro amino acid sequence. A and B) Sequence alignments between HRV14 2A^pro and HRV2 2A^pro (A) and HRV14 2A^pro and PV1 2A^pro (B). HRV 14 2A^pro shares 40% identity with HRV2 2A^pro and 47% with PV1 2A^pro. Conserved residues are represented in blue. The alignments were done with the clustalW2 program. **C) Tree based on the amino acid identity of HRV2, HRV14 and PV1 2A^pro, showing that HRV14 2A^pro amino acid sequence is closer related to PV1 2A^pro than to HRV2 2A^pro.** The tree was made using the program jalview.

In order to understand why HRV14 2A^pro behaves so differently from HRV2 2A^pro, we performed site directed mutagenesis at several sites of the proteinase sequence. Our work was based in amino acid sequence comparisons, among several picornaviruses, and on the crystal structure of HRV2 2A^pro (Petersen *et al.*, 1999). At present, this is the only HRV 2A^pro crystal structure solved. The NMR structure of CVB4 2A^pro is also available (Baxter *et al.*, 2006); however, we did not consider it due to the low resolution of the region surrounding the catalytic triad.

One region which seemed likely to be important was the substrate binding region of HRV14 (Gly85, Asn86 and Pro87), identified from the equivalent residues in HRV2 (Glu84, Ser83 and Glu84) (Petersen *et al.*, 1999). Figure 84 shows the position of this region (black

rectangle). However, changes in this region had no effect on the HRV14 2A^{pro} mutant bearing an arginine at P1. Furthermore, in the reciprocal experiment, when the residues from HRV14 2A^{pro} were introduced into HRV2 2A^{pro} sequence (Glu84Pro and Glu82Gly), no influence on the recognition of substrate by the HRV2 2A^{pro} was observed.
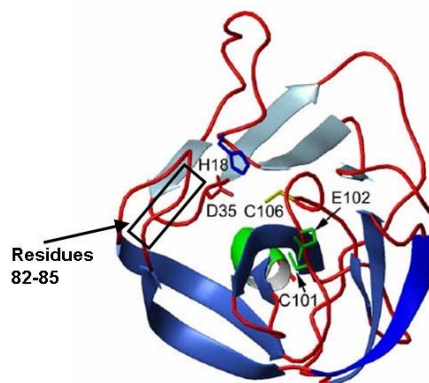
Figure 84: The structure of HRV2 2A^{pro}. Ribbon diagrams of the overall structure of HRV2 2A^{pro} (Same as figure 23). The single α-helix is shown in green, the β-strands of the N-terminal and C-terminal domains are shown in silver and deep blue, respectively. The three residues of the catalytic triad are shown as are residues C101 and E102. Residues 82 to 85 are marked with a black rectangle. The figure was generated using the program Molscript (Kraulis, 1991) and was a kindly prepared by Christina Mayer.

Further analysis of HRV2 2A^{pro} identified the Cys101 side chain (corresponding to Ala104 in HRV14 2A^{pro}) as a important residue for substrate recognition. This residue protrudes into the S1 pocket, the site on the enzyme that recognizes the P1 substrate residue (figure 84). At the end of the pocket, the presence of Glu102 provides a negative charge which presumably assists in accepting the positive charge of the arginine at position P1 (Petersen *et al.*, 1999). Further support for the importance of Cys101 and Glu102 was obtained from the structure of the *Streptomyces griseus* proteinase B (SGPB). This enzyme is the closest related serine protease to picornaviral 2A^{pro}. Interestingly, the equivalent residues in this protease to the ones mentioned above are Ala192 and Glu192A (Bateman *et al.*, 2000). Bateman *et al.* (2000) found that an inhibitor with tyrosine at the P1 position bound to SGPB 10 to 20 times stronger than another inhibitor with arginine at P1 position. These results support the role of Cys101 and thus of the equivalent Ala104 in the specificity of HRV14 2A^{pro}. Additionally, the residue content at position 101 (for HRV2 and correspondent residue for other picornaviruses) is consistent with the amino acid content at the P1 position (see table 13). Based on these analyses, we decided to replace the Ala104 of HRV14 2A^{pro}, containing the arginine at P1 position, by a cysteine and by a serine. We were expecting that the HRV14 2A^{pro} would

accept the arginine at P1 position and perform the cleavage from VP1, like HRV2 2A^{pro}, at least for the mutant containing a cysteine at position 104. However, the rate of self-processing was far from being restored to the wild type levels. Evidently, other residues are also involved in recognition of the P1 residue. Thus, the structure of HRV14 2A^{pro} is required before identification of such residues can be made, given the low level of identity between HRV2 and HRV14 2A^{pro}.

In PV1 2A^{pro}, the residue at position 104 is alanine as for HRV14 2A^{pro}; however, the residue corresponding to Glu102 is a serine. This could help explain why PV1 2A^{pro} can accept an arginine at P1 position, in contrast with HRV14 2A^{pro}. However, once again, the low level of similarity between the two proteins renders difficult the identification of other residues involved in determining specificity.

We have shown that HRV2 2A^{pro} and HRV14 2A^{pro} differ significantly in the specificity at P1 position. It will be interesting to investigate whether these differences are related with differences in pathogenicity of viruses from the two genetic groups. Furthermore, these differences have to be taken into account when designing inhibitors. Indeed, Deszcz *et al.* (2006) reported recently a specific inhibitor for 2A^{pro} which is active against several HRV 2A^{pro} and CVB4 2A^{pro} *in vitro* (see sections 1.1.8.3.1 and 4.1.2). However, zVAM.fmk inhibits different 2A^{pro} to different extents. HRV2 2A^{pro} is inhibited in the intermolecular cleavage of eIF4GI and not during the self-processing whilst HRV14 2A^{pro} is affected during the self-processing and, to a lesser extent, in the intermolecular cleavage. The sensitivity of 2A^{pro} to zVAM.fmk during the intermolecular cleavage varies from the nanomolar range for HRV2 2A^{pro} to the micromolar range for HRV14 2A^{pro}. CBV4 is inhibited at intermediate levels between HRV2 and HRV14 2A^{pro}. We showed that PV1 2A^{pro} is not inhibited at the intramolecular cleavage. In contrast, the intermolecular cleavage as well as viral replication are inhibited by zVAM.fmk (K. Kirkegaard, personal communication). These results are summarised in table 15.

zVAM.fmk effect in picornaviral 2A^{pro} and caspases activity		
Protein	**Polyprotein cleavage (intramolecular)**	**Cleavage of eIF4GI (intermolecular)**
HRV2 2A^{pro}	++	+++
HRV14 2A^{pro}	+++	+
PV1 2A^{pro}	-	+++
CVB4 2A^{pro}	?	+
Pro-caspase 9	-	-

Table 15: Summary of the effect of zVAM.fmk on the inhibition of picornaviral 2A^{pro}.

In conclusion, we have shown that HRV2 and HRV14 2A^{pro} have different specificities at the P1 position in the polyprotein context. Furthermore, our results showed that the residue in position 101 of HRV2 2A^{pro} (104 for HRV14 2A^{pro}) is involved in the discrimination of the residues accepted by these proteinases at the P1 site. These results, together with the structure of HRV14 2A^{pro}, will help to understand the mechanisms of HRV 2A^{pro} and facilitate the discovery of new inhibitors.

5.2 Protein purification for crystallization and NMR experiments

Rhinoviral and enteroviral 2A^{pro} cleavage mechanisms vary at a great extent. For instance, it was shown that PV 2A^{pro} cleaves eIF4G in the same manner as HRV2 2A^{pro} (Cencic, 2005) and not as HRV14 2A^{pro}, although PV is closer related to group B HRVs (Laine *et al.*, 2005). Additionally, the mechanisms used by 2A^{pro} to cleave eIF4G are still a matter of controversy (see section 1.1.8.3.4).

To better understand HRV14 2A^{pro} mechanisms, we set out to purify and crystallize HRV14 2A^{pro}. In addition, we wanted to understand the interaction of this and other picornaviral proteinases, such as FMDV Lb^{pro}, with the cellular protein eIF4G. For that we planned to obtain a fragment of eIF4GII, containing the binding site for eIF4E and the cleavage sites for FMDV Lb^{pro} and HRV2 2A^{pro} (residues 552 to 744) for crystallization and for NMR experiments. Although the structures of two fragments of eIF4GI are available (residues 393 to 490 (Gross *et al.*, 2003) and residues 745 to 1003 (Marcotrigiano *et al.*, 2001), none of these fragments contain neither binding sites nor cleavage sites for picornaviral proteases.

The purification of both proteins was successful, although the expression levels were low and the proteins were mainly insoluble. We obtained 1.2 mg of HRV14 2A^{pro} at a concentration of 2.83 mg/ml; 1.5 mg of eIF4GII at a concentration of 2.4 mg/ml and 0.25 mg of ^{15}N labelled eIF4GII at a concentration of 150 µM. However, it was not possible to set either protein for crystallization because they appeared unstructured after purification.

We found HRV14 2A^{pro} to be unstable at high concentrations under pH 9.0 in the buffers used throughout this work, remarkably different from HRV2 2A^{pro} which is folded and active at pH 8.0. The buffer contents are mainly 50 mM Tris-HCl pH 9.0 and 50 mM NaCl. Perhaps a higher concentration of NaCl will help HRV14 2A^{pro} to keep its structure during the purification process.

The domain of eIF4GII purified was also unstructured, both in the samples prepared for crystallization and in the labelled sample prepared for NMR studies. However, this observation was not surprising as it has been shown that the binding of eIF4E induces

changes in the conformation of eIF4GI (Gross *et al.*, 2003; Hershey *et al.*, 1999). We believe that eIF4E and picornaviral proteinases such as FMDV Lb^{pro} can also introduce modifications in the structure of eIF4GII. Therefore, we performed a second NMR experiment in which a four fold excess of inactive FMDV Lb^{pro} was added to the ^{15}N labelled eIF4GII. Unfortunately, the results showed that eIF4GII was, once again, unstructured. One of the reasons could have been the rather low concentration of eIF4GII upon addition of FMDV Lb^{pro}. However, we believe that the complex with eIF4E is of primary importance, as the formation of the complex eIF4GII-eIF4E seems to acquire a structure that is better recognized by picornaviral 2A^{pro} (Haghighat *et al.*, 1996). To this end, we expressed and purified eIF4E to a level of purity and concentration sufficient to perform preliminary NMR experiments. Unfortunately, these experiments fall out of the time frame of this thesis. Nevertheless, we believe that the addition of an excess of non labelled eIF4E to ^{15}N labelled eIF4GII will form a stable and well structured complex and we will be able to solve the structure of this important domain. However, the expression of eIF4GII probably needs to be done in eukaryotic cells, as our results showed that only the fragment of eIF4GII expressed in Sf9 cells was putatively recognized by the HRV14 3C^{pro} (see section 4.3.1). These results indicate that eIF4GII only acquires a correctly folding state when expressed in a eukaryotic system, perhaps due to post-translation modifications.

5.3 Screening of HRV2 and HRV14 2A^{pro} binding partners

Picornaviral 2A^{pro} bind and cleave several cellular proteins. Rhinovirus and enterovirus 2A^{pro} cleave eIF4G and PABP. HRV14 2A^{pro} cleaves cytokeratin 8. PV 2A^{pro} cleave TATA-box binding protein (TBP) and two nuclear pore complex (NPC) proteins, Nup153 and Nup62. CV 2A^{pro} cleave dystrophin causing cardiomyopathy (Badorff *et al.*, 2000; Badorff *et al.*, 1999; Foeger *et al.*, 2002; Kerekatte *et al.*, 1999; Park *et al.*, 2008; Seipelt *et al.*, 2000; Yalamanchili *et al.*, 1997a).

Despite this long list we wanted to find out whether other and yet undetected partners in the host cell for HRV2 and HRV14 2A^{pro} exist. To that end, we chose the TAP method developed by Rigaut *et al.* (1999). We used a different approach in that the 2A^{pro} were over expressed in *E. coli* and after sonication and binding to IgG beads they were incubated with HeLa extracts.

Two proteins that are known to bind HRV2 2A^{pro} were found, eIF4GI and PABP ((Foeger *et al.*, 2002) and Luiza Deszcz, personal communication). We considered the interaction of these proteins with the 2A^{pro} as positive controls for the method. However, cytokeratin 8 was not found. One of the reasons for this result could have been that the interaction of cytokeratin 8 with HRV14 2A^{pro} is very weak or that the expression levels of this

protein is below the limit of sensitivity of the detection method used. The amount of total protein extract was very high and proteins that are highly expressed can mask other proteins that have very low expression levels.

We selected some proteins co-purified with the HRV2 and HRV14 2A^{pro} and identified by mass spectroscopy analysis to use in further experiments in order to confirm their interaction with 2A^{pro}. The criteria for the choice were the role of the proteins in the cell. For instance, the identified proteins should be involved in transcription, translation or be part of the cytoskeleton. A literature search excluded some of the candidates such as retinoblastoma-associated factor 600 (RBAF600), which binds to calmodulin beads (Nakatani *et al.*, 2005). Our interest in this protein was based on the known interaction of other viral proteins with retinoblastoma, namely simian virus 40 (SV40) (Moens *et al.*, 2007). Some of the proteins selected like ribosomal protein S17 or hnRNPU could not be investigated due to lack of antibodies. It will be of interest to acquire antibodies and perform pull-down experiments to confirm whether there is an interaction with HRV2 and HRV14 2A^{pro}.

In the end, three of the selected proteins were tested for interaction with HRV2 and HRV14 2A^{pro}. β-actin and PABP were tested for binding and cleavage. The translation factor eEF1α was tested for cleavage. The results showed that PABP binds and is cleaved by HRV2 2A^{pro}, confirming the results of Luiza Deszcz (data not shown). In contrast, β-actin does not bind neither is cleaved by HRV2 and HRV14 2A^{pro}. Finally, the eEF1α is not cleaved by any of the two proteases *in vitro*; therefore we did not perform the binding experiments. The outcome of this work suggests that the method used was not optimal; perhaps the amount of cell extract used for incubation was too high, which raised such an elevated number of false positives.

To achieve conditions closer to physiological levels we used the vector (pMZI) for human cells transfection which contains the TAP tag, developed by Zeghouf *et al.* (2004). We introduced the inactive forms of HRV2 and HRV14 2A^{pro} in this vector and transfected transiently human HEK 293T cells with the two constructs. We did not success in expressing the viral proteases in large scale experiments; only cells transfected with the empty vector expressed the TAP tag. We hypothesised that HRV2 and HRV14 2A^{pro} can be toxic for the cells, even the inactive form, and maybe the expression would have been blocked. Therefore, we decided to clone the inactive forms of HIV 1 protease, CVB4 2A^{pro} and FMDV Lb^{pro} in the pMZI vector and tried to express them. Only FMDV Lb^{pro} was successfully expressed; however, the results from the mass spectroscopy analysis did not reveal any potential Lb^{pro} binding partner. For the other proteins, it is possible that they are toxic for the cells.

In conclusion, the TAP method is a useful tool for identification of protein-protein interactions. The modifications that we introduced in the method only worked partially. We

were able to confirm two interactions of cellular proteins with 2A^{pro}; however we failed in identifying new binding partners for these proteinases. Further optimization of the method is necessary, namely find the optimal expression conditions in the HEK 293T cells or even try the expression of 2A^{pro}-TAP tag in yeast by creating stable clones expressing the inactive viral proteins, as described in the original method (Rigaut *et al.*, 1999).

6 Appendixes

6.1 Appendix A

Mass spectroscopy results for the TAP experiments

HRV14-2A^{pro} C109A negative control

protein	Mass kDa	score
gi|223036 troponin C-like protein	16696	889
gi|109327 myosin-light-chain kinase (EC 2.7.1.117), skeletal muscle - rabbit	65997	635
gi|162648 albumin [Bos taurus]	71244	494
gi|106586 Ig kappa chain V-III (KAU cold agglutinin) - human	23037	170
gi|27806751 alpha-2-HS-glycoprotein [Bos taurus]	39193	105
gi|33700 immunoglobulin lambda light chain [Homo sapiens]	25519	72
gi|29649713 protease serine 1 [Homo sapiens]	9218	64

Table 16: HRV14-2A^{pro} C109A negative control. Search against the mammalian subset of the NCBI nr database.

HRV14-2A^{pro} C109A positive

protein	Mass kDa	score
gi|4506787 IQ motif containing GTPase activating protein 1 [Homo sapiens]	189761	1610
gi|12667788 myosin, heavy polypeptide 9, non-muscle [Homo sapiens]	227646	1591
gi|223036 troponin C-like protein	16696	1553
gi|18088719 Tubulin, beta polypeptide [Homo sapiens]	50096	1342
gi|15277503 ACTB protein [Homo sapiens]	40536	1039
gi|42476013 NHL repeat containing 2 [Homo sapiens]	80249	760
gi|2119266 tubulin alpha-1 chain - human	50804	705
gi|5729877|ref|NP_006588.1| heat shock 70kDa protein 8 isoform		
gi|14993776 skeletal myosin light chain kinase [Homo sapiens]	65214	539
gi|16507237 heat shock 70kDa protein 5 (glucose-regulated protein, 78kDa) [Homo sapiens]	72402	386
gi|162648 albumin [Bos taurus]	71244	374
gi|17986258 smooth muscle and non-muscle myosin alkali light chain isoform 1 [Homo sapiens]	17090	323
gi|19070472 **retinoblastoma-associated factor 600 [Homo sapiens]**	**580607**	**308**
gi|5123454|ref|NP_005336.2| heat shock 70kDa protein 1A [Homo sapiens]		

127

protein	Mass kDa	score
gi|57209936 melanoma antigen, family D, 2 [Homo sapiens]	55932	266
gi|4506693 **ribosomal protein S17 [Homo sapiens]**	**15597**	**256**
gi|266992 Splicing factor, arginine/serine-rich 2 (Splicing factor SC35) (SC-35) (Splicing component, 35 kDa)	25560	245
gi|14141163 **heterogeneous nuclear ribonucleoprotein U isoform a [Homo sapiens]**	**91164**	**225**
gi|189998 M2-type pyruvate kinase	58447	201
gi|5032069 splicing factor 3b, subunit 4 [Homo sapiens]	44414	179
gi|16741043 MRCL3 protein [Homo sapiens]	19839	174
gi|54696696 annexin A1 [Homo sapiens]	38918	173
gi|7706310 LUC7-like 2 [Homo sapiens]	48104	169
gi|48734733 **Eukaryotic translation elongation factor 1 alpha 1 [Homo sapiens]**	**50438**	**161**
gi|42490910 Ribosomal protein L13 [Homo sapiens]	24308	127
gi|538581 **polyadenylate-binding protein - human**	**70508**	**126**
gi|54696638 heat shock 27kDa protein 1 [Homo sapiens]	22826	125
gi|45219787 Ribosomal protein S3a [Homo sapiens]	30184	120
gi|106529 Ig kappa chain C region (allotype Inv(1,2)) - human (fragment)	11161	109

protein	Mass kDa	score
gi|12803339 PAI-RBP1 protein [Homo sapiens]	44291	100
gi|4506455 reticulocalbin 1 precursor [Homo sapiens]	38866	99
gi|62897725|dbj|BAD96802.1| ribosomal protein L19 variant [Homo		
gi|2521983|dbj|BAA22652.1| alpha2-HS glycoprotein [Homo sapiens]		
gi|33150766 heparin-binding protein HBp15 [Homo sapiens]	14866	86
gi|19343694 MAP7 protein [Homo sapiens]	84146	81
gi|61369330|gb|AAX43318.1| nuclease sensitive element binding		
gi|7657532|ref|NP_055439.1| S100 calcium-binding protein A6		
gi|56205102 single stranded DNA binding protein 3 [Homo sapiens]	28692	69
gi|16924231 ribosomal protein S19 [Homo sapiens]	17271	66
gi|51471019 PREDICTED: similar to 60S ribosomal protein L29 (Cell surface heparin binding protein HIP) [Homo sapiens]17146		59

Table 17: HRV14-2A^{pro} C109A positive. Search against the mammalian subset of the NCBI nr database. The highlighted proteins were considered relevant for this work.

HRV2-2A^{pro} C106A negative control

protein	Mass kDa	score
gi|7766868 Chain B, 2a Cysteine Proteinase From Human Rhinovirus 2	16596	2954
gi|54306511 CTAP-tag [Cloning vector pUAST-CTAP]	20524	1229
gi|50507914 yellow cameleon 2.60 [synthetic construct]	73565	1031
gi|38491478 GroEL [Escherichia coli]	57434	719
gi|208991 protein A signal fusion protein	27046	454
gi|71665 calmodulin - electric eel	16799	432
gi|223036 troponin C-like protein	16696	408
gi|26246446 Trigger factor [Escherichia coli CFT073]	48221	250
>gi|16131182|ref|NP_417762.1| 30S ribosomal subunit protein S5 [Escherichia coli K12]		
gi|229552 albumin [Bos taurus]	68083	147
gi|16974825 Chain A, Solution Structure Of Calcium-Calmodulin N-Terminal Domain	8483	135
gi|106529 Ig kappa chain C region (allotype Inv(1,2)) - human (fragment)	11161	130
gi|12516297 galactitol-specific enzyme IIA of phosphotransferase system [Escherichia coli O157:H7]	17011	99
gi|29649713 protease serine 1 [Homo sapiens]	9218	93
gi|25013638 NIa-Pro protein [Tobacco etch virus]	27738	82

protein	Mass kDa	score
gi|261553 GTP cyclohydrolase I (N-terminal) [Escherichia coli, Peptide Partial, 50 aa, segment 1 of 2]	5544	73
gi|4506773 S100 calcium-binding protein A9 [Homo sapiens]	13291	68
gi|457116 S20 protein	9763	61
>gi|16131199|ref|NP_417779.1| 50S ribosomal subunit protein L3 [Escherichia coli K12]		
gi|226334 myosin L kinase	36258	1854

Table 18: HRV2-2A^{pro} C106A negative control. Search against all entries in the NCBI nr database.

HRV2-2A^{pro} C106A positive

protein	Mass kDa	score
gi|7766868 Chain B, 2a Cysteine Proteinase From Human Rhinovirus 2	16596	18034
gi|38490010 polyprotein [Human rhinovirus 30]	53303	5710
gi|4506787 IQ motif containing GTPase activating protein 1 [Homo sapiens]	189761	5026
gi|109327 myosin-light-chain kinase (EC 2.7.1.117), skeletal muscle - rabbit	65997	2317
gi|54306511 CTAP-tag [Cloning vector pUAST-CTAP]	20524	2020
gi|50507914 yellow cameleon 2.60 [synthetic construct]	73565	1490
gi|56205916 **retinoblastoma-associated factor 600 (RBAF600) [Homo sapiens]**	**580547**	**1294**
gi|4506693 **ribosomal protein S17 [Homo sapiens]**	**15597**	**1238**
gi|4885109 calmodulin 3 [Homo sapiens]	17152	1059
gi|4586876 huntingtin [Homo sapiens]	351557	1025
gi|24111820 trigger factor [Shigella flexneri 2a str. 301]	48163	1015
gi|14250401 **actin, beta [Homo sapiens]**	**41321**	**956**
gi|18088719 Tubulin, beta polypeptide [Homo sapiens]	50096	741

protein	Mass kDa	score
gi|2119266 tubulin alpha-1 chain - human	50804	700
gi|48734733 **Eukaryotic translation** **elongation factor 1 alpha 1** **[Homo sapiens]**	**50438**	**624**
gi|31645 glyceraldehyde-3-phosphate dehydrogenase [Homo sapiens]	36202	544
gi|693933 2-phosphopyruvate-hydratase alpha-enolase; carbonate dehydratase [Homo sapiens]	47421	518
gi|20072478 PAI-RBP1 protein [Homo sapiens]	44995	505
gi|30583577 vesicle amine transport protein 1 homolog (T californica) [Homo sapiens]	42122	493
gi|189998 M2-type pyruvate kinase	58447	416
>gi|5729877|ref|NP_006588.1| heat shock 70kDa protein 8 isoform 1 [Homo sapiens]		
gi|12667788 myosin, heavy polypeptide 9, non-muscle [Homo sapiens]	227646	362
gi|52783777 Phosphoglycerate kinase 1	44973	355
gi|17986258 smooth muscle and non-muscle myosin alkali light chain isoform 1 [Homo sapiens]	17090	354
gi|32358 **hnRNP U protein [Homo** **sapiens]**	**89631**	**342**
gi|4507895 vimentin [Homo sapiens]	53710	296
gi|32454741 serine (or cysteine) proteinase inhibitor, clade H, member 1 precursor [Homo sapiens]	46525	289

protein	Mass kDa	score
gi|16507237 heat shock 70kDa protein 5 (glucose-regulated protein, 78kDa) [Homo sapiens]	72402	288
gi|27676004 similar to ribosomal protein L9 [Rattus norvegicus]	21994	281
gi|10863927 peptidylprolyl isomerase A isoform 1 [Homo sapiens]	18098	280
gi|54696696 annexin A1 [Homo sapiens]	38918	265
gi|57036493 PREDICTED: similar to ribosomal protein S19 [Canis familiaris]	16051	243
gi|18645167 Annexin A2, isoform 2 [Homo sapiens]	38780	237
gi|15559443 Hypothetical protein BC014089 [Homo sapiens]	14669	236
gi|3309539 liprin-beta1 [Homo sapiens]	113632	229
gi|28614 aldolase A [Homo sapiens]	39706	227
gi|56972440 Ribosomal protein L3 [Homo sapiens]	46365	224
gi|38201623 **eukaryotic translation** **initiation factor 4 gamma, 1** **isoform 1 [Homo sapiens]**	**176094**	**223**
gi|999893 Chain B, Triosephosphate Isomerase (Tim) (E.C.5.3.1.1) Complexed With 2- Phosphoglycolic Acid	36807	211
gi|57209936 melanoma antigen, family D, 2 [Homo sapiens]	55932	200

protein	Mass kDa	score
gi|2773160 neuronal tissue-enriched acidic protein [Homo sapiens]	22941	183
gi|6016838|dbj|BAA85184.1| 14-3-3gamma [Homo sapiens]		
gi|33187679 hypothetical protein [Homo sapiens]	14682	177
gi|185945 immunoglobulin kappa chain constant region [Homo sapiens]	11773	166
gi|35871 RAP74 [Homo sapiens]	58276	161
gi|5031857 lactate dehydrogenase A [Homo sapiens]	36950	154
gi|107082 microtubule-associated protein 4 - human	121618	153
gi|180985 CpG island protein	39022	149
gi|19343933 PPP3CA protein [Homo sapiens]	58306	148
gi|4092054 GTP binding protein [Homo sapiens]	24668	93
gi|16418383 transcriptional repressor NAC1 [Homo sapiens]	57906	90
gi|460317 chaperonin	58598	79
gi|55959887 peroxiredoxin 1 [Homo sapiens]	19135	78
gi|54695918 flap structure-specific endonuclease 1 [Homo sapiens]	42908	76
gi|13569488 OSBP related protein 11 [Homo sapiens]	35076	75
gi|55859705 tropomyosin 2 (beta) [Homo sapiens]	37010	74

protein	Mass kDa	score
gi|55749406 transcription elongation factor A (SII)-like 1 [Homo sapiens]	18686	68
gi|27802691 caspase 9, apoptosis-related cysteine protease [Homo sapiens]	47035	66

Table 19: HRV2-2A^{pro} C106A positive. Search against the mammalian subset of the NCBI nr database. The highlighted proteins were considered relevant for this work.

Lb^{pro} negative control

protein	Mass kDa	score
gi|825635 calmodulin [Homo sapiens]	17152	4097
gi|16974825 Chain A, Solution Structure Of Calcium-Calmodulin N-Terminal Domain	8483	2405
gi|29649713 protease serine 1 [Homo sapiens]	9218	66
gi|38051823 Plasminogen [Homo sapiens]	93263	59
gi|14993776 skeletal myosin light chain kinase [Homo sapiens]	65214	55

Table 20: Lb^{pro} negative control. Search against the mammalian subset of the NCBI nr database.

Lb^{pro} positive

protein	Mass kDa	score
gi|825635 calmodulin [Homo sapiens]	17152	7812
gi|4506773 S100 calcium-binding protein A9 [Homo sapiens]	13291	372
gi|18490211 Unknown (protein for MGC:23888) [Homo sapiens]	26503	239
gi|21614544 S100 calcium-binding protein A8 [Homo sapiens]	10885	233
gi|14043538 Unknown (protein for IMAGE:4110141) [Homo sapiens]	27865	199
gi|16554039 unnamed protein product [Homo sapiens]	65755	179
gi|4885111 calmodulin-like 3 [Homo sapiens]	16937	173
gi|31645 glyceraldehyde-3-phosphate dehydrogenase [Homo sapiens]	36202	160
gi|8393159 calmodulin-like skin protein [Homo sapiens]	15911	144
gi|29649713 protease serine 1 [Homo sapiens]	9218	111
gi|38348366 suprabasin [Homo sapiens]	25377	100
gi|62122917 filaggrin 2 [Homo sapiens]	249296	94
gi|3891470 Chain A, Crystal Structure Of Human Galectin-7 In Complex With Galactosamine	14992	91

protein	Mass kDa	score
gi|6912286 caspase 14 precursor [Homo sapiens]	27947	87
gi|18645167 Annexin A2 [Homo sapiens]	38780	71
gi|62897625 beta actin variant [Homo sapiens]	42080	67
gi|5803225 tyrosine 3/tryptophan 5 - monooxygenase activation protein, epsilon polypeptide [Homo sapiens]	29326	65
gi|4506671 ribosomal protein P2 [Homo sapiens]	11658	64
gi|38051823 Plasminogen [Homo sapiens]	93263	63
gi|4885375 histone cluster 1, H1c [Homo sapiens]	21352	60
gi|38014625 RPL8 protein [Homo sapiens]	23114	60
gi|338695 beta-tubulin	50240	56
gi|229532 ubiquitin	8446	55
gi|5729877 heat shock 70kDa protein 8 isoform 1 [Homo sapiens]	71082	51
gi|4503113 cystatin M precursor [Homo sapiens]	16785	45
gi|494296 Chain B, Cathepsin D (E.C.3.4.23.5)	26457	43
gi|60097902 filaggrin [Homo sapiens]	435036	39
gi|178995 arginase (EC 3.5.3.1)	34884	38

Table 21: Lb^{pro} positive. Search against the mammalian subset of the NCBI nr database.

6.2 Appendix B
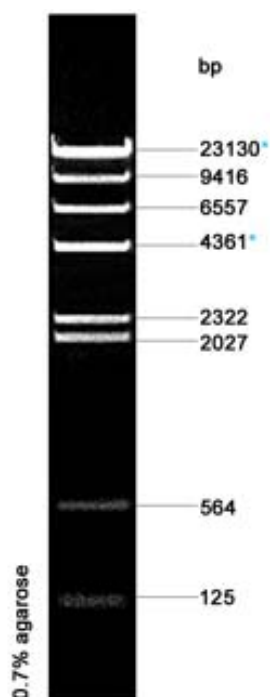
DNA and protein markers

Figure 85: DNA marker. λ-DNA (Promega) digested with the restriction enzyme HindIII. 1µg/well was loaded.
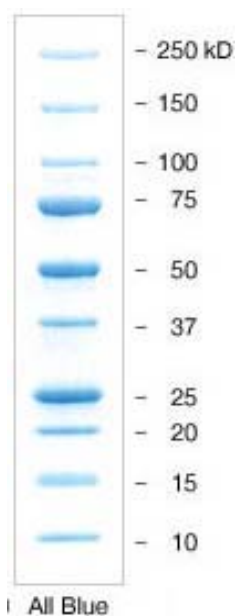

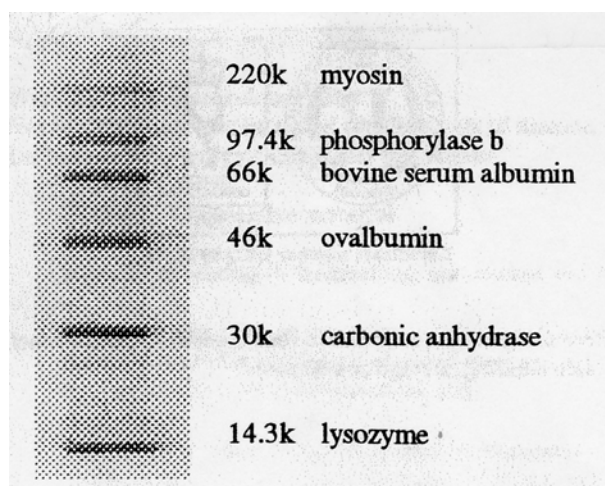**Figure 86: Biorad prestained protein marker.** Catalog number 161-0373. 5µl of marker were loaded.

Figure 87: [¹⁴C] Methylated proteins (Amersham Biosciences). Catalog number CFA-626. 5µl of marker were loaded.

6.3 Appendix C

Amino acids abbreviations

Amino acid	Three letters abbreviation	One letter abbreviation
Alanine	Ala	A
Cysteine	Cys	C
Aspartate	Asp	D
Glutamate	Glu	E
Phenylalanine	Phe	F
Glycine	Gly	G
Histidine	His	H
Isoleucine	Ile	I
Lysine	Lys	K
Leucine	Leu	L
Methionine	Met	M
Asparagine	Asn	N
Proline	Pro	P
Glutamine	Gln	Q
Arginine	Arg	R
Serine	Ser	S
Threonine	Thr	T
Valine	Val	V
Tryptophan	Trp	W
Tyrosine	Tyr	Y

Table 22: **List and abbreviations of the 20 amino acids.**

6.4 Appendix D

List of figures

Figure 24: Fluorography of a 17.5% SDS-PAGE showing the processing of HRV14 VP1-2A^{pro} containing an arginine at the P1 site and a mutation in position 104.

Figure 25: Fluorography of a 17.5% SDS-PAGE showing the processing of HRV2 VP1-2A^{pro} containing a mutation in position 101.

Figure 26: 17.5% SDS-PAGE showing the inhibition of self-processing of HRV2 and HRV14 2A^{pro} by zVAM.fmk.

Figure 27: Cloning strategy to introduce the inactive form of HRV14 2A^{pro} carrying a His tag into pGEX-6P-1.

Figure 28: Coomassie stained SDS-PAGE (10% (A) and 15% (B) polyacrylamide) of the expression of HRV14 2A^{pro}-GST-His (A) and the protein after incubation with PreScission proteinase (Amersham) (B).

Figure 29: A) Chromatogram of HRV14 2A^{pro}-His purification performed on a HisTrap column 1 ml (Amersham). B) Coomassie stained 15% SDS-PAGE of the fractions collected.

Figure 30: Coomassie stained 12.5% SDS-PAGE of the expression of HRV14 2A^{pro}-GST-His (A) and the protein after incubation with PreScission protease (Amersham) (B).

Figure 31: A) Chromatogram of HRV14 2A^{pro}-His purification performed on a HisTrap column 1 ml (Amersham). B) Coomassie stained 12.5% SDS-PAGE of the fractions collected.

Figure 32: A) Chromatogram of gel filtration performed on a superdex 26/60 column. B) Coomassie stained 12.5% SDS-PAGE of the fractions collected.

Figure 33: Coomassie stained 12.5% SDS-PAGE of the concentrated HRV14 2A^{pro}-His.

Figure 34: Determination of the melting temperature of a protein.

Figure 35: Graphic showing the melting temperature curve of HRV14 2A^{pro}-His.

Figure 36: Cloning strategy to introduce the inactive form of HRV14 2A^{pro} carrying a His tag into pET11d.

Figure 37: Coomassie stained 12.5% SDS-PAGE of the expression HRV14 2A^{pro}-His.

Figure 38: A) Chromatogram of HRV14 2A^{pro}-His purification performed on a HisTrap column 1 ml (Amersham). B) Coomassie stained 12.5% SDS-PAGE of the fractions collected. C) Coomassie stained 12.5% SDS-PAGE of the concentrated (pool of lanes 9 to 13 of panel B) HRV14 2A^{pro}-His.

Figure 39: A) Cromatogram of gel filtration performed on a superdex 26/60 column. B) and C) Coomassie stained 12.5% SDS-PAGE of the fractions collected.

Figure 40: Scheme for the pGEX-6P1-eIF4GII-(aa 445-744)-FLAG vector provided by A. Gradi.

Figure 41: Coomassie stained 10% SDS-PAGE of the expression eIF4GII-GST aminoacids 445 to 744.

Figure 42: Coomassie stained 10% SDS-PAGE of eIF4GII aminoacids 445 to 744 after cleavage from the GST-tag.

Figure 43: A) Chromatogram of gel filtration of the sample from figure 43, after being concentrated to 2 ml, performed on a superdex 26/60 column. B) Coomassie stained 10% SDS-PAGE of the fractions corresponding to peak 1 and 2 respectively.

Figure 44: Coomassie stained 10% SDS-PAGE of the pooled and concentrated fractions of eIF4GII.

Figure 45: Cloning strategy to introduce the GST tag and eIF4GII residues 445 to 744 into the pFastBac vector (Invitrogen).

Figure 46: immunoblot of 12.5% SDS-PAGE showing the expression of eIF4GII-GST.

Figure 47: Coomassie stained 10% SDS-PAGE of eIF4GII after incubation with PreScission protease (Amersham).

Figure 48: fragment of eIF4GII (residues 445 to 744) cloned in pGEX-6P1 (Amersham).

Figure 49: Cloning strategy to introduce the fragment corresponding to the residues 552 to 744 of eIF4GII into pGEX-6P-1.

Figure 50: Coomassie stained 10% SDS-PAGE of the expression eIF4GII-GST-His aminoacids 552 to 744 (A) and the protein after incubation with PreScission protease (Amersham) (B).

Figure 51: Cloning strategy to introduce the fragment corresponding to the residues 552 to 744 of eIF4GII carrying a His tag into pET11d.

Figure 52: Coomassie stained 12.5% SDS-PAGE of the expression eIF4GII-GST aminoacids 552 to 744.

Figure 53: A) Chromatogram of eIF4GII-His aminoacid 552 to 744 performed on a HisTrap column 1 ml (Amersham). B) Commassie stained 10% SDS-PAGE of the fractions collected.

Figure 54: Commassie stained 12.5% SDS-PAGE of the pooled and concentrated fractions of eIF4GII.

Figure 55: A) Chromatogram of gel filtration performed on a superdex 26/60 column. B) Commassie stained 10% SDS-PAGE of the fractions collected.

Figure 56: Commassie stained 12.5% SDS-PAGE of the pooled and concentrated fractions 13 to 16 of eIF4GII of figure 56B.

Figure 57: Melting temperature curve of eIF4GII-His amino acids 552 to 744.

Figure 58: Superimposition of ^{1}H-^{15}N-HSQC of ^{15}NLb^{pro}C51A and ^{1}H-^{15}N-HSQC of ^{15}N/^{13}C Lb^{pro}C51A.

Figure 59: A) Chromatogram of eIF4GII-His aminoacid 552 to 744 performed on a HisTrap column 1 ml (Amersham). B) and C) Commassie stained 10% SDS-PAGE of the fractions collected.

Figure 60: Commassie stained 12.5% SDS-PAGE of the pooled and concentrated fractions of eIF4GII.

Figure 61: Superimposition of ^{15}N-eIF4GII (red) and ^{15}N-eIF4GII plus FMDV Lb (blue).

Figure 62: Commassie stained 12.5% SDS-PAGE of the expression eIF4EΔ27.

Figure 63: Scheme for the $_p$pro ExHTA-meIF4E vector provided by Regina Cencic.

Figure 64: Commassie stained 12.5% SDS-PAGE of the expression eIF4E.

Figure 65: A) Chromatogram of eIF4E performed on a MonoQ 10/10 column (Amersham). B) and C) Commassie stained 10% SDS-PAGE of the fractions collected.

Figure 66: Commassie stained 12.5% SDS-PAGE of eIF4E eluted from m^{7}GTP beads.

Figure 67: eIF4E after purification and concentration.

Figure 68: Overview of TAP procedure (adapted from Rigaut *et al.*, 1999).

Figure 69: Cloning strategy to introduce the TAP tag into pET11d.

Figure 70: Cloning strategy to introduce the inactive forms of HRV2 and HRV14 2A^{pro} into pET11d-TAP.

Figure 71: Commassie stained 10% SDS-PAGE of the expression of: A) Tap tag, B) HRV2 2A^{pro}-TAP and C) HRV14 2A^{pro}-TAP.

Figure 72: Commassie stained 10% SDS-PAGE of the soluble fractions from the expressions of TAP, HRV2 2A^{pro}-TAP and HRV14 2A^{pro}-TAP.

Figure 73: Silver stained 7 to 20% SDS-PAGE of TAP (A), HRV2 2A^{pro}-TAP (B) and HRV14 2A^{pro}-TAP (C).

Figure 74: Commassie stained 12.5% SDS-PAGE of GST tag (lane 1), HRV2 2A^{pro} C106A – GST (lane2) and HRV14 2A^{pro} C109A – GST (lane 3).

Figure 75: GST pulldown of eIF4GI (6% SDS-PAGE) (A), PABP (12.5% SDS-PAGE) (B) and β-actin (12.5% SDS-PAGE) (C).

Figure 76: Immunoblot of 12.5% SDS-PAGE of β actin, PABP and eIF1 α.

Figure 77: Cloning strategy to introduce the inactive forms of HRV2 and HRV14 2A^{pro} into pMZI.

Figure 78: immunoblot of 12.5% SDS-PAGE showing the expression of HRV2 2A^{pro}-TAP and HRV14 2A^{pro}-TAP after a small scale transfection of HEK-293T cells.

Figure 79: Immunoblot of 12.5% SDS-PAGE showing the expression of HRV2 2A^{pro}-TAP and HRV14 2A^{pro}-TAP after transfection of 2×10^{6} HEK-293T cells and 48 hours expression.

Figure 80: Cloning strategy to introduce the inactive forms of HIV1 protease, CBV4 2A^{pro} and FMDV Lb^{pro} into pMZI.

Figure 81: immunoblot of 12.5% SDS-PAGE showing the expression pMZI-TAP (A), HIV 1^{pro}-TAP (B), CBV4 2A^{pro}-TAP (C) and FMDV Lb^{pro}-TAP after a large scale transfection of HEK-293T cells and 48 hours expression (D).

Figure 82: Silver stained 7 to 20% SDS-PAGE of TAP FMDV Lb^{pro}-TAP.

Figure 83: Analysis of HRV2, HRV14 and PV1 2A^{pro} amino acid sequence. A and B) Sequence alignments between HRV14 2A^{pro} and HRV2 2A^{pro} (A) and HRV14 2A^{pro} and PV1 2A^{pro} (B). C) Tree based on the amino acid identity of HRV2, HRV14 and PV1 2A^{pro}, showing that HRV14 2A^{pro} amino acid sequence is closer related to PV1 2A^{pro} than to HRV2 2A^{pro}.

Figure 84: The structure of HRV2 2A^{pro}. Ribbon diagrams of the overall structure of HRV2 2A^{pro} (Same as figure 24).

Figure 85: DNA marker (Promega).

Figure 86: Biorad prestained protein marker.

Figure 87: [^{14}C] Methylated proteins (Amersham Biosciences).

List of tables

Table 1: The Genera of the family of Picornaviruses.

Table 2: Viruses and their receptors. Adapted from (Fields *et al.*, 2007).

Table 3: Lb^{pro} cleavage sites on known substrates.

Table 4: List of the plasmids used in this work.

Table 5: List of primers used for cloning experiments.

Table 6: List of primers used for sequencing.

Table 7: Composition of Separating Gels (Laemmli, 1970).

Table 8: Composition of separating gels (Dasso & Jackson, 1989).

Table 9: List of primary antibodies used in this work.

Table 10: List of secondary antibodies used in this work.

Table 11: Dilutions of protein/SYPRO Orange dye for protein melting point detection.

Table 12: 2A^{pro} cleavage sites on the respective polyproteins and eIF4G homologues.

Table 13: Occupancy of the P1 residue of the 2A^{pro} cleavage site and residue 101 or its equivalent of 2A^{pro}.

Table 14: Proteins purified with the TAP method and identified by mass spectroscopy.

Table 15: Summary of the effect of zVAM.fmk on the inhibition of picornaviral 2A^{pro}.

Table 16: HRV14-2A^{pro} C109A negative control.

Table 17: HRV14-2A^{pro} C109A positive.

Table 18: HRV2-2A^{pro} C106A negative control.

Table 19: HRV2-2A^{pro} C106A positive.

Table 20: Lb^{pro} negative control.

Table 21: Lb^{pro} positive.

Table 22: List and abbreviations of the 20 amino acids.

7 Literature

Acharya, R., Fry, E., Stuart, D., Fox, G., Rowlands, D. and Brown, F. (1989) The three-dimensional structure of foot-and-mouth disease virus at 2.9 A resolution. *Nature,* **337**, 709-716.

Agol, V.I. (2002) Picornavirus genome: an overview. In Semler, B.L. and Wimmer, E. (eds.), *Molecular Biology of Picornaviruses.* ASM Press, Washington, D. C., pp. 127-148.

Allaire, M., Chernaia, M.M., Malcolm, B.A. and James, M.N. (1994) Picornaviral 3C cysteine proteinases have a fold similar to chymotrypsin-like serine proteinases. *Nature*, **369**, 72-76.

Amann, E., Ochs, B. and Abel, K.J. (1988) Tightly regulated tac promoter vectors useful for the expression of unfused and fused proteins in Escherichia coli. *Gene*, **69**, 301-315.

Arnold, E., Luo, M., Vriend, G., Rossmann, M.G., Palmenberg, A.C., Parks, G.D., Nicklin, M.J. and Wimmer, E. (1987) Implications of the picornavirus capsid structure for polyprotein processing. *Proc Natl Acad Sci U S A*, **84**, 21-25.

Arruda, E., Pitkaranta, A., Witek, T.J., Jr., Doyle, C.A. and Hayden, F.G. (1997) Frequency and natural history of rhinovirus infections in adults during autumn. *J Clin Microbiol*, **35**, 2864-2868.

Badorff, C., Berkely, N., Mehrotra, S., Talhouk, J.W., Rhoads, R.E. and Knowlton, K.U. (2000) Enteroviral protease 2A directly cleaves dystrophin and is inhibited by a dystrophin-based substrate analogue. *J Biol Chem*, **275**, 11191-11197.

Badorff, C., Lee, G.H., Lamphear, B.J., Martone, M.E., Campbell, K.P., Rhoads, R.E. and Knowlton, K.U. (1999) Enteroviral protease 2A cleaves dystrophin: evidence of cytoskeletal disruption in an acquired cardiomyopathy. *Nat Med*, **5**, 320-326.

Barton, D.J., Morasco, B.J. and Flanegan, J.B. (1999) Translating ribosomes inhibit poliovirus negative-strand RNA synthesis. *J Virol*, **73**, 10104-10112.

Bateman, K.S., Anderson, S., Lu, W., Qasim, M.A., Laskowski, M., Jr. and James, M.N. (2000) Deleterious effects of beta-branched residues in the S1 specificity pocket of Streptomyces griseus proteinase B (SGPB): crystal structures of the turkey ovomucoid third domain variants Ile18I, Val18I, Thr18I, and Ser18I in complex with SGPB. *Protein Sci*, **9**, 83-94.

Baxter, N.J., Roetzer, A., Liebig, H.D., Sedelnikova, S.E., Hounslow, A.M., Skern, T. and Waltho, J.P. (2006) Structure and dynamics of coxsackievirus B4 2A proteinase, an enyzme involved in the etiology of heart disease. *J Virol*, **80**, 1451-1462.

Beck, E., Forss, S., Strebel, K., Cattaneo, R. and Feil, G. (1983) Structure of the FMDV translation initiation site and of the structural proteins. *Nucleic Acids Res*, **11**, 7873-7885.

Belsham, G.J. and Jackson, R.J. (2000) Translation initiation on picornavirus RNA. In Sonenberg, N., Hershey, J.W. and Mathews, M. (eds.), *Tranlational control of gene expression.* Cold Spring Harbor Laboratory Press, New York, pp. 869-900.

Belsham, G.J., McInerney, G.M. and Ross-Smith, N. (2000) Foot-and-mouth disease virus 3C protease induces cleavage of translation initiation factors eIF4A and eIF4G within infected cells. *J Virol*, **74**, 272-280.

Bergelson, J.M. (2008) New (fluorescent) light on poliovirus entry. *Trends Microbiol.*

Bergmann, E.M., Mosimann, S.C., Chernaia, M.M., Malcolm, B.A. and James, M.N. (1997) The refined crystal structure of the 3C gene product from hepatitis A virus: specific proteinase activity and RNA recognition. *J Virol*, **71**, 2436-2448.

Bienz, K., Egger, D. and Pfister, T. (1994) Characteristics of the poliovirus replication complex. *Arch Virol Suppl*, **9**, 147-157.

Binford, S.L., Maldonado, F., Brothers, M.A., Weady, P.T., Zalman, L.S., Meador, J.W., 3rd, Matthews, D.A. and Patick, A.K. (2005) Conservation of amino acids in human rhinovirus 3C protease correlates with broad-spectrum antiviral activity of rupintrivir, a novel human rhinovirus 3C protease inhibitor. *Antimicrob Agents Chemother*, **49**, 619-626.

Binford, S.L., Weady, P.T., Maldonado, F., Brothers, M.A., Matthews, D.A. and Patick, A.K. (2007) In vitro resistance study of rupintrivir, a novel inhibitor of human rhinovirus 3C protease. *Antimicrob Agents Chemother*, **51**, 4366-4373.

Borman, A.M. and Kean, K.M. (1997) Intact eukaryotic initiation factor 4G is required for hepatitis A virus internal initiation of translation. *Virology*, **237**, 129-136.

Bovee, M.L., Lamphear, B.J., Rhoads, R.E. and Lloyd, R.E. (1998) Direct cleavage of elF4G by poliovirus 2A protease is inefficient in vitro. *Virology*, **245**, 241-249.

Brändén, C.-I. and Tooze, J. (1999) *Introduction to protein structure.* Garland Publishing, New York.

Brandenburg, B., Lee, L.Y., Lakadamyali, M., Rust, M.J., Zhuang, X. and Hogle, J.M. (2007) Imaging Poliovirus Entry in Live Cells. *PLoS Biol*, **5**, e183.

Brown, D.M., Cornell, C.T., Tran, G.P., Nguyen, J.H. and Semler, B.L. (2005) An authentic 3' noncoding region is necessary for efficient poliovirus replication. *J Virol*, **79**, 11962-11973.

Bubeck, D., Filman, D.J. and Hogle, J.M. (2005) Cryo-electron microscopy reconstruction of a poliovirus-receptor-membrane complex. *Nat Struct Mol Biol*, **12**, 615-618.

Burroughs, J.N., Sangar, D.V., Clarke, B.E., Rowlands, D.J., Billiau, A. and Collen, D. (1984) Multiple proteases in foot-and-mouth disease virus replication. *J Virol*, **50**, 878-883.

Calandria, C., Irurzun, A., Barco, A. and Carrasco, L. (2004) Individual expression of poliovirus 2Apro and 3Cpro induces activation of caspase-3 and PARP cleavage in HeLa cells. *Virus Res*, **104**, 39-49.

Cao, X., Bergmann, I.E., Fullkrug, R. and Beck, E. (1995) Functional analysis of the two alternative translation initiation sites of foot-and-mouth disease virus. *J Virol*, **69**, 560-563.

Cencic, R. (2005) Structure and Function Relationships in the FMDV Leader Protease. *PhD thesis.* University of Vienna, Vienna.

Chau, D.H., Yuan, J., Zhang, H., Cheung, P., Lim, T., Liu, Z., Sall, A. and Yang, D. (2007) Coxsackievirus B3 proteases 2A and 3C induce apoptotic cell death through mitochondrial injury and cleavage of eIF4GI but not DAP5/p97/NAT1. *Apoptosis*, **12**, 513-524.

Choe, S.S., Dodd, D.A. and Kirkegaard, K. (2005) Inhibition of cellular protein secretion by picornaviral 3A proteins. *Virology*, **337**, 18-29.

Clark, M.E., Hammerle, T., Wimmer, E. and Dasgupta, A. (1991) Poliovirus proteinase 3C converts an active form of transcription factor IIIC to an inactive form: a mechanism for inhibition of host cell polymerase III transcription by poliovirus. *Embo J*, **10**, 2941-2947.

Clark, M.E., Lieberman, P.M., Berk, A.J. and Dasgupta, A. (1993) Direct cleavage of human TATA-binding protein by poliovirus protease 3C in vivo and in vitro. *Mol Cell Biol*, **13**, 1232-1237.

Clarke, B.E., Sangar, D.V., Burroughs, J.N., Newton, S.E., Carroll, A.R. and Rowlands, D.J. (1985) Two initiation sites for foot-and-mouth disease virus polyprotein in vivo. *J Gen Virol*, **66 (Pt 12)**, 2615-2626.

Cordingley, M.G., Callahan, P.L., Sardana, V.V., Garsky, V.M. and Colonno, R.J. (1990) Substrate requirements of human rhinovirus 3C protease for peptide cleavage in vitro. *J Biol Chem*, **265**, 9062-9065.

Cornelis, S., Bruynooghe, Y., Denecker, G., Van Huffel, S., Tinton, S. and Beyaert, R. (2000) Identification and characterization of a novel cell cycle-regulated internal ribosome entry site. *Mol Cell*, **5**, 597-605.

Coyne, C.B., Kim, K.S. and Bergelson, J.M. (2007) Poliovirus entry into human brain microvascular cells requires receptor-induced activation of SHP-2. *Embo J*, **26**, 4016-4028.

Crowder, S. and Kirkegaard, K. (2004) Complete three-dimensional structures of picornaviral RNA-dependent RNA polymerases. *Structure*, **12**, 1336-1339.

Crowder, S. and Kirkegaard, K. (2005) Trans-dominant inhibition of RNA viral replication can slow growth of drug-resistant viruses. *Nat Genet*, **37**, 701-709.

Dasso, M.C. and Jackson, R.J. (1989) On the fidelity of mRNA translation in the nuclease-treated rabbit reticulocyte lysate system. *Nucleic Acids Res*, **17**, 3129-3144.

De Gregorio, E., Preiss, T. and Hentze, M.W. (1999) Translation driven by an eIF4G core domain in vivo. *Embo J*, **18**, 4865-4874.

Deszcz, L., Cencic, R., Sousa, C., Kuechler, E. and Skern, T. (2006) An antiviral peptide inhibitor that is active against picornavirus 2A proteinases but not cellular caspases. *J Virol*, **80**, 9619-9627.

Deszcz, L., Gaudernak, E., Kuechler, E. and Seipelt, J. (2005) Apoptotic events induced by human rhinovirus infection. *J Gen Virol*, **86**, 1379-1389.

Deszcz, L., Seipelt, J., Vassilieva, E., Roetzer, A. and Kuechler, E. (2004) Antiviral activity of caspase inhibitors: effect on picornaviral 2A proteinase. *FEBS Lett*, **560**, 51-55.

Duncan, R., Milburn, S.C. and Hershey, J.W. (1987) Regulated phosphorylation and low abundance of HeLa cell initiation factor eIF-4F suggest a role in translational control. Heat shock effects on eIF-4F. *J Biol Chem*, **262**, 380-388.

Ehrenfeld, E. and Teterina, N.L. (2002) Initiation of translation of picornavirus RNAs: structure and function of the Internal Ribosome Entry Site. In Semler, B.L. and Wimmer, E. (eds.), *Molecular Biology of Picornaviruses*. ASM Press, Washington, D. C., pp. 159-169.

Etchison, D., Milburn, S.C., Edery, I., Sonenberg, N. and Hershey, J.W. (1982) Inhibition of HeLa cell protein synthesis following poliovirus infection correlates with the proteolysis of a 220,000-dalton polypeptide associated with eucaryotic initiation factor 3 and a cap binding protein complex. *J Biol Chem*, **257**, 14806-14810.

Fauquet, C. and International Committee on Taxonomy of, V. (2005) *Virus taxonomy: classification and nomenclature of viruses; 8th report of the International Committee on Taxonomy of Viruses*. Elsevier/Academic Press, Oxford.

Feigenblum, D. and Schneider, R.J. (1993) Modification of eukaryotic initiation factor 4F during infection by influenza virus. *J Virol*, **67**, 3027-3035.

Fendrick, A.M., Monto, A.S., Nightengale, B. and Sarnes, M. (2003) The economic burden of non-influenza-related viral respiratory tract infection in the United States. *Arch Intern Med*, **163**, 487-494.

Fields, B.N., Knipe, D.M. and Howley, P.M. (2007) *Fields' virology*. Wolters Kluwer Health/Lippincott Williams & Wilkins, Philadelphia.

Flanegan, J.B., Petterson, R.F., Ambros, V., Hewlett, N.J. and Baltimore, D. (1977) Covalent linkage of a protein to a defined nucleotide sequence at the 5'-terminus of virion and replicative intermediate RNAs of poliovirus. *Proc Natl Acad Sci U S A*, **74**, 961-965.

Flint, S.J. (2004) *Principles of virology: molecular biology, pathogenesis, and control of animal viruses.* ASM Press, Washington, D.C.

Foeger, N., Glaser, W. and Skern, T. (2002) Recognition of eukaryotic initiation factor 4G isoforms by picornaviral proteinases. *J Biol Chem*, **277**, 44300-44309.

Gamarnik, A.V. and Andino, R. (1998) Switch from translation to RNA replication in a positive-stranded RNA virus. *Genes Dev*, **12**, 2293-2304.

Gamarnik, A.V. and Andino, R. (2000) Interactions of viral protein 3CD and poly(rC) binding protein with the 5' untranslated region of the poliovirus genome. *J Virol*, **74**, 2219-2226.

Goldstaub, D., Gradi, A., Bercovitch, Z., Grosmann, Z., Nophar, Y., Luria, S., Sonenberg, N. and Kahana, C. (2000) Poliovirus 2A protease induces apoptotic cell death. *Mol Cell Biol*, **20**, 1271-1277.

Goodfellow, I.G., Polacek, C., Andino, R. and Evans, D.J. (2003) The poliovirus 2C cis-acting replication element-mediated uridylylation of VPg is not required for synthesis of negative-sense genomes. *J Gen Virol*, **84**, 2359-2363.

Gorbalenya, A.E., Donchenko, A.P., Blinov, V.M. and Koonin, E.V. (1989) Cysteine proteases of positive strand RNA viruses and chymotrypsin-like serine proteases. A distinct protein superfamily with a common structural fold. *FEBS Lett*, **243**, 103-114.

Gorbalenya, A.E., Svitkin, Y.V., Kazachkov, Y.A. and Agol, V.I. (1979) Encephalomyocarditis virus-specific polypeptide p22 is involved in the processing of the viral precursor polypeptides. *FEBS Lett*, **108**, 1-5.

Goyer, C., Altmann, M., Lee, H.S., Blanc, A., Deshmukh, M., Woolford, J.L., Jr., Trachsel, H. and Sonenberg, N. (1993) TIF4631 and TIF4632: two yeast genes encoding the high-molecular-weight subunits of the cap-binding protein complex (eukaryotic initiation factor 4F) contain an RNA recognition motif-like sequence and carry out an essential function. *Mol Cell Biol*, **13**, 4860-4874.

Gradi, A., Foeger, N., Strong, R., Svitkin, Y.V., Sonenberg, N., Skern, T. and Belsham, G.J. (2004) Cleavage of eukaryotic translation initiation factor 4GII within foot-and-mouth disease virus-infected cells: identification of the L-protease cleavage site in vitro. *J Virol*, **78**, 3271-3278.

Gradi, A., Imataka, H., Svitkin, Y.V., Rom, E., Raught, B., Morino, S. and Sonenberg, N. (1998a) A novel functional human eukaryotic translation initiation factor 4G. *Mol Cell Biol*, **18**, 334-342.

Gradi, A., Svitkin, Y.V., Imataka, H. and Sonenberg, N. (1998b) Proteolysis of human eukaryotic translation initiation factor eIF4GII, but not eIF4GI, coincides with the shutoff of host protein synthesis after poliovirus infection. *Proc Natl Acad Sci U S A*, **95**, 11089-11094.

Gradi, A., Svitkin, Y.V., Sommergruber, W., Imataka, H., Morino, S., Skern, T. and Sonenberg, N. (2003) Human rhinovirus 2A proteinase cleavage sites in eukaryotic initiation factors (eIF) 4GI and eIF4GII are different. *J Virol*, **77**, 5026-5029.

Greve, J.M., Davis, G., Meyer, A.M., Forte, C.P., Yost, S.C., Marlor, C.W., Kamarck, M.E. and McClelland, A. (1989) The major human rhinovirus receptor is ICAM-1. *Cell*, **56**, 839-847.

Gross, J.D., Moerke, N.J., von der Haar, T., Lugovskoy, A.A., Sachs, A.B., McCarthy, J.E. and Wagner, G. (2003) Ribosome loading onto the mRNA cap is driven by conformational coupling between eIF4G and eIF4E. *Cell*, **115**, 739-750.

Guarne, A., Tormo, J., Kirchweger, R., Pfistermueller, D., Fita, I. and Skern, T. (1998) Structure of the foot-and-mouth disease virus leader protease: a papain-like fold adapted for self-processing and eIF4G recognition. *Embo J*, **17**, 7469-7479.

Haghighat, A. and Sonenberg, N. (1997) eIF4G dramatically enhances the binding of eIF4E to the mRNA 5'-cap structure. *J Biol Chem*, **272**, 21677-21680.

Haghighat, A., Svitkin, Y., Novoa, I., Kuechler, E., Skern, T. and Sonenberg, N. (1996) The eIF4G-eIF4E complex is the target for direct cleavage by the rhinovirus 2A proteinase. *J Virol*, **70**, 8444-8450.

Hanecak, R., Semler, B.L., Anderson, C.W. and Wimmer, E. (1982) Proteolytic processing of poliovirus polypeptides: antibodies to polypeptide P3-7c inhibit cleavage at glutamine-glycine pairs. *Proc Natl Acad Sci U S A*, **79**, 3973-3977.

Hanecak, R., Semler, B.L., Ariga, H., Anderson, C.W. and Wimmer, E. (1984) Expression of a cloned gene segment of poliovirus in E. coli: evidence for autocatalytic production of the viral proteinase. *Cell*, **37**, 1063-1073.

Harber, J.J., Bradley, J., Anderson, C.W. and Wimmer, E. (1991) Catalysis of poliovirus VP0 maturation cleavage is not mediated by serine 10 of VP2. *J Virol*, **65**, 326-334.

Hentze, M.W. (1997) eIF4G: a multipurpose ribosome adapter? *Science*, **275**, 500-501.

Hershey, J.W. and Merrick, W.C. (2000) The pathway and mechanism of initiation of protein synthesis. In Sonenberg, N., Hershey, J.W. and Mathews, M. (eds.), *Tranlational control of gene expression*. Cold Spring Harbor Laboratory Press, New York, pp. 33-88.

Hershey, P.E., McWhirter, S.M., Gross, J.D., Wagner, G., Alber, T. and Sachs, A.B. (1999) The Cap-binding protein eIF4E promotes folding of a functional domain of yeast translation initiation factor eIF4G1. *J Biol Chem*, **274**, 21297-21304.

Hindiyeh, M., Li, Q.H., Basavappa, R., Hogle, J.M. and Chow, M. (1999) Poliovirus mutants at histidine 195 of VP2 do not cleave VP0 into VP2 and VP4. *J Virol*, **73**, 9072-9079.

Hofer, F., Gruenberger, M., Kowalski, H., Machat, H., Huettinger, M., Kuechler, E. and Blaas, D. (1994) Members of the low density lipoprotein receptor family mediate cell entry of a minor-group common cold virus. *Proc Natl Acad Sci U S A*, **91**, 1839-1842.

Hogle, J.M., Chow, M. and Filman, D.J. (1985) Three-dimensional structure of poliovirus at 2.9 A resolution. *Science*, **229**, 1358-1365.

Imataka, H., Gradi, A. and Sonenberg, N. (1998) A newly identified N-terminal amino acid sequence of human eIF4G binds poly(A)-binding protein and functions in poly(A)-dependent translation. *Embo J*, **17**, 7480-7489.

Imataka, H. and Sonenberg, N. (1997) Human eukaryotic translation initiation factor 4G (eIF4G) possesses two separate and independent binding sites for eIF4A. *Mol Cell Biol*, **17**, 6940-6947.

Jackson, T., Ellard, F.M., Ghazaleh, R.A., Brookes, S.M., Blakemore, W.E., Corteyn, A.H., Stuart, D.I., Newman, J.W. and King, A.M. (1996) Efficient infection of cells in culture by type O foot-and-mouth disease virus requires binding to cell surface heparan sulfate. *J Virol*, **70**, 5282-5287.

Jacobson, M.F. and Baltimore, D. (1968) Morphogenesis of poliovirus. I. Association of the viral RNA with coat protein. *J Mol Biol*, **33**, 369-378.

Jacobson, S.J., Konings, D.A. and Sarnow, P. (1993) Biochemical and genetic evidence for a pseudoknot structure at the 3' terminus of the poliovirus RNA genome and its role in viral RNA amplification. *J Virol*, **67**, 2961-2971.

Ji, H., Fraser, C.S., Yu, Y., Leary, J. and Doudna, J.A. (2004) Coordinated assembly of human translation initiation complexes by the hepatitis C virus internal ribosome entry site RNA. *Proc Natl Acad Sci U S A*, **101**, 16990-16995.

Joachims, M., Harris, K.S. and Etchison, D. (1995) Poliovirus protease 3C mediates cleavage of microtubule-associated protein 4. *Virology*, **211**, 451-461.

Joachims, M., Van Breugel, P.C. and Lloyd, R.E. (1999) Cleavage of poly(A)-binding protein by enterovirus proteases concurrent with inhibition of translation in vitro. *J Virol*, **73**, 718-727.

Jore, J., De Geus, B., Jackson, R.J., Pouwels, P.H. and Enger-Valk, B.E. (1988) Poliovirus protein 3CD is the active protease for processing of the precursor protein P1 in vitro. *J Gen Virol*, **69 (Pt 7)**, 1627-1636.

Kean, K.M., Teterina, N.L., Marc, D. and Girard, M. (1991) Analysis of putative active site residues of the poliovirus 3C protease. *Virology*, **181**, 609-619.

Kerekatte, V., Keiper, B.D., Badorff, C., Cai, A., Knowlton, K.U. and Rhoads, R.E. (1999) Cleavage of Poly(A)-binding protein by coxsackievirus 2A protease in vitro and in vivo: another mechanism for host protein synthesis shutoff? *J Virol*, **73**, 709-717.

Khan, A.G., Pichler, J., Rosemann, A. and Blaas, D. (2007) Human rhinovirus type 54 infection via heparan sulfate is less efficient and strictly dependent on low endosomal pH. *J Virol*, **81**, 4625-4632.

Kleijn, M., Vrins, C.L., Voorma, H.O. and Thomas, A.A. (1996) Phosphorylation state of the cap-binding protein eIF4E during viral infection. *Virology*, **217**, 486-494.

Kleina, L.G. and Grubman, M.J. (1992) Antiviral effects of a thiol protease inhibitor on foot-and-mouth disease virus. *J Virol*, **66**, 7168-7175.

Kolatkar, P.R., Bella, J., Olson, N.H., Bator, C.M., Baker, T.S. and Rossmann, M.G. (1999) Structural studies of two rhinovirus serotypes complexed with fragments of their cellular receptor. *Embo J*, **18**, 6249-6259.

Kolupaeva, V.G., Pestova, T.V. and Hellen, C.U. (2000) An enzymatic footprinting analysis of the interaction of 40S ribosomal subunits with the internal ribosomal entry site of hepatitis C virus. *J Virol*, **74**, 6242-6250.

Kolupaeva, V.G., Pestova, T.V., Hellen, C.U. and Shatsky, I.N. (1998) Translation eukaryotic initiation factor 4G recognizes a specific structural element within the internal ribosome entry site of encephalomyocarditis virus RNA. *J Biol Chem*, **273**, 18599-18604.

Kozak, M. (2001) New ways of initiating translation in eukaryotes? *Mol Cell Biol*, **21**, 1899-1907.

Kozak, M. (2005) A second look at cellular mRNA sequences said to function as internal ribosome entry sites. *Nucleic Acids Res*, **33**, 6593-6602.

Kozak, M. (2007) Lessons (not) learned from mistakes about translation. *Gene*, **403**, 194-203.

Kraulis, P.J. (1991) MOLSCRIPT: a program to produce both detailed and schmatic plots of protein structures. *J. Appl. Crystallogr.*, **24**, 946-950.

Kuyumcu-Martinez, N.M., Joachims, M. and Lloyd, R.E. (2002) Efficient cleavage of ribosome-associated poly(A)-binding protein by enterovirus 3C protease. *J Virol*, **76**, 2062-2074.

Laemmli, U.K. (1970) Cleavage of structural proteins during the assembly of the head of bacteriophage T4. *Nature*, **227**, 680-685.

Laine, P., Blomqvist, S., Savolainen, C., Andries, K. and Hovi, T. (2006) Alignment of capsid protein VP1 sequences of all human rhinovirus prototype strains: conserved motifs and functional domains. *J Gen Virol*, **87**, 129-138.

Laine, P., Savolainen, C., Blomqvist, S. and Hovi, T. (2005) Phylogenetic analysis of human rhinovirus capsid protein VP1 and 2A protease coding sequences confirms shared genus-like relationships with human enteroviruses. *J Gen Virol*, **86**, 697-706.

Lamphear, B.J., Yan, R., Yang, F., Waters, D., Liebig, H.D., Klump, H., Kuechler, E., Skern, T. and Rhoads, R.E. (1993) Mapping the cleavage site in protein synthesis initiation factor eIF-4 gamma of the 2A proteases from human Coxsackievirus and rhinovirus. *J Biol Chem*, **268**, 19200-19203.

Lamson, D., Renwick, N., Kapoor, V., Liu, Z., Palacios, G., Ju, J., Dean, A., St George, K., Briese, T. and Lipkin, W.I. (2006) MassTag polymerase-chain-reaction detection of respiratory pathogens, including a new rhinovirus genotype, that caused influenza-like illness in New York State during 2004-2005. *J Infect Dis*, **194**, 1398-1402.

Lau, S.K., Yip, C.C., Tsoi, H.W., Lee, R.A., So, L.Y., Lau, Y.L., Chan, K.H., Woo, P.C. and Yuen, K.Y. (2007) Clinical features and complete genome characterization of a distinct human rhinovirus (HRV) genetic cluster, probably representing a previously undetected HRV species, HRV-C, associated with acute respiratory illness in children. *J Clin Microbiol*, **45**, 3655-3664.

Lee, W.M., Monroe, S.S. and Rueckert, R.R. (1993) Role of maturation cleavage in infectivity of picornaviruses: activation of an infectosome. *J Virol*, **67**, 2110-2122.

Lee, Y.F., Nomoto, A., Detjen, B.M. and Wimmer, E. (1977) A protein covalently linked to poliovirus genome RNA. *Proc Natl Acad Sci U S A*, **74**, 59-63.

LeFebvre, A.K., Korneeva, N.L., Trutschl, M., Cvek, U., Duzan, R.D., Bradley, C.A., Hershey, J.W. and Rhoads, R.E. (2006) Translation initiation factor eIF4G-1 binds to eIF3 through the eIF3e subunit. *J Biol Chem*, **281**, 22917-22932.

Liebig, H.D., Seipelt, J., Vassilieva, E., Gradi, A. and Kuechler, E. (2002) A thermosensitive mutant of HRV2 2A proteinase: evidence for direct cleavage of eIF4GI and eIF4GII. *FEBS Lett*, **523**, 53-57.

Long, A.C., Orr, D.C., Cameron, J.M., Dunn, B.M. and Kay, J. (1989) A consensus sequence for substrate hydrolysis by rhinovirus 3C proteinase. *FEBS Lett*, **258**, 75-78.

Lopez-Lastra, M., Rivas, A. and Barria, M.I. (2005) Protein synthesis in eukaryotes: the growing biological relevance of cap-independent translation initiation. *Biol Res*, **38**, 121-146.

Lyle, J.M., Bullitt, E., Bienz, K. and Kirkegaard, K. (2002) Visualization and functional analysis of RNA-dependent RNA polymerase lattices. *Science*, **296**, 2218-2222.

Mader, S., Lee, H., Pause, A. and Sonenberg, N. (1995) The translation initiation factor eIF-4E binds to a common motif shared by the translation factor eIF-4 gamma and the translational repressors 4E-binding proteins. *Mol Cell Biol*, **15**, 4990-4997.

Marcotrigiano, J., Lomakin, I.B., Sonenberg, N., Pestova, T.V., Hellen, C.U. and Burley, S.K. (2001) A conserved HEAT domain within eIF4G directs assembly of the translation initiation machinery. *Mol Cell*, **7**, 193-203.

Marcotte, L.L., Wass, A.B., Gohara, D.W., Pathak, H.B., Arnold, J.J., Filman, D.J., Cameron, C.E. and Hogle, J.M. (2007) Crystal structure of poliovirus 3CD protein: virally encoded protease and precursor to the RNA-dependent RNA polymerase. *J Virol*, **81**, 3583-3596.

Martin, A., Escriou, N., Chao, S.F., Girard, M., Lemon, S.M. and Wychowski, C. (1995) Identification and site-directed mutagenesis of the primary (2A/2B) cleavage site of the hepatitis A virus polyprotein: functional impact on the infectivity of HAV RNA transcripts. *Virology*, **213**, 213-222.

Matthews, D.A., Dragovich, P.S., Webber, S.E., Fuhrman, S.A., Patick, A.K., Zalman, L.S., Hendrickson, T.F., Love, R.A., Prins, T.J., Marakovits, J.T., Zhou, R., Tikhe, J., Ford, C.E., Meador, J.W., Ferre, R.A., Brown, E.L., Binford, S.L., Brothers, M.A., DeLisle, D.M. and Worland, S.T. (1999) Structure-assisted design of mechanism-based irreversible inhibitors of human rhinovirus 3C protease with potent antiviral activity against multiple rhinovirus serotypes. *Proc Natl Acad Sci U S A*, **96**, 11000-11007.

Matthews, D.A., Smith, W.W., Ferre, R.A., Condon, B., Budahazi, G., Sisson, W., Villafranca, J.E., Janson, C.A., McElroy, H.E., Gribskov, C.L. and et al. (1994) Structure of human rhinovirus 3C protease reveals a trypsin-like polypeptide fold, RNA-binding site, and means for cleaving precursor polyprotein. *Cell*, **77**, 761-771.

McLean, C., Matthews, T.J. and Rueckert, R.R. (1976) Evidence of ambiguous processing and selective degradation in the noncapsid proteins of rhinovirus 1A. *J Virol*, **19**, 903-914.

Medina, M., Domingo, E., Brangwyn, J.K. and Belsham, G.J. (1993) The two species of the foot-and-mouth disease virus leader protein, expressed individually, exhibit the same activities. *Virology*, **194**, 355-359.

Moens, U., Van Ghelue, M. and Johannessen, M. (2007) Oncogenic potentials of the human polyomavirus regulatory proteins. *Cell Mol Life Sci*, **64**, 1656-1678.

Morino, S., Imataka, H., Svitkin, Y.V., Pestova, T.V. and Sonenberg, N. (2000) Eukaryotic translation initiation factor 4E (eIF4E) binding site and the middle one-third of eIF4GI constitute the core domain for cap-dependent translation, and the C-terminal one-third functions as a modulatory region. *Mol Cell Biol*, **20**, 468-477.

Mosimann, S.C., Cherney, M.M., Sia, S., Plotch, S. and James, M.N. (1997) Refined X-ray crystallographic structure of the poliovirus 3C gene product. *J Mol Biol*, **273**, 1032-1047.

Mosser, A.G., Vrtis, R., Burchell, L., Lee, W.M., Dick, C.R., Weisshaar, E., Bock, D., Swenson, C.A., Cornwell, R.D., Meyer, K.C., Jarjour, N.N., Busse, W.W. and Gern, J.E. (2005) Quantitative and qualitative analysis of rhinovirus infection in bronchial tissues. *Am J Respir Crit Care Med*, **171**, 645-651.

Muckelbauer, J.K., Kremer, M., Minor, I., Diana, G., Dutko, F.J., Groarke, J., Pevear, D.C. and Rossmann, M.G. (1995) The structure of coxsackievirus B3 at 3.5 A resolution. *Structure*, **3**, 653-667.

Nakatani, Y., Konishi, H., Vassilev, A., Kurooka, H., Ishiguro, K., Sawada, J., Ikura, T., Korsmeyer, S.J., Qin, J. and Herlitz, A.M. (2005) p600, a unique protein required for membrane morphogenesis and cell survival. *Proc Natl Acad Sci U S A*, **102**, 15093-15098.

Neff, S., Sa-Carvalho, D., Rieder, E., Mason, P.W., Blystone, S.D., Brown, E.J. and Baxt, B. (1998) Foot-and-mouth disease virus virulent for cattle utilizes the integrin alpha(v)beta3 as its receptor. *J Virol*, **72**, 3587-3594.

Nugent, C.I. and Kirkegaard, K. (1995) RNA binding properties of poliovirus subviral particles. *J Virol*, **69**, 13-22.

Ohlmann, T., Rau, M., Morley, S.J. and Pain, V.M. (1995) Proteolytic cleavage of initiation factor eIF-4 gamma in the reticulocyte lysate inhibits translation of capped mRNAs but enhances that of uncapped mRNAs. *Nucleic Acids Res*, **23**, 334-340.

Oliveira, M.A., Zhao, R., Lee, W.M., Kremer, M.J., Minor, I., Rueckert, R.R., Diana, G.D., Pevear, D.C., Dutko, F.J., McKinlay, M.A. and et al. (1993) The structure of human rhinovirus 16. *Structure*, **1**, 51-68.

Olson, N.H., Kolatkar, P.R., Oliveira, M.A., Cheng, R.H., Greve, J.M., McClelland, A., Baker, T.S. and Rossmann, M.G. (1993) Structure of a human rhinovirus complexed with its receptor molecule. *Proc Natl Acad Sci U S A*, **90**, 507-511.

Orr, D.C., Long, A.C., Kay, J., Dunn, B.M. and Cameron, J.M. (1989) Hydrolysis of a series of synthetic peptide substrates by the human rhinovirus 14 3C proteinase, cloned and expressed in Escherichia coli. *J Gen Virol*, **70 (Pt 11)**, 2931-2942.

Ozols, J. (1990) Amino acid analysis. *Methods Enzymol*, **182**, 587-601.

Pain, V.M. (1996) Initiation of protein synthesis in eukaryotic cells. *Eur J Biochem*, **236**, 747-771.

Palmenberg, A.C., Pallansch, M.A. and Rueckert, R.R. (1979) Protease required for processing picornaviral coat protein resides in the viral replicase gene. *J Virol*, **32**, 770-778.

Papadopoulos, N.G., Bates, P.J., Bardin, P.G., Papi, A., Leir, S.H., Fraenkel, D.J., Meyer, J., Lackie, P.M., Sanderson, G., Holgate, S.T. and Johnston, S.L. (2000) Rhinoviruses infect the lower airways. *J Infect Dis*, **181**, 1875-1884.

Park, N., Katikaneni, P., Skern, T. and Gustin, K.E. (2008) Differential targeting of nuclear pore complex proteins in poliovirus-infected cells. *J Virol*, **82**, 1647-1655.

Parks, G.D., Baker, J.C. and Palmenberg, A.C. (1989) Proteolytic cleavage of encephalomyocarditis virus capsid region substrates by precursors to the 3C enzyme. *J Virol*, **63**, 1054-1058.

Pata, J.D., Schultz, S.C. and Kirkegaard, K. (1995) Functional oligomerization of poliovirus RNA-dependent RNA polymerase. *Rna*, **1**, 466-477.

Patick, A.K., Brothers, M.A., Maldonado, F., Binford, S., Maldonado, O., Fuhrman, S., Petersen, A., Smith, G.J., 3rd, Zalman, L.S., Burns-Naas, L.A. and Tran, J.Q. (2005) In vitro antiviral activity and single-dose pharmacokinetics in humans of a novel, orally bioavailable inhibitor of human rhinovirus 3C protease. *Antimicrob Agents Chemother*, **49**, 2267-2275.

Paul, A.V., van Boom, J.H., Filippov, D. and Wimmer, E. (1998) Protein-primed RNA synthesis by purified poliovirus RNA polymerase. *Nature*, **393**, 280-284.

Pelham, H.R. (1978) Translation of encephalomyocarditis virus RNA in vitro yields an active proteolytic processing enzyme. *Eur J Biochem*, **85**, 457-462.

Pelham, H.R. and Jackson, R.J. (1976) An efficient mRNA-dependent translation system from reticulocyte lysates. *Eur J Biochem*, **67**, 247-256.

Pestova, T.V., Hellen, C.U. and Shatsky, I.N. (1996a) Canonical eukaryotic initiation factors determine initiation of translation by internal ribosomal entry. *Mol Cell Biol*, **16**, 6859-6869.

Pestova, T.V., Kolupaeva, V.G., Lomakin, I.B., Pilipenko, E.V., Shatsky, I.N., Agol, V.I. and Hellen, C.U. (2001) Molecular mechanisms of translation initiation in eukaryotes. *Proc Natl Acad Sci U S A*, **98**, 7029-7036.

Pestova, T.V., Shatsky, I.N. and Hellen, C.U. (1996b) Functional dissection of eukaryotic initiation factor 4F: the 4A subunit and the central domain of the 4G subunit are sufficient to mediate internal entry of 43S preinitiation complexes. *Mol Cell Biol*, **16**, 6870-6878.

Petersen, J.F., Cherney, M.M., Liebig, H.D., Skern, T., Kuechler, E. and James, M.N. (1999) The structure of the 2A proteinase from a common cold virus: a proteinase responsible for the shut-off of host-cell protein synthesis. *Embo J*, **18**, 5463-5475.

Pettersson, R.F., Ambros, V. and Baltimore, D. (1978) Identification of a protein linked to nascent poliovirus RNA and to the polyuridylic acid of negative-strand RNA. *J Virol*, **27**, 357-365.

Pilipenko, E.V., Gmyl, A.P., Maslova, S.V., Khitrina, E.V. and Agol, V.I. (1995) Attenuation of Theiler's murine encephalomyelitis virus by modifications of the oligopyrimidine/AUG tandem, a host-dependent translational cis element. *J Virol*, **69**, 864-870.

Pilipenko, E.V., Gmyl, A.P., Maslova, S.V., Svitkin, Y.V., Sinyakov, A.N. and Agol, V.I. (1992) Prokaryotic-like cis elements in the cap-independent internal initiation of translation on picornavirus RNA. *Cell*, **68**, 119-131.

Pollard, T.D., Earnshaw, W.C. and Johnson, G.T. (2002) *Cell biology*. Saunders, Philadelphia, Penn.; London.

Pyronnet, S., Imataka, H., Gingras, A.C., Fukunaga, R., Hunter, T. and Sonenberg, N. (1999) Human eukaryotic translation initiation factor 4G (eIF4G) recruits mnk1 to phosphorylate eIF4E. *Embo J*, **18**, 270-279.

Reed, L.J. and Muench., H. (1938) A simple method of estimating 50 per cent end-points. *Amer. Jour. Hygiene*, **27**, 493-497.

Renwick, N., Schweiger, B., Kapoor, V., Liu, Z., Villari, J., Bullmann, R., Miething, R., Briese, T. and Lipkin, W.I. (2007) A recently identified rhinovirus genotype is associated with severe respiratory-tract infection in children in Germany. *J Infect Dis*, **196**, 1754-1760.

Rigaut, G., Shevchenko, A., Rutz, B., Wilm, M., Mann, M. and Seraphin, B. (1999) A generic protein purification method for protein complex characterization and proteome exploration. *Nat Biotechnol*, **17**, 1030-1032.

Roetzer, A. (2004) Untersuchung der Wechselwirkung von Enteroviralen 2A Proteinasen mit dem Eukaryotishen Initiationfaktor eIF4GI. *Diploma thesis*. University of Vienna, Vienna.

Rossmann, M.G., Arnold, E., Erickson, J.W., Frankenberger, E.A., Griffith, J.P., Hecht, H.J., Johnson, J.E., Kamer, G., Luo, M., Mosser, A.G. and et al. (1985) Structure of a human common cold virus and functional relationship to other picornaviruses. *Nature*, **317**, 145-153.

Rossmann, M.G., Bella, J., Kolatkar, P.R., He, Y., Wimmer, E., Kuhn, R.J. and Baker, T.S. (2000) Cell recognition and entry by rhino- and enteroviruses. *Virology*, **269**, 239-247.

Rossmann, M.G., He, Y. and Kuhn, R.J. (2002) Picornavirus-receptor interactions. *Trends Microbiol*, **10**, 324-331.

Ryan, M.D., Donnelly, M., Lewis, A., Mehrotra, A.P., Wilkie, J. and Gani, D. (1999) A Model for Nonstoichiometric, Costranslational Protein Scission in Eukaryotic Ribosomes. *Bioorganic Chemistry*, **27**, 55-79.

Sambrok, J., Fritsch, E.F. and Maniatis, T. (1989) *Molecular Cloning: A Laboratory Manual*. Cold Spring Harbour Laboratory, New York.

Sangar, D.V., Newton, S.E., Rowlands, D.J. and Clarke, B.E. (1987) All foot and mouth disease virus serotypes initiate protein synthesis at two separate AUGs. *Nucleic Acids Res*, **15**, 3305-3315.

Sarkany, Z., Szeltner, Z. and Polgar, L. (2001) Thiolate-imidazolium ion pair is not an obligatory catalytic entity of cysteine peptidases: the active site of picornain 3C. *Biochemistry*, **40**, 10601-10606.

Savolainen, C., Blomqvist, S., Mulders, M.N. and Hovi, T. (2002) Genetic clustering of all 102 human rhinovirus prototype strains: serotype 87 is close to human enterovirus 70. *J Gen Virol*, **83**, 333-340.

Schechter, I. and Berger, A. (1967) On the size of the active site in proteases. I. Papain. *Biochem Biophys Res Commun*, **27**, 157-162.

Scheper, G.C., van Kollenburg, B., Hu, J., Luo, Y., Goss, D.J. and Proud, C.G. (2002) Phosphorylation of eukaryotic initiation factor 4E markedly reduces its affinity for capped mRNA. *J Biol Chem*, **277**, 3303-3309.

Schlegel, A., Giddings, T.H., Jr., Ladinsky, M.S. and Kirkegaard, K. (1996) Cellular origin and ultrastructure of membranes induced during poliovirus infection. *J Virol*, **70**, 6576-6588.

Schlick, P. (2004) Investigation of the HIV proteinase substrate specificity and inhibitor sensitivity using a bacterial genetic screen. *PhD thesis*. University of vienna, Vienna.

Schmid, E. (2002) Strukturspezifische Untersuchung rhinoviraler Proteasen unter besonderer Berückschtigung der Spaltung der eIF4G Isoformen. *Diploma thesis*. University of Vienna, Vienna.

Schneider, R., Agol, V.I., Andino, R., Bayard, F., Cavener, D.R., Chappell, S.A., Chen, J.J., Darlix, J.L., Dasgupta, A., Donze, O., Duncan, R., Elroy-Stein, O., Farabaugh, P.J., Filipowicz, W., Gale, M., Jr., Gehrke, L., Goldman, E., Groner, Y., Harford, J.B., Hatzglou, M., He, B., Hellen, C.U., Hentze, M.W., Hershey, J., Hershey, P., Hohn, T., Holcik, M., Hunter, C.P., Igarashi, K., Jackson, R., Jagus, R., Jefferson, L.S., Joshi, B., Kaempfer, R., Katze, M., Kaufman, R.J., Kiledjian, M., Kimball, S.R., Kimchi, A., Kirkegaard, K., Koromilas, A.E., Krug, R.M., Kruys, V., Lamphear, B.J., Lemon, S., Lloyd, R.E., Maquat, L.E., Martinez-Salas, E., Mathews, M.B., Mauro, V.P., Miyamoto, S., Mohr, I., Morris, D.R., Moss, E.G., Nakashima, N., Palmenberg, A., Parkin, N.T., Pe'ery, T., Pelletier, J., Peltz, S., Pestova, T.V., Pilipenko, E.V., Prats, A.C., Racaniello, V., Read, G.S., Rhoads, R.E., Richter, J.D., Rivera-Pomar, R., Rouault, T., Sachs, A., Sarnow, P., Scheper, G.C., Schiff, L., Schoenberg, D.R., Semler, B.L., Siddiqui, A., Skern, T., Sonenberg, N., Tahara, S.M., Thomas, A.A., Toulme, J.J., Wilusz, J., Wimmer, E., Witherell, G. and Wormington, M. (2001) New ways of initiating translation in eukaryotes. *Mol Cell Biol*, **21**, 8238-8246.

Schultheiss, T., Kusov, Y.Y. and Gauss-Muller, V. (1994) Proteinase 3C of hepatitis A virus (HAV) cleaves the HAV polyprotein P2-P3 at all sites including VP1/2A and 2A/2B. *Virology*, **198**, 275-281.

Seipelt, J., Liebig, H.D., Sommergruber, W., Gerner, C. and Kuechler, E. (2000) 2A proteinase of human rhinovirus cleaves cytokeratin 8 in infected HeLa cells. *J Biol Chem*, **275**, 20084-20089.

Skern, T., Hampölz, B., Guarné, A., Fita, I., Bergmann, E., Petersen, J. and James, M.N. (2002) Structure and function of picornavirus proteinases. In Semler, B.L. and Wimmer, E. (eds.), *Molecular Biology of Picornaviruses*. ASM Press, Washington, D. C., pp. 199-212.

Skern, T., Sommergruber, W., Auer, H., Volkmann, P., Zorn, M., Liebig, H.D., Fessl, F., Blaas, D. and Kuechler, E. (1991) Substrate requirements of a human rhinoviral 2A proteinase. *Virology*, **181**, 46-54.

Sommergruber, W., Ahorn, H., Zophel, A., Maurer-Fogy, I., Fessl, F., Schnorrenberg, G., Liebig, H.D., Blaas, D., Kuechler, E. and Skern, T. (1992) Cleavage specificity on synthetic peptide substrates of human rhinovirus 2 proteinase 2A. *J Biol Chem*, **267**, 22639-22644.

Sousa, C., Schmid, E.M. and Skern, T. (2006) Defining residues involved in human rhinovirus 2A proteinase substrate recognition. *FEBS Lett*, **580**, 5713-5717.

Spector, D.H. and Baltimore, D. (1974) Requirement of 3'-terminal poly(adenylic acid) for the infectivity of poliovirus RNA. *Proc Natl Acad Sci U S A*, **71**, 2983-2987.

Staunton, D.E., Merluzzi, V.J., Rothlein, R., Barton, R., Marlin, S.D. and Springer, T.A. (1989) A cell adhesion molecule, ICAM-1, is the major surface receptor for rhinoviruses. *Cell*, **56**, 849-853.

Strong, R. and Belsham, G.J. (2004) Sequential modification of translation initiation factor eIF4GI by two different foot-and-mouth disease virus proteases within infected baby hamster kidney cells: identification of the 3Cpro cleavage site. *J Gen Virol*, **85**, 2953-2962.

Studier, F.W. (1991) Use of bacteriophage T7 lysozyme to improve an inducible T7 expression system. *J Mol Biol*, **219**, 37-44.

Svitkin, Y.V., Gorbalenya, A.E., Kazachkov, Y.A. and Agol, V.I. (1979) Encephalomyocarditis virus-specific polypeptide p22 possessing a proteolytic activity: preliminary mapping on the viral genome. *FEBS Lett*, **108**, 6-9.

Svitkin, Y.V., Gradi, A., Imataka, H., Morino, S. and Sonenberg, N. (1999) Eukaryotic initiation factor 4GII (eIF4GII), but not eIF4GI, cleavage correlates with inhibition of host cell protein synthesis after human rhinovirus infection. *J Virol*, **73**, 3467-3472.

Svitkin, Y.V., Hahn, H., Gingras, A.C., Palmenberg, A.C. and Sonenberg, N. (1998) Rapamycin and wortmannin enhance replication of a defective encephalomyocarditis virus. *J Virol*, **72**, 5811-5819.

Svitkin, Y.V., Imataka, H., Khaleghpour, K., Kahvejian, A., Liebig, H.D. and Sonenberg, N. (2001) Poly(A)-binding protein interaction with eIF4G stimulates picornavirus IRES-dependent translation. *Rna*, **7**, 1743-1752.

Svitkin, Y.V., Ovchinnikov, L.P., Dreyfuss, G. and Sonenberg, N. (1996) General RNA binding proteins render translation cap dependent. *Embo J*, **15**, 7147-7155.

Tesar, M. and Marquardt, O. (1990) Foot-and-mouth disease virus protease 3C inhibits cellular transcription and mediates cleavage of histone H3. *Virology*, **174**, 364-374.

Toyoda, H., Nicklin, M.J., Murray, M.G., Anderson, C.W., Dunn, J.J., Studier, F.W. and Wimmer, E. (1986) A second virus-encoded proteinase involved in proteolytic processing of poliovirus polyprotein. *Cell*, **45**, 761-770.

Turner, R.B. (2007) Rhinovirus: more than just a common cold virus. *J Infect Dis*, **195**, 765-766.

van Kuppeveld, F.J., de Jong, A.S., Melchers, W.J. and Willems, P.H. (2005) Enterovirus protein 2B po(u)res out the calcium: a viral strategy to survive? *Trends Microbiol*, **13**, 41-44.

van Vlijmen, H.W., Curry, S., Schaefer, M. and Karplus, M. (1998) Titration calculations of foot-and-mouth disease virus capsids and their stabilities as a function of pH. *J Mol Biol*, **275**, 295-308.

Vance, L.M., Moscufo, N., Chow, M. and Heinz, B.A. (1997) Poliovirus 2C region functions during encapsidation of viral RNA. *J Virol*, **71**, 8759-8765.

Ventoso, I., MacMillan, S.E., Hershey, J.W. and Carrasco, L. (1998) Poliovirus 2A proteinase cleaves directly the eIF-4G subunit of eIF-4F complex. *FEBS Lett*, **435**, 79-83.

Vlasak, M., Blomqvist, S., Hovi, T., Hewat, E. and Blaas, D. (2003) Sequence and structure of human rhinoviruses reveal the basis of receptor discrimination. *J Virol*, **77**, 6923-6930.

Wang, Q.M., Johnson, R.B., Sommergruber, W. and Shepherd, T.A. (1998) Development of in vitro peptide substrates for human rhinovirus-14 2A protease. *Arch Biochem Biophys*, **356**, 12-18.

Wells, S.E., Hillner, P.E., Vale, R.D. and Sachs, A.B. (1998) Circularization of mRNA by eukaryotic translation initiation factors. *Mol Cell*, **2**, 135-140.

Witherell, G.W., Schultz-Witherell, C.S. and Wimmer, E. (1995) Cis-acting elements of the encephalomyocarditis virus internal ribosomal entry site. *Virology*, **214**, 660-663.

Wyckoff, E.E., Lloyd, R.E. and Ehrenfeld, E. (1992) Relationship of eukaryotic initiation factor 3 to poliovirus-induced p220 cleavage activity. *J Virol*, **66**, 2943-2951.

Xatzipsalti, M., Kyrana, S., Tsolia, M., Psarras, S., Bossios, A., Laza-Stanca, V., Johnston, S.L. and Papadopoulos, N.G. (2005) Rhinovirus viremia in children with respiratory infections. *Am J Respir Crit Care Med*, **172**, 1037-1040.

Yalamanchili, P., Banerjee, R. and Dasgupta, A. (1997a) Poliovirus-encoded protease 2APro cleaves the TATA-binding protein but does not inhibit host cell RNA polymerase II transcription in vitro. *J Virol*, **71**, 6881-6886.

Yalamanchili, P., Datta, U. and Dasgupta, A. (1997b) Inhibition of host cell transcription by poliovirus: cleavage of transcription factor CREB by poliovirus-encoded protease 3Cpro. *J Virol*, **71**, 1220-1226.

Yalamanchili, P., Weidman, K. and Dasgupta, A. (1997c) Cleavage of transcriptional activator Oct-1 by poliovirus encoded protease 3Cpro. *Virology*, **239**, 176-185.

Yamamoto, T., Davis, C.G., Brown, M.S., Schneider, W.J., Casey, M.L., Goldstein, J.L. and Russell, D.W. (1984) The human LDL receptor: a cysteine-rich protein with multiple Alu sequences in its mRNA. *Cell*, **39**, 27-38.

Yeh, A.P., McMillan, A. and Stowell, M.H. (2006) Rapid and simple protein-stability screens: application to membrane proteins. *Acta Crystallogr D Biol Crystallogr*, **62**, 451-457.

Ypma-Wong, M.F., Dewalt, P.G., Johnson, V.H., Lamb, J.G. and Semler, B.L. (1988) Protein 3CD is the major poliovirus proteinase responsible for cleavage of the P1 capsid precursor. *Virology*, **166**, 265-270.

Zamora, M., Marissen, W.E. and Lloyd, R.E. (2002) Multiple eIF4GI-specific protease activities present in uninfected and poliovirus-infected cells. *J Virol*, **76**, 165-177.

Zeghouf, M., Li, J., Butland, G., Borkowska, A., Canadien, V., Richards, D., Beattie, B., Emili, A. and Greenblatt, J.F. (2004) Sequential Peptide Affinity (SPA) system for the identification of mammalian and bacterial protein complexes. *J Proteome Res*, **3**, 463-468.

Zoll, J., Melchers, W.J., Galama, J.M. and van Kuppeveld, F.J. (2002) The mengovirus leader protein suppresses alpha/beta interferon production by inhibition of the iron/ferritin-mediated activation of NF-kappa B. *J Virol*, **76**, 9664-9672.

Curriculum Vitae

Name: Carla Cristina Jacinto de Sousa

Date of birth: 1979/06/10

Nationality: Portuguese

Address: Sankt Johann Gasse 1-5/4/15 1050 Wien, Austria

Telephone: +43 699 10776107

Email: carla.sousa@univie.ac.at; sousac6@gmail.com

Academic degrees, fields of study, dates
1997-2002-Graduated in Biochemistry, Faculty of Sciences, Oporto University. Final mark: 13/20.

Present position, institution, starting date

PhD student at the department of Biochemistry of The Medical University of Vienna, Austria, under supervision of Professor Tim Skern. Started on October 2004.

Previous positions, institutions, dates
- Mar. 2004 – Sept. 2004: work on the department of Animal Breeding and Genetics of the Veterinary Medicine University of Vienna, under the supervision of Professor Christian Schlötterer, on population genetics.

- Jan. 2003 - Jan. 2004: started as recipient of a "Initiation to Research Grant" in the Molecular Immunology Unit of the Molecular and Cellular Biology Institute, Oporto, under the supervision of Dr. Ana M. Tomás on the subject " Functional analysis of two tryparedoxins of *Leishmania infantum* and their validation as drug targets ".

- Sep. 2001 - Sept. 2002: Diploma project on the subject "Isolation and characterization of tryparedoxins of *Leishmania infantum*", under the supervision of Dr. Ana M. Tomás, in the Molecular Immunology Unit of the Molecular and Cellular Biology Institute, Oporto. Final mark: 18/20.

- Mar. 2001 - Sept. 2001: voluntary work at the Molecular Immunology Unit of the Molecular and Cellular Biology Institute, Oporto, under the supervision of Dr. Ana M. Tomás.

Main scientific area of research
Molecular Biology

Interests
Cell Biology, Molecular Biology, Biochemistry, Virology, Microbiology, Immunology.

Publications

- **Sousa C**., Schmid E.M., Skern T. (2006) Defining residues involved in human rhinovirus 2A proteinase substrate recognition, FEBS letters, 580, 5713-5717.

 - Deszcz L., Cencic R., **Sousa C.**, Kuechler E. and Skern T. (2006) An anti-viral peptide inhibitor active against picornaviral 2A proteinases but not cellular caspases, J. of Virology, 80, 9619-9627.

- Schlötterer C., Neumeier H., **Sousa C.**, and Nolte V. (2006) Highly Structured Asian Drosophila melanogaster Populations: A New Tool for Hitchhiking Mapping?,Genetics 172, 287-292.

- Castro H, **Sousa C.**, Novais M, Santos M, Budde H, Cordeiro-da-Silva A, Flohé L, Tomás A. M. (2004) Two linked genes of Leishmania infantum encode tryparedoxins localized to cytosol and mitochondrion, Mol Biochem Parasitol, 136, 137-147.

- Castro H.; **Sousa C**.; Santos M.; Cordeiro-da-Silva A.; Flohé L.; Tomás A. M. (2002) Complementary antioxidant defence by cytoplasmic and mitochondrial peroxiredoxin of Leishmania infantum, Free Radic Biol Med, 33, 1552-1562.